ETEC-82-1

I-3888

Energy Technology Engineering Center (ETEC) Annual Technical Progress Report January-December 1981

MASTER

~~APPLIED TECHNOLOGY~~

~~Any further distribution by any holder of this document of the data therein to third parties representing foreign interests, foreign governments, foreign companies and foreign subsidiaries or foreign divisions of U. S. companies should be coordinated with the Director, Division of Reactor Research and Technology, U. S. Department of Energy.~~

Prepared for the U.S. Department of Energy
Division of Nuclear Power Development
under Contract Number DE-AM03-76-SF00700

Energy Technology Engineering Center

Operated for the U.S. Department of Energy
by Energy Systems Group, Rockwell International

P.O. Box 1449, Canoga Park, California 91304

DISCLAIMER

ETEC-82-1
UC-79T

ETEC--82-1

DE82 016909

Energy Technology Engineering Center (ETEC)

Annual Technical Progress Report January-December 1981

Energy Technology Engineering Center

Operated for the U.S. Department of Energy
by Energy Systems Group, Rockwell International

P.O. Box 1449, Canoga Park, California 91304

CONTRACT: DE-AM03-76-SF00700
ISSUED: MAY 15, 1982

DISTRIBUTION

Energy Technology Engineering Center — Internal:

L. J. Auge
J. O. Bates
L. B. Copeland
W. S. DeBear
R. E. Fenton
F. L. Fletcher
K. T. Stafford
M. J. Tessier
H. C. Wieseneck
H. R. Zweig
D. J. Zweng
(15) Library

External:

Director, RRT, HQ (NE-530)
Director, ETEC Project Office, SS
Actg Chief, Facilities Management Division, RRT, HQ (NE-530)
(3) J. W. Semko, Facilities Management Division, RRT, HQ (NE-530)
Chief, DOE Calif. Patent Group, SAN
Manager, SAN
Patent Counsel, Energy Systems Group, Rockwell International
Information Services, Energy Systems Group, Rockwell International

(97) DOE Technical Information Center for distribution under DOE/TIC-4500-R68, Category UC-79T

CONTENTS

CONTENTS

CONTENTS

CONTENTS

CONTENTS

CONTENTS

TABLES

FIGURES

FIGURES

FIGURES

FIGURES

FIGURES

FIGURES

FIGURES

INTRODUCTION

The Energy Technology Engineering Center (ETEC) is operated for the U.S. Department of Energy (DOE) by the Energy Systems Group (ESG) of Rockwell International.

The ETEC complex contains several multipurpose test facilities, including some of the world's largest circulating sodium loops. These facilities are maintained and operated in support of DOE's Liquid Metal Fast Breeder Reactor (LMFBR) Program. Major components of the Fast Flux Test Facility (FFTF), located in Hanford, Washington, have been tested here, and similar testing for the Clinch River Breeder Reactor (CRBR), in Tennessee, is planned or underway.

This technical progress report covers all of ETEC's activities in support of the LMFBR program during Calendar Year 1981.

SUMMARY

ETEC test components and systems associated with liquid metal reactors include heat exchangers, circulating pumps, valves, and related instrumentation. Reactor core mechanisms are evaluated for performance in sodium, but no nuclear fuels or radioactive materials are handled on site. This summary provides a brief overview of all testing activities during Calendar Year 1981. A detailed description of all major test programs forms the balance of this report.

PUMPS

INTERMEDIATE-SIZE INDUCER PUMP

Sodium Performance

An FFTF pump (14,500 gal/min) fitted with an inducer was assembled, installed, and tested to determine head-flow characteristics and suction performance over a wide range of operating conditions. Subsequently, a 1000-h endurance test was conducted at reduced NPSH.

1/5-SCALE INDUCER PUMP

Water Performance

Facility modifications were completed for testing a 1/5-scale inducer pump (3200 gal/min). The pump was received and installed, facility checkouts were completed, and testing was initiated. Testing will continue through FY 1982 to fully characterize head-flow and cavitation performance of the unit.

CRBR FLAT, LINEAR INDUCTION PUMP

Sodium Performance

The CRBR EM pump was tested in sodium in the SCTI at flows up to 800 gal/min and head pressures of 200 psi. Testing occurred at temperatures between 450 and 1130^{o}F. Included were performance testing, off-limits testing, emergency conditions testing, and extended operations (endurance) at 900^{o}F.

TRANSITION JOINT LIFE TEST

Thermal Transient Testing

Two 18-in.-diameter, 1-in.-thick piping test articles, each containing a bi-metallic and a tri-metallic welded joint, were subjected to a continuous 400,000-lb tensile load. While under load, the test articles were subjected to 10^{o}F/s thermal transients from 1100 to 800^{o}F and then, at a lower transient rate, down to 200^{o}F. Testing was terminated at 81 transients on one test article and 50 on the other after the discovery of cracks that exceeded the maximum size specified for shutdown.

INSERVICE INSPECTION TESTS

Simulated Reactor Inspection Conditions

A 16-in.-diameter test pipe section containing circumferential welds with calibrated defects was installed in a circulating sodium loop. The test section was maintained at reactor refueling conditions in order to test an ultrasonic scanning inspection mechanism.

8-IN. PIPE TEST

Creep Ratchetting

An 8-in.-diameter Type 304 stainless steel pipe was subjected to a series of thermal downramps from 1100 to 500^{o}F at a rate of 60^{o}F/s, followed by 16-h hold periods at 1100^{o}F. A continuous tensile load of 180,000 lb was maintained on the test article. The test article failed after 19 cycles and was replaced by a second one, which is undergoing an identical test series.

ELECTRICAL HEATERS

Life Testing

The electric heater test program evaluates heater performance under typical operating conditions and overstress condition to accelerate failure rate. A total of 81,000 h of typical operation was accumulated on 20 mineral-insulated cables. Six mineral-insulated cables were subjected to 26,000 thermal cycles (overstress tests). The cables were manufactured in the U.S., France, and Germany. Nine tubular heaters were subjected to 58,000 thermal cycles. Tubular heater testing was also conducted. Ten heaters were tested to failure in accelerated life evaluation.

INSTRUMENTATION

SODIUM LEVEL MEASUREMENT

Dry Checkout and Sodium Testing

Several systems were evaluated, including inductive, displacer float, and differential pressure. The test program included foreign-made devices as part of an international exchange program. Sodium level transducers accumulated 43,000 h of performance and life testing at sodium temperatures between 400 and 1200^{o}F.

SODIUM PRESSURE MEASUREMENT

Dry Checkout and Sodium Testing

Two types of high-temperature pressure measurement systems were evaluated: steady-state and dynamic pressure. The first type is used in LMFBR plants for performance information and plant protective systems. The second type is used primarily in test facilities to record off-normal conditions. Sodium testing parameters ranged from 0 to 300 psi and from 250 to 1200^{o}F. Testing of 13 sodium

pressure transducers from three different manufacturers totalled more than 100,000 h of elevated-temperature performance.

LARGE SODIUM FLOWMETERS

Sodium Testing

Three sodium flowmeters with 16-in.-diameter pipes were evaluated for output versus flow, sodium temperature effects, and response time. The flowmeter types were saddle coil, single path ultrasonic, and venturi bypass. Calibrations were conducted over a flow range of 1,000 to 18,000 gal/min at temperatures from 400 to 1050°F.

SODIUM FLOWMETERS

Sodium Testing

Four permanent magnet flowmeters with pipes 1 in. in diameter were calibrated over a flow range of 2 to 10 gal/min in sodium between 400 and 800°F. These flowmeters were calibrated in support of the annular linear induction pumps (ALIPs) used by HEDL in the transient fuel pin tests.

HIGH-TEMPERATURE STRAIN GAGES

Operational Testing

High-temperature strain gages are used to measure stresses during sodium component testing. Strain gage data are used to evaluate thermally induced creep ratchet in pipes and transition joints, dynamic response of piping, and in-stream generator testing. The two types of gages being tested are capacitance and weldable resistance gages. Capacitance gages are tested from ambient to 1200°F. Resistance gages, depending on their intended application, are tested up to 900 or 1100°F. Resistance gages are also tested in sodium. More than 95,000 h of strain gage testing time were recorded in 1981.

PUMP BEARING PROXIMITY MEASUREMENT

Proximity Transducers

The ultrasonic proximity transducer design progressed from the experimental level to an operational model. More than 5800 h of static sodium operation were accumulated on the first operational unit. Calibrations were conducted at sodium temperatures between 400 and 1100^{o}F. The displacement range was extended to 250 mils to accommodate LSBR pump requirements. The signal conditioning was improved to simplify operation and increase signal-to-noise ratio.

VALVES

COMMERCIALLY AVAILABLE VALVES

A test program was initiated to investigate the suitability of commercially available valves for sodium service. Program objectives are reductions in cost and in procurement lead time. Promising test results were obtained this year on more than 61 valves from four different manufacturers.

CRBR VALVES

A hardware testing program aimed at qualifying valves of different sizes for CRBR sodium service is underway. In addition to out-of-sodium checkouts, in-sodium testing included cycling tests, leak tests, flow tests, thermal transient tests under simulated pipe-loading conditions, and seismic testing.

HEAT EXCHANGERS

SODIUM-WATER REACTION TEST

Sodium Testing

During 1981, three tests in which failures were induced in steam generator tubes were conducted. Two of the tests were double-ended guillotine failures of

a central and a peripheral tube using high-pressure subcooled water on the tube side. The third tube failure was induced using a presized orifice with high-pressure steam on the tube side.

Wastage effects on adjacent tubes and leak detection performance capabilities were monitored for all three tube failure tests.

AUXILIARY EQUIPMENT

SELF-ACTUATED SHUTDOWN SYSTEM

Based on proof-of-principle testing in FY 1980, facility modifications were implemented to improve injection performance and to prepare for a series of "bowed-tube" tests. Renewed testing of this improved articulated control assembly and Curie-point magnet will begin early in FY 1982.

LEAK DETECTOR EVALUATION
Sodium Testing

Acoustic monitoring systems built by three different manufacturers were evaluated for their ability to detect steam/water leakage in steam generators. The devices were tested in conjunction with the large leak sodium-water reaction test program.

MATERIALS TESTING

ABSORBER BALL ALLOY CORROSION
Sodium Testing

Tests were conducted on candidate materials for an LMFBR shutdown mechanism. Six neutron-absorbing metals (tantalum, tantalum alloys, and tantalum with protective coatings) were exposed to sodium for 500 h over a temperature range of 700 to 1200^{o}F.

I. LARGE LEAK TEST RIG
SODIUM-WATER REACTION TESTING

H. H. NEELY AND L. M. PRESS

A. INTRODUCTION

The Large Leak Test Rig (LLTR) was designed and built to measure the total effects of steam generator tube failures in near prototypical steam generator internals and plant piping. Series II LLTR testing (Reference I-1) utilized the large leak test internals (LLTI), which are full size in diameter but shortened in length and prototypic of the Clinch River Breeder Reactor (CRBR) steam generator. The LLTI was installed in the large leak test vessel (LLTV).

The Series II program was designed to measure the effects of intermediate to large double-ended-guillotine (DEG) steam tube failures. Tube failure in a liquid-metal fast breeder reactor (LMFBR) steam generator results in an exothermic, high-temperature, corrosive sodium-water reaction (SWR) that can waste surrounding tubes at a rapid rate. Point source leak injection of this type causes heterogeneous heating (Reference I-1) of nearby steam tubes in the reaction region. Also, upon rupture disc failure, continued injection will tend to rapidly quench the reaction and subsequently the SWR-heated surfaces of the surrounding medium. These two effects result in thermoplastic deformation of the steam tubes (Reference I-2). Continued injection has also been shown to cause pool wastage on a static heel and excessive sodium-water reaction product (SWRP) buildup (Reference I-3). When the sodium heel is drained from a generator, the SWRP that was generated tends to hang up on tube support spacers and other hardware and can effectively plug this portion of a generator.

Sodium-water reaction testing in large steam generator models results in specific phenomena. Previously, there has not been equipment available to measure these phenomena. Therefore, to fully understand the SWR test results, some instrumentation to make the measurements had to be conceived and built. These phenomena were principally steam tube wastage and deformation, spacer plate deformation and location, and SWRP deposition in the tube bundle.

Anticipating the problem of wastage measurement, in Series I testing, ETEC designed and built an ultrasonic testing (UT) device (Reference I-4) to measure the tube wall thickness from the boreside of the tube. This device measured a single path about 20^{o} wide. Realizing that this was time-consuming, ETEC conceived and built a boreside rotating ultrasonic tester (BRUT) (References I-2, -3, and -5) designed to make the measurement in a single pass; it is presently in the checkout phase. Series I tests indicated steam tube deformation to be a problem. For Series II, ETEC conceived and built an isotope scanning tester (IST) (References I-2 and -3) to measure tube deformation, spacer location, and SWRP deposition. The IST has proven very useful for measuring these phenomena in Series II testing.

Previous ETEC annual reports have reported on four Series II tests, two nonreactive and one reactive DEG and one directed intermediate leak test. In 1981, there were three SWR tests performed. The first, A-6, was a subcooled water DEG on the periphery in the upper region of the LLTI. The test measured the dynamic system pressure due to a DEG at the bundle edge. The second test, A-7, was also a subcooled water DEG but in the central location nearer the bottom of the LLTI. That test was designed to measure the effects of a DEG at elevated sodium pressure in the same location as a previous nonreactive test. The third test, A-8, was an intermediate-directed-superheated-steam test in the upper central region of the LLTI. The test was designed to measure and determine experimentally the SWR effects during the time required for a reactor automatic shutdown system to sense the failure and deactivate the plant.

During CY 1981, ETEC published a number of general technical papers and two company reports on each test. The technical publications and presentations were on SWR testing, in-service inspection, and ETEC-devised inspection equipment. They are listed in References I-1 through I-8. The ETEC reports discussing each test are listed as References I-9 through I-14.

B. DESCRIPTION

1. Facility

The LLTR consists of three principal process systems (Figure I-1): (1) a static sodium system, Figures I-1 and -2, which is electrically heated to obtain temperature gradients that will exist in an LMFBR plant and a steam generator in particular; (2) a rupture relief system that seals the sodium system with a double rupture disc assembly designed for CRBR; and (3) a three-tank water supply system that supplies water/steam to both ends of the rupture tube and preconditioned water/steam to the secondary tubes. In the double rupture disc assembly of the second system, when the discs burst, the sodium and SWRP drain into the reaction products tank (RPT) through a tangential nozzle that effectively represents a cyclone separator. The reaction gases (hydrogen and unreacted steam) vent to the atmosphere through an ignited stack.

2. Test Article

For Series II testing, the test article is comprised of the LLTI, a shortened tube bundle that simulates the CRBR steam generator (Figure I-3), and the LLTV,

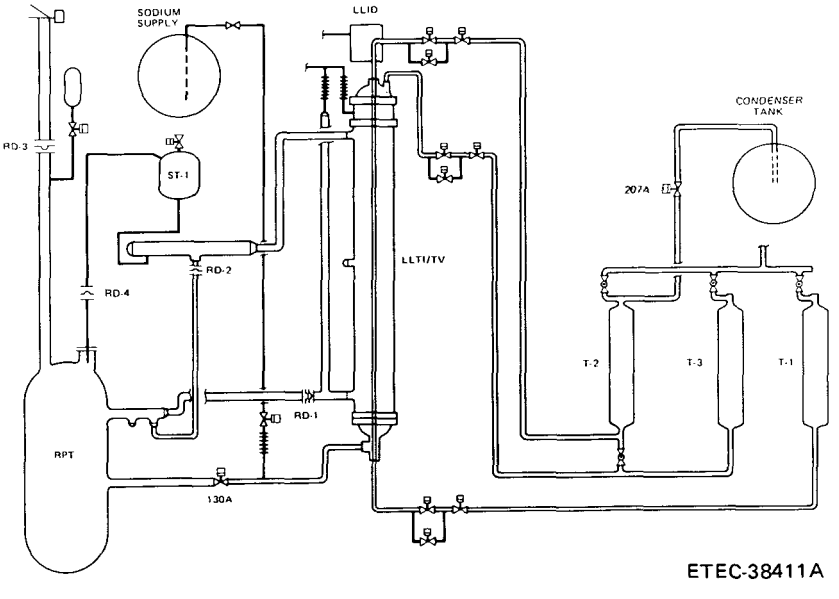

Figure I-1. Simplified Schematic of Series II LLTR

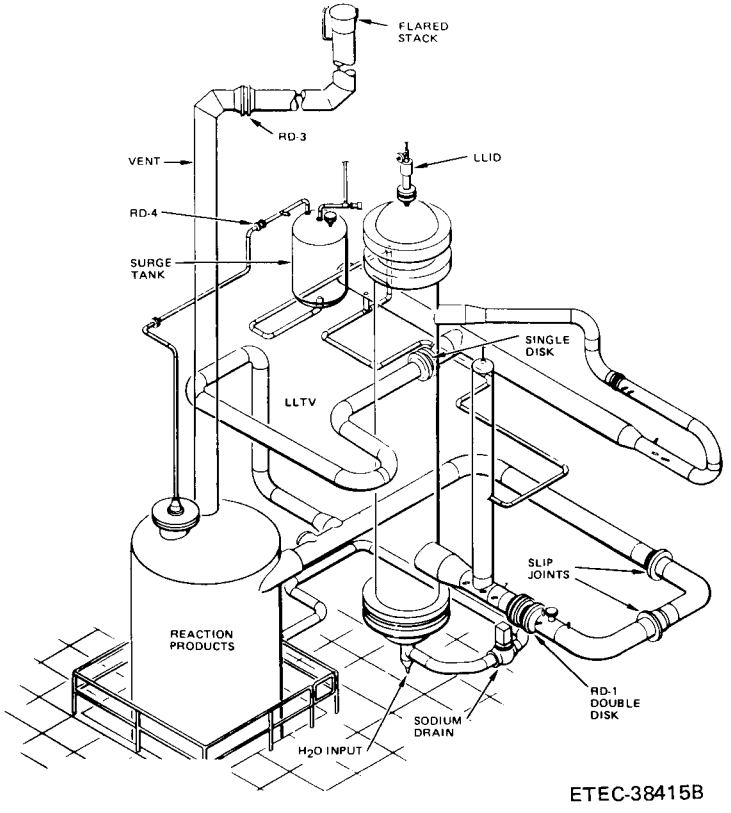

Figure I-2. LLTR Test Article, Sodium and Rupture Relief Systems

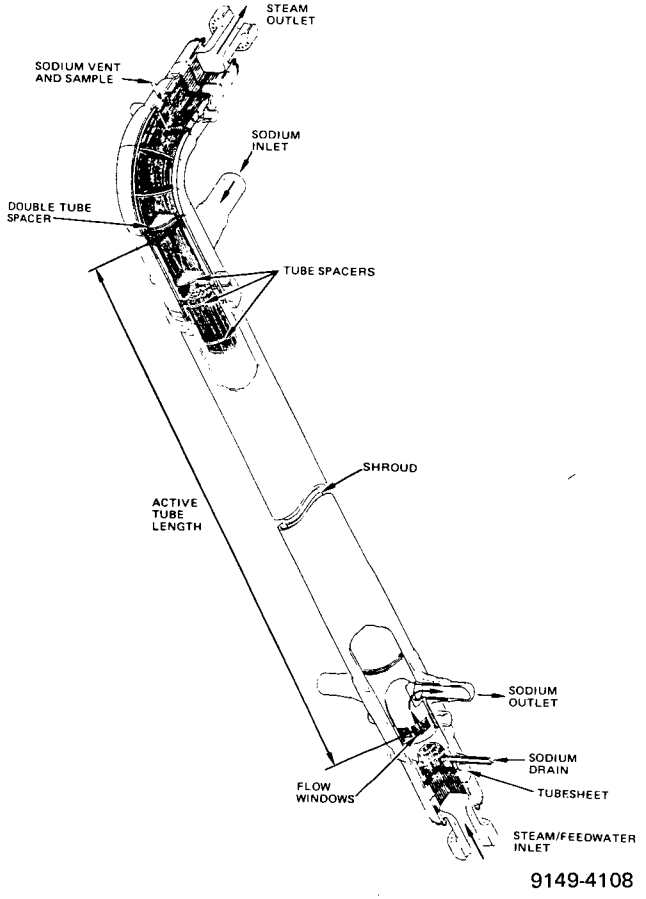

Figure I-3. The CRBR Steam Generator

which simulates the steam generator shell. The tube bundle diameter is full scale and, when combined with prototypic tubes, tube supports, and a simulated tubesheet, results in a component suitable for duplicating the effects of a water/steam tube failure in a full-sized steam generator.

The reason for a two-part test assembly (LLTI-LLTV) is that the LLTI internals have been designed for removal from the LLTV for refurbishment and instrumentation (if needed) between tests. Instrumented tubes may be removed, replaced, or relocated. A schematic showing salient features of the LLTI instrumented tube locations is presented in Figure I-4. Initially, 19 instrumented tubes were installed in the LLTI. The instruments shown are for a low central break; after the A-3 test, instrumentation (thermocouples) tubes were added for peripheral testing (Figure I-5). The instrumented tubes contained thermocouples, pressure transducers, and strain gages to measure test parameters and propagation of the SWR event radially and axially.

During an SWR test, sodium occupies the shell side of the LLTV (which simulates a steam generator section) and is in a static condition. Thermal gradients, which simulate plant flowing sodium conditions through a steam generator, are established by electrical heaters on the external wall of the LLTV. The sodium system is isolated from the relief system by rupture discs. When SWR test pressure attains a specified range, the discs burst and the sodium plus SWRP flow from the LLTV through the relief lines to the RPT.

In the water system, a static or dynamic flow condition can be established in the LLTI rupture tube prior to test with water flowing under pressure from Tank T-1, through the rupture tube, and then to Tank T-2. In all cases, the other LLTI (secondary) tubes are filled with water/steam supplied from Tank T-3 under specified conditions.

Tube rupture that initiates a DEG or intermediate event is effected by the large leak injection device (LLID),* shown in Figure I-6. The LLID consists of

*Supplied by the test requester, GE.

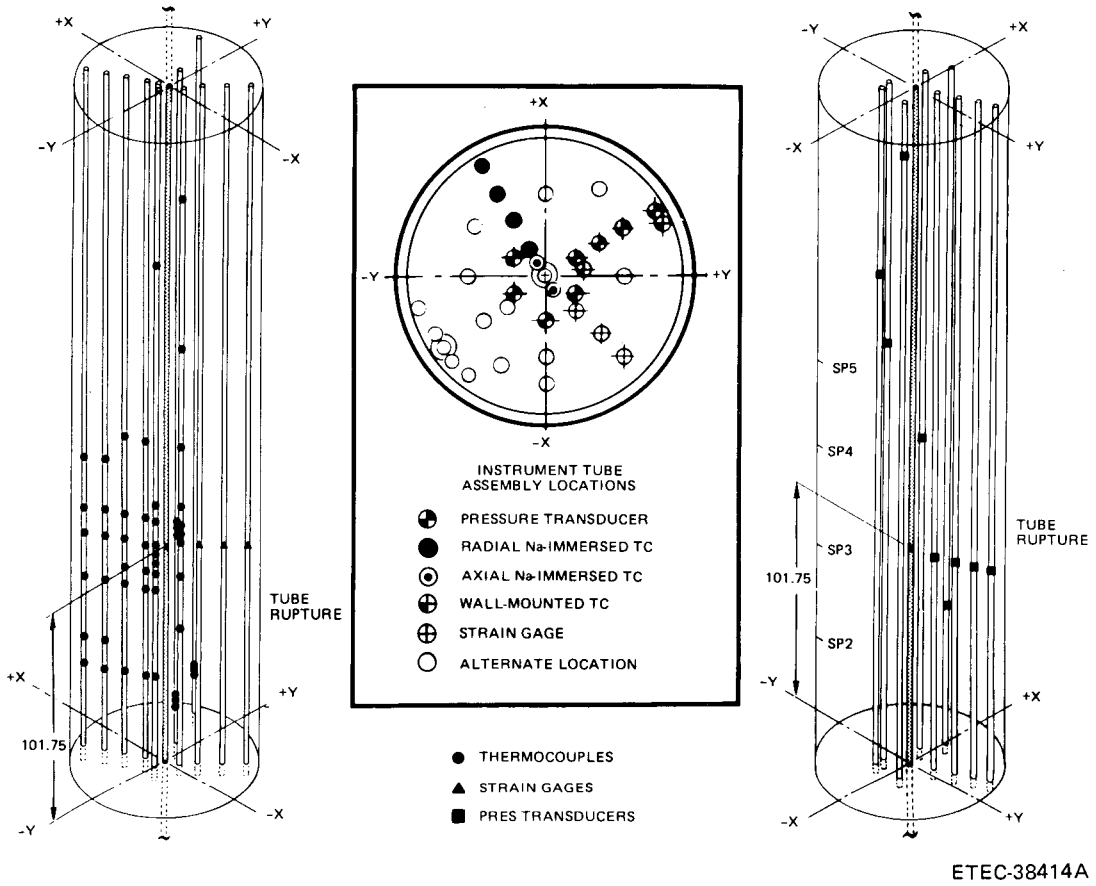

Figure I-4. Large Leak Test Internals Instrumentation

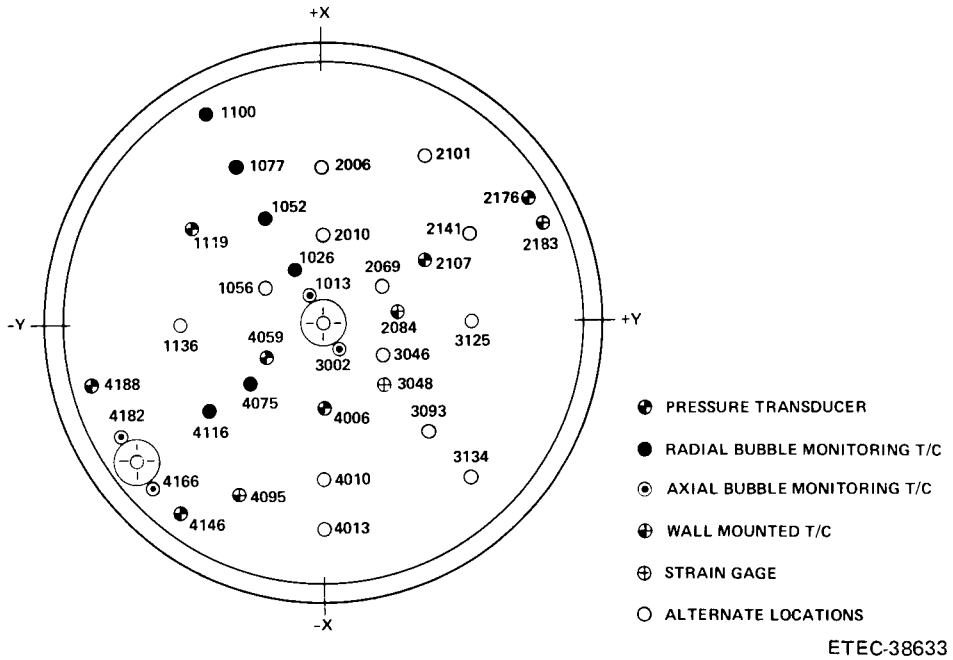

Figure I-5. LLTI Instrumented Tubes for Central and Peripheral Testing

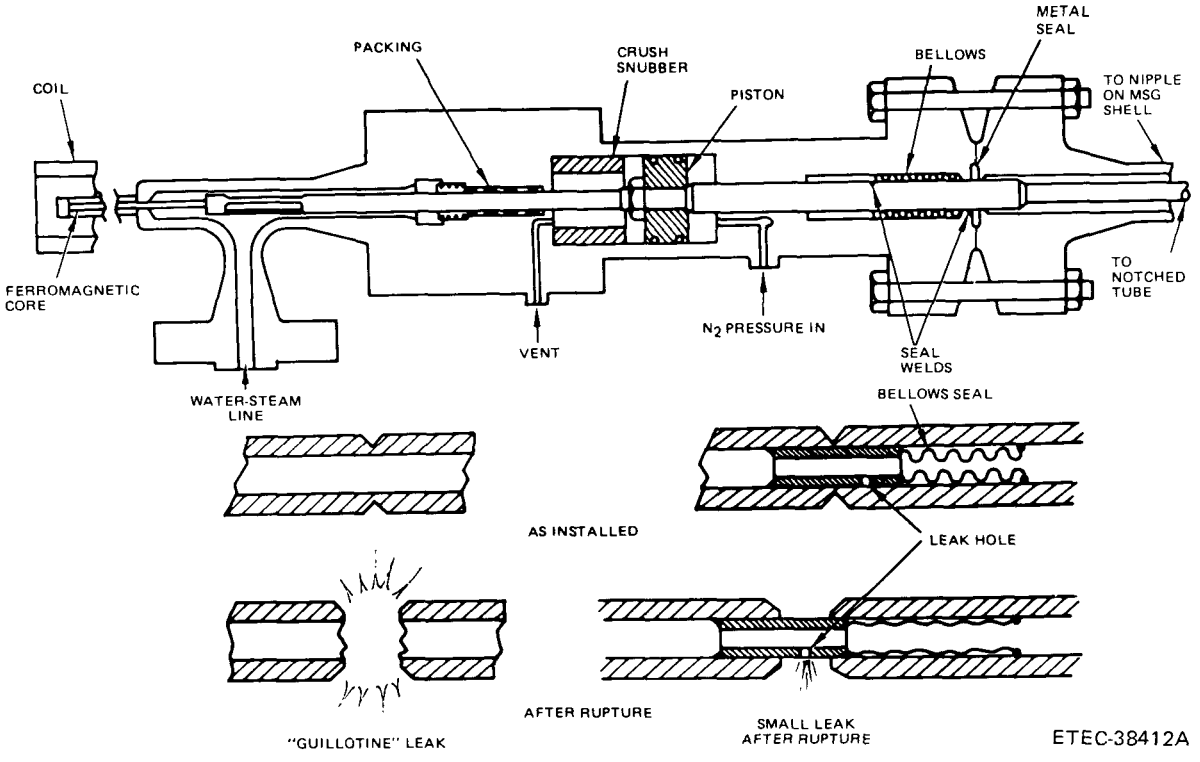

Figure I-6. Large Leak Injection Device

a cylinder with a pneumatic piston that can apply tension loading to the rupture tube (pre-weakened at the test site by a machined circumferential groove). The LLID is located above the LLTV head, and the piston is linked to the upper end of the rupture tube. The lower end of the rupture tube is welded to a nozzle attached to the bottom head of the LLTV. When adequate gas pressure is applied to the LLID piston, the rupture tube is pulled apart to yield failure at the pre-weakened groove, resulting in a instantaneous guillotine-type failure. Should a leak smaller than guillotine be desired, the flow of water from the guillotine failure would be constrained by means of an internally mounted sleeve with a presized leak hole drilled through the wall. A schematic of the two injection devices is included in Figure I-6.

3. Test Program

The original Series II test matrix was divided into two separate groups. Group A consisted of seven tests (two gas injection tests and five water injection tests) directed at identifying which type and size of primary leak would generate the maximum tube damage. Group B consisted of five additional tests using the worst leak characteristics from Group A; however, this portion of the program has been cancelled. At present, the only test remaining in Series IIA is A-5, possibly followed by destructive examination of the LLTI. Upon conclusion of the test program, the following objectives are anticipated:

1) The potential for secondary tube failure will be defined in order to establish a basis for selection of design-basis leaks (DBLs) for LMFBR steam generators.
2) Peak pressures experienced for large leak events in large steam generators will be determined experimentally.
3) Design-basis methods for large steam generators will be confirmed (or corrected).
4) Data will be provided to confirm adequacy of LMFBR design features to withstand SWR events.
5) LMFBR relief system performance will be determined.
6) Data will be provided for fast drain, cleanup, and recovery actions following major steam generator leak events.

In addition to sodium-water reaction testing, various intertest inspections are specified to meet program objectives. Intertest examinations are performed following each test to identify the effects of the previous test, verify the integrity of the test article for subsequent tests, and establish test article instrumentation availability. Most intertest examinations are conducted with the LLTI installed in the LLTV and include ultrasonic, isotope scanning, borescopic, and leak testing examinations on the LLTI, plus visual dye-penetrant, ultrasonic, and radiographic examination on selected portions of the LLTR.

The test program is primarily intended to provide data required to establish steam generator design parameters. To achieve this goal, the following test variations have been planned:

1) Leak Location – Various axial and radial rupture tube positions will be selected relative to internal components such as tube supports, flow baffles, and proximity to instrument elements.
2) Leak Size – Sizes will range from intermediate leak to full guillotine.
3) Fluid Conditions – Water/steam distribution and flow rates will be varied.

To meet various test requirements, the following techniques have been used as required:

1) Pressure wave magnitude and propagation mapping
2) Bubble growth mapping
3) Visual damage inspection
4) Pneumatic, hydraulic, and helium leak testing
5) Isotope scanning for SWR deposition and bowed tubes
6) Ultrasonic signature comparison of tube diameter and wall thickness with original baseline (wastage)
7) Borescopic examination for tube damage and reaction product depositions
8) Measurement of water/steam injection conditions
9) Piping and vessel transient pressure, temperature, and strain
10) Secondary line loading from the acoustic pressure wave propagation
11) Relief system transient pressure, temprature, flow, and strain responses
12) Transient conditions in the RPT resulting from the entry of sodium and reaction products
13) Vent system performance, including airborne particulate size and distribution and downwind deposition from the LLTR stack.

C. TEST CHRONOLOGY, CONDITIONS, AND RESULTS

During the 1981 report period, three SWR tests, SWRs A-6, A-7, and A-8 (November 26, 1980, April 13, 1981, and July 30, 1981, respectively), were run in the LLTR at ETEC. SWRs A-4 and A-5 and the Series B portion of the program were put on hold; then later in the year, A-4 was canceled and A-5 was reprogrammed to be run in CY 1982. When A-5 (peripheral intermediate superheated steam) has been run, the LLTI is expected to have almost no test regions available where there is no previous SWR damage. At that time, the LLTI will be ready for refurbishment for future testing and/or post-test destructive examination.

1. SWR A-6

Series II SWR A-6 was a DEG SWR test with the primary and secondary tubes filled with subcooled water, typically at reactor startup conditions. The purposes of this test were to obtain data on dynamic pressure wave propagation, secondary sodium system line loading from the acoustic pulse, and rupture disc response to a peripheral reactive DEG in a hard sodium system and to ascertain the potential for tube bundle damage from this particular test at prescribed conditions.

Series II SWR A-6 was performed on November 26, 1980. LLTR test conditions for this test were as follows:

1) DEG rupture of a single tube with the break site located 222.9 in. above the end of the LLTI shroud. The test was reactive with flow through the rupture tube prior to rupture. The LLTI/LLTV was in the evaporator startup power mode; the LLTV sodium system was to have been hard, with the system pressurized with nitrogen through the surge tank.
2) Injection medium: subcooled water ($580^{o}F$).
3) Injection water flow rate: upper, 41 gal/min; lower, 13.5 gal/min.
4) Rupture tube supply pressure: T-1, 1680 psig; T-2, 1695 psig.
5) Water/steam secondary system: 1615 psig.

6) Water/steam tubes and lines: 580 ± 10°F.

7) Sodium pressure (P-513): 127 psig.

8) Sodium temperature: 580 ± 10°F.

9) LLTV with a linear temperature gradient from 570 ± 10°F at the lower tubesheet to 590 ± 10°F at the upper tubesheet.

10) The RD-1 rupture disc assembly (double discs, 325 psid) was preheated with an isothermal temperature of 573 ± 20°F.

This test generally duplicated the conditions and sequence of previous DEG rupture sodium-water tests, with dynamic flow in the primary tube and the plant in reactor startup conditions. The preprogrammed test event sequence shown in Table I-1 was typical of all DEG test activities.

TABLE I-1

TUBE RUPTURE SEQUENCE EVENT SCHEDULE

Sequence	Function	Time (sec)	
		Total	Set
0-	On; terminate heater and fan power; start analog tape.	0	-
1	Close LLID vent, V-231B, and start cameras. (Rapidly complete opening of Valve V-201C.)	10	10
2	DNA	-	
3	Activate LLID, open V-231A; fire flash bulbs, start time.	15	15
4	Deactivate LLID; close V-231A.	-	999
5	RD-1 rupture: vent and close secondary tubes; close V-204A&B, open V-204F.	R*+4	4
6&7	Injection termination; close V-201A and V-203A&B (V-201B not open during test).	R*+30	30
8	DNA		999
9	Sodium drain and rupture tube vent; open V-130A and V-203F.	R*S+34	4
10	Purge H_2 systems; open V-201D&E, V-204D&E, V-203D&E.	R*S+44	10
11	Terminate test; shut down HSC and igniter.	R*S244	200

R* = time of RD-1 failure
R*S = timer activated by Sequence 7 or 8

When the tube was failed, the acoustic pressure pulse at RD-1 resulted in only ∿285 psi (Figure I-7a). Consequently, the disc did not fail until the total system was pressurized to hydraulic disc failure by the SWR injection. The upstream rupture disc failed 6.56 s into the test (Figure I-7b), followed 54 ms later by the failure of the downstream disc. Both discs failed at 325 psi. Prior to the test, the LLTV and sodium piping were hard filled (no gas). During the SWR event, the gas space in the surge tank (Figure I-2) was displaced by the SWR pressurization. The test resulted in a displacement of ∿19 ft^3 of sodium before RD-1 rupture disc failure.

The amplitude of the acoustic pulse in this test was not as high as had been anticipated from previous SWR tests in the central region. Test parameters were checked to be quite certain that all test conditions were met. However, post-test review of the process instrumentation data indicated that the rupture tube had a leak in one of the four welds. Just after the rupture tube was filled with water (the secondary tubes had been filled for days), the sodium level in the surge tank (L-505) and the sodium pressure (P-531) indicated an increase; the surge tank gas was vented to sustain the required sodium pressure for the test. It is believed that a major factor in reducing the acoustic pressure pulse was probably the gas space (∿8 ft^3) at the LLTI tubesheet where the pulse was attenuated, i.e., not reinforced. All the welds except one were destroyed before they could be examined; the remaining weld checked out.

The amplitude of the initial portion of the acoustic pulse, measured near the injection site, was on the order of 280 psig, which was not necessarily low for times of early pressurization, but since the test was in the upper portion of the LLTV and there was a gas interface at the tubesheet, the acoustic pulse was not reinforced. From the initial measured portion of the acoustic pulse, and if there had been reinforcement, i.e., solid sodium at the tubesheet, the rupture discs would have been failed during this time rather than by hydraulic pressurization at 6.56 s.

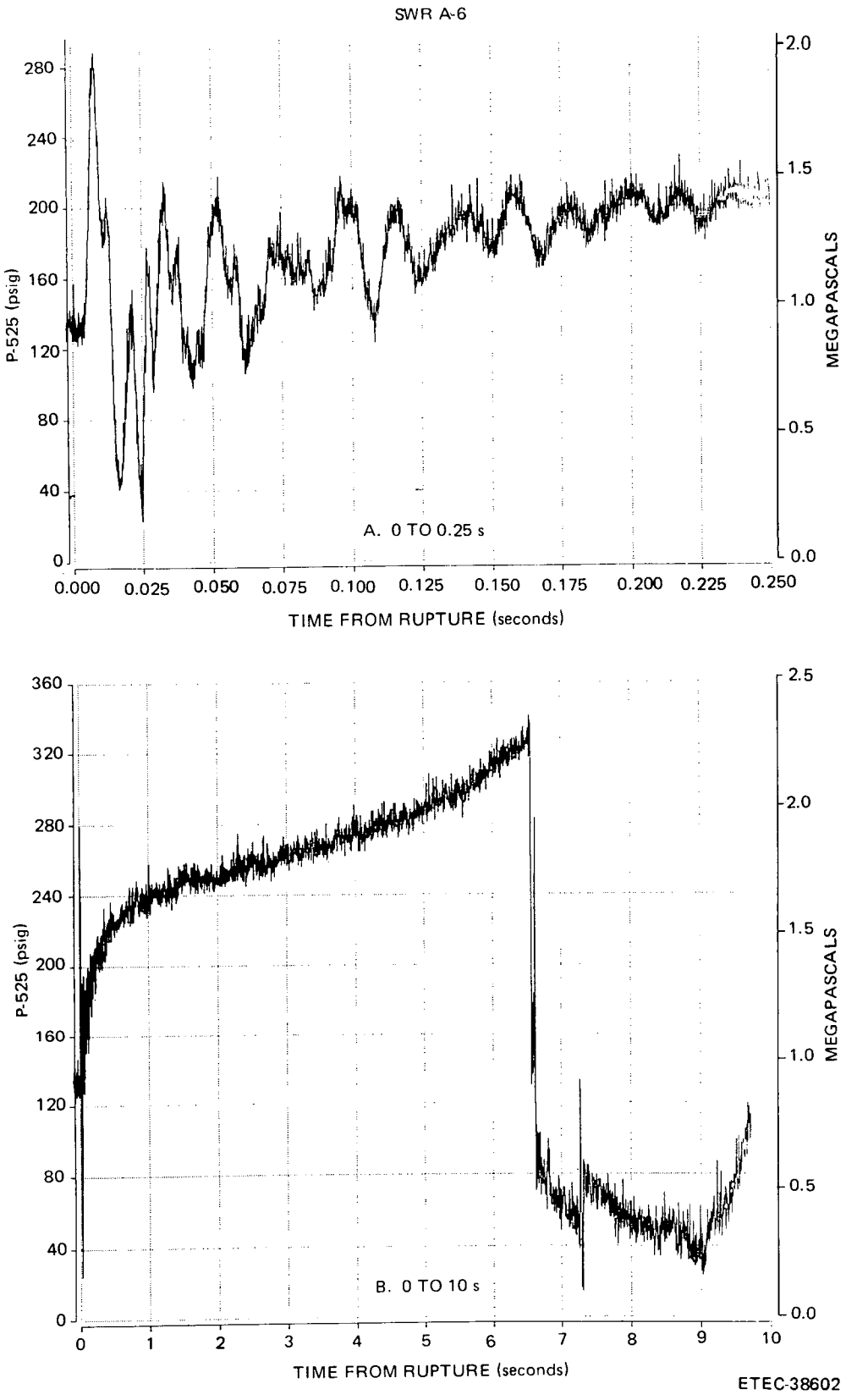

Figure I-7. Acoustic Pressure Pulse and System Pressurization Required to Fail the RD-1 Discs, Measured Near the Rupture

A temperature-vs-time plot of an LLTI transient thermocouple (TE-12-80) nearest the rupture site is shown in Figure I-8. The thermocouple is located at a 1.5-in. radial distance from and 26 in. below the rupture. The reaction temperature increased to ∿2100°F before the disc failed at 6.5 s. When the sodium had drained from the general area, the temperature dropped quickly to ∿900°F in less than 1 s and then cooled more slowly to 400°F in about 8 s.

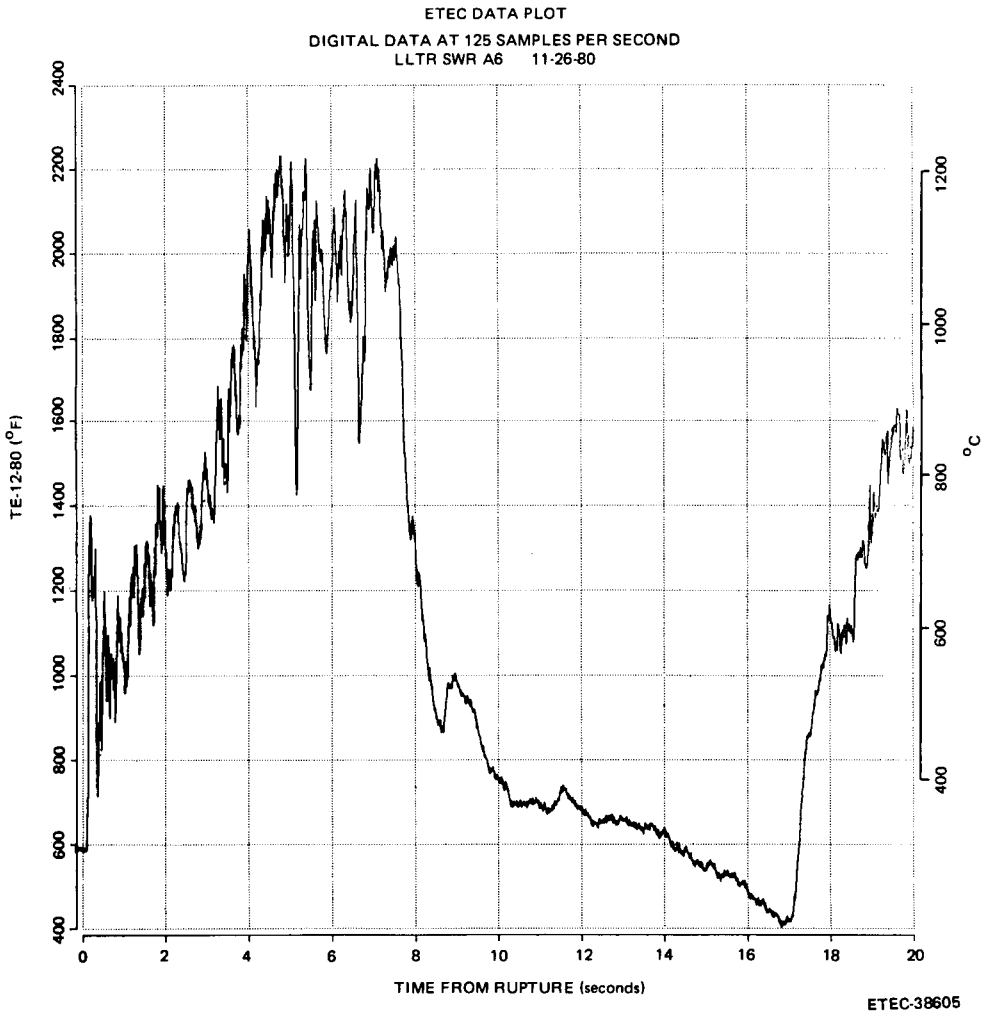

Figure I-8. SWR Bubble Temperature Nearest the Rupture 26 in. Below and 1.5 in. Radial

Water injection was programmed through rupture disc failure plus 30 s (Table I-1). During the injection, prior to disc failure, ∿35 lb of subcooled water at 1700 psi and 580°F was injected from the upper and lower ends of the DEG

failure. The total test resulted in the injection of ∿200 lb of water, the major portion after disc failure. The lengthened injection, in this case, did not result in appreciable pool reaction in the lower relief line area.

At the time of the test, wind velocity was 9 mph from the north. Twelve trays were positioned on the ETEC site at distances from 49 to 1370 m from the LLTR stack. There was significant (5.6×10^{-3} mg/cm^2/day NaOH) downwind ground deposition at 130 m.

The 90-ft hydrogen-ignited exhaust stack from the RPT has a 5-psid rupture disc to allow environmental control of the relief system prior to test. The exhaust stack and igniter served to ensure the controlled burning of the hydrogen evolved from the SWR event. Before test, the RPT and stack were purged with 5 lb•mass/min of nitrogen to prevent inside burning. During the test, still photographs and 16-mm movies were taken of the stack flame. These movie strips were compared to previous test movies to evaluate the SWR intensity. Figure I-9 shows photographs made during the test. The flame pulsated near the start and finish of the test, which was typical of all the tests.

Accelerometers were added to the LLTR system to measure the dynamic structural response of sodium piping during Series II DEG tests. This information is of no consequence during the intermediate leak tests but will be used to evaluate piping support structure and computational models. Initial instrumentation placed on the upper relief line consisted of nine high-temperature accelerometers (A502 through A510, Endevco Model N22845M3-120) to measure axial, lateral, and vertical accelerations of Lines 106 and 107 as shown in Figure I-10. The accelerometers (A511 and A512) added on structural supports for Test A-6 are indicated. In addition, vertical line accelerometers, A503, A506, and A509, were remounted on the top of the pipe. Vertical mounting should help eliminate the effect of pipe twist and thus allow the accelerometers to measure true vertical components.

Figure I-9. RPT Stack Fire Taken Sequentially During the Test

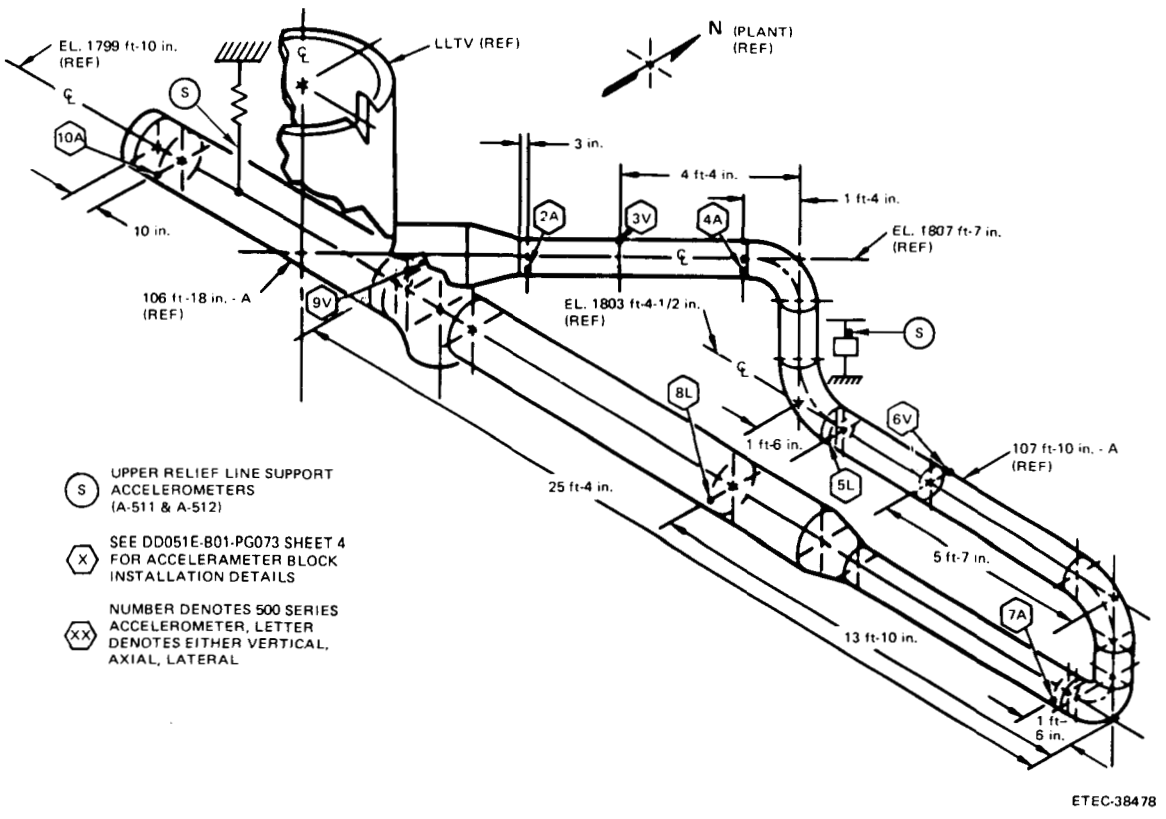

Figure I-10. Location of Load Accelerometers on Secondary Sodium System

2. SWR A-7

SWR A-7 was the fifth double-ended-guillotine rupture test in the LLTI with reactor startup conditions. For this test, the LLTV was hard filled with sodium, i.e., there was no gas space. The test was run in the same location and with the same conditions as the nonreactive test, A-1a, just above Spacer 4, and near the SWR A-2 site for direct pressure-wave comparison. It was designed to be a short-term test that represented a wastage propagation leak scenario in progress with creation of an effective DEG at an elevated sodium system pressure generated by the SWR. Prime measurements desired of the test were dynamic pressure-wave propagation, amplitude, secondary sodium line loading response, rupture disc response, and damage resulting from a short DEG injection at elevated pressure. A short injection duration (1.5 s) was required in order to limit the potential for damage to the LLTI. For this test, water in the primary tube was in the

dynamic (flowing) mode prior to tube failure; the secondary tubes were filled with low-pressure nitrogen. The RD-1 rupture disc assembly (Figure I-2) had two 325-psid diaphragms.

Series II SWR A-7 was performed on April 13, 1981, at 20:16:30:970. LLTR test conditions for this test were as follows:

1) DEG rupture of a single tube with the break site located in the central tube and 127.75 in. above the end of the LLTI shroud. The test was reactive, with flow through the rupture tube prior to rupture. The LLTI/LLTV was in the evaporator startup power mode; the LLTV sodium system was hard, with the system pressurized with nitrogen through the surge tank.
2) Injection medium: subcooled water ($580^{o}F$).
3) Injection water flow rate: upper, 40 gal/min (estimated); lower, 14 gal/min.
4) Lower inlet water orifice: 0.141 in.
5) Rupture tube supply pressure: T-1, 1800 psig; T-2, 1750 psig.
6) Water/steam tubes and lines: $580 \pm 10^{o}F$.
7) Sodium pressure (P-523A): 255 psig.
8) Sodium temperature at injection: $580 \pm 10^{o}F$.
9) Sodium level in surge tank: 24 ft^3.
10) LLTV with a linear temperature gradient from $570 \pm 10^{o}F$ at the lower tubesheet to $590 \pm 10^{o}F$ at the upper tubesheet.
11) The RD-1 rupture disc assembly was preheated isothermally to $573 \pm 20^{o}F$.

The water injection for SWR A-7 is characterized by Figure I-11. The sequencer activated test termination (Table I-1 changed to reflect 1.5-s activation of R*) at 1.5 s; valve closure was between 2 and 3 s, indicated by a rapid dropoff of flow and pressure. Even though F-503 (upper injection flow) failed, the flow was choked and, therefore, proportional to previous tests at 40 gal/min. Termination of upper injection flow is indicated by the system pressure drop measured by P-554 (Figure I-11). During the test, 3.2 lb and 11.6 lb of water were injected from the lower and upper ends, respectively, of the rupture tube.

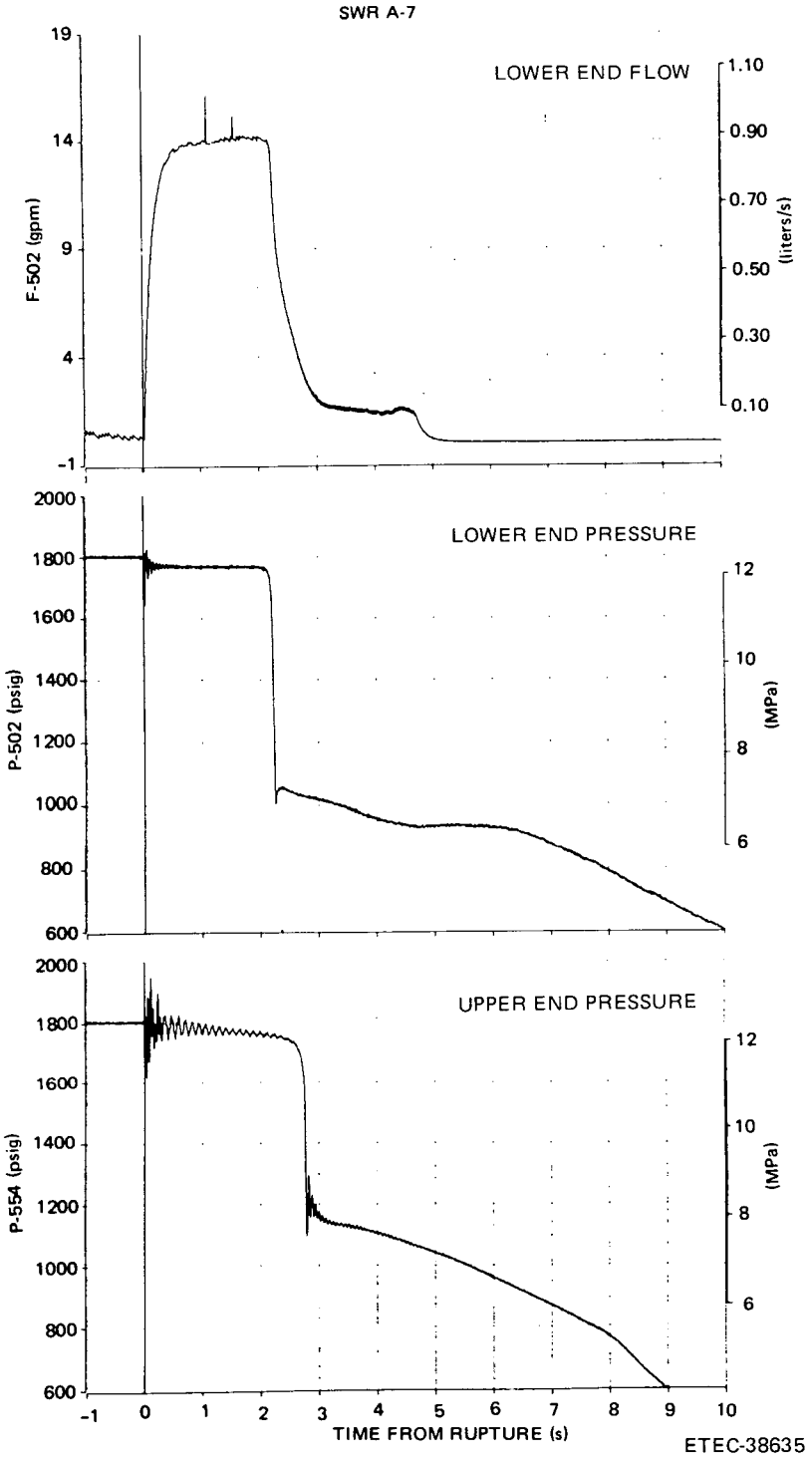

Figure I-11. Plots of the Water Injection Characteristics

Typical pressure activity during the elevated sodium side pressure DEG test at subcooled conditions is shown in Figure I-12. The pressure measurements were made on the LLTV shell near the rupture site, upstream from the RD-1 rupture disc, and in the cavity of RD-1 between the two discs. The pressure nearest the rupture site (Figure I-12, P-617) shows an acoustic pulse of 300 psi being reinforced to 385 psi at 10 ms. A pressure transducer ∿1 m upstream of RD-1 (P-525 failed) indicated that the front disc buckled at about 5 ms and 325 psig, which was the design rating. PRD-1C indicated that the cavity pressure was 280 psi at the time of disc failure. The second disc pressurization and the failure were hardly reflected at the leak site. This was the first measurement of cavity pressure, and since P-525 failed, it was hard to directly compare the dynamics in this repair with previous tests; but PRD-1C did indicate that the instantaneous pressure in the cavity prior to the second disc failure may have been higher than previously thought.

Figure I-13 shows three typical temperatures measured during the test at locations below the injection site at 127.75 in. Thermocouples 12-6, 12-5, and 12-4 were for measurement of reaction bubble propagation mounted radially 5 cm away in Tube 3002 at 121, 113, and 109 in., respectively. The maximum temperature indicated during the test was below the injection site and was ∿2000°F (1110°C) at about 7 to 8 s, even though injection was terminated at about 2 s by valve closure and the sodium should have been drained from the area ∿5 s into the test. The reaction at 109 in., TE12-4, was out of the primary reaction region, and there was no appreciable temperature increase until the sodium started to move from the area; however, it attained ∿1300°F (720°C) and held it for more than 20 s, when the reaction nearer the injection quenched. Other temperature measurements in this region (at 5 cm radial) indicated a somewhat heterogeneous pattern, as expected, but in general showed ∿800°F (440°C) during the first 6 s and between 1250 and 1450°F (700 and 800°C), continuing to more than 20 s while not quenching. Indication was that a slightly larger portion of the upper injection could have been off to the direction of the tube that contained the Series 12 thermocouples.

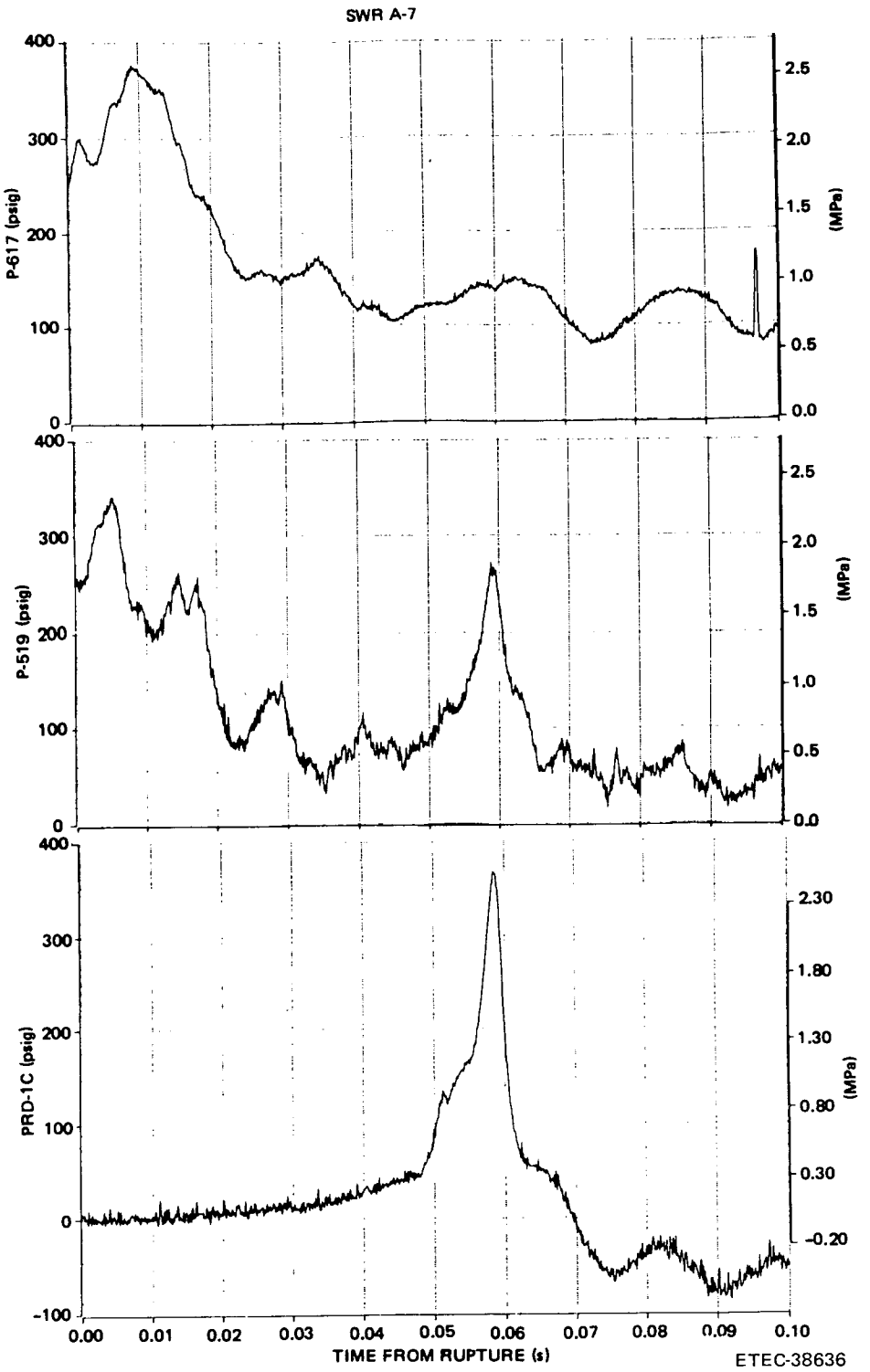

Figure I-12. SWR A-7 Pressure Measurements

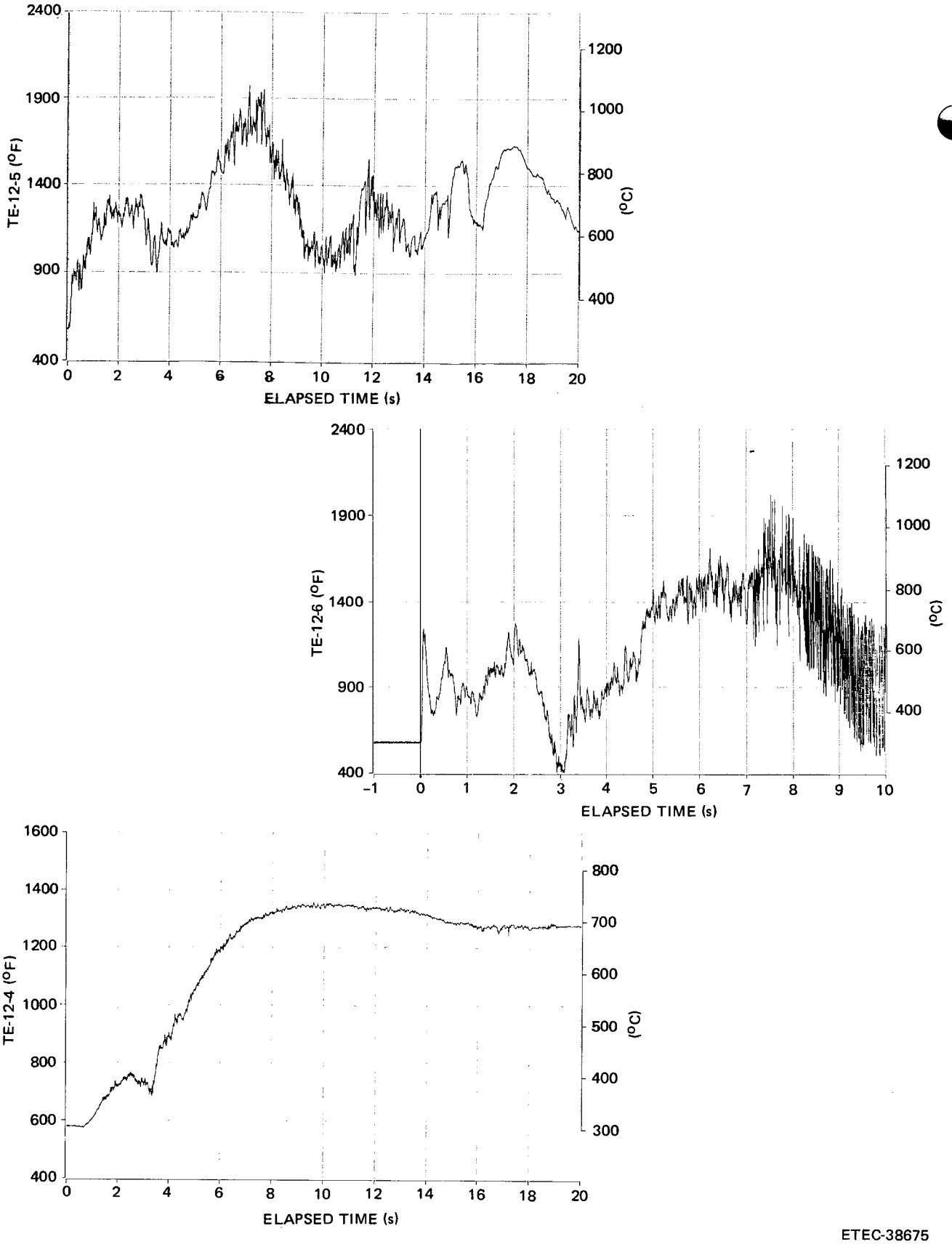

Figure I-13. Temperatures Measured During SWR A-7, Axially Located at 121, 113, and 109 in. in Tube 3002

At the time of the test, the wind was from the NNE at 0 to 1 mph. During this test, trays were put out to sample stack fallout in the same positions as in the previous test. No significant downwind ground deposition was received in any of the trays, with an average deposition of 8.5×10^{-6} mg/cm^2 per day. Average airborne concentration as sodium hydroxide was 17×10^{-3} mg/m^3.

The exhaust flame from the RPT stack was much less intense than in other tests due to the short test.

Since the RD-1 reverse-buckling double rupture disc assembly was installed in the LLTR to obtain information on disc failure characteristics, a number of different approaches were taken to measure the time at which the discs buckled and were subsequently cut by the knife blades. One of these approaches was to measure disc movement with a linear voltage differential transformer (LVDT), which proved not to work due to the disc dynamics. In another approach, spark plugs used for plant information seem to be very reliable and to give reasonable information on failure of the disc; however, they gave no information on disc buckling. To get further information on disc activity, accelerometers were added on the upstream flange of each rupture disc. These data proved unsatisfactory for this measurement. Consequently, spark plugs are being recommended for use in CRBR only in conjunction with other measurement for disc activity.

3. SWR A-8

SWR A-8 was the second intermediate leak test performed during Series II testing. The intermediate leak test was run at superheater conditions and directed at a second-row tube. The test was designed to determine damage to a steam generator from an intermediate leak during the time required for an automatic leak detection system to function. For this test, the steam injection from the primary tube was initiated from the static mode (not flowing); the secondary water system was filled with superheated steam at the same conditions as the primary for prototypic injection in case of tube failure. The RD-1 rupture disc assembly was installed with only one 325-psid diaphragm. Upon test termination at 40 s, the sodium system was pressurized with nitrogen to fail the rupture disc.

The test was located in the upper central portion of the LLTI in Tube 4001, midway between Spacers 7 and 8 at 197 in. from the lower portion of the LLTI shroud. The injection orifice was a drilled hole 0.054 in. in diameter directed at Tube 1029 (Figure I-14) in the second row. The distance from the injection orifice to the target tube was 1.6 in. These dimensions resulted in an L/D_O ratio (the ratio of the distance of the orifice from the target to the orifice diameter) of 30, which would predict a maximum wastage rate of the target tube at these conditions. This type of injection assembly is shown in Figure I-6. The LLTI/LLTV was run in the 100% superheater mode; the sodium system was run at an elevated pressure and "soft" (the upper portion of the LLTV, the upper secondary sodium header, and the surge tank pressurized with gas) to extend the running time of the test; the injection medium was superheated steam at $900^{O}F$.

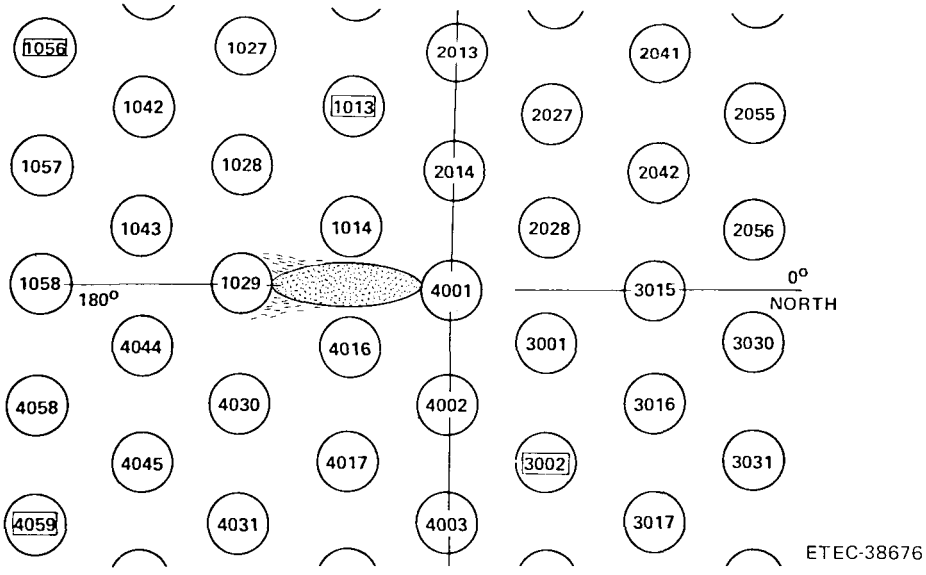

Figure I-14. LLTI Tube Array, SWR A-8

Prime measurements desired from the test were failure propagation, acoustic emission from the leak process, SWR bubble temperature, rupture disc response, and damage resulting from this type of test, i.e., tube wastage and deformation. The acoustic emissions resulting from the leak were recorded by AI, ANL, and GE. These data were not analyzed by ETEC. The sensors were mounted on the LLTV wall at the plane of the leak and on the LLTI tubesheet.

Series II SWR A-8 was performed in the LLTR on July 30, 1981, at 17:42:07:537. LLTR test conditions for the test were as follows:

1) DEG rupture of a single tube, exposing an injection orifice of 0.054-in. diameter. The test was with superheated steam, with no flow through the rupture tube prior to rupture.
2) Injection medium: superheated steam (900°F at 1550 psig).
3) Injection flow rate: 0.07 lb/s, measured.
4) Test elevation: 197 in., between Spacers 7 and 8.
5) Secondary water system: 1550 psig steam from T-1 and T-3 valved together on the top.
6) Sodium pressure (P-523A): 180 psig.
7) Sodium temperature at injection: 900 ± 10°F.
8) Sodium system: soft, about 140 ft^3 gas space.
9) Sodium fill: to inlet header only.
10) LLTV temperature: Zones 1 and 2 — 825 to 900°F
    Zones 3 through 5 — 900 ± 10°F
    Zone 6 (steam head and tubesheet) — 750°F
11) RD-1 rupture disc assembly: 790 to 675°F, single disc.
12) The test was designed to run for a predetermined time (40 s) before termination and not activated by RD-1 failure (R* set to 0 and Sequences 5, 6, and 7 activated to inject for 40 s — Table I-1).

The steam injection of SWR A-8 is characterized by Figure I-15; the injection measured 0.073 lb/s. The sequencer activated injection termination at 40 s after the LLID was activated (Table I-1). A total of about 2.7 lb of steam was injected during the 40-s portion of the test, not including blowdown. The increase in flow at 40 s was due to the injection tube vent valve's opening prior to closure of the system supply valves, which were timed on the same sequence. The injection pressure and system blowdown are shown in Figure I-16. The flow and pressure data indicate that the injection orifice did not vary, i.e., there was no self-wastage or bellows failure during the test, and that the system was blown down in 10 s.

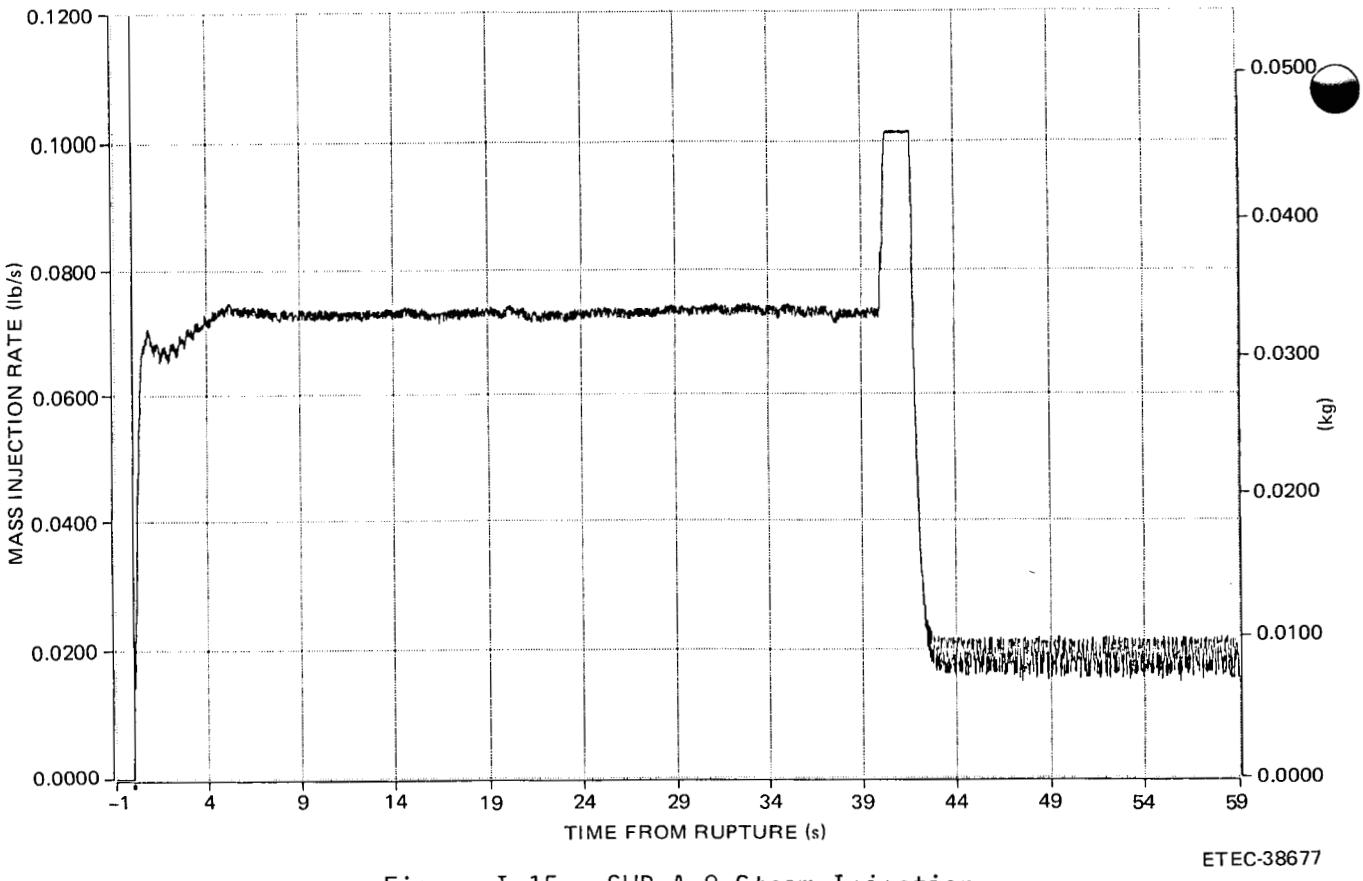

Figure I-15. SWR A-8 Steam Injection

The temperature spectrum of Thermocouple 12-8, which was located in Tube 3002 at 197 in., is shown in Figure I-17. The thermocouple, while at the same level as the test, was 3.3 in. from the target tube and 2.1 in. from the injection orifice (Figure I-14). The heat of reaction of the event measured at this location indicated an increase of only about 70^{o}F. This was the only thermocouple near the injection site. Temperatures and pressures measured during the test indicated that there was probably no secondary tube failure.

During the test, the event recorder indicated that all valves functioned properly, including the sodium drain valve, V-130. However, there was a malfunction in the nitrogen pressurization system, which failed to adequately pressurize the sodium cover gas to fail the RD-1 rupture disc within 2 min; actual time of failure was about 5 min. This prolonged time for disc failure was probably the reason for deposition of SWRP in the region of the injection such that no borescope examination of this area could be done until after cleaning. It has been

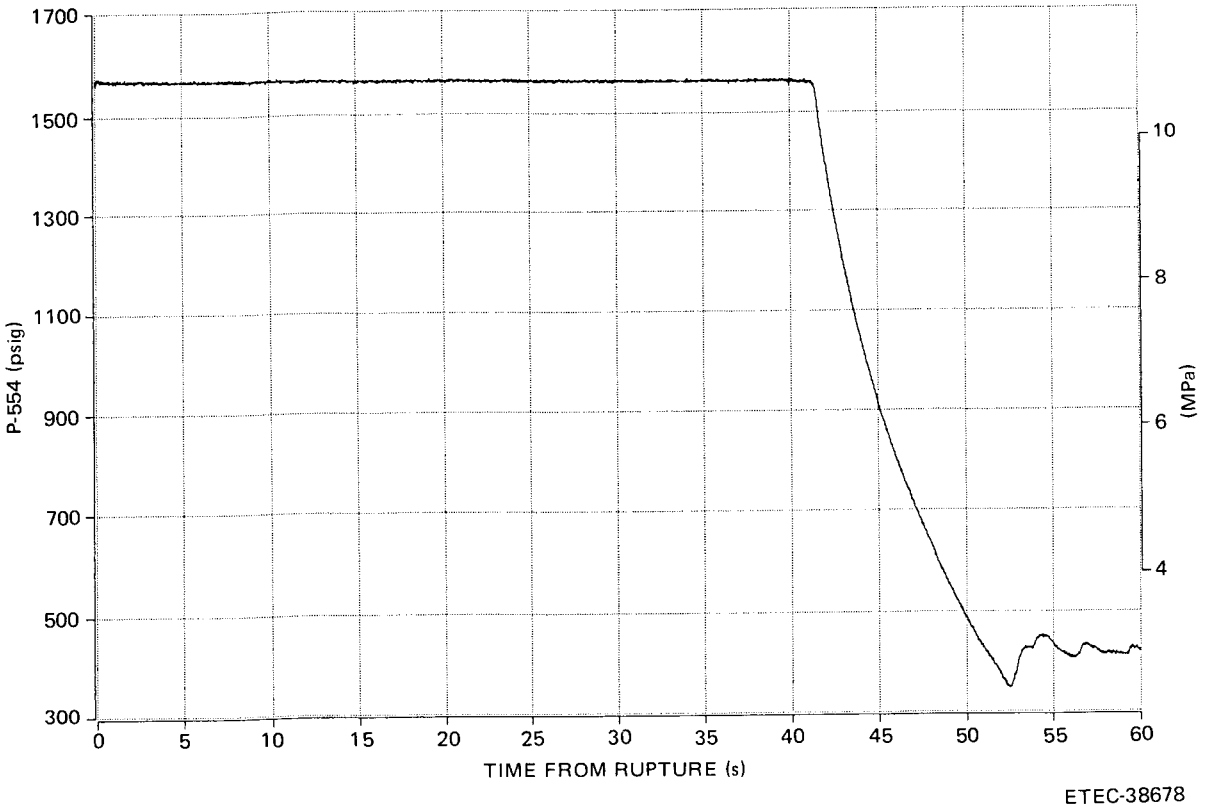

Figure I-16. SWR A-8 Injection Pressure and Rupture Tube Blowdown

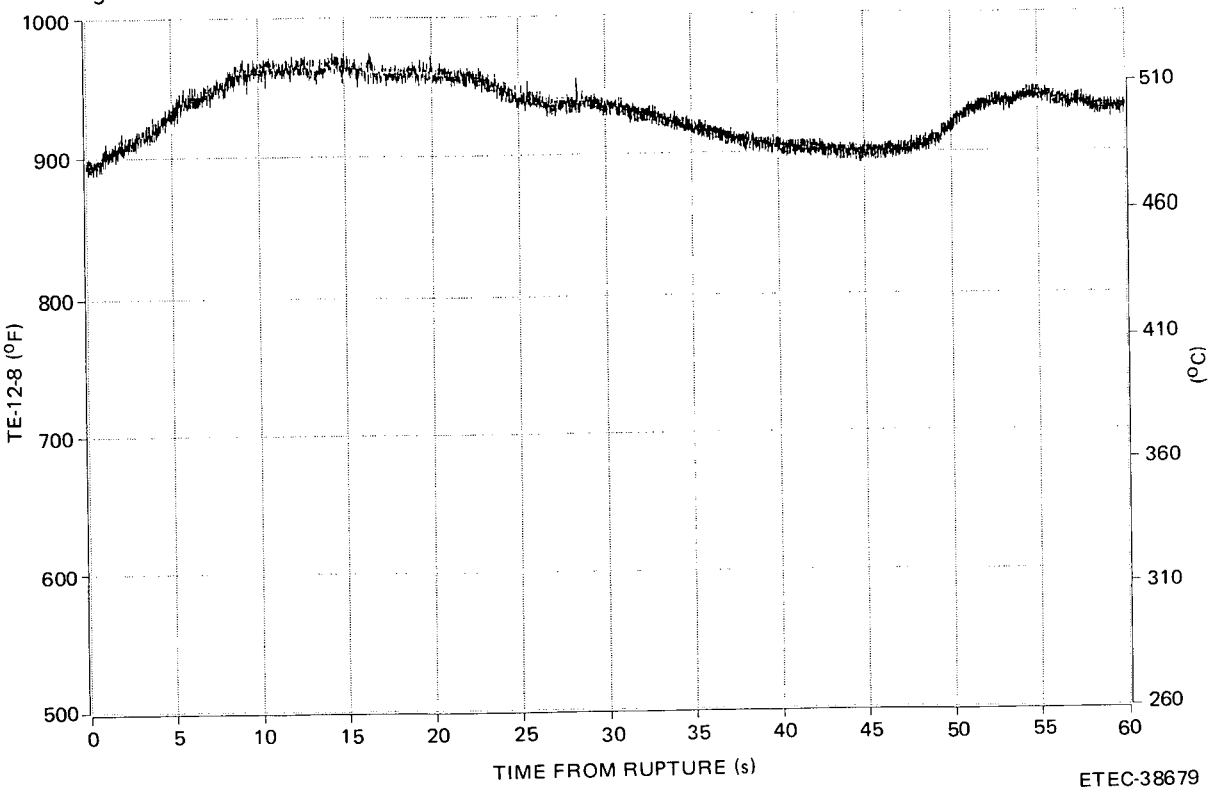

Figure I-17. Temperature Measured Near the Injection Site in SWR A-8

shown in the past that if the sodium-containing reaction products are not drained in a short time, the SWRP will tend to agglomerate. However, as will be discussed later in this report, not only was there a deposition at the test site, but during test preparation to superheater temperatures, the lower portion of the LLTV, explicitly the L-130 drain line, had become plugged with precipitated SWRP that did not drain the heel at all when the valve was opened.

After the system had cooled appreciably, the LLID and the upper end of the rupture tube were removed. To remove the upper end of the rupture tube, the bellows in the injection assembly must be severed.

When the lower portion of the rupture tube was to be removed, it was found to be stuck in its position. This was at the time the isotope scanning test was being run to ascertain sodium/SWRP deposition in the lower portion of the LLTI/LLTV. IST deposition tests indicated deposition almost to the lower nozzle. This was partially confirmed by visual observation of the LLTI through Line 124 at RD-1. Therefore, the lower portion of the rupture tube was not removed until after cleaning.

In the previous test, it was noted that there was appreciable SWRP in the lower portion of the LLTV and that before a peripheral test could be run, the system would have to be cleaned. However, as mentioned previously, the lower portion of the rupture tube could not be removed. IST deposition tests revealed that the sodium heel had only drained ∿2 to 4 in., leaving a sodium level just below the lower outlet header. It was calculated that ∿1500 lb of sodium remained in the vessel.

This undrained sodium heel represented a major problem for conventionally cleaning the LLTV with alcohol. Further investigation of the problem revealed that the tee nozzle (N-20) and Line 130 were completely filled with reaction products, which was the reason for the system's not draining even though the drain valve (V-130) opened as scheduled during the test. It was found that there was no flow communication through the LLTV, the drain line, and some nozzles;

therefore, cleaning would have to be done by flowing the solvent in and out of various ports. This approach would have been an extremely slow process that would have required a large volume of alcohol and a great deal of plant operator time.

In solving this problem, it was found that the material above the peripheral injection nozzle (N-11) was predominantly sodium. Therefore, a line was connected to this port and routed to Line 131, the drain line to the reaction products tank, bypassing Line 130. The lower portion of the LLTV, the added line, and Line 131 were programmed to be heated to as much as 400°F. During heatup, there was indication of sodium drain by a temperature change in the drain line and evidence that gas flow communication was made through the LLTV but not through L-130. After this heatup and drain process was completed, the system was cooled and the drain piping removed. This allowed the system to be cleaned with alcohol to remove the lower portion of the rupture tube and clear a passage for the A-5 rupture tube. After cleaning, L-130 was cut between the LLTV tee and V-130 removed for mechanical cleaning before reinstallation.

The LLTR was cleaned only with Dowanol. The alcohol cleaning system was essentially the same as was used previously and is shown schematically in Figure I-18. It was not rinsed with ethanol due to a fire that destroyed the pump. Sodium dissolution as a function of time is given in Figure I-19. Initially, the Dowanol-PM contained 10.9 gm/l of sodium and 6.7 vol % of water. As in previous LLTR solvent cleanings, the major dissolution was in the first hour. The total sodium removed was ∿400 lb.

D. INTERTEST ACTIVITIES AND RESULTS

1. General

As mentioned previously, intertest inspection information is vital to attaining the total program objectives. These inspection tests reveal the effects of the SWR test on the test article and associated piping as well as the double rupture disc assembly, which is a test article in itself. The intertest examinations, plus others if required, are:

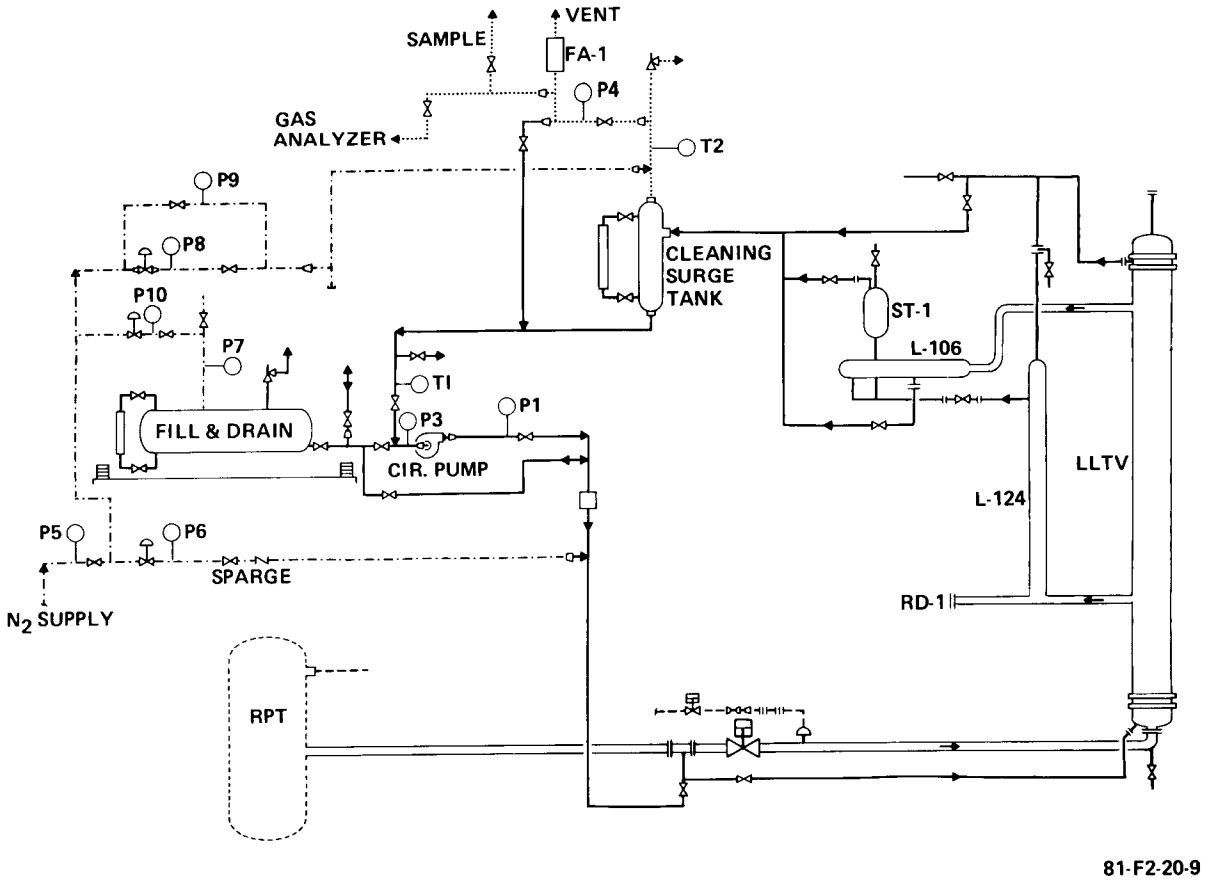

Figure I-18. LLTR Cleaning System

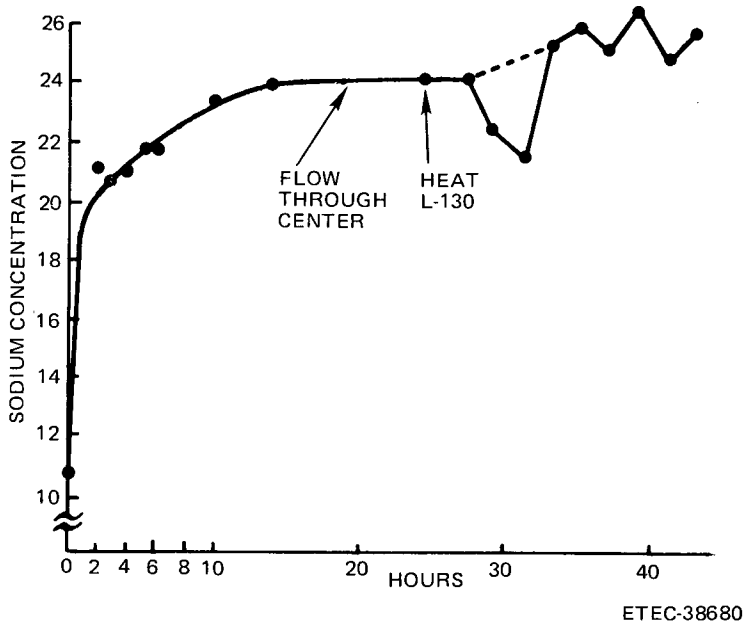

Figure I-19. SWR A-8 Solvent Cleaning Showing Sodium Dissolution in Dowanol-PM

1) Tube leak testing, including helium, pressure decay, and hydrostatic testing
2) Visual inspection of relief lines
3) Examination of the RD-1 assembly for failure characteristics
4) Dye-penetrant and UT examination of selected relief line piping weld heat-affected zones (WHAZ) for stress corrosion cracking (SCC)
5) Radiography of the LLTV drain system for SWRP residue
6) IST of LLTI steam tubes for deformation and SWRP deposition in the LLTV
7) UT examination of LLTI steam tubes to measure SWR wastage.

In most cases, the intertest examinations were performed with conventional equipment and technique. However, in at least two cases, UT inspection for wall wastage and deformation/SWRP deposition, there was no equipment available to make the required measurements. In these cases, ETEC conceived tests and built equipment to permit the required measurements.

Series I SWR testing in the LLTR resulted in steam tube deformation and SWRP deposition. These phenomena require developing special nondestructive equipment (NDE) and techniques to achieve the test objectives of Series II. The LLTR tests have resulted in basic failure phenomena, as a consequence of SWR testing, that will be typical of LMFBR steam generator tube failure. Therefore, NDE developed for experimental SWR testing could be adapted for use in future plants. The equipment and tests designed to measure tube deformation, SWRP deposition, and tube wall thickness were the IST (References I-2 and -3) and UT (References I-2, -3, and -4) devices.

2. IST and UT Devices

IST — To study tube deformation and reaction production deposition as a function of SWR testing, an isotope scanning test was conceived and developed by ETEC to measure in situ these parameters resulting from the Series II tests. The

device, shown in Figure I-20, is computer assessed. IST measures gamma-ray dispersion for tube deformation and attenuation for SWRP deposition. In both cases, an isotope gamma source and a Geiger-Muller (GM) tube are simultaneously passed through steam tubes, and count rate vs axial distance is measured to determine the desired parameter.

During impingement leak testing (large or small), the tube bundle in the area of the SWR must be prototypical for the testing to be valid. In the past, inspection has been a very cumbersome process and has been inconclusive in the tube bundle of the modular steam generator. Prototypical steam generator models used in SWR testing may have as many as 800 steam tubes and shell thicknesses of $\sim$10 cm. With these larger test articles, it would be impractical to use conventional radiography. Even if a tube bundle could be removed for inspection and refurbishment (in the case of a central tube test site), it could not be inspected, radiographically or otherwise, to ensure a prototypical test site.

Cobalt-60 was used to study deformation because of its long half-life (5.4 years) and high-energy gammas (1.17 and 1.34 MeV). In Figure I-21, a theoretical curve of gamma intensity transmitted vs tube deformation is plotted for Co-60. Clearly, this is a very sensitive measurement, in that a 1-cm bend outward (+) from normal reduces gamma intensity by 45%, while an inward (-) 1-cm bend increases gamma intensity by 100%.

In the present tests, it is advantageous to replace the ruptured tube with a straight tube. Near-neighbor tubes (line-of-sight) are measured with respect to this tube. Actual deformation is ascertained by taking the algebraic sum of sequential sets of scans. Of course, in the case of a plant-type accident or ISI, when an IST measurement is required, the number of detectors would be increased to the number of nearest-neighbor tubes. The scanning would be started in an area where there was no deformation and continued into the damaged area.

For this series of tests, the rupture tube is replaced with a known straight tube and all line-of-sight tube measurements are with respect to this tube. When deformation measurements are required for tubes past the second row, tube-to-tube

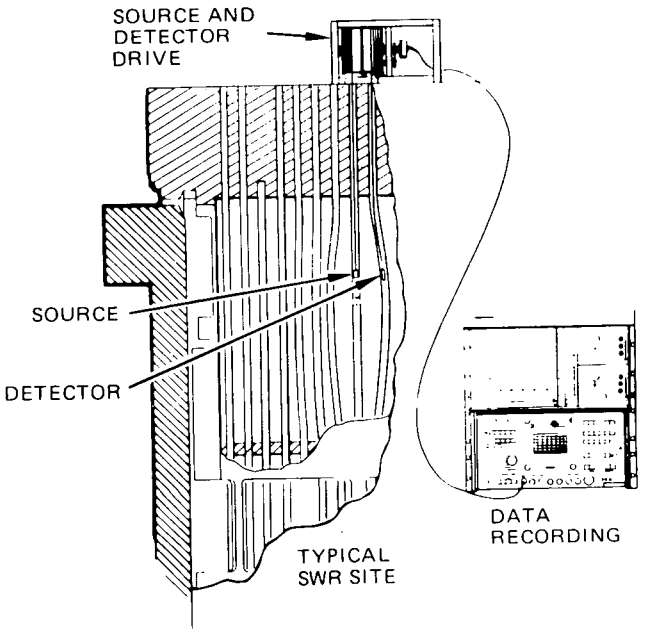

Figure I-20. Isotope Scanning Test (IST)

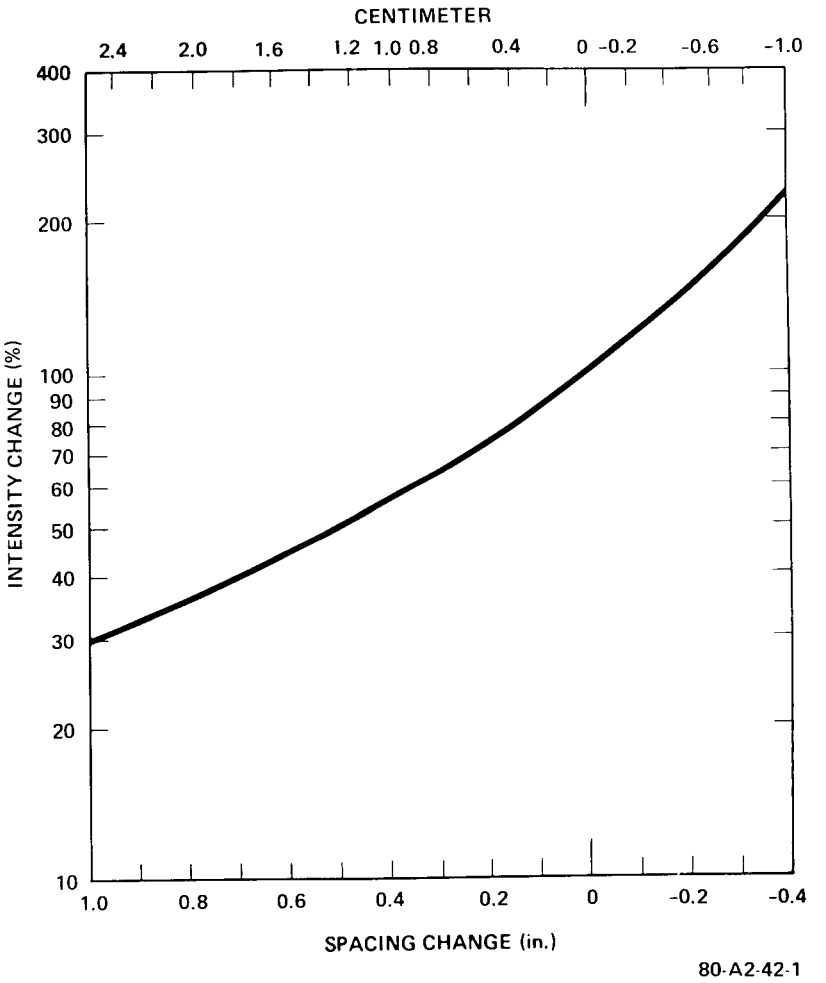

Figure I-21. Theoretical Gamma Intensity as a Function of Deformation for Co-60

measurements are made and then the algebraic sum is taken to ascertain the deformation of the array. Deformation in the first two rows results in a finite probability that the intervening tube has been deformed in such a way that it does not homogeneously shield the scanned tube. This could result in an error of up to 22%. Since a distance calibration is, in effect, made each time the unit traverses a spacer plate, the ISI may be moved toward the outside of the tube bundle, where there is no deformation, and then worked back into the deformed area for actual measurement.

For the tests described above, a 10-mCi Co-57 source was used, but others could have been substituted. The edge of the spacer plate is better defined with Co-57 than Co-60 due to the lower energy of Co-57. Co-57 yields good spacer deformation and location measurement, since there is but a small amount of spacer material to attenuate a beam. Measurements for SWRP deposition are relevant in the area on top of the spacer. However, if deformation is present, it must be integrated into the results for proper SWRP measurements. A calculated plot for Co-57 gamma attenuation in SWRP (μ = 0.25 cm^{-1} and ρ = 1.8 g/cm^3) is shown in Figure I-22.

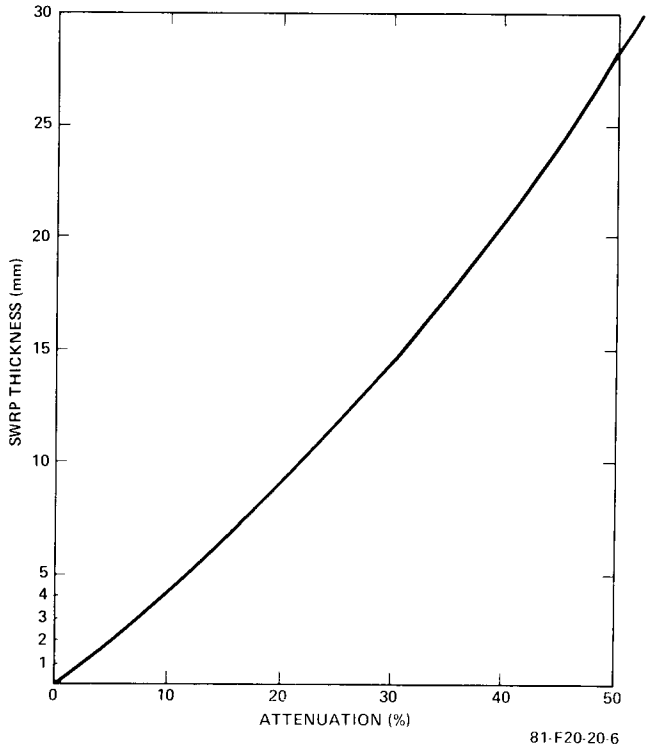

Figure I-22. Calculated Attenuation for Co-57 Gammas in SWRP

Ultrasonic Examination of LLTI Steam Tubes — The objective of the UT intertest examinations was to survey steam tubes in the area of a rupture site for wastage due to the SWR event. The pool reaction area at the lower relief line was also tested for wastage. The standing pool reaction, located on top of the sodium heel at the lower rupture relief nozzle, is due to continued water injection after most of the sodium has been expelled from the LLTV through the rupture relief system by the SWR event. Mapping tube wastage as a function of axial and azimuthal locations will yield information leading to an understanding of the dynamic SWR front propagation and intensity.

The UT instrument (Figure I-23) presently used for this inspection (Reference I-4) was designed to examine a single slice of steam tube wall with a 15-MHz PZT transducer operated in the pulse-echo compression-wave mode at a sampling rate of 10,000/s. System outputs are inside diameter, wall thickness, attitude, and axial position. All are displayed digitally and may be recorded. Sensitivity of the instrument is 0.002 in. (0.051 mm). A boreside rotating ultrasonic tester has been developed (References I-2 and -3). The device head is shown in Figure I-24. It would examine, with a helical scan, almost an entire tube in a single pass. It would equal or better the sensitivity of the present device and have capabilities of computer data storage as well as on-line digital and CRT display of a number of revolutions. Development efforts on this device have been suspended at this time.

During the present LLTR tests, wall thickness data were plotted by an on-line X-Y recorder; no data were stored by computer. Scans were typically in the direction of the rupture tube, $\pm 45^{o}$ and 180^{o} from the rupture tube. Where wastage greater than 0.006 in. was encountered, scans were made every 22.5^{o} to encompass it.

Before UT tests were started, the tubes were lightly brushed and a go/no-go gage was traversed through the tubes to ascertain passage of the UT head. The go/no-go gage measures 0.34 in. in diameter by 2.62 in. in length.

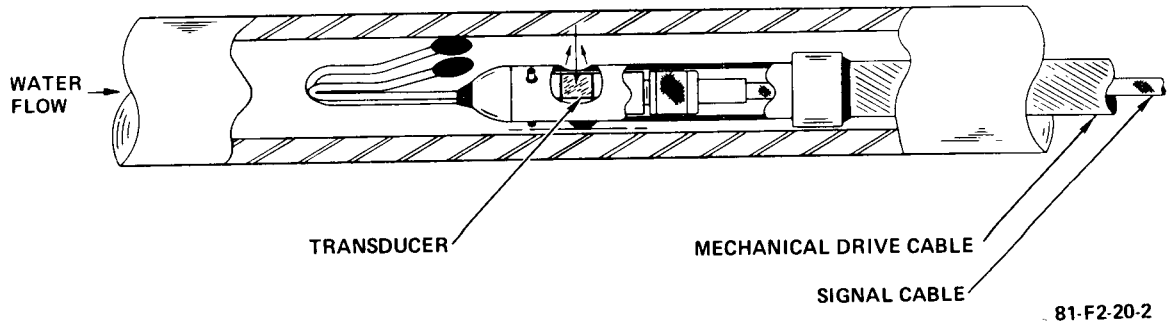

Figure I-23. Fixed UT Wall Thickness and ID Measurement Probe

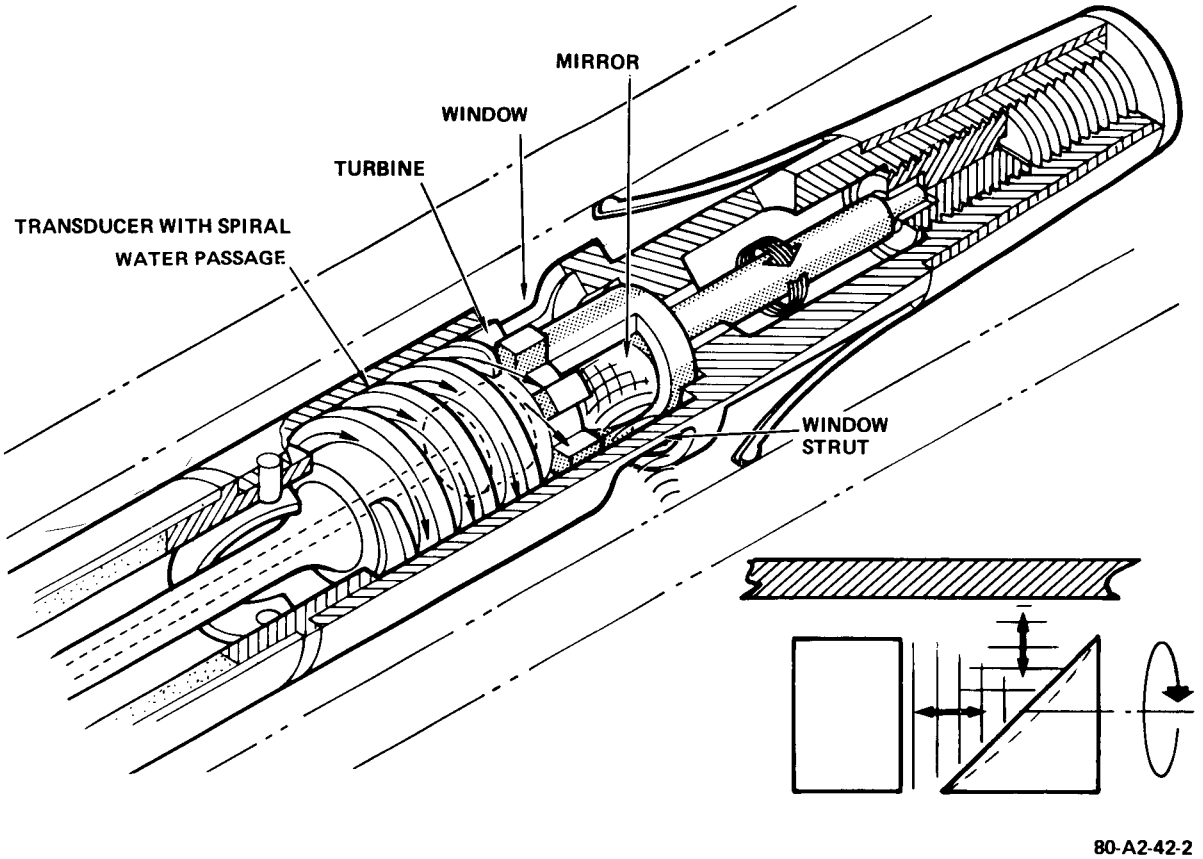

Figure I-24. Boreside Rotating Ultrasonic Tester for Helical Measurement of Steam Tube Characteristics

3. Intertest Results

Peripheral Test A-6 — In general, the measured intertest effects of this DEG failure were minor, with the only appreciable measurement being with IST. The results of the intertest are summarized as follows:

1) Secondary tube leaks — None.
2) Relief line inspection — SWRP deposition light due to short injection and rapid disc failure.
3) RD-1 assembly — Failed at 325 psid and opened 60 and 80% on hydraulic pressurization; the disc knife blades were dulled appreciably and replaced for the next test.
4) Dye-penetrant and UT examination of relief line WHAZs — Indicated only minor UT changes.
5) LLTI tube UT — Minimal wastage at the level of injection, 0.004 in. maximum.
6) IST — Minor deformed array, seven tubes bowed and two kinked (sharp bend at spacer); the A-3 deformed region was also outlined (Figure I-25). Results from the IST examination in a particular direction from the wall through the deformed region are presented in Figure I-26.

During the intertest, ISTs were run in the central region to outline the area of deformation created by the SWR A-3 intermediate leak test (Figure I-25). To outline this region, the approach was to begin with IST measurements in the nondeformed region and to continue making measurements inward toward the test site. Tubes measured were the nearest-neighbor tubes, 0.6 in. apart. The criterion for deformation was that bowing from tube to tube be $\geq$0.3 in. Tubes measured for deformation that were on the outside of the marked array and do not meet the deformation criterion are not shown. The test results indicate that 37% of the tube bundle, including the "kinked" tubes, were deformed due to the A-3 test. The deformed array of Test A-6 was somewhat different but no larger than the deformed array of tubes of SWR A-2.

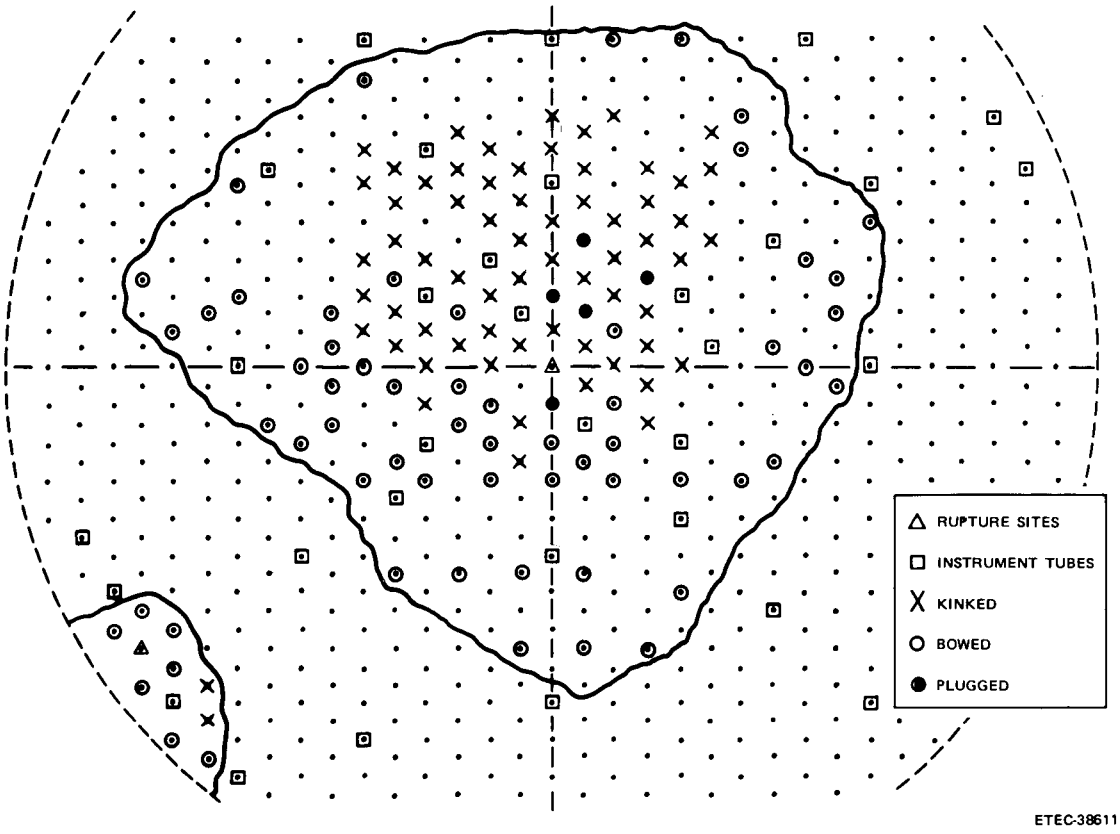

Figure I-25. The Deformed Areas of SWRs A-3 and A-6

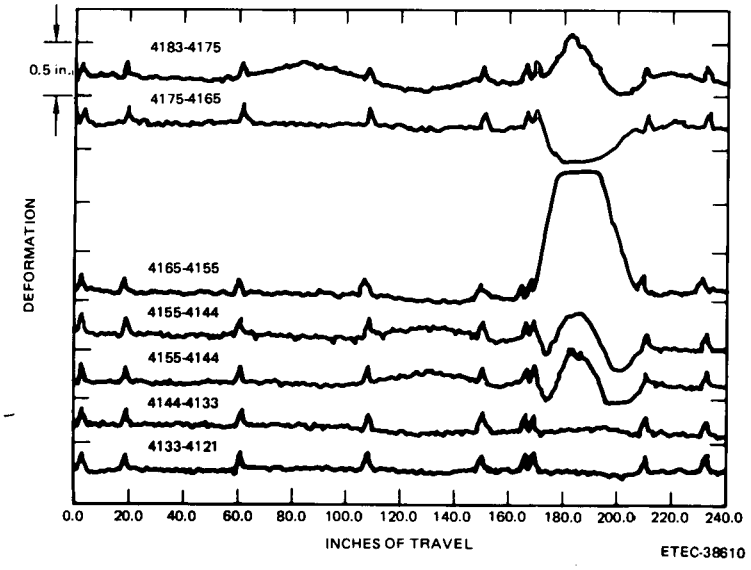

Figure I-26. IST Measurements in a Line Through the Rupture Site into the Unaffected Region

Central DEG SWR A-7 — SWR A-7 was required only to measure the pressure resulting from a DEG at high sodium pressure, from a location where previous tests had been run, for comparison to previous test results at lower pressures. Therefore, in order that there be no effect on the predamaged region, the test was run for only 1.5 s to minimize damage.

All of the intertest examinations were run with no significant damage reported in any of the tests. Prior to the test, the RD-1 knife blades had been resharpened. During the test, the upstream and downstream discs opened 60 and 90%, respectively, and at the required pressure.

Central Intermediate Superheated SWR A-8 — Injection for this test was superheated steam for only 40 s. Therefore, as expected, there was only minor damage to any portion of the system except the predicted tube leakage or wastage. The rupture disc (single) was failed by hydraulic pressurization to 320 psid; it opened ~80%.

Tubes in the region of the directed SWR event were tested for leakage by helium leak tests and hydrostatic testing; then pH measurements were made of the UT water to ascertain sodium in-leakage. All of these results were negative, indicating no secondary tube failure.

Ultrasonic examination of the tube array in the direction of the flame indicated a maximum wastage of 28 mils. Maximum wastage was about 45^{o} from the predicted target point (0^{o}) on Tube 1029. Tube 4016, Figure I-14, also showed more wastage than did 1014, indicating that the injection could have been slightly in that direction. Tube 4044 showed shallow wastage; other tubes showed only minor wastage.

REFERENCES

I-1 H. H. Neely and M. J. Tessier, "Sodium-Water Reaction Testing in Support of LMFBR Steam Generator Development," 1981 ASME Joint Power Conference, St. Louis, Missouri, 81-JPGC-NE-3

I-2 H. H. Neely, "Sodium-Water Reaction Testing — NDE Requirements and Approach for ISI of the LMFBR Steam Generator," 1981 4th International Conference on Nondestructive Evaluation in the Nuclear Industry, Lindau, Germany

I-3 H. H. Neely, "Sodium-Water Reaction Test Results and LMFBR Steam Generator Inspection," 1981 ASME Winter Annual Meeting, Washington, D.C., 81-WA/NE-8

I-4 H. H. Neely and H. L. Renger, "Ultrasonic Inspection for Wastage in the LMFBR Steam Generator Due to Sodium-Water Reaction," 1977 ASNT Spring Conference Summaries, Phoenix, Arizona

I-5 R. W. McClung (ORNL), R. A. Day (GE), H. H. Neely (ETEC), and T. Powers (B&W), "Techniques for In-Service Inspection of Heat Transfer Tubes in Steam Generators," The 1981 Second Joint US/Japan LMFBR Steam Generator Seminar at Sunnyvale, California, CONF-810615 UC-79TK

I-6 J. C. Amos, T. K. Odegaard, and J. C. Whipple (GE), R. E. Fenton and H. H. Neely (ETEC), and C. E. Ockert (DOE), "LLTR Large Leak Test Results and Evaluation," The 1981 Second Joint US/Japan LMFBR Steam Generator Seminar at Sunnyvale, California, CONF-810615 UC-79TK

I-7 J. C. Whipple, D. A. Greene, and K. Chen (GE), H. H. Neely (ETEC), and C. E. Ockert (DOE), "Test Results and Evaluation of LLTR Leak Propagation Tests and Supporting Small Leak Tests," The 1981 Second Joint US/Japan LMFBR Steam Generator Seminar at Sunnyvale, California, CONF-810615 UC-79TK

I-8 R. A. Meyer, J. C. Whipple, H. H. Neely, and C. E. Ockert, "U.S. Program for Sodium-Water Reaction Testing in LMFBR Steam Generators," 1981, Genoa, Italy; topical meeting on R&D, Fabrication and Operating Experience on Steam Generators for LMFBRs

I-9 H. H. Neely, "LLTR Series II Sodium-Water Reaction Test SWR A-6," Parts I and II ETEC-TDR-81-2 and -4

I-10 H. H. Neely and L. M. Press, "LLTR SWR A-7 Central DEG Test," Parts I and II ETEC-TDR-81-7 and -6

I-11 H. H. Neely and L. M. Press, "LLTR SWR A-8 Central Intermediate Superheat Leak Test," Part I ETEC-TDR-81-15

II. PRESSURE TRANSDUCER TESTING

G. J. TWA

A. INTRODUCTION

Testing of pressure measuring systems continued throughout CY 1981. Out-of-sodium testing was conducted on an MTI capacitance-type pressure transducer and started on a Gould prototype NaK/oil pressure measurement system. In-sodium testing continued throughout the year on the 13 pressure transducers that were in test at the end of last year.

B. OUT-OF-SODIUM TESTING

Out-of-sodium tests of pressure measuring systems are performed to evaluate their performance at temperature without the complication of using liquid sodium. Argon gas is used as the pressurizing medium. These tests provide the baseline data for comparison with subsequent sodium tests.

During CY 1981, limited testing was performed on a Mechanical Technology, Inc., (MTI) capacitance pressure transducer and a Gould prototype NaK/oil pressure measurement system.

The MTI transducer was a Model 212D194 Serial Number 6 with a nominal range specified as 120 psig. Figure II-1 shows a metallographic sample, sectioned to show the internal structure. The center electrode forms one plate of a capacitor, with the pressure-sensing diaphragm forming the other plate. An annular guard-ring surrounds the center electrode to minimize stray capacitance effects.

The following tests were performed on the MTI transducer:

1) Insulation resistance
2) Dielectric leakage current
3) Proof pressure test at 180 psi and 1000^{o}F (538^{o}C)
4) Repeatability test at room temperature

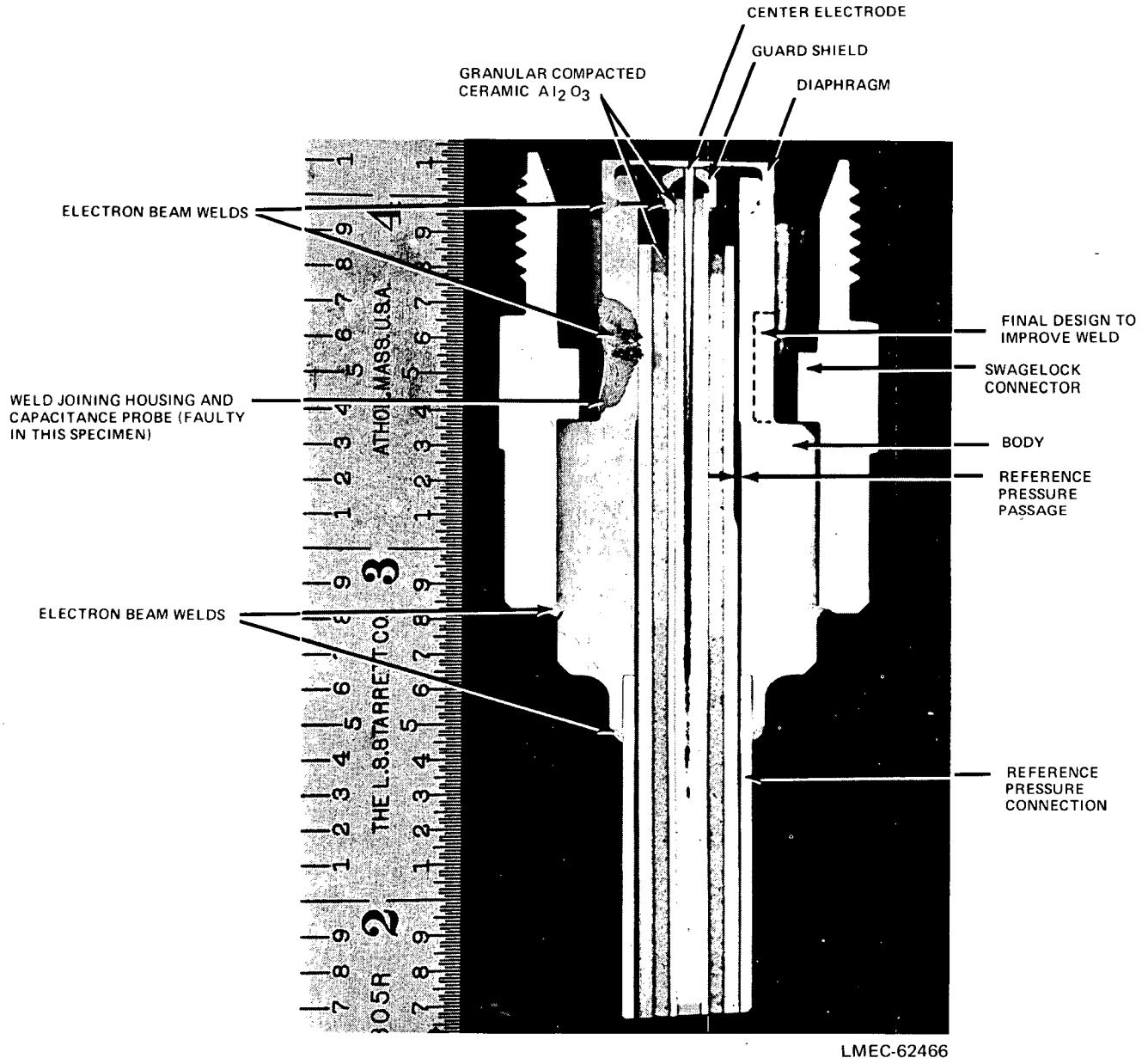

Figure II-1. Metallophotographic Section of High-Temperature Capacitance Pressure Transducer (for Use in Liquid Metals)

5) Temperature calibrations at 200, 400, 600, 800, and 1000°F (93, 204, 316, 427, and 538°C)

6) Ten temperature cycles from room temperature to 1000°F (538°C) with pressure calibrations at room temperature and 1000°F (538°C)

7) Short-term stability test.

During the initial calibration of this unit, it was found that above 114 psig (785 kPa), the transducer output became erratic. Therefore, the full-range pressure was reduced to 100 psig (689 kPa) for subsequent calibrations.

A Wayne-Kerr Model TE200 capacitance bridge was used to convert the change in capacitance of the pressure transducer to millivolts.

During the short-term stability test, with the transducer at 1000°F (538°C), the output became unstable after ∿26 h. In order to find a stable operating temperature, the temperature was incrementally reduced to 800°F (427°C) before stable operation was obtained.

Figure II-2 shows the typical linearity error for this transducer. The linearity error was essentially unaffected by temperature.

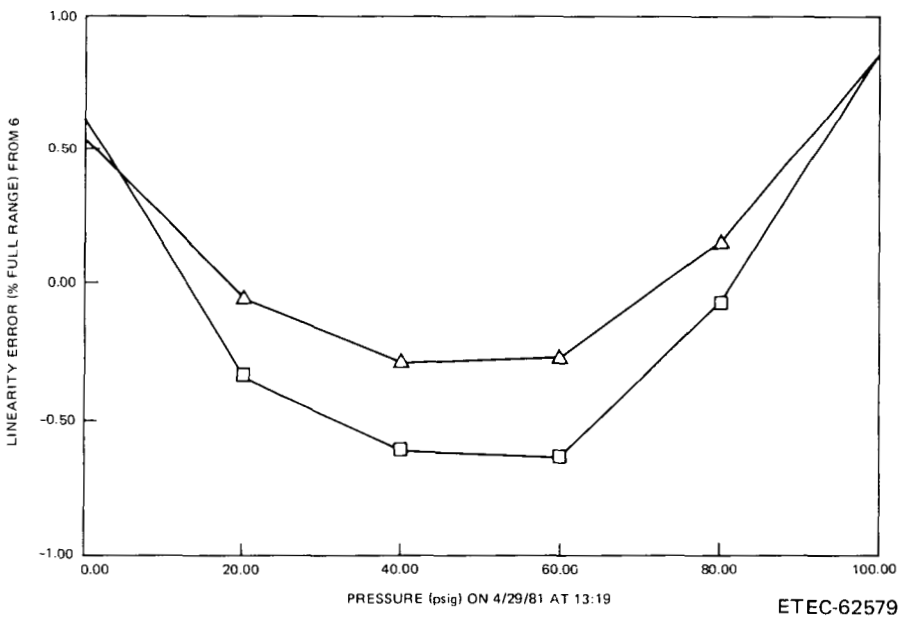

Figure II-2. MTI Linearity Error

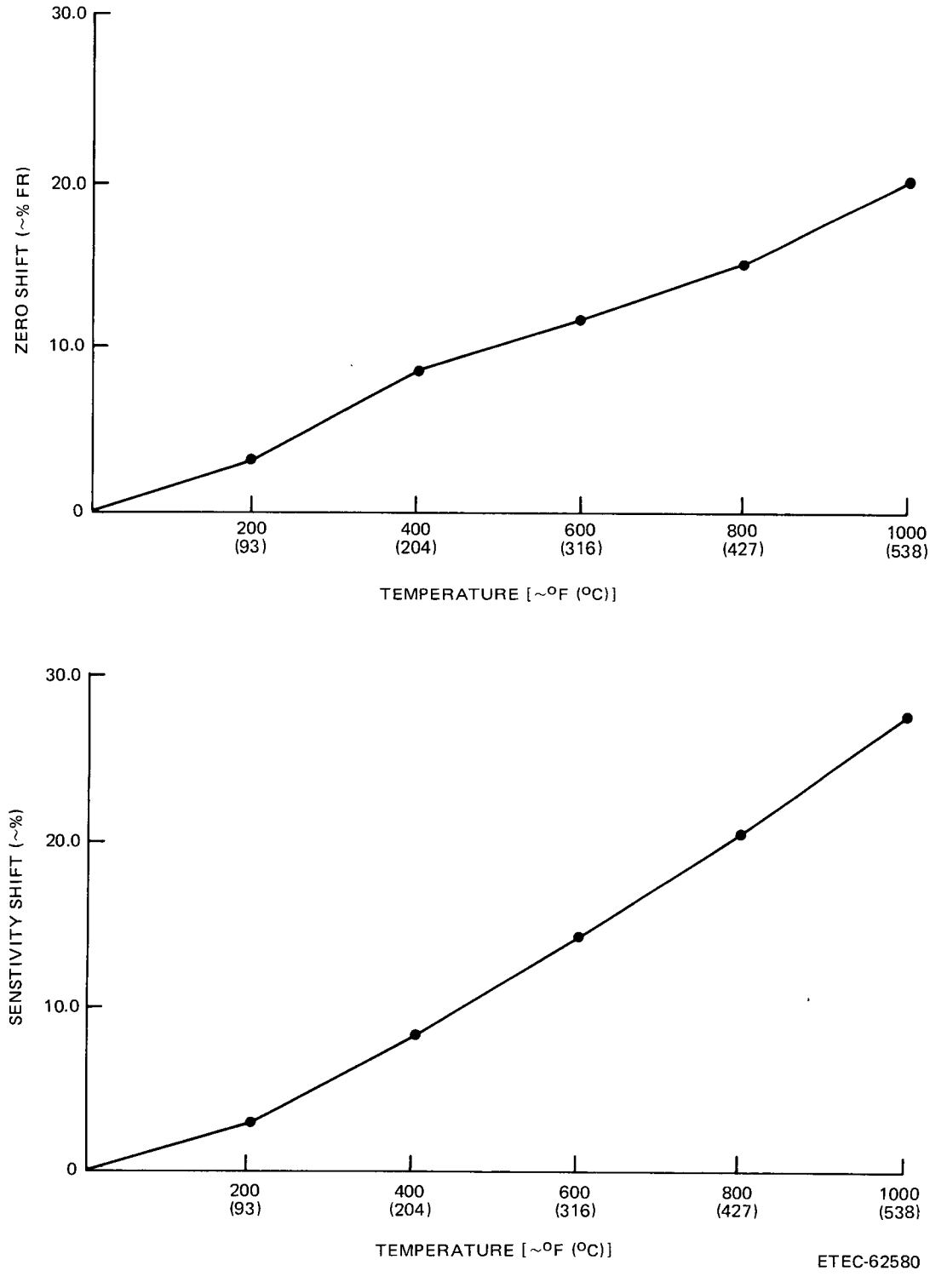

Figure II-3. MTI Zero and Sensitivity Shift vs Temperature

Figure II-3 shows the zero shift and sensitivity shift vs temperature. The maximum zero shift was 20.25% of full range (FR) at 1000^{o}F, and the maximum sensitivity shift was 27.56%.

Because of the erratic behavior at temperature and the extremely large zero shift and sensitivity shift with temperature, testing of this device has been terminated.

The prototype NaK/oil pressure measuring system is shown schematically in Figure II-4. The incorporation of an additional interface from NaK to oil in the conventional NaK transmission high-temperature pressure transducer theoretically has the following advantages:

1) The pressure transducer can be easily replaced in the field without breaching the sodium containment. (Oil filling can be done in a field environment, whereas NaK filling is not practical.)
2) A pressure range change for a measurement system can be implemented by removing and replacing just the pressure transducer assembly and refilling with oil.
3) Periodic transducer recalibration in the laboratory is practical, since the transducer can be removed from the system.
4) In-place calibration is also possible if the NaK capillary is frozen to isolate the process pressure.

During CY 1981, the oil filling system and procedures were developed, and the first system was satisfactorily filled with oil. Figure II-5 shows the oil-fill setup. Basically, the procedure is to evacuate the transducer system,

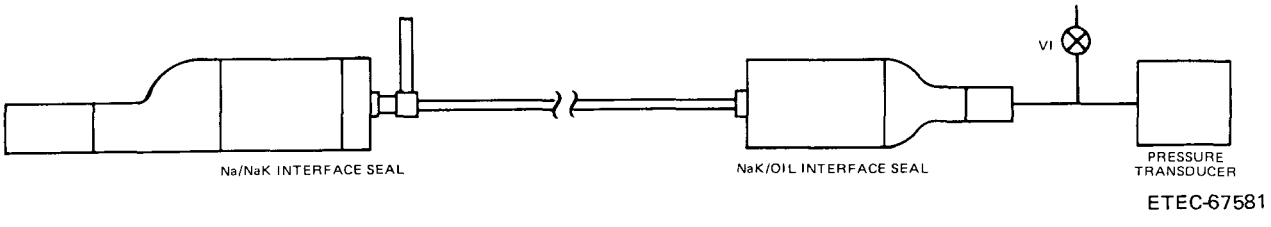

Figure II-4. NaK/Oil System

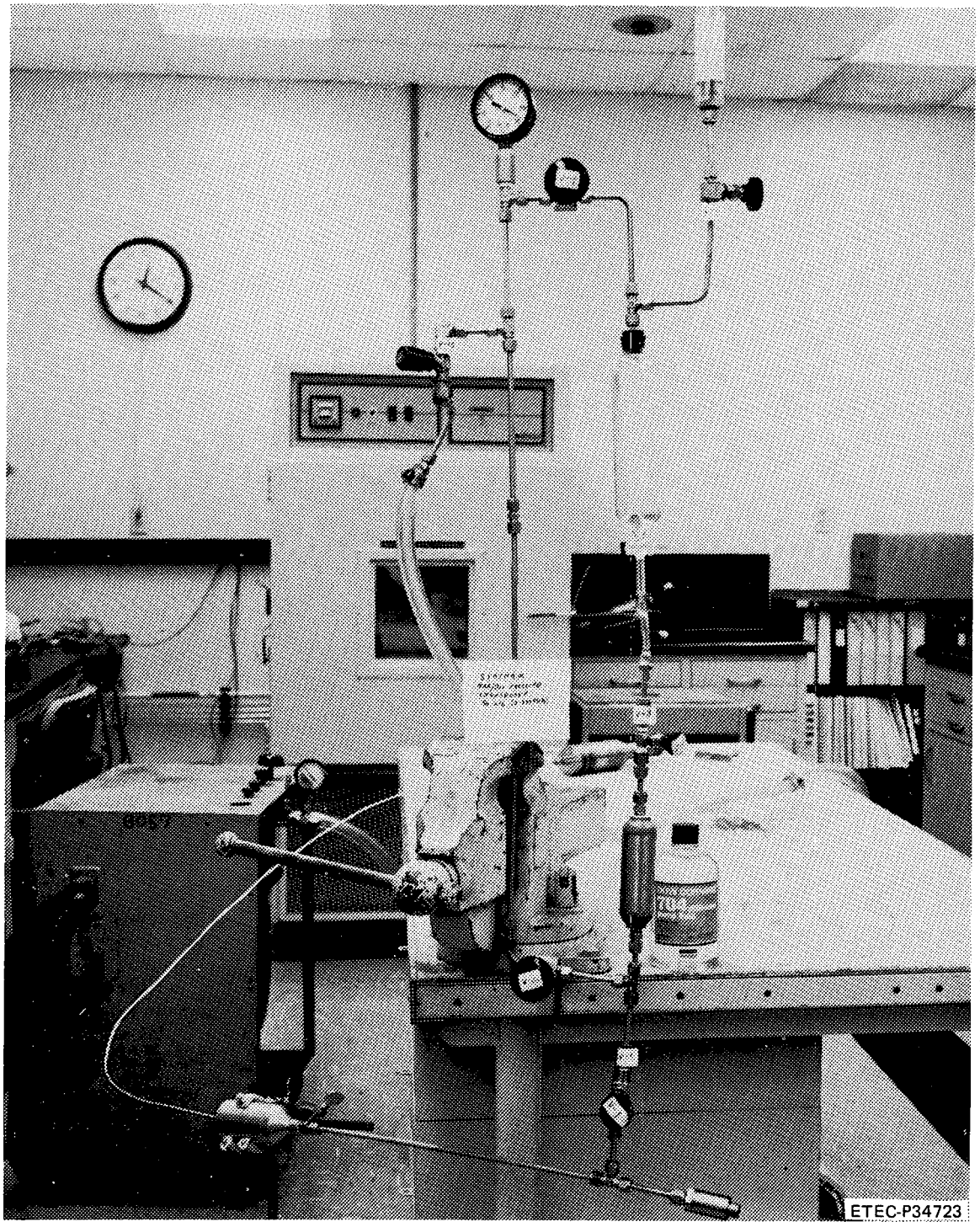

Figure II-5. NaK/Oil Pressure Measurement System — Oil-Fill Setup

deaerate the oil, then gravity-drop the oil into the transducer system. Testing of this first unit was initiated in CY 1981 and will continue in CY 1982.

C. IN-SODIUM TESTING

The sodium tests of the pressure transducers are conducted to determine the effects on the transducer of long-term exposure to liquid sodium at temperatures to 1200°F (649°C) and repeated temperature cycles from 500°F (260°C) to 1200°F (649°C). These tests are accomplished by using the high-pressure Test Rigs 032-R4, 032-R5, and 032-R6 (see Figure II-6). Each test rig contains a small sodium

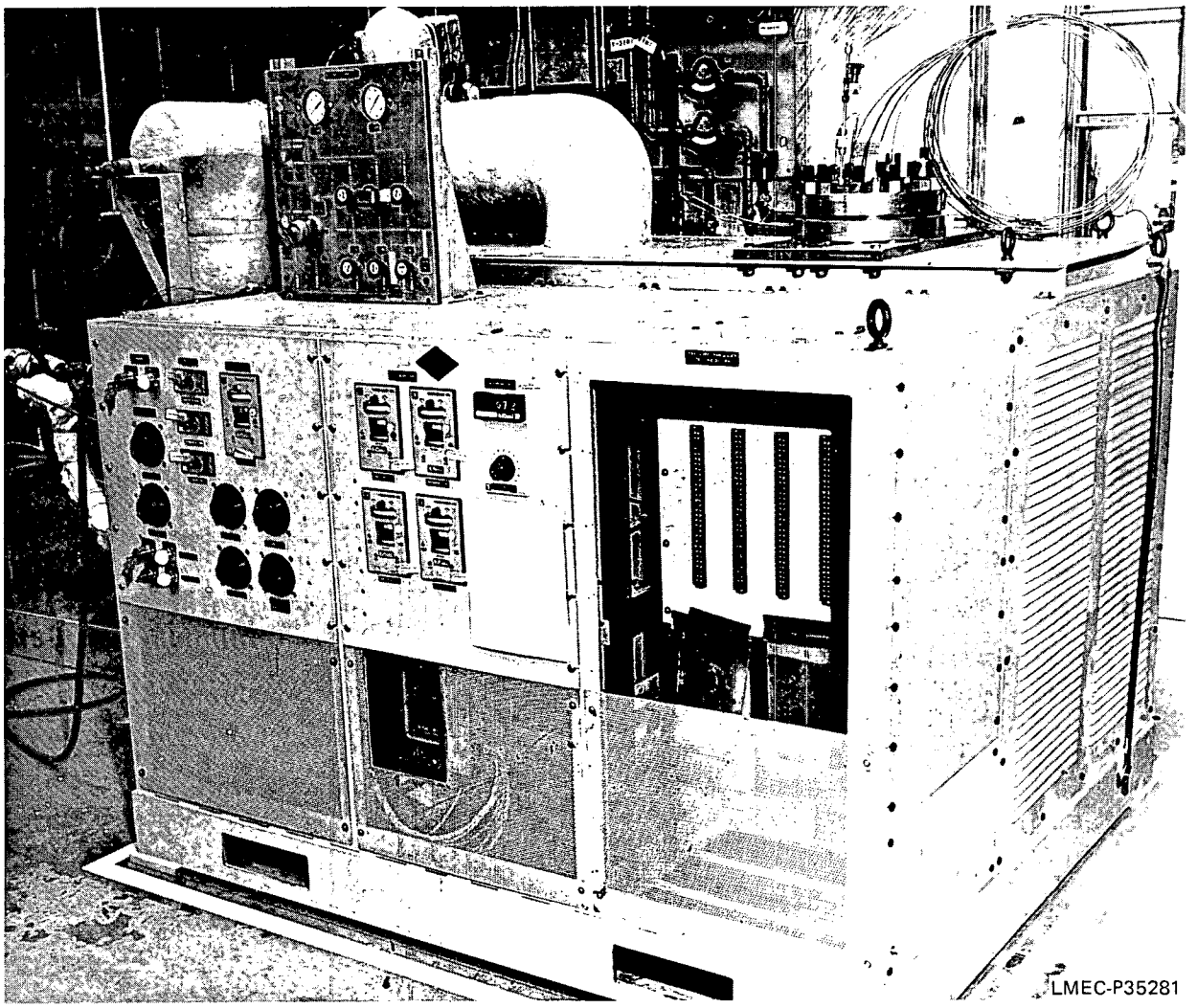

Figure II-6. In-Sodium Test Bench

vessel, the necessary argon system for local pressure application and remote pressurization for calibration, electrical heaters and controls, and provision for mounting transducers. The test rig is filled at a fill station, then isolated by freeze sections and moved to its test position, where it is connected to the electrical power, cooling water, argon calibration pressure source, alarm wiring, and instrumentation wiring. Calibration pressure is provided by a Gilmore pressure calibrator, and the output of the transducer and associated temperature measurements is recorded on a digital data acquisition system (DDAS).

The test sequence for all sodium testing is similar: Ten temperature cycles are performed from 500°F (260°C) to the maximum temperature of (1000°F (538°C) for Test Rigs 032-R4 and 032-R6 and 1200°F (649°C) for Test Rig 032-R5), followed by a 1000-h hold period at the maximum temperature, then by a single temperature cycle. (During the hold period, a pressure calibration is performed each working day.) The 1000-h hold at maximum temperature and single temperature cycle are repeated until the test is terminated. Normally, a minimum of 10,000 h is accumulated on a transducer before the test is terminated. During the temperature cycle, the sodium temperature is stabilized at 500, 600, 800, and 1000°F (260, 316, 427, and 538°C) for Test Rigs 032-R4 and 032-R6 and an additional temperature point at 1200°F (649°C) for Test Rig 032-R5.

1. Sodium Test Rig 032-R4

Sodium testing continued on this test rig throughout CY 1981 except for a short period when it was interrupted to repair a failed valve in the Gilmore pressure calibrator. At the end of CY 1980, the test rig was in the second 1000-h hold period. During CY 1981, Temperature Cycles 12 through 16 and Hold Periods 2 through 7 were completed.

Table II-1 lists the transducers installed on this test rig. Table II-2 provides a summary of the data for each of the hold periods. Data are presented for the start, the middle (500 h), and the end (1000 h) of each hold period.

TABLE II-1

TRANSDUCERS INSTALLED IN SODIUM TEST RIGS

Test Rig	Manufacturer	Model	S/N	Range (∿ psi)	Date Installed
032-R4	Gould	S63-2	68	0 to 300	10/13/75
032-R4	Barton	368	1505	0 to 300	10/15/78
032-R4	Barton	368	1506	0 to 300	01/15/78
032-R4	Barton	273A	6845	0 to 300	07/18/80
032-R4	Kaman	KP1911	01	0 to 500	07/18/80
032-R4	Kaman	KP1911	02	0 to 500	07/18/80
032-R5	Gould	S63-4	3	0 to 300	11/27/74
032-R5	Gould	S76-2	119	0 to 300	08/16/77
032-R5	Barton	758	891	0 to 300	08/16/77
032-R6	Gould	S76-2	1	0 to 50	02/22/79
032-R6	Barton	758	893	0 to 50	02/22/79
032-R6	Kaman	KP1911	03	0 to 100	06/09/80
032-R6	Kaman	KP1911	04	0 to 100	06/09/80

The maximum and minimum zero and sensitivity shifts observed during the year for each transducer are as follows:

Transducers	Zero Shift (∿ % FR)		Sensitivity Shift (∿ %)	
	Max.	Min.	Max.	Min.
Barton 368 S/N 1505	2.39	1.59	0.01	-0.33
Barton 368 S/N 1506	5.91	5.34	0.04	-0.44
Barton 273A S/N 6845	0.71	0.07	-3.12	-3.99
Gould S62-2 S/N 68	1.68	1.24	0.06	-0.34
Kaman KP1911 S/N 1	5.22	-9.05	-3.30	-6.00
Kaman KP1911 S/N 2	-18.53	-33.05	-3.04	-7.12

TABLE II-2

TEST RIG 032-R4 — TEST DATA SUMMARY

Hold Period	Hours	S63-2/68		386/1505		368/1506		KP1911/01		KP1911/02		273A/6845	
		Zero (~ % FR)	Sensitivity (~ %)	Zero (~ % FR)	Sensitivity (~ %)	Zero (~ % FR)	Sensitivity (~ %)	Zero (~ % FR)	Sensitivity (~ %)	Zero (~ % FR)	Sensitivity (~ %)	Zero (~ % FR)	Sensitivity (~ %)
2	480	1.64	-0.27	2.22	-0.15	5.91	-0.27	5.22	-4.89	-18.53	-5.14	0.07	-3.21
2	1032	1.51	-0.15	2.09	-0.23	5.87	-0.16	3.30	-4.98	-20.80	-4.67	0.13	-3.74
3	0	1.45	-0.23	2.21	-0.20	5.84	-0.38	2.44	-4.40	-22.47	-4.48	0.15	-3.85
3	500	1.54	-0.23	2.24	-0.27	5.85	-0.40	0.15	-4.58	-23.53	-4.20	0.18	-3.45
3	1000	1.43	-0.24	2.24	-0.33	5.89	-0.29	-0.77	-4.39	-23.40	-4.27	0.15	-3.70
4	0	1.40	-0.24	2.18	-0.15	5.87	-0.37	-2.14	-5.10	-22.94	-4.42	0.44	-3.44
4	500	1.43	-0.19	1.98	-0.06	5.86	-0.22	1.04	-3.30	-23.22	-4.77	0.22	-3.12
4	1000	1.68	-0.34	2.06	-0.14	5.85	-0.44	0.56	-4.70	-27.06	-3.76	0.38	-3.43
5	0	1.57	-0.14	2.39	-0.11	5.82	-0.21	-0.56	-3.63	-26.37	-3.45	0.71	-3.18
5	500	1.61	-0.07	2.26	-0.13	5.83	-0.02	-3.60	-3.89	-29.18	-3.04	0.65	-3.27
5	1000	1.58	0.06	2.26	0.01	5.73	-0.01	-3.82	-3.83	-29.39	-3.99	0.66	-3.41
6	0	1.28	0.01	2.02	-0.10	5.42	0.04	-5.48	-4.14	-29.78	-4.55	0.51	-3.36
6	500	1.24	-0.07	1.96	-0.16	5.39	-0.03	-5.28	-4.07	-26.53	-4.21	0.50	-3.36
6	1000	1.19	-0.26	1.61	-0.28	5.34	-0.36	-6.28	-4.29	-31.93	-4.05	0.34	-3.99
7	0	1.42	-0.25	1.76	-0.22	5.51	-0.41	-9.05	-6.00	-33.05	-5.40	0.65	-3.70
7	500	1.37	-0.11	1.69	-0.16	5.44	-0.29	-7.15	-4.32	-34.15	-4.21	0.63	-3.55
7	1000	1.37	-0.18	1.59	-0.08	5.46	-0.34	1.31	-5.47	-24.98	-7.12	0.15	-3.48
Max.		1.68	0.06	2.39	0.01	5.91	0.04	5.22	-3.30	-18.53	-3.04	0.71	-3.12
Min.		1.24	-0.34	1.59	-0.33	5.34	-0.44	-9.05	-6.00	-33.05	-7.12	0.07	-3.99

The reference values used to compute zero and sensitivity shifts were those obtained from the last room-temperature calibration taken during the out-of-sodium tests.

2. Sodium Test Rig 032-R5

Testing of the transducers installed in this rig was conducted from the first of the year until mid-September, when testing was halted because of a failed valve in the argon pressurizing system. Testing was resumed in December, following the repairs. At the end of CY 1980, Temperature Cycle 20 had been completed. During CY 1981, Temperature Cycles 21 through 24 and Hold Periods 11 through 15 were completed.

Table II-1 lists the transducers installed on this test rig. Table II-3 provides a summary of the data for each of the hold periods. Data are presented for the start, the middle (500 h), and the end (1000 h) of each hold period.

The maximum and minimum zero and sensitivity shifts observed during the year for each transducer are as follows:

Transducers	Zero Shift (∿ % FR)		Sensitivity Shift (∿ %)	
	Max.	Min.	Max.	Min.
Gould S76-2 S/N 119	0.18	-0.79	-1.36	-2.42
Gould S63-4 S/N 3	1.65	-0.19	0.43	-0.85
Barton 758 S/N 891	-1.74	-3.19	0.85	-0.80

The Gould (originally Statham) transducer Model S63-4 is one of the original FFTF PPS transducers installed in November of 1974. This transducer was re-ranged from its original 0-250 psi (0-1723 kPa) to 0-300 psi (0-2608 kPa) to be compatible with the other two transducers. All zero and sensitivity shift data are referenced to the last out-of-sodium room-temperature calibration for the Gould S76-2 and Barton 758 and to the initial calibration at 500^{o}F following the range change for the Gould S63-4.

TABLE II-3

TEST RIG 032-R5 — TEST DATA SUMMARY

Hold Period	Hours	S76/119		S63-4/3		758/891	
		Zero (∿ % FR)	Sensitivity (∿ %)	Zero (∿ % FR)	Sensitivity (∿ %)	Zero (∿ % FR)	Sensitivity (∿ %)
11	480	-0.01	-1.73	1.61	0.06	-1.89	-0.52
11	1000	0.18	-1.95	1.17	0.09	-1.74	-0.36
12	0	0.16	-1.81	1.51	-0.04	-2.74	0.04
12	500	-0.46	-1.36	1.27	0.43	-2.60	-0.25
12	1000	-0.04	-1.73	1.34	0.08	-2.38	-0.71
13	0	0.09	-1.80	1.65	-0.14	-2.61	0.60
13	500	-0.18	-1.57	1.12	0.01	-2.52	0.26
13	1000	-0.19	-1.53	0.77	0.04	-2.60	-0.04
14	0	-0.22	-1.60	0.76	0.00	-2.41	-0.80
14	500	-0.35	-1.54	0.81	-0.07	-2.82	-0.15
14	1000	-0.19	-1.80	-0.19	0.26	-2.38	-0.17
15	0	-0.48	-2.00	-0.08	-0.20	-3.19	0.85
15	312	-0.79	-2.42	0.74	-0.85	-3.03	-0.64
Max.		-0.79	-2.42	1.65	-0.43	-3.19	0.85
Min.		0.09	-1.36	-0.08	-0.85	-1.74	-0.80

3. Sodium Test Rig 032-R6

Sodium testing continued on this test rig throughout CY 1981 except for the short period during repair of the Gilmore pressure calibrator. At the end of CY 1980, the test rig was in the second 1000-h hold period at 1000°F (538°C). During CY 1981, Temperature Cycles 12 through 16 and Hold Periods 2 through 7 were completed.

Table II-2 lists the transducers installed on this test rig. Table II-4 provides a summary of the data for each of the hold periods. Data are presented for the start, the middle (500 h), and the end (1000 h) of each hold period.

TABLE II-4

TEST RIG 032-R6 — TEST DATA SUMMARY

Hold Period	Hours	758/893		S76-2/01		KP1911/03		KP1911/04	
		Zero (∿ % FR)	Sensitivity (∿ %)	Zero (∿ % FR)	Sensitivity (∿ %)	Zero (∿ % FR)	Sensitivity (∿ %)	Zero (∿ % FR)	Sensitivity (∿ %)
3	0	3.54	-0.62	4.09	-0.38	42.13	3.24	-28.68	-2.39
3	500	3.11	-0.58	4.65	-0.51	41.19	3.59	-68.61	-2.83
3	1000	2.87	-0.46	5.70	-0.65	46.82	3.19	-25.23	-1.74
4	0	3.01	-0.88	4.80	-0.72	49.70	3.16	-21.65	-1.81
4	500	3.63	-1.42	4.23	-0.71	49.70	2.23	-17.87	-1.64
4	1000	2.90	-0.49	5.98	-0.69	49.51	2.81	-13.03	-1.31
5	0	2.82	-0.85	4.16	-0.60	48.16	2.35	-0.67	-1.55
5	500	2.99	-0.34	5.27	-0.14	49.92	2.15	1.21	-0.65
5	1270	2.55	-0.32	5.41	-0.30	48.91	1.98	-3.84	-0.67
6	0	3.74	-0.86	5.92	-0.60	48.35	1.96	-3.96	-1.06
6	500	2.90	-0.33	7.10	-0.57	44.36	2.91	-16.31	-1.37
6	1000	3.80	-1.99	6.23	-1.91	45.37	-0.28	-57.00	-1.86
Max.		3.80	-1.99	7.10	-1.91	49.92	3.59	-68.61	-2.83
Min.		2.55	-0.32	4.09	-0.14	41.19	-0.28	1.21	-0.65

The maximum and minimum zero and sensitivity shifts observed during the year for each transducer are as follows:

Transducers	Zero Shift (∿ % FR)		Sensitivity Shift (∿ %)	
	Max.	Min.	Max.	Min.
Barton 758 S/N 893	3.80	2.55	-1.99	-0.32
Gould S76-2 S/N 1	7.10	4.09	-1.91	-0.14
Kaman KP1911 S/N 03	49.92	41.19	3.59	-0.28
Kaman KP1911 S/N 04	-68.61	1.21	-2.83	-0.65

The reference values used to compute zero and sensitivity shifts were those obtained from the last room-temperature calibration taken during the out-of-sodium tests.

Both Kaman pressure transducers were quite erratic throughout the sodium testing.

III. HEDL FLOWMETERS

V. DE VITA

A. INTRODUCTION

This report discusses the results from testing an annular linear induction pump (ALIP) for the Single-Pin Test Loop (SPTL) designed and supplied by HEDL. This test article also included the calibration of two permanent magnet (PM) flowmeters mounted on the inlet side of the pump. A second pump, SPTL-2 ALIP, is currently being calibrated in the same manner but is not yet completed.

The reference flow for these calibrations was determined by flowing sodium from a supply tank to a receiver tank. By measuring the change in the sodium free surface level in the supply tank as a function of time, the volumetric flow rate was computed. A final report (Ref. III-1) has been completed and distributed this year for SPTL ALIP. The testing of these test articles was very similar to the DUAL-ALIP calibrated in 1979 and 1980. Reference to detailed testing descriptions can be found in the 1979 and 1980 ETEC annual reports.

B. TEST DESCRIPTION

The test article includes an annular linear induction pump and an extension tube where the two PM flowmeters were installed. An isometric sketch (Figure III-1) depicts the position of these sections with respect to each other. The ALIP consists of a Type 316 stainless steel pump ~58 in. (147.3 cm) long. Around the pump tube are six magnetic stators made of vanadium Permendur (49 Fe, 49 Co, 2 V) and 24 anodized aluminum coils. A return magnetic path is provided by a nickel-plated vanadium Permendur core contained inside the pump tube. The magnetic stators are protected from the hot sodium by a "multi-foil" insulation tube surrounding the pump. Silicon coolant (Dow 200) is pumped continuously through each stator to cool the aluminum coils.

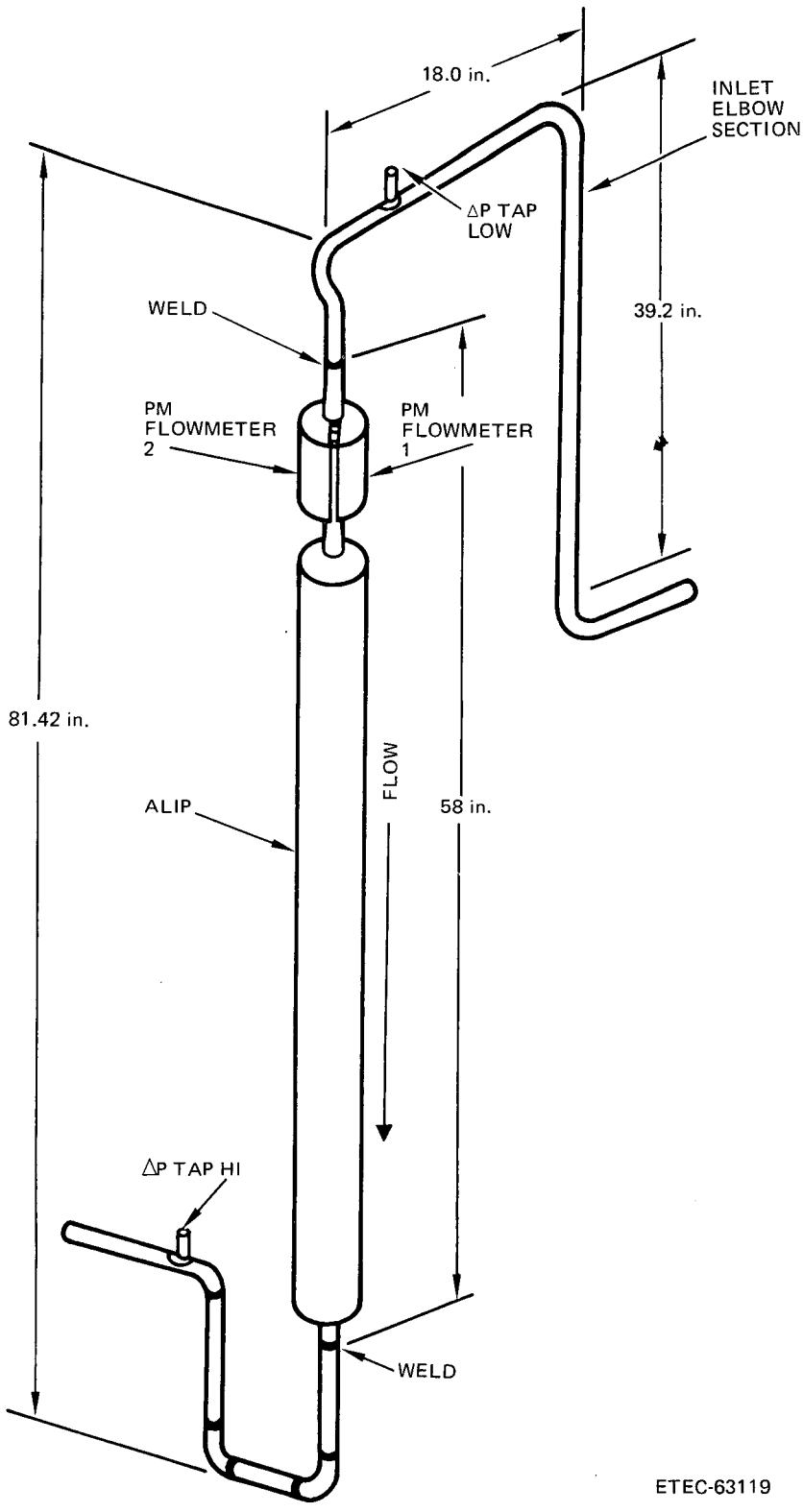

Figure III-1. SPTL-ALIP Calibration Test Article

The PM flowmeters consist of two Alnico VB magnets with two 1.75-in. (4.44-cm) pole pieces. Stainless steel wires are welded to the flow duct and terminated into an insulated, twisted, shielded cable. The temperature of the ALIP case is monitored by a thermocouple strapped to its exterior. Five internal ALIP thermocouples are also installed for monitoring of coil and lamination temperatures. An immersion thermocouple inserted at the inlet to the ALIP was used for establishing the required sodium temperature.

Electrical power is supplied to the sodium pump coils by ceramic-to-metal feedthrough seals in the upper end of the pump from a programmable three-phase motor-driven auto transformer supply situated at a 10-ft (305-cm) distance from the operating loop. The pump phases are closed-delta connected to achieve isolation from ground. A photo depicting the installed ALIP, PM flowmeter, pump console, oil cart, and facility PM flowmeter is shown in Figure III-2.

C. FACILITY AND TEST METHOD DESCRIPTION

1. General

The desired flows and temperatures required for the test programs were achieved utilizing Tanks T-6 and T-7 in the General Test Facility (Building 032). The facility description and test-method description are identical to those in Reference III-2. Fixed flows of 2, 4, 6, 7, 8, and 10 gal/min (12.6, 25.2, 37.8, 44.1, 50.4, and 63 x 10^{-5} m^3/s) with each of the required pump pressures of 5, 8, 10, 15, 20, 30, 40, and 50 psid (34.5, 55.2, 69, 103.5, 138, 207, 276, and 345 kPa) were performed at each of the five test temperatures: 400, 500, 600, 700, and 800^{o}F (204.4, 260, 315.5, 371.1, and 426.7^{o}C).

2. Computations of Reference Flow

The level sensor, LE-2, was wired through an amplifier and ranged from -10 to +10 V for a 120-in. (305-cm) level change. This was done to maximize resolution to the digital data acquisition system (DDAS), thereby maximizing the accuracy of the level change. The reference flow was computed as follows:

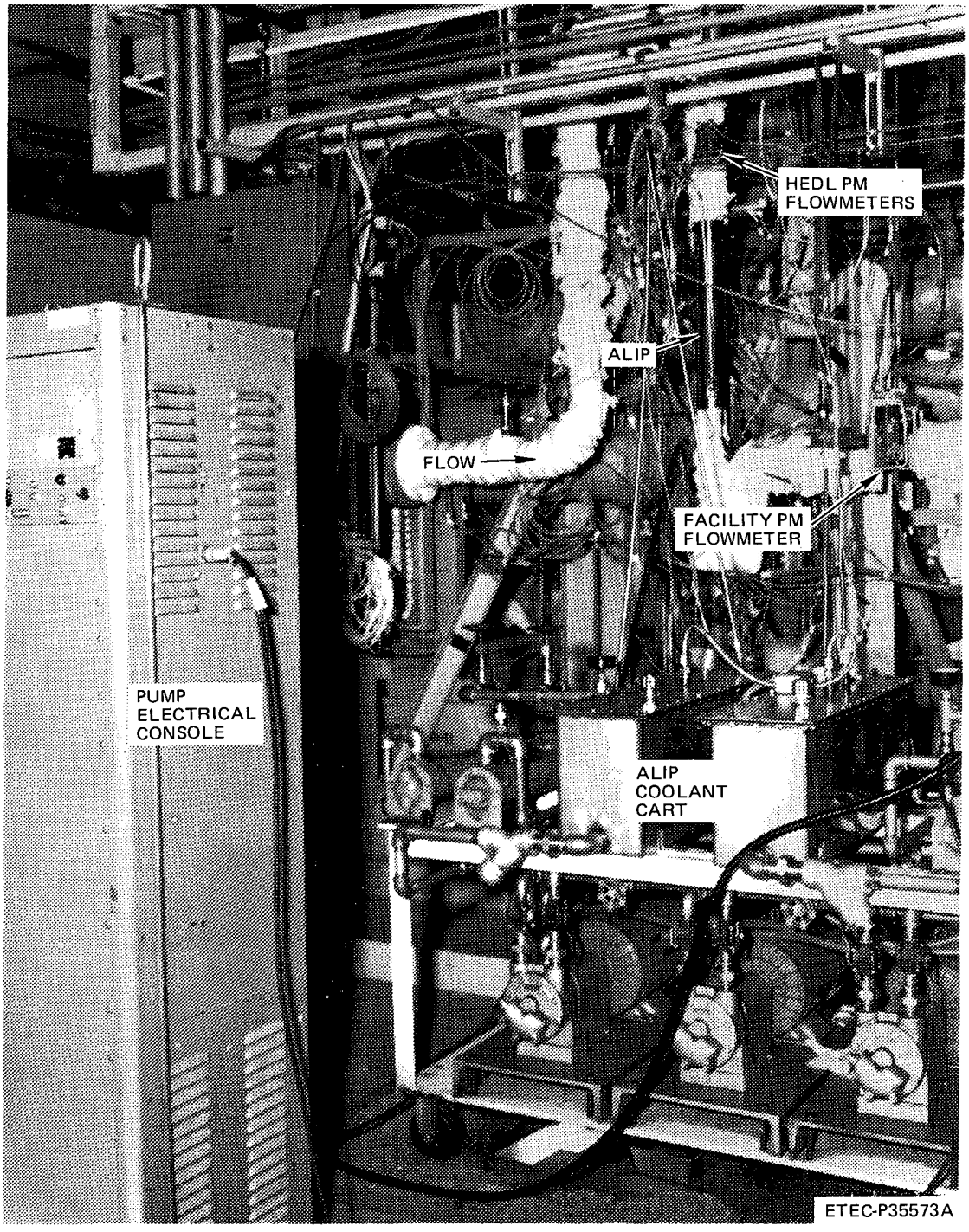

Figure III-2. Complete ALIP Test Article Installation

1) The level data from LE-2 (Interatom) was computed for every data point (15 points/s), over a selected slice of test time (minimum of 20 s).
2) A curve fit of the level data to the third degree was computed over the selected time slice.
3) The above curve-fit equation was differentiated with respect to test time, thereby establishing data for $\Delta L/\Delta t$.
4) $(\Delta V/\Delta t) = 0.983\ (\Delta L/\Delta t)\left[1 + (19.2 \times 10^{-6})\ (T-70)\right] \times 60$ is the final equation used for computing flow rate in gal/min.

D. TEST RESULTS

A listing of all the test data, including the two PM flowmeters, internal pump temperature, total input power, each of the three phase currents to the ALIP for each of the required sodium flow, differential pump pressure, and sodium temperature, are presented in ETEC-TDR-81-9, dated November 5, 1981. ETEC-TDR-81-9 also includes plots of (1) Phase A current vs flow for each of the pump differential pressures, (2) total input power vs flow for each of the pump differential pressures, and (3) HEDL PM Flowmeters FE-1 and FE-2 vs flow. Representative plots of these parameters are shown in Figures III-3, III-4, III-5, and III-6. As can be seen, at several sodium flows above 6 gal/min (37.8 m^3/s) and high differential pressures, no data are presented. This is due to pump performance limitations in the form of internal pump cavitation. The characteristics of pump cavitation were manifested by sudden loss of sodium flow with increasing input current and differential pressure and, in some severe cases, an audible high-frequency noise emanating from the pump.

Per HEDL requirements, the data for Phase A current, pump differential pressure, and sodium flow were characterized and curve fit to form the following relationships:

$$I_A = 6.34 + 0.168Q + 0.608\Delta P + 0.0929Q^2 - 0.0037(\Delta P)^2 \pm 2.08\% \text{ or } \pm 0.57\ A^*$$

at 400^oF (204.4^oC)

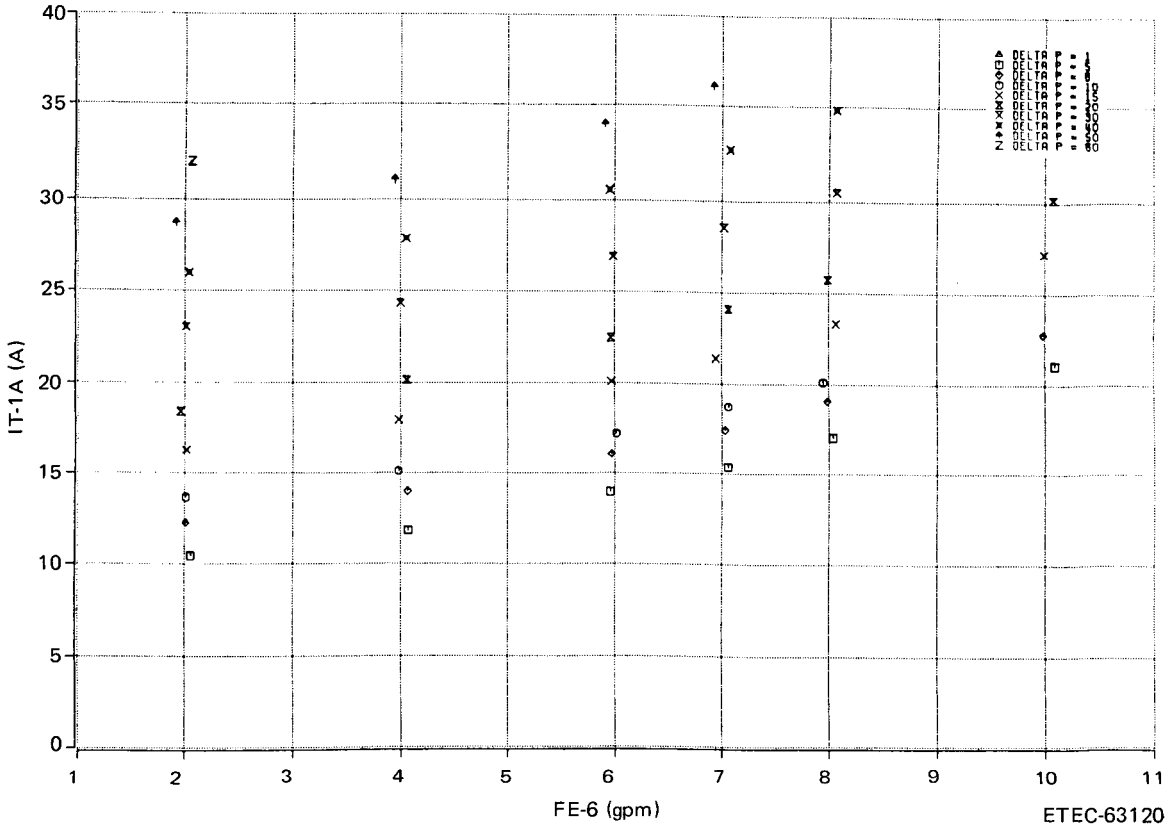

Figure III-3. Phase A Current at 500°F (260°C)

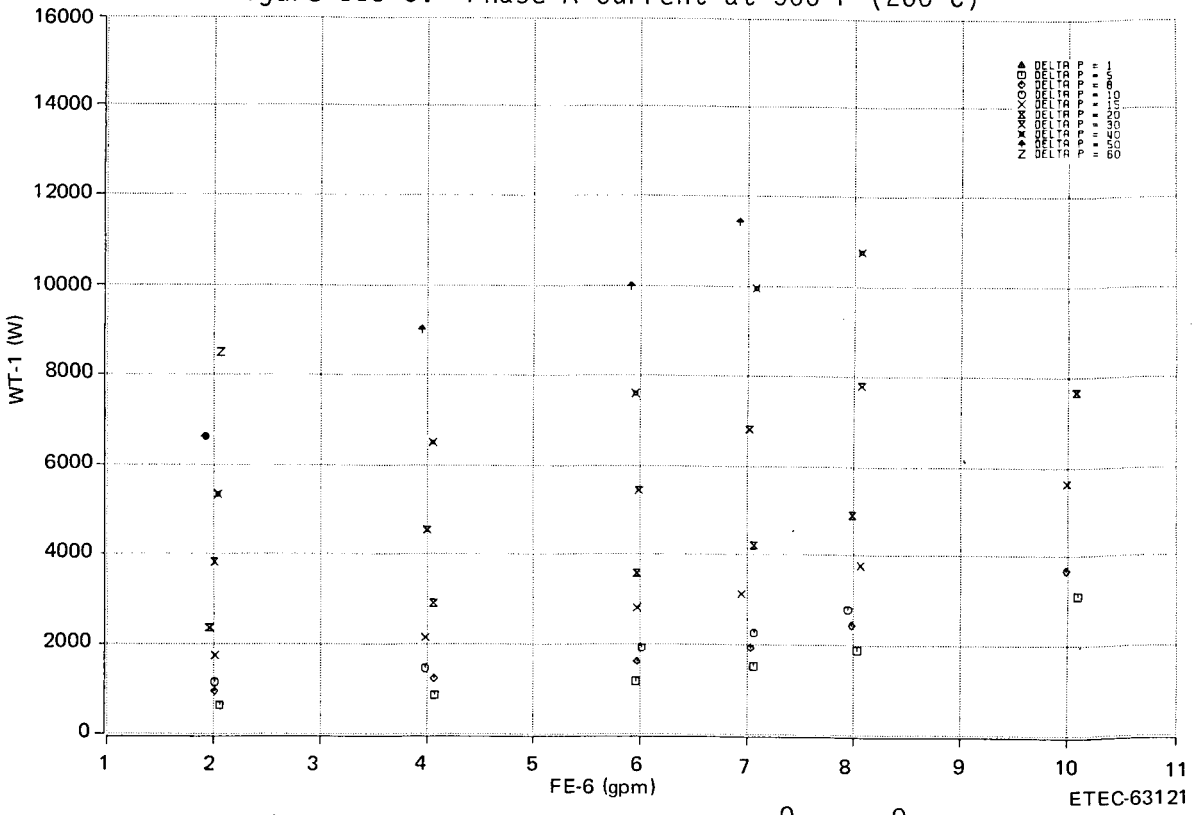

Figure III-4. Total Power at 500°F (260°C)

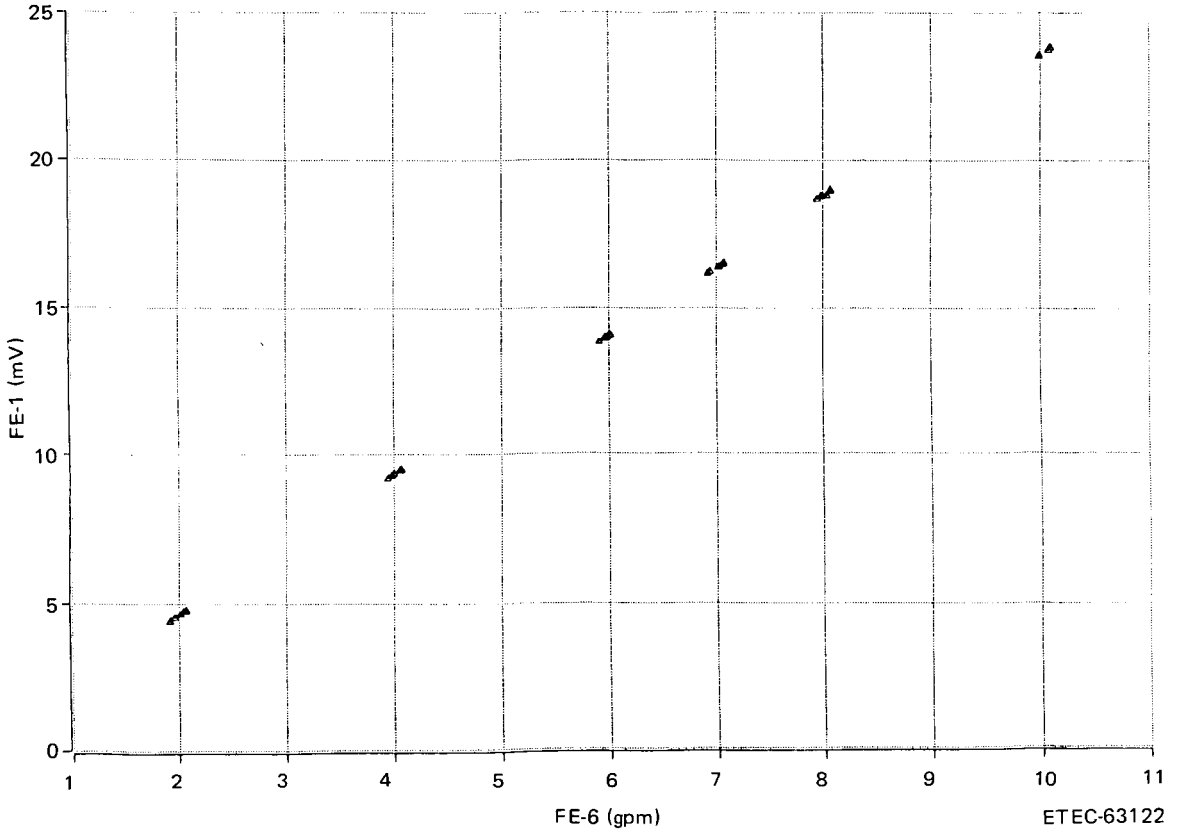

Figure III-5. PM-1 Flowmeter at 500°F (260°C)

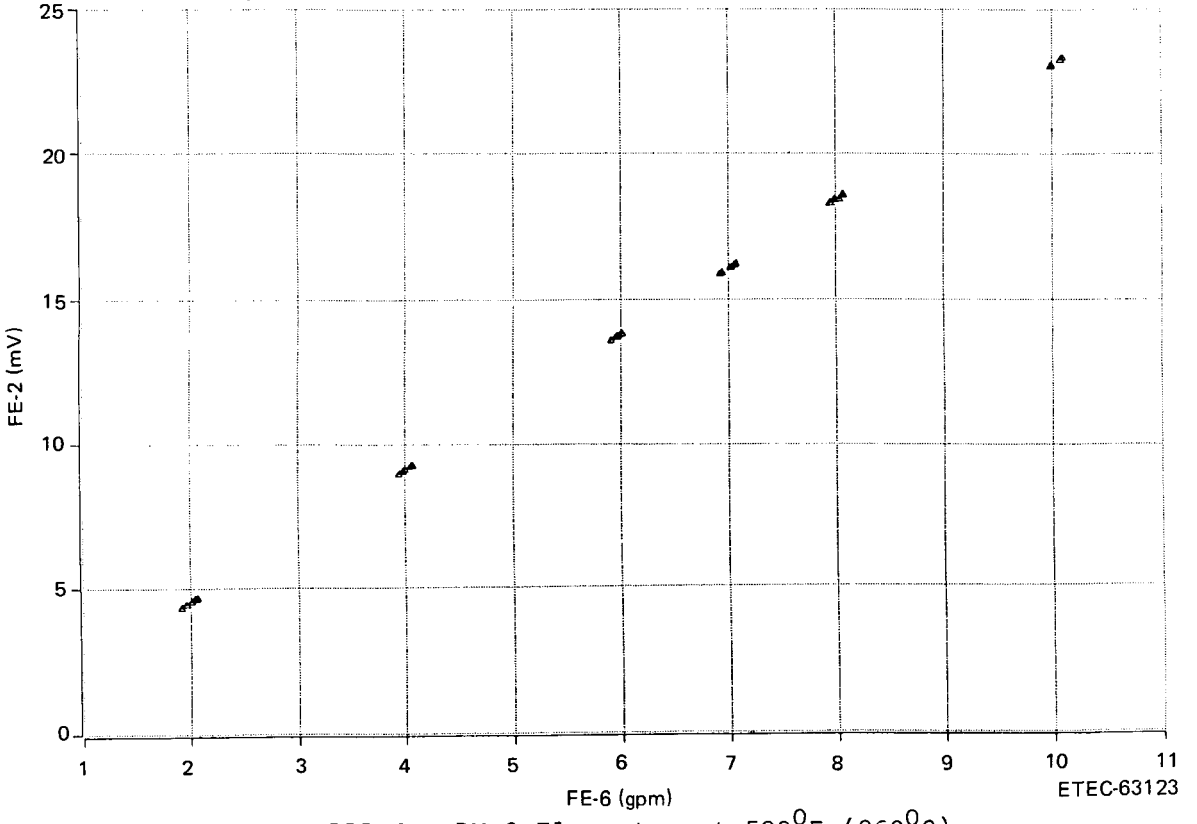

Figure III-6. PM-2 Flowmeter at 500°F (260°C)

$$I_A = 5.91 + 0.300Q + 0.657\Delta P + 0.0915Q^2 - 0.00405(\Delta P)^2 \pm 2.55\% \text{ or } \pm 0.54 \text{ A*}$$
at 500^oF (260^oC)

$$I_A = 5.58 + 0.446Q + 0.705\Delta P + 0.085Q^2 - 0.00450(\Delta P)^2 \pm 2.0\% \text{ or } \pm 0.68 \text{ A*}$$
at 600^oF (315.5^oC)

$$I_A = 6.13 + 0.355Q + 0.741\Delta P + 0.102Q^2 - 0.00467(\Delta P)^2 \pm 3.2\% \text{ or } \pm 0.78 \text{ A*}$$
at 700^oF (371.1^oC)

$$I_A = 5.43 + 0.544Q + 0.805\Delta P + 0.0946Q^2 - 0.00527(\Delta P)^2 \pm 3.5\% \text{ or } \pm 0.83 \text{ A*}$$
at 800^oF (426.7^oC)

The curve fits for total input power were attempted for the same independent variables of differential pressure and current, but the resultant curve fits are extremely poor, measuring in the order of 20-30% errors. The failure to curve-fit to a polynomial is attributed to higher internal power losses in pump coils, which does not contribute to pump performance but is measured as a part of total input power.

REFERENCES

III-1. ETEC Report, ETEC-TDR-81-9, "SPTL ALIP and PM FM Calibration," dated November 5, 1981

III-2. ETEC Report, ETEC-TDR-80-11, "Dual-ALIP Calibration," dated July 10, 1980

*Whichever is greater, for 95% of all data points

IV. LARGE FLOWMETERS

V. DE VITA

A. INTRODUCTION

This report discusses the results from testing three types of sodium flowmeter. All three flowmeters were tested simultaneously, measuring sodium flow in a 16-in. (40.6-cm) pipe. A 16-in. venturi was used as the reference flowmeter. The three types of flowmeter are:

1) Ultrasonic – This flowmeter was designed, manufactured, and supplied by Argonne National Laboratories.
2) Electromagnetic (Saddle Coil) – The coil was designed and manufactured by Reactor Equipment Division of GEC, Leicester, England. The power supply that energizes the saddle coil was manufactured by Electronic Measurements, Inc. The overall measurement system was supplied by Argonne National Laboratories.
3) Venturi Bypass – This flowmeter was designed and manufactured by Energy Technology Engineering Center (ETEC).

Test conditions included sodium temperatures from 400 to 1050°F (204.4 to 565.5°C) and flow rates from 1000 to 17,500 gal/min (6.3×10^{-2} to 1.1 m^3/s). The final reports for each of the three flowmeters have been completed and distributed. They are identified as follows:

1) ETEC-81-17, "16-Inch Ultrasonic Flowmeter Performance in Liquid Sodium"
2) ETEC-82-3, "16-Inch Electromagnet Flowmeter Performance in Liquid Sodium"
3) ETEC-82-5, "16-Inch Venturi Bypass Flowmeter Performance in Liquid Sodium."

B. TEST DESCRIPTION

1. Ultrasonic

This test article included two ultrasonic (UT) transducers, operating in a single-path transmit-receive mode. The transducers were clamped to the outside surface on opposite sides of the 16-in. pipe as shown pictorially in Figure IV-1. The transducers, manufactured by Argonne National Laboratories (ANL), featured shear mode X-cut lithium niobate ($LiNbO_3$) piezoelectric crystals mounted on a laminated wedge. Each transducer was clamped under 400 lb (181 kg) of force on optically polished flats (Figure IV-2) on the pipe as shown in Figure IV-3. Further assembly details are described in ETEC Report ETEC-81-17.

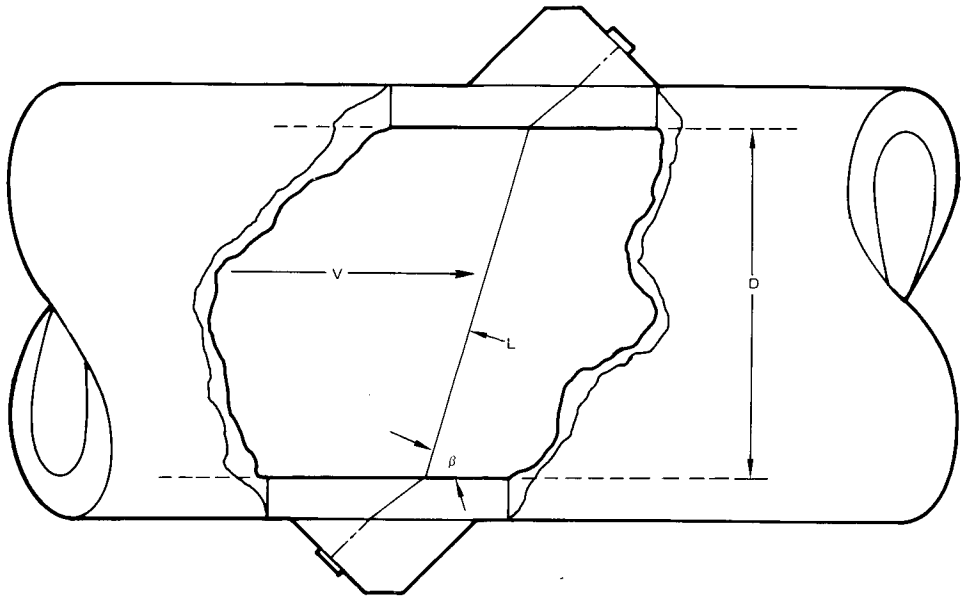

Figure IV-1. Typical Path for an Acoustic Pulse

The transducers were driven through 150 ft (45.7 m) of coaxial cable, RG-71/u, from rack-mounted control electronics identified as MCD 168-2. In addition to providing the output/input for the two transmit/receive signals to the transducers, three digital outputs and four analog outputs are generated by MCD 168-2.

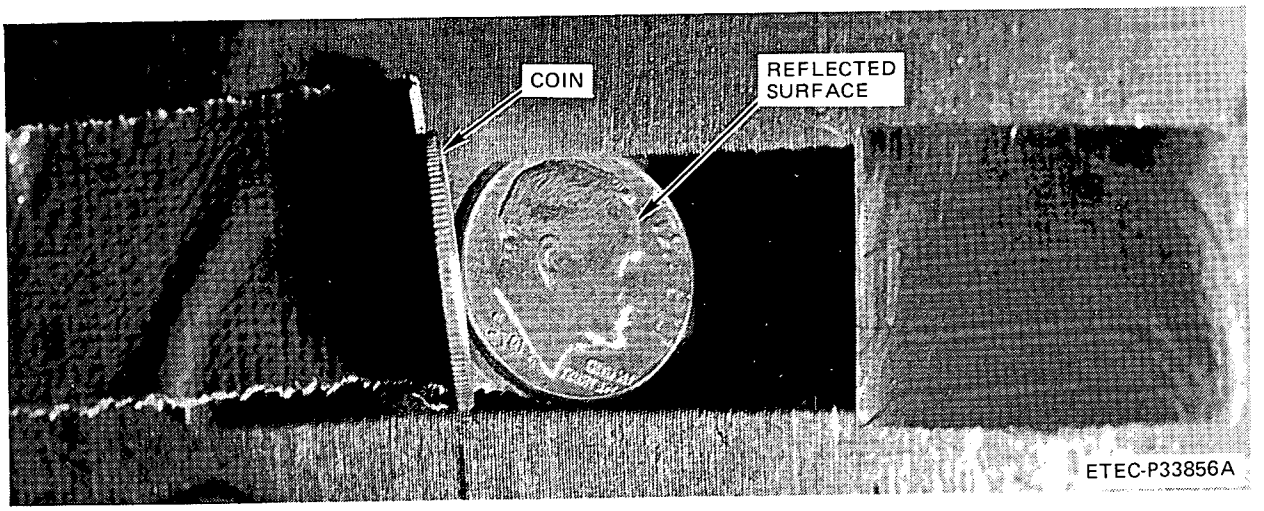

Figure IV-2. Polished Face on Pipe for Transducer Mounting

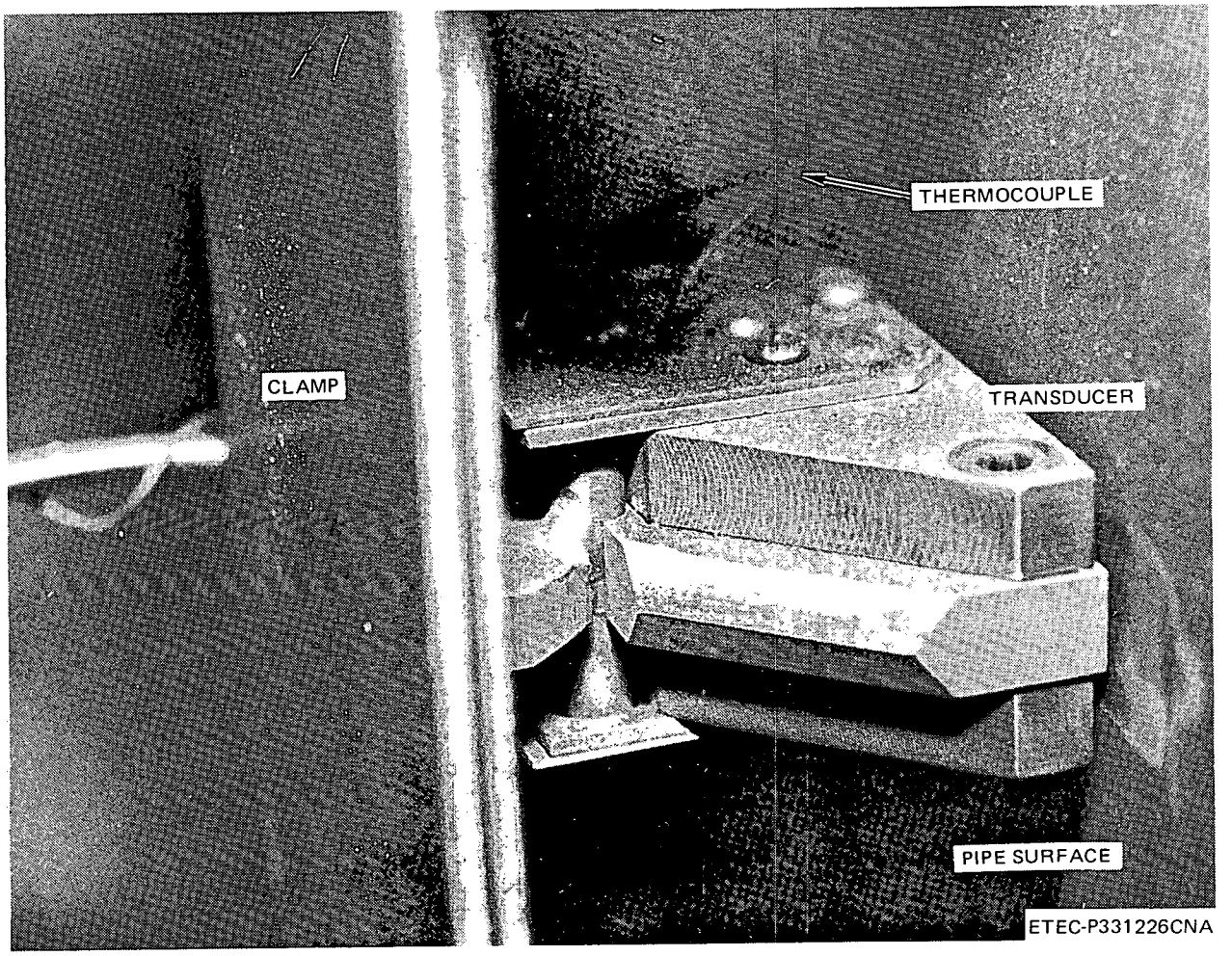

Figure IV-3. Mounted UT Transducer — In Place

In operation, the transducers, clamped on opposite sides of the pipe, are separated by a calculated distance such that the sonic pulse, initiated by an electrical pulse to the crystals, travels through the coupling block, the pipe wall, the fluid, and the opposite pipe wall and is then received by the transducer on the opposite side. The path through the fluid is set at an angle, β, to the pipe axis such that the velocity of sound, c, along the direction of the sound path is increased by the component of the fluid velocity in that direction. By interchanging the transmission and receiving functions of the two transducers, the direction of sound propagation is reversed. In this manner, time delays in the electronics, transducers, and pipe walls affect upstream and downstream travel times equally and have no effect on the time difference.

2. Saddle Coil (Electromagnetic)

As is shown in Figure IV-4, the saddle coil flowmeter is 96 in. (2.44 m) long by 31 in. (0.78 m) inside diameter. The coil assembly, weighing 416 lb (188 kg), is mounted over a 16-in. (40.6-cm) insulated pipe and is supported by six pipe clamps. Flow signals are obtained from electrodes attached to the pipe as in permanent magnet (PM) flowmeters. In order to obtain full characterization of the flowmeter, nine sets of electrodes were spaced at 12-in. (30.5-cm) intervals along the pipe. Four additional electrodes were attached downstream of the center electrode to better define the area of most probable interest (Figure IV-5). The coil was energized from a locally mounted power supply that provided up to 200 A of constant dc current. The dc power supply is an Electronics Measurement, Inc., Model SCR30-200. Its input requirements are 190 to 240 V, three-phase, 25 A, 60 Hz. The millivolt signals from all the electrodes were measured directly on the digital data acquisition system (DDAS).

3. Bypass Venturi

The flowmeter used a spare pair of pressure taps off the 16-in. venturi flowmeter and simply attached a 0.5-in. pipe from the upstream tap to the throat

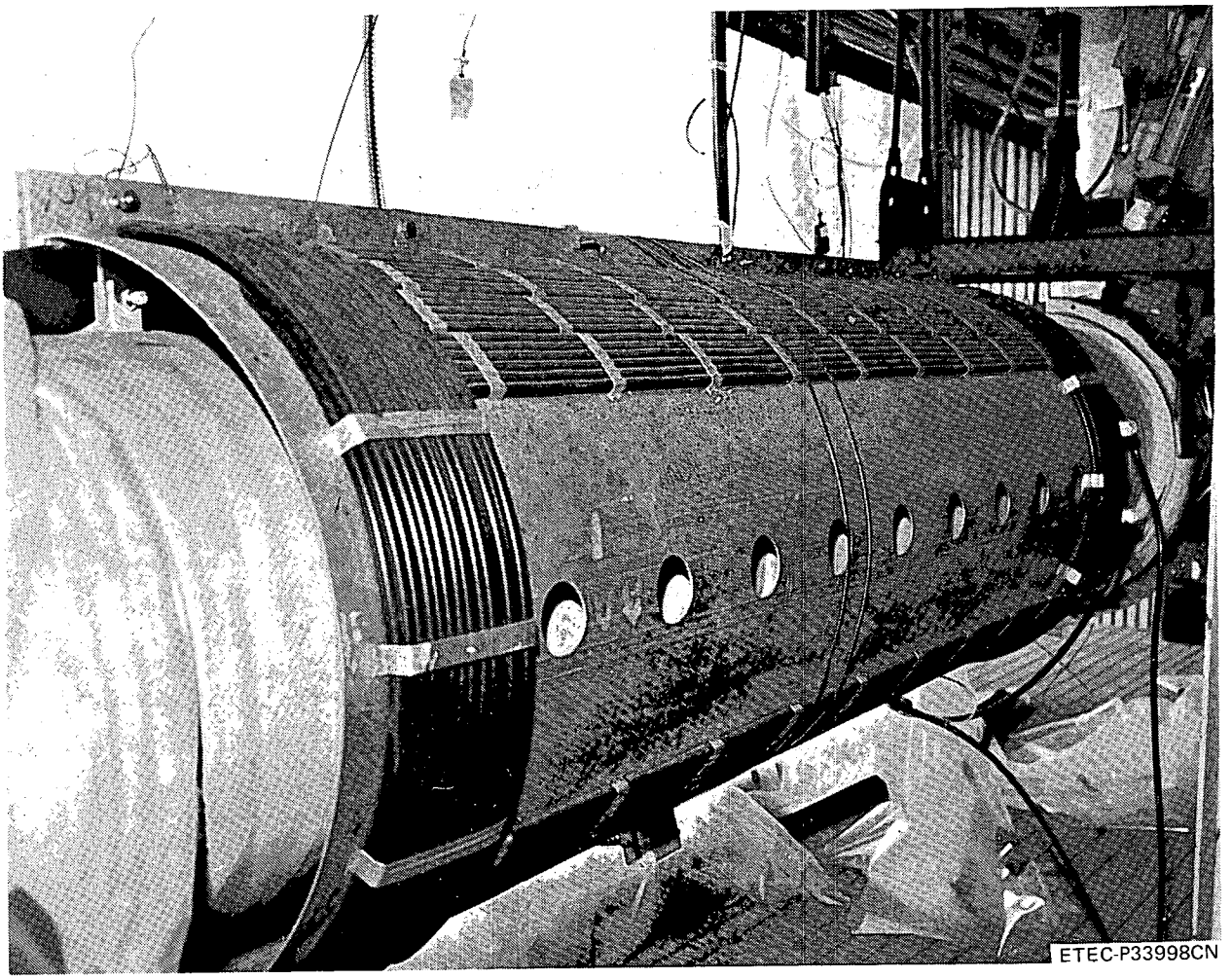

Figure IV-4. Saddle Coil Flowmeter Installation

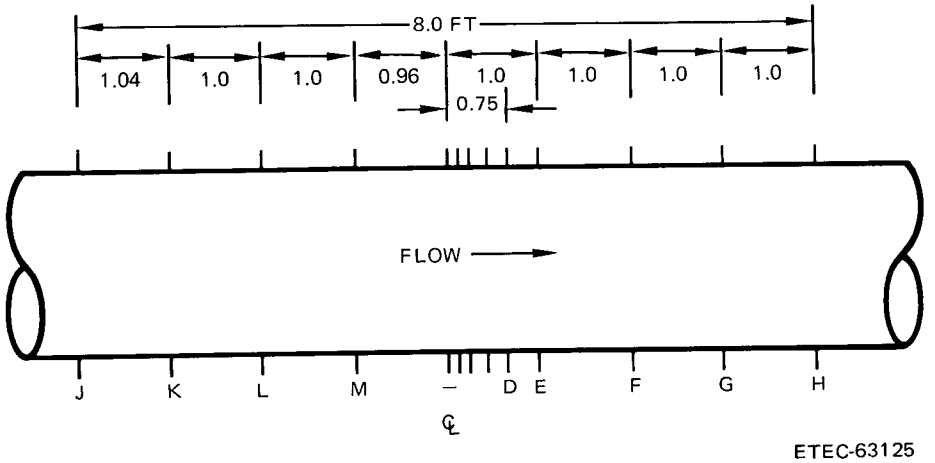

Figure IV-5. Electrode Positioning on 16-in. Pipe

tap. A pair of electrodes was attached to the 0.5-in. (1.27-cm) pipe, and a small permanent magnet was mounted on the pipe, thereby providing a PM flowmeter measurement on this bypass line (see Figure IV-6). An orifice, sized at 0.375 in. (0.95 cm), was assembled into the bypass line to satisfy a velocity limit of 30 ft/s (9.14 m/s). The output from the electrode pair was measured directly by the DDAS.

In theory, the venturi flow rate vs bypass flow rate relationship should be linear. This is due to the flow rate's dependence on the square root of the differential pressure and the same square root of differential pressure in a line that drives the flow.

C. FACILITY AND TEST METHOD DESCRIPTION

The desired temperatures and flows required for these test programs were achieved with the ISIP-II (modified FFTF) pump. All three test flowmeters are installed in the main flow loop at SPTF. There are 11.0 pipe diameters of straight-section piping between the first elbow, downstream of the pump discharge, and the centerline of the UT installation. There are 14.8 pipe diameters between the elbow and venturi upstream pressure tap. A distance of 7.7 diameters separates the first elbow and the centerline of the saddle coil flowmeter.

Sodium flow rates were set by adjusting both the pump speed and the loop resistance, which was varied by adjusting the five butterfly flow control valves.

The 16-in. venturi output was used as the reference flowmeter for the simultaneous readings from all three flowmeters.

D. TEST RESULTS

All flowmeter calibrations were conducted in conjunction with the ISIP-II Pump Test Program.

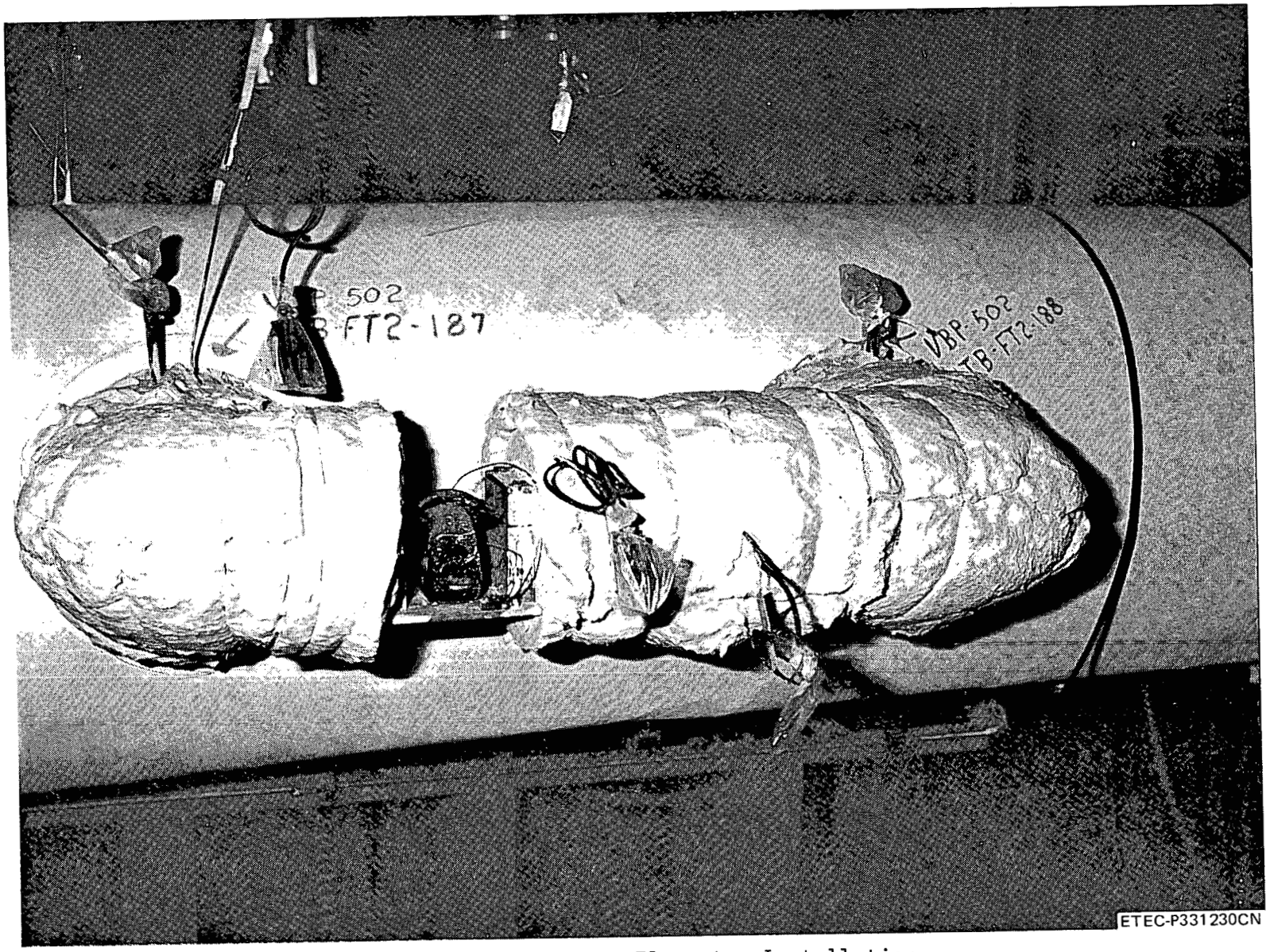

Figure IV-6. Bypass Flowmeter Installation

1. Ultrasonic

Initial pump testing included sodium flows at 400, 500, and 600°F (204.4, 260, and 315.5°C). No UT data were generated until the sodium temperature reached 700°F (371.1°C) when inner pipe walls became wetted. Once they were wetted, calibrations at all temperatures were attempted.

At all measured temperatures, digitized flow output was consistently in error on the low side by as much as 4% of the measured reference flow. Figure IV-7 is a typical UT output, along with the straight-line reference flow. Only at 400 and 600°F (204.4 and 315.5°C), however, were full-range and stable data attained. In general, electronic signal threshold voltage levels were periodically adjusted in order to attain data. When operable, the flowmeter generated a linear output with increasing flow. The nonlinearity was on the order of ±1% compared to a best-fit straight line.

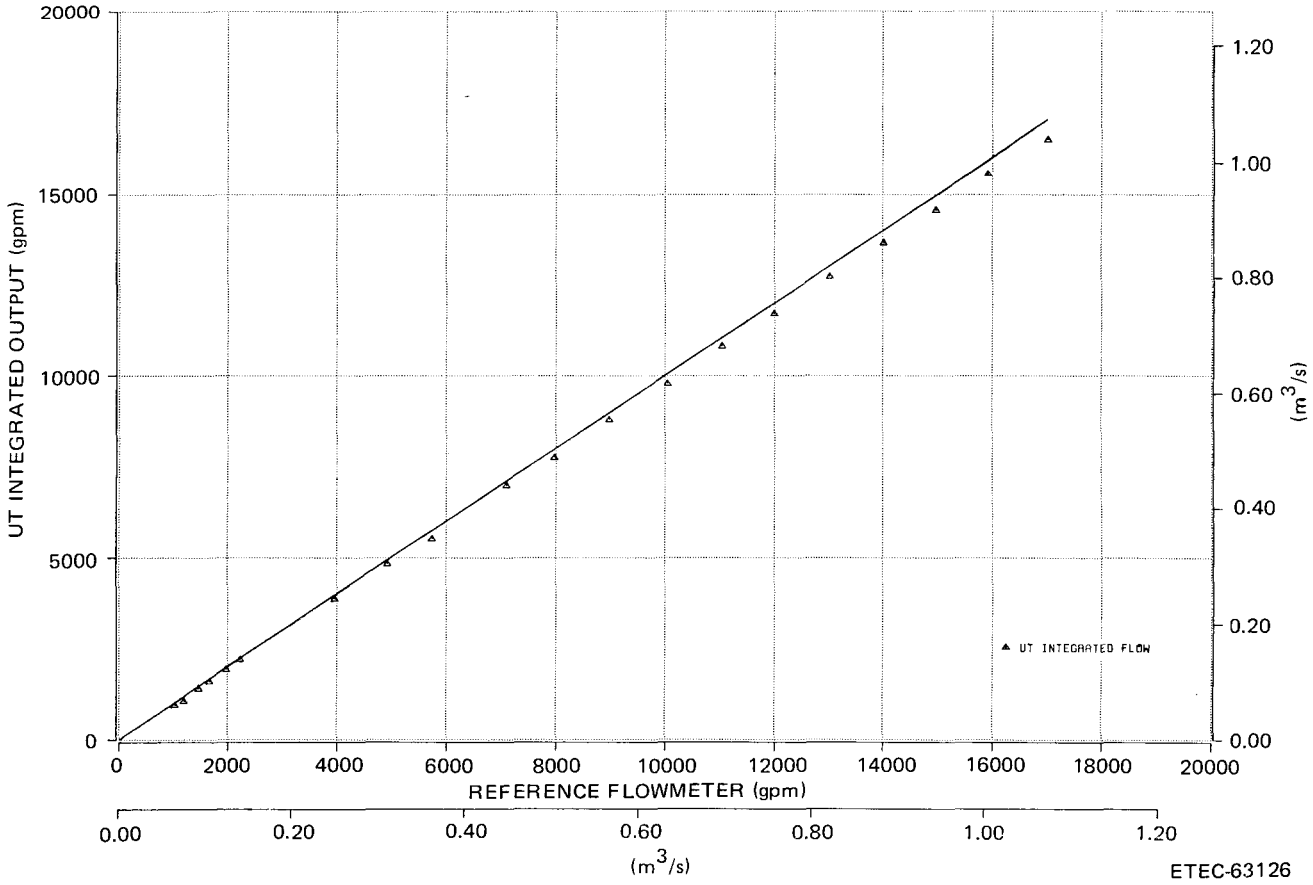

Figure IV-7. 16-in. Ultrasonic Sodium Flowmeter Calibration, 600°F, August 29, 1981

During a normal cooldown of sodium temperature from 950 to 400°F (510 to 204.4°C), the temperature-compensated flow measurement technique was evaluated while the facility maintained a nominal flow of 7500 gal/min (0.423 m^3/s). The digitized UT output flow varied only ±2% when compared to the reference flow during this cooldown. However, the full effects of temperature with flow greater than 12,000 gal/min (0.756 m^3/s) are incomplete due to malfunctioning of the UT flowmeter under those conditions.

The sensitivity of the flowmeter was measured to a flow as low as 1000 gal/min (6.3×10^{-2} m^3/s). It would appear that even lower flows would be measurable with the UT flowmeter.

2. Saddle Coil (EM)

Figure IV-8 shows the composite output from Electrode D, which is located 9 in. (22.9 cm) downstream of the center electrode, for the entire range of test temperatures. The degree of nonlinearity, however, is less than that of the 16-in. (40.6-cm) permanent magnet flowmeter results from earlier tests. Figure IV-9 shows the difference between the two at 400°F when normalized at low flow rates. All EM flow data were normalized to a coil current of 50 A.

The typical output sensitivity from each of seven pairs of electrodes over a wide flow range is plotted in Figure IV-10. This plot demonstrates the different degrees of nonlinearity as a function of axial position of the electrodes. The most linear, relative to others, is FE-108D, E, and F.

Output sensitivity as a function of electrode position is also shown in Figure IV-11. All data were normalized to Electrode Pair FE-108D. The nominal flow for these temperatures is 12,500 gal/min (0.788 m^3/s).

Flux density as measured by electrode voltage as a function of coil current is shown in Figure IV-12. Flux density varies linearly with coil current from 0 to 200 A to within less than 1%.

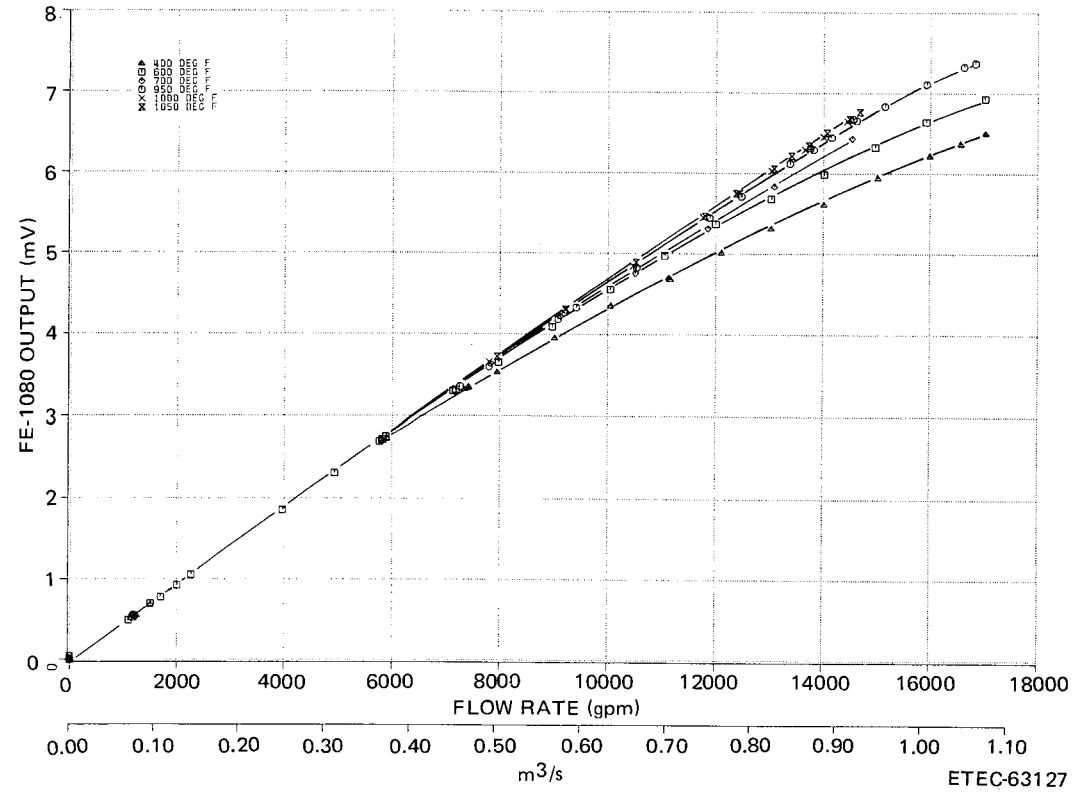

Figure IV-8. 16-in. EM Flowmeter Calibration, 50 A, August 29, 1981

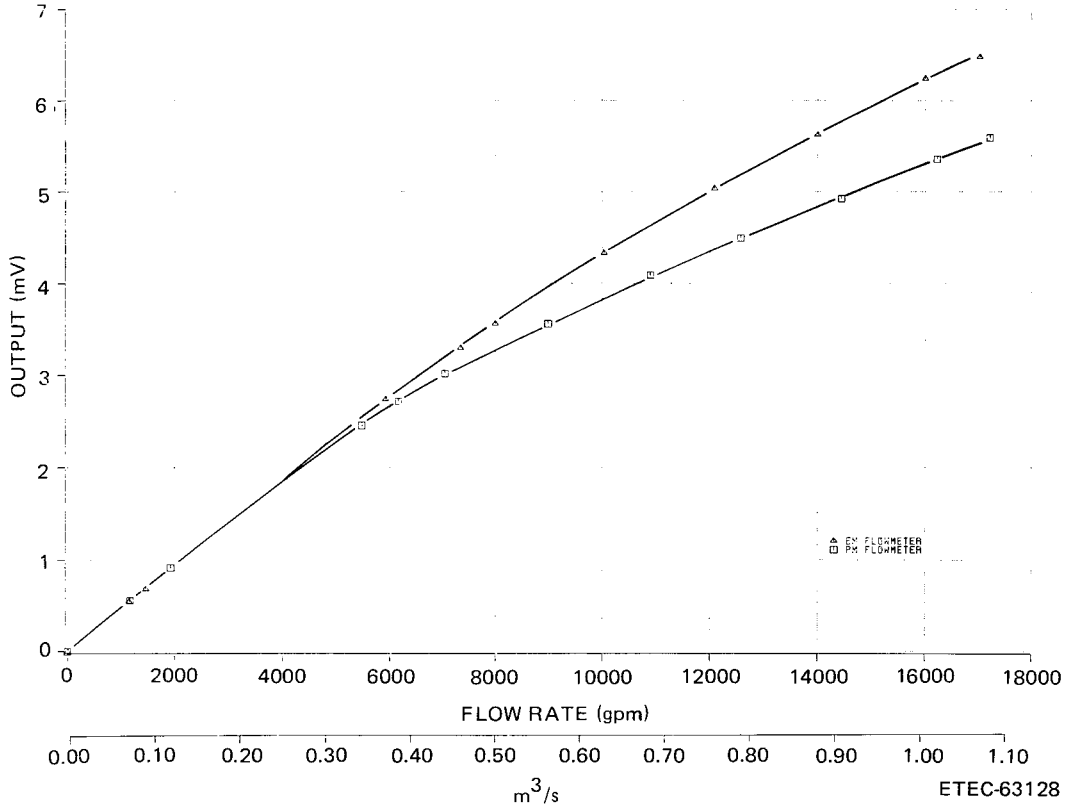

Figure IV-9. 16-in. EM and PM Flowmeter Comparison at 400°F (204°C), PM Flux Density Normalized to EM Flux Density at 22.95 gauss

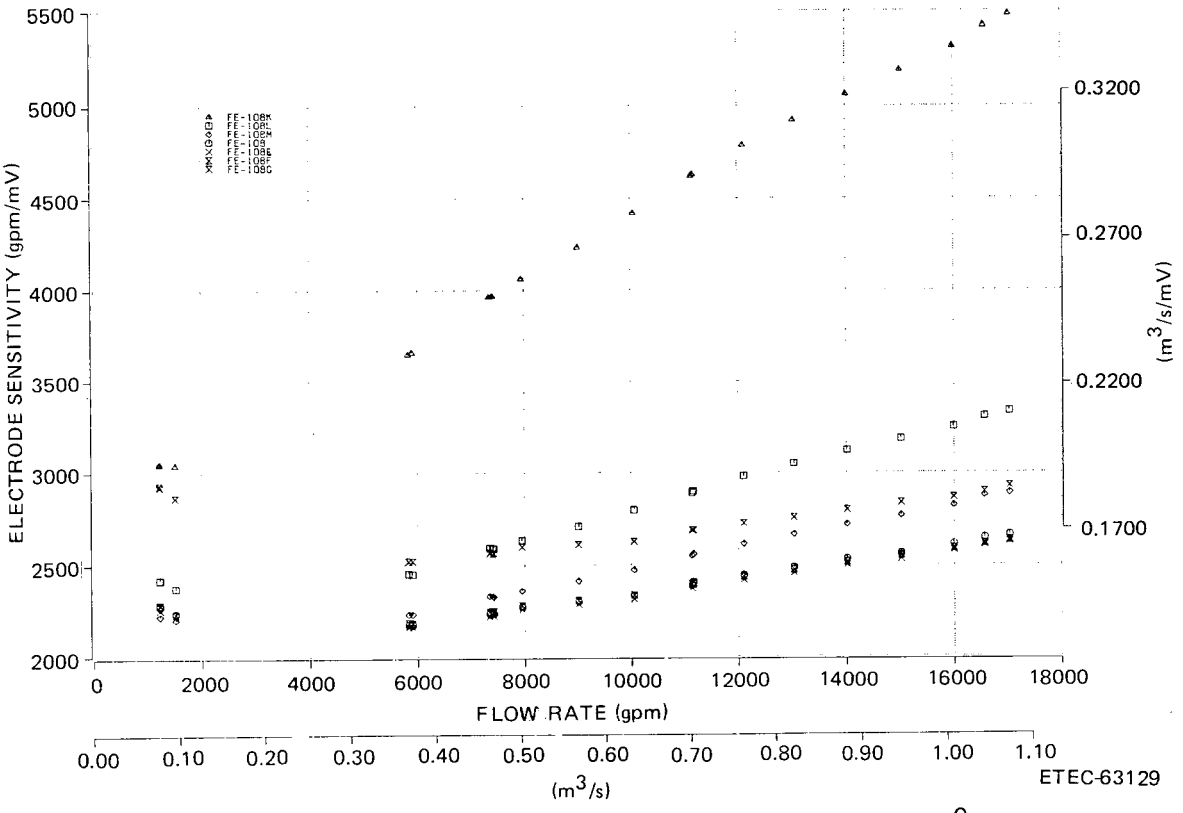

Figure IV-10. 16-in. Flowmeter Calibration, 400°F, August 29, 1981

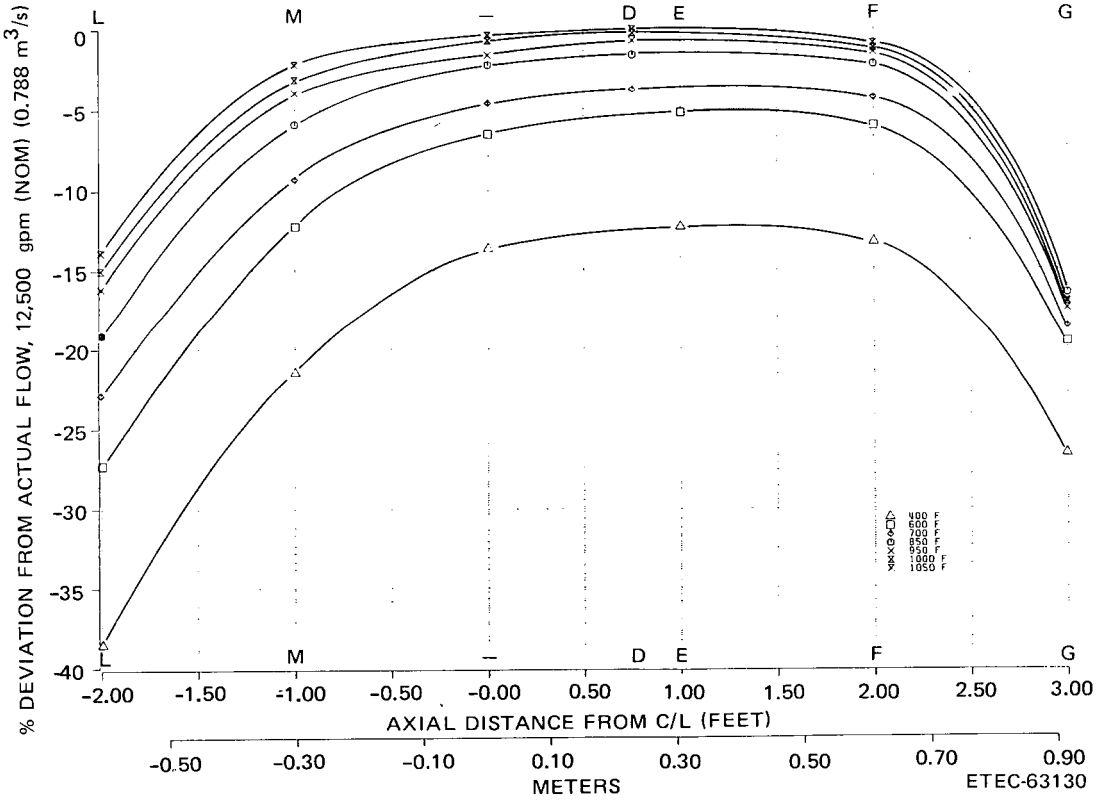

Figure IV-11. 16-in. EM FM Axial Sensitivity Variation

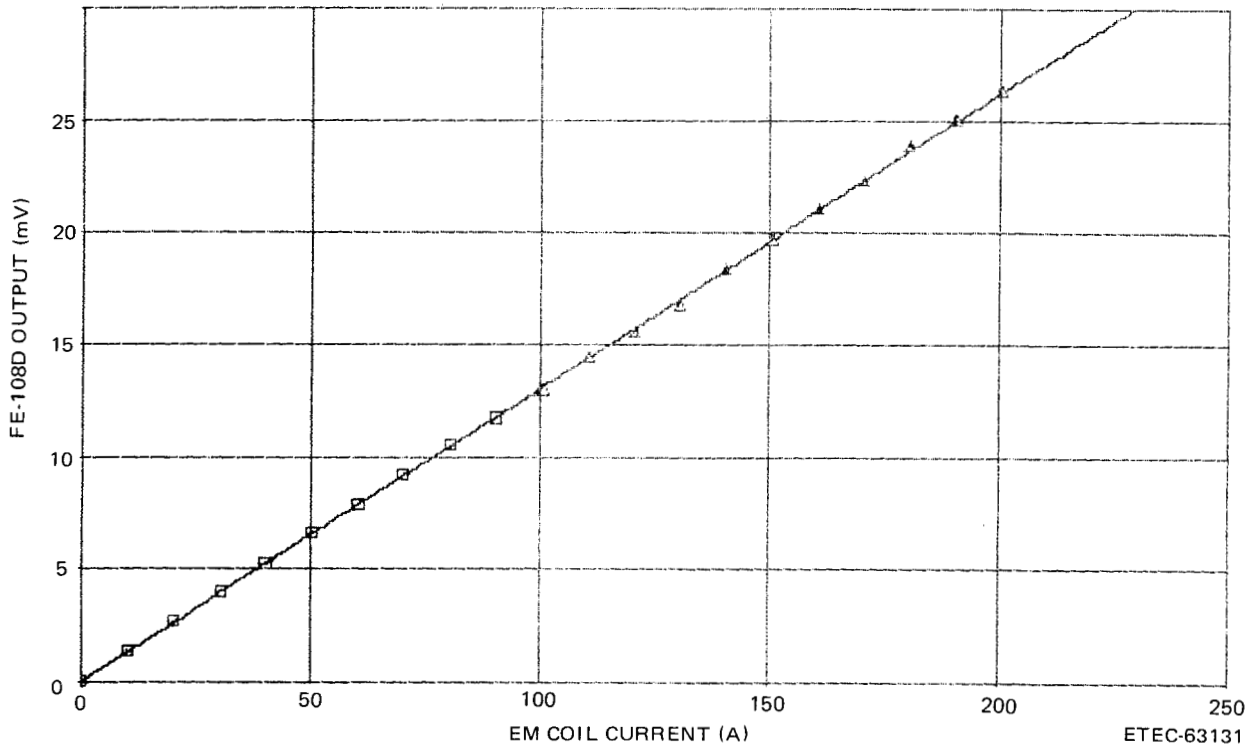

Figure IV-12. EM Flowmeter Output at a Constant Flow of 14,400 gal/min vs EM Coil Current

Some operational problems with the power supply or coil current terminations were encountered that caused occasional loss of current above 50 A. Since the exact solution could not be resolved during the pump test program, all tests were conducted at 50 A.

3. Bypass Venturi

Plotting the output of the 0.5-in. (1.27-cm) permanent magnet flowmeter mounted on the venturi bypass line against the reference venturi calculated flow rate at 600°F produces the curve shown in Figure IV-13. The plot at this temperature is typical of those produced at all temperatures. Note the as-predicted linear relationship between 1000 and 17,000 gal/min (6.3×10^{-2} to 1.07 m^3/s). Figure IV-14 is a composite plot of the bypass flowmeter outputs from 400 to 1050°F (204.4 to 565.5°C). There appear to be two groupings of data, differing by about 4% — that of 400 and 600°F (204.4 and 315.5°C) and that of the remaining temperatures. The calibrations at 400 and 600°F (204.4 and 315.5°C) were performed

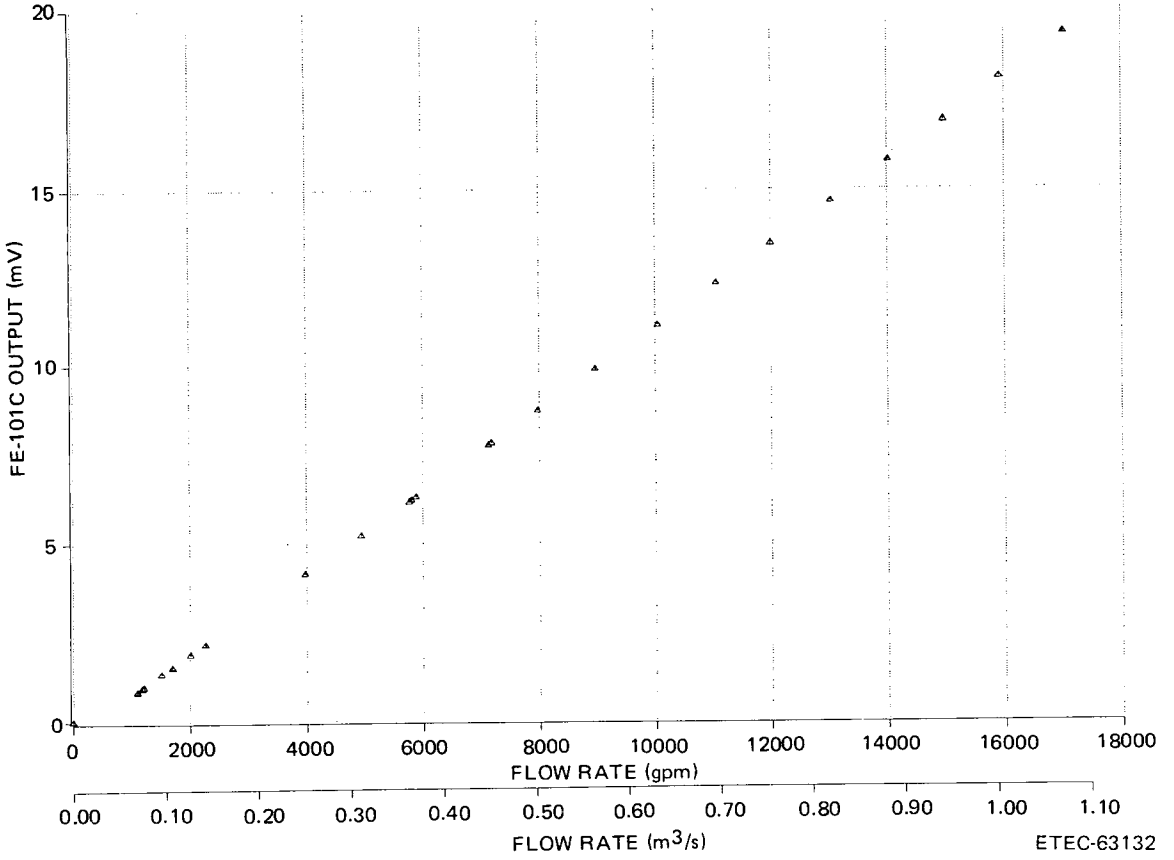

Figure IV-13. 16-in. Venturi Bypass Flowmeter Calibration, Composite Output

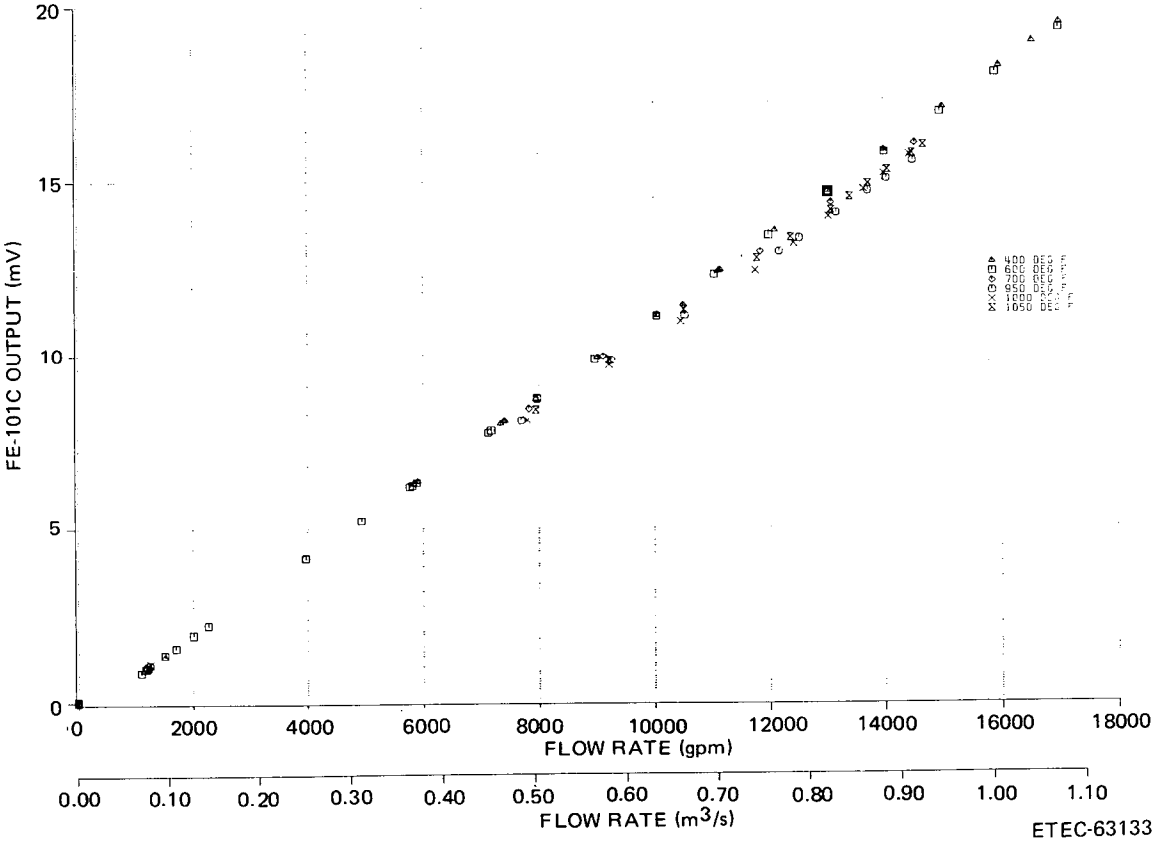

Figure IV-14. 16-in. Venturi Bypass Flowmeter Calibration Data, 600°F

at the very end of the test program. One possibility is that the orifice edge may have eroded, thereby shifting the discharge coefficient. Hence, a higher flow is generated in the bypass line for the same developed differential pressure in the venturi. The bypass line will be disassembled at a later date to verify any orifice dimensional change.

V. SODIUM LEVEL MEASUREMENT SYSTEM TESTING

J. A. KLEA

A. INTRODUCTION

During 1981, the following sodium level measurement systems were tested: (1) two second-generation continuous-measuring inductive systems procured from Westinghouse Industrial and Government Tube Division (W-IGTD); (2) a continuous-measuring inductive system procured from Mine Safety Appliances (MSA); (3) one displacement-float-type system from Fisher Controls Corp.; (4) two differential pressure systems, one procured from Barton Instrument Corp. and one from Statham Instrument Co.; and (5) a continuous-measuring inductive system with alarm set points from PNC (Hitachi) of Japan.

The PNC level measuring system testing was completed and the instrument returned to PNC (Hitachi) of Japan. A formal topical report (ETEC-81-10) that summarized all of the data accumulated over a 1-year evaluation period was published.

B. TEST FACILITY AND TEST ARTICLE DESCRIPTION

The sodium level calibration system facility is located in Building 032 at ETEC. The sodium calibration test facility (Rig 3) contains five sodium tanks used primarily for sodium level measurement system evaluation. Two of the sodium tanks are used together to perform the level calibrations on the level measuring systems under test. Each of the test tanks is equipped with four 1-in. Schedule 40 pipe thimbles and four flanged ports for access to the sodium. Tubular heaters are mounted on the tanks and covered with insulation, which permits control of the sodium temperature up to 1200^{o}F.

The test level measurement systems under evaluation use three different principles for operation. The Barton and Statham level measurement systems are delta pressure transducers, which are welded to the side of the T6 tank. Sodium

head pressure is used to determine the liquid level in this method. The Fisher level measurement system employs a float, which is used to measure the buoyant force exerted by the sodium column. This method requires the float to be in direct contact with the sodium. The third device under evaluation does not require direct contact with the sodium and is the inductive type of level transducer. This type of level measuring system consists of a probe (containing a primary and secondary coil winding, which is used as a transformer) inserted into a stainless steel thimble within the sodium tank and a signal conditioning electronics package. By exciting one coil and detecting the signal change in the other coil, the sodium level can be determined. The signal conditioner is generally located remotely from the coil-wound level probe.

The method used to calibrate the level measuring systems under evaluation is to move the sodium from one tank into another, using argon gas pressure, to set incremental sodium levels. The tank levels are positioned by using a discrete point probe (dipstick) that is inserted into one of the thimbles. The output of the probe causes a peak on a peaking meter when the balance point is at a level equal to the sodium level. An incremental scale along the probe is read to determine the distance from the top of the tank to the sodium level. At each incremental level over the range of the measuring system, the output is read out on a CRT or line printer that is part of the data acquisition system. The calibration data are also stored on magnetic tape for data reduction and reduced for graphical presentation at a later time.

1. Inductive Level Measuring Systems — PNC

The PNC level measurement system continued to undergo sodium level calibration testing at ETEC during the first 6 months of 1981. No additional problems were encountered during the sodium level calibration testing.

The first phase of the test program consisted of a series of presodium tests. A summary of the results of these tests is given in Table V-1. The second phase

TABLE V-1

PRESODIUM TESTING DATA SUMMARY
PNC LEVEL MEASURING SYSTEM, MFG. NO. 199761

PRESODIUM TESTS	
Input Voltage Effects (100-132 V)	
Zero Shift (% FR)	-0.107%
Sensitivity Shift (%)	+0.152%
Input Frequency Effects (57-63 Hz)	
Zero Shift (% FR)	+0.016%
Sensitivity Shift (%)	+0.049%
Output Load (50-500 r)	
Zero Shift (% FR)	+0.102%
Sensitivity Shift (%)	-0.208%
Cable Lengths Effects (33-300 ft)	
Zero Shift (% FR)	-0.220%
Sensitivity Shift (%)	+0.238%
Electronics Temperature Effects (32-140^{O}F)	
Zero Shift (% FR)	+0.516%
Sensitivity Shift (%)	+0.217%
Cable Temperature Effects (32-140^{O}F)	
Zero Shift (% FR)	-0.055%
Sensitivity Shift (%)	+0.033%
Time Response	∿340 ms
Short-Term Stability (% FR), 7 Days	
Zero Shift	+0.70%

of the testing consisted of a series of sodium level calibrations at temperatures between 300 and 1100°F (149 and 593°C). The zero shift and sensitivity shift at the various sodium test temperatures can be evaluated by reviewing Figures V-1 and V-2. In Figure V-1, a negative zero shift with time can be observed. While the drift is relatively small, ~2% of full scale per year, periodic re-zeroing would be required. Figure V-2 shows the sensitivity shift vs time at each repeated sodium level calibration temperature. The sensitivity shift does not display a positive or negative trend.

The system also contains discrete level sensors at the 30 and 70% points of the 63-in. (160-cm) measurement range. Their performance as alarm functions and/or in-place calibration points can be evaluated by reviewing Figures V-3 and V-4. Figure V-3 shows the 30% discrete point function output in dimensional units (centimeters) vs time for each of the test temperatures. The 30% output value appears to be repeatable within ±1.5 cm of the designed alarm output value (48 cm). Figure V-4 is the 70% discrete point output (designed to be 112 cm) in centimeters vs time, which also appears stable (within ±1.5 cm) and independent of temperature with the exception of the few points that appeared during the 300°F (149°C) level calibration testing.

The sodium level calibration evaluation testing of the PNC level measurement system was completed in June of 1981. At that time, the unit was removed from the sodium test facility, repackaged into the original containers, and shipped back to Japan within the 1-year loan period.

A formal report entitled "PNC Sodium Level Measuring System Performance Test," ETEC-81-10, has been published. The report summarizes all of the evaluation testing results on the PNC sodium level measurement device.

2. Inductive Level Measuring Systems – Westinghouse (W-IGTD)

During the past year, both of the second-generation signal conditioners were subjected to sodium level calibration testing. They were matched with existing

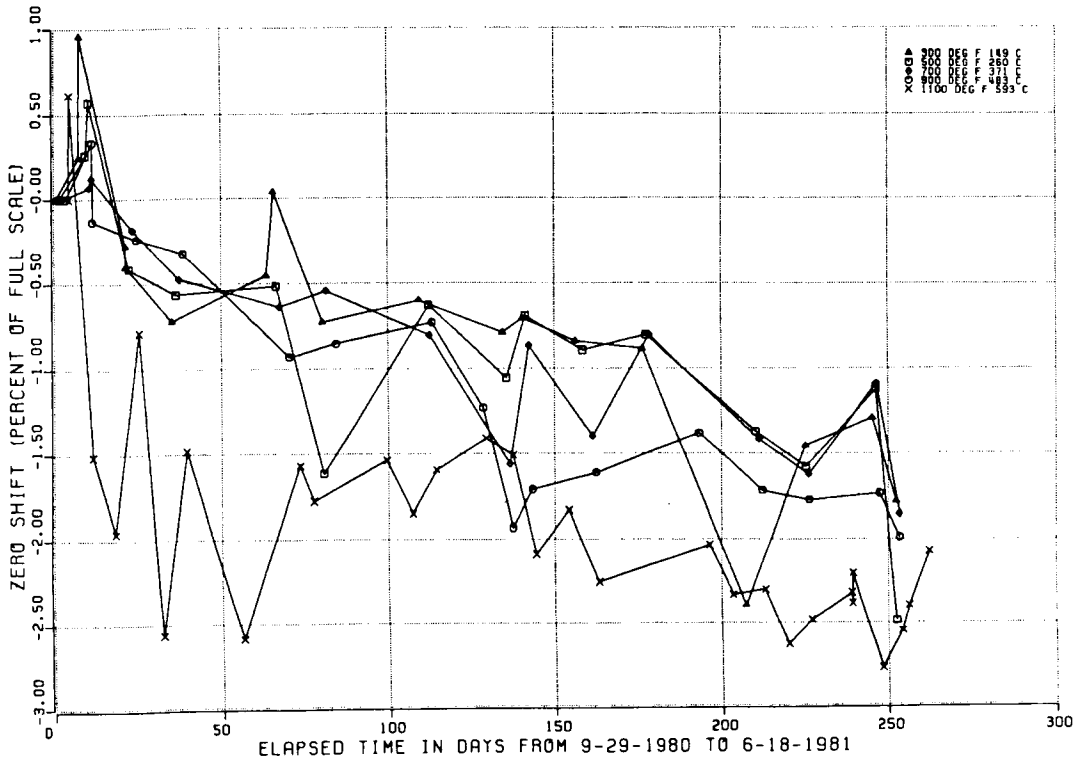

Figure V-1. PNC Level Measuring System — Composite 300 to 1100°F (149 to 593°C) Sodium System Using First Calibration at Each Temperature as Reference — Zero Shift

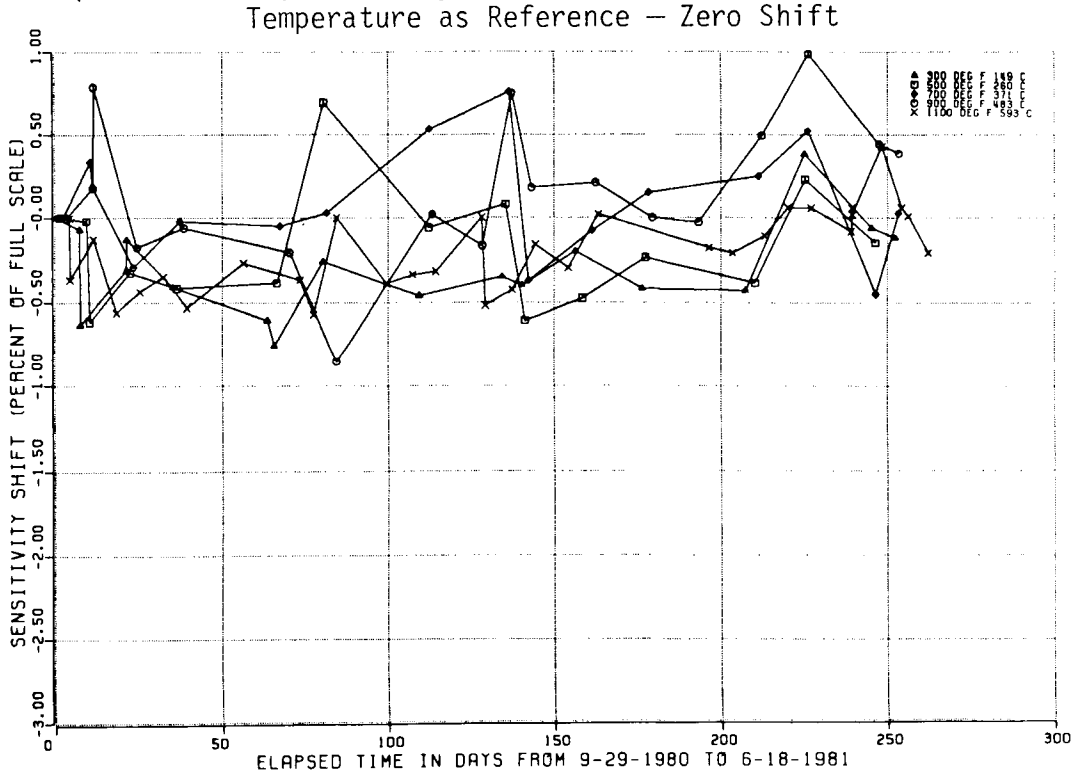

Figure V-2. PNC Level Measuring System — Composite 300 to 1100°F (149 to 593°C) Sodium System Using First Calibration at Each Temperature as Reference — Sensitivity Shift

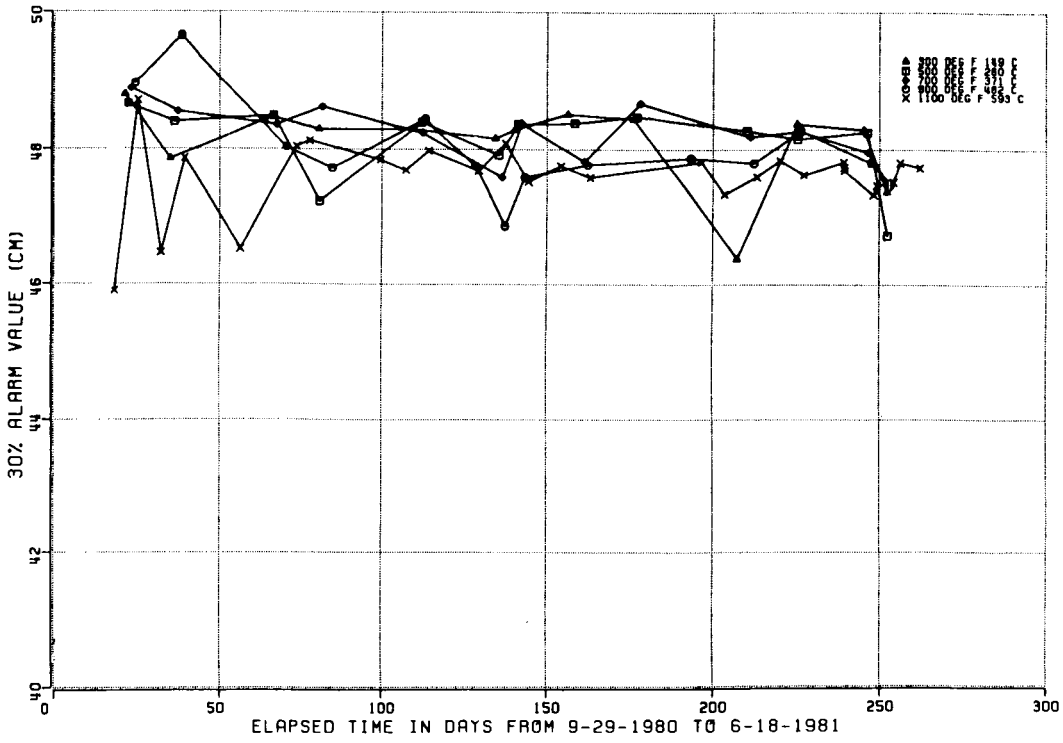

Figure V-3. PNC Level Measuring System — 300 to 1100°F (149 to 593°C) Sodium Calibration Composite of 30% Alarm Values

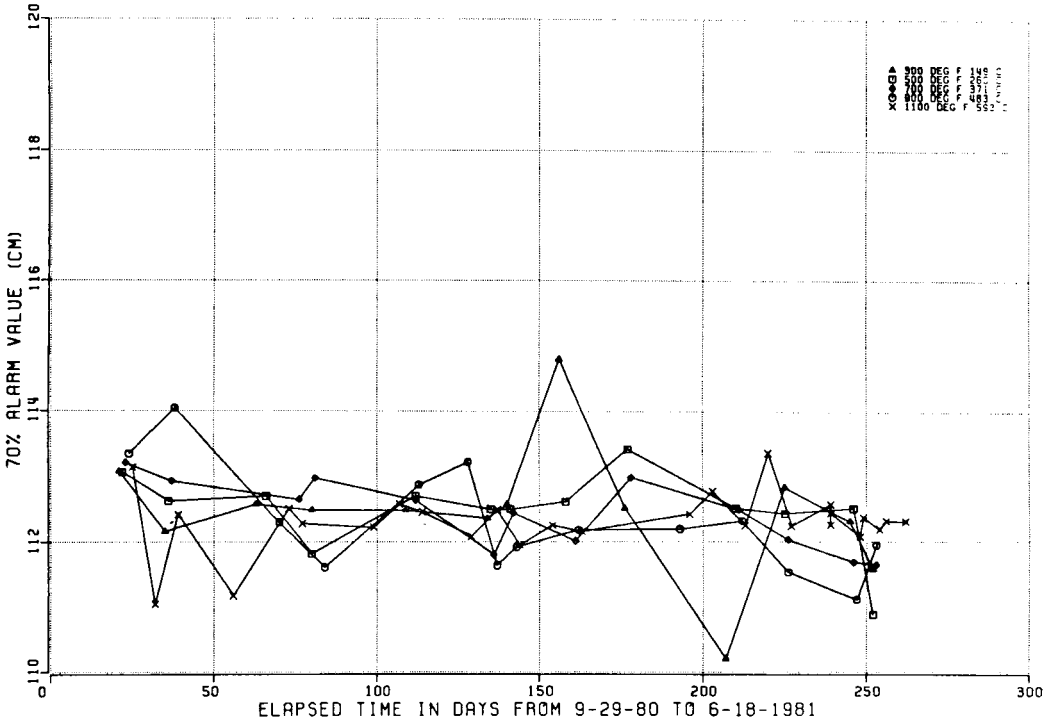

Figure V-4. PNC Level Measuring System — 300 to 1100°F (149 to 593°C) Sodium Calibration Composite of 70% Alarm Values

20-in. (50.8-cm) and 10-ft (304.8-cm) measurement range level transducers. The calibration testing only occurred over the first half of the year, as another test program utilized the level test facility during the second half. During this period, the units were exposed to high-temperature sodium but not undergoing continuous level calibrations. Both units were operating satisfactorily before the inactive period. Level calibration testing of these devices resumed in late 1981.

3. Inductive Level Measuring Systems – Mine Safety Appliances

At about mid-year, the remaining 20-in. (50.8-cm) level measuring system from MSA failed. The level transducer was tested for continuity and found to be open circuit. The transducer was X-rayed, and a break was found in both coils. The device will be sectioned for further examination.

A formal report covering the evaluation test results that occurred over the 4-year period will be written and published in early 1982.

4. Inductive Level Measuring Systems – Kaman

During the past year, one of two Kaman (S/N 7880) level measurement systems was repaired and working for a period of time. The zero and sensitivity shifts exceeded 30% over the test temperature range of 300 to 1200°F (149 to 649°C). This transducer also failed prior to mid-year. At present, both of the systems fail to respond to sodium level changes. Additional efforts to modify the signal conditioners and get them working will be made in 1982.

5. Displacement Level Measuring Systems – Fisher

One 10-ft (304.8-cm) displacement-float-type level measuring system is under evaluation at ETEC. The transducer continues to operate in a satisfactory manner as long as the transducer head is kept at ~300°F (149°C). This heating is necessary to prevent sodium vapor from depositing on the mechanical linkage, which

would inhibit freedom of movement of the float. The disadvantage of this system is that the sodium boundary must be entered in order for this principle of operation to function. This type of unit, because of its cost and reliability, is used in many sodium facility tanks at ETEC.

6. Delta Pressure Level Measuring System – Barton

A Barton NaK capillary level measuring transducer remains under evaluation test at ETEC. For several years, the device exhibited nonlinear characteristics in the area of 15 to 16%. During 1980, the zero and span controls were adjusted and the nonlinearity was improved, but only to about 9%. It was suspected that the manner in which the sensors were attached to the tank might be influencing the linearity of the sensing device. Both of the sensors were welded to elbows and mounted in a vertical direction, one of the sensors at the near bottom cylindrical surface of the tank and one on the cylindrical surface near the top. With the elbow configuration, the sodium would always drain out of the sensor to permit removal if required. However, with this arrangement, a gas pocket formed between the sodium surface and the pressure transducer diaphragm. Of course, this gas pocket would be compressible, depending on the tank head pressure and the sodium temperature. In early 1981, the tank (T8) was completely drained of sodium and the pressure transducer sensors were cut from the tank. The sensor bellows were cleaned of any sodium residue and examined for any cracks or imperfections; none was found. Next, the device was sent to the calibration laboratory, where a calibration was performed using gas as the sensing medium. Additional efforts were made to adjust the zero and span controls of the device to idealize the milliamp output (4 to 20 mA) to match the pressure equivalent to 120 in. of sodium at $900^{o}F$ ($482^{o}C$). After the laboratory calibration, the sensors were rewelded to the T8 sodium tank. The bottom sensor was welded to the tank in the opposite direction, however. The elbow configuration remained but the sensing diaphragm was lower than the tank port. In this manner, sodium would always remain on the diaphragm because it was no longer self-draining.

Figure V-5 shows the calibration data of the Barton delta pressure transducer before the device was removed from the tank. Figure V-6 shows a calibration at approximately the same sodium temperature after the transducer was recalibrated in the laboratory and the bottom sensor was rewelded to the tank in a downward fashion. The fourth column of data, to the right, indicates the difference between an end-point line and actual data values. This difference is the linearity error of the device. It may be noted that the linearity greatly improved after the modification to the standard installation configuration.

7. Delta Pressure Level Measuring System – Statham

Since the Statham delta pressure transducer exhibited nonlinear characteristics similar to the Barton transducer, it, too, was removed at the same time as the Barton. It was cleaned, examined, recalibrated in the laboratory, and reinstalled in the same manner as the Barton transducer. Figure V-7 indicates a typical calibration prior to the modification, and Figure V-8 reveals the calibration results after the modification. The linearity can be seen to have improved by an order of magnitude. Additional evaluation testing will be continued during 1982.

BARTON LEVEL PR XDUCER SN 368-132

SODIUM TEMPERATURE = 1218 DEGREES F. SENSITIVITY = .12598 MA PER INCH
SODIUM CALIBRATION 12/15/80 AT 15:35 ZERO VALUE = 4.23058 MA
TANK 6 STICK = M2059 RANGE VALUE = 19.34873 MA

TECH.
PROC. 232-TP-100
PAR. 13.7

TEST DATA		END POINT FIT	
LEVEL(INCH)	OUTPUT(MA)	CURVE VAL	% DIFF
120.00	19.349	19.349	.000
107.75	17.385	17.805	2.780
96.00	15.679	16.325	4.276
71.75	12.303	13.270	6.397
60.00	10.634	11.790	7.646
48.00	8.998	10.278	8.464
23.75	6.437	7.223	5.196
12.00	5.322	5.742	2.782
-.25	4.199	4.199	.000

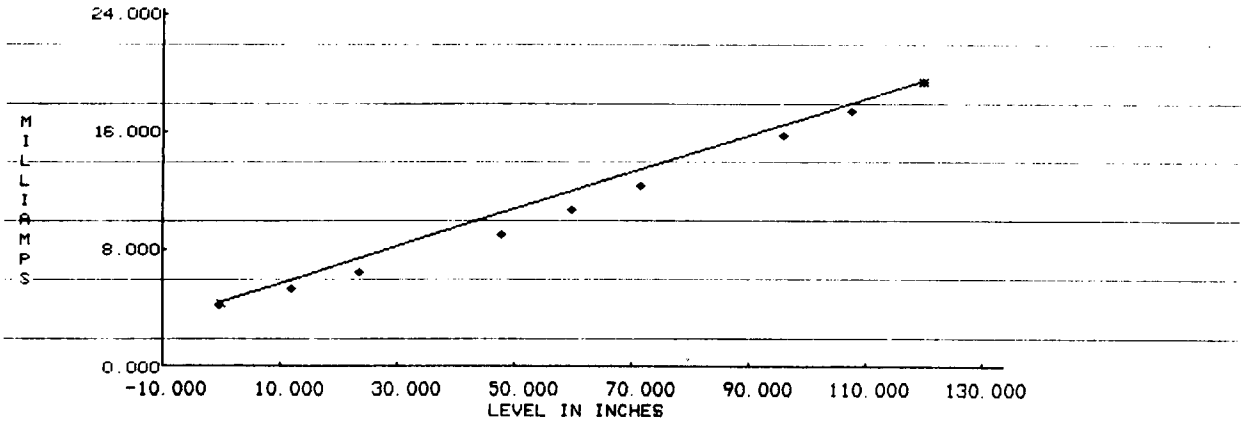

Figure V-5. Barton Level Transducer (SN 368-132) Calibration Test Prior to Installation Modification

BARTON LEVEL PR XDUCER SN 368-132

SODIUM TEMPERATURE = 1184 DEGREES F. SENSITIVITY = .11478 MA PER INCH
SODIUM CALIBRATION 3/ 3/81 AT 10:42 ZERO VALUE = 5.02867 MA
TANK 7 STICK = M5727 RANGE VALUE = 18.80232 MA

TECH.
PROC. 232-TP-100
PAR. 13.9

TEST DATA		END POINT FIT	
LEVEL(INCH)	OUTPUT(MA)	CURVE VAL	% DIFF
.00	5.029	5.029	.000
12.00	6.305	6.406	.735
24.00	7.700	7.783	.609
48.00	10.412	10.538	.918
60.00	11.824	11.915	.666
72.00	13.190	13.293	.748
96.00	15.998	16.048	.360
108.00	17.424	17.425	.008
120.00	18.802	18.802	.000

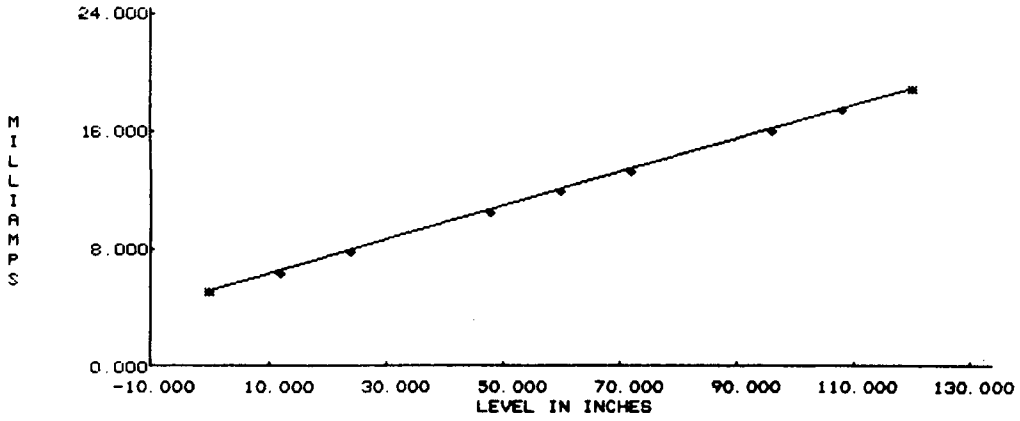

Figure V-6. Barton Level Transducer (SN 368-132) Calibration Test After Installation Modification

STATHAM LEVEL PR XDUCER SN S62-2

SODIUM TEMPERATURE = 493 DEGREES F.
SODIUM CALIBRATION 12/18/80 AT 15:29
TANK 6 STICK = M5727

SENSITIVITY = -.10853 MA PER INCH
ZERO VALUE = 18.22940 MA
RANGE VALUE = 5.20535 MA

TECH.
PROC.
PAR.

TEST DATA LEVEL(INCH)	OUTPUT(MA)	END POINT FIT CURVE VAL	% DIFF
120.00	5.205	5.205	.000
108.00	5.416	6.508	-8.382
96.00	6.847	7.810	-7.397
71.99	9.593	10.417	-6.323
60.00	10.799	11.717	-7.048
48.00	12.412	13.020	-4.666
23.75	15.387	15.652	-2.036
12.00	16.916	16.927	-.081
.00	18.229	18.229	.000

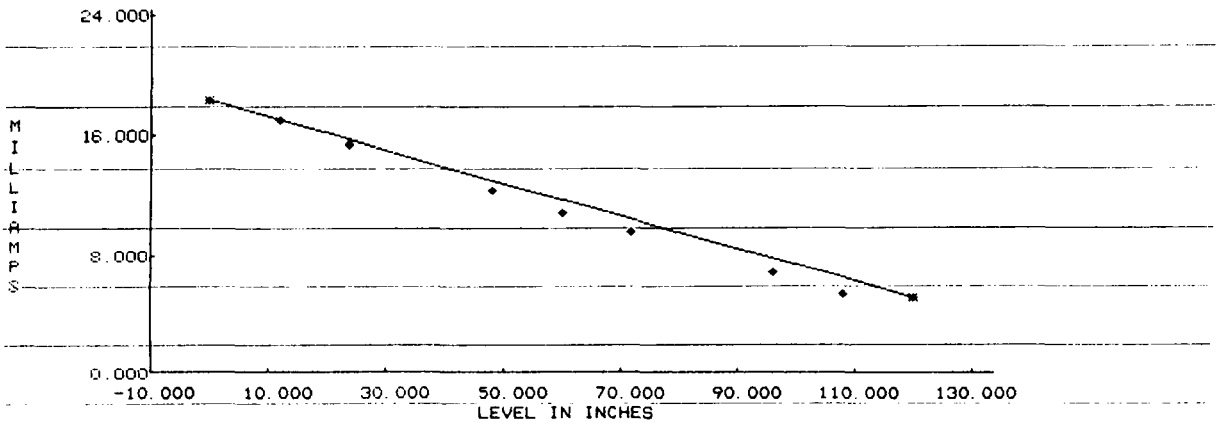

Figure V-7. Statham Level Transducer (SN S62-2) Calibration Test Prior to Installation Modification

STATHAM LEVEL PR XDUCER SN S62-2

SODIUM TEMPERATURE = 514 DEGREES F.
SODIUM CALIBRATION 3/ 9/81 AT 8:53
TANK 6 STICK = M2059

SENSITIVITY = -.11955 MA PER INCH
ZERO VALUE = 19.32665 MA
RANGE VALUE = 4.98089 MA

TECH.
PROC.
PAR.

TEST DATA LEVEL(INCH)	OUTPUT(MA)	END POINT FIT CURVE VAL	% DIFF
120.00	4.981	4.981	.000
108.00	6.281	6.415	-.935
96.00	7.728	7.850	-.848
72.00	10.599	10.719	-.839
60.00	12.048	12.154	-.734
48.00	13.531	13.588	-.402
24.00	16.424	16.457	-.236
12.00	17.895	17.892	.017
.00	19.327	19.327	.000

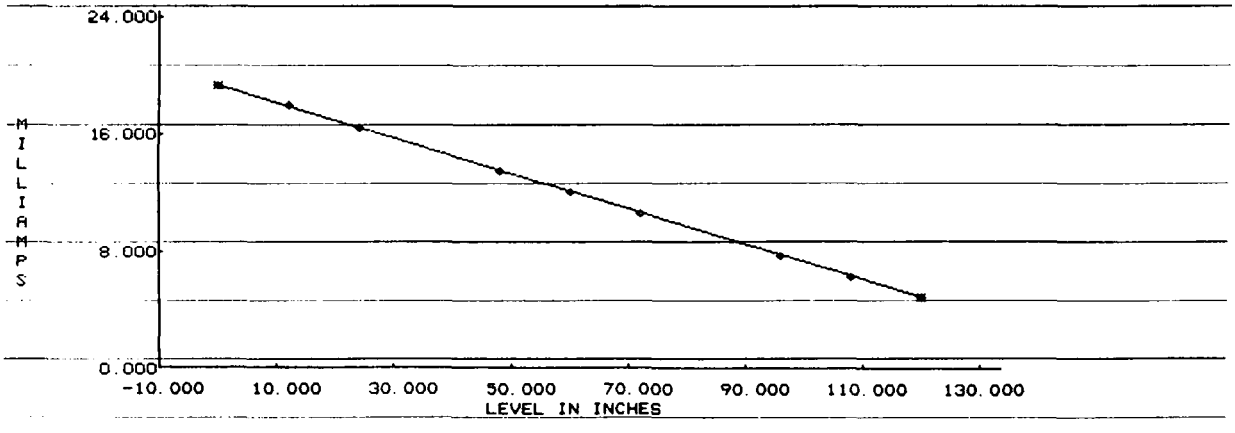

Figure V-8. Statham Level Transducer (SN S62-2) Calibration Test After Installation Modification

VI. ELECTRICAL RESISTANCE HEATER TESTS — TUBULAR HEATERS

J. A. KLEA

A. INTRODUCTION

An electrical heater evaluation test program is being conducted at ETEC. Heaters from several manufacturers are being evaluated to determine heater quality, reliability, and expected lift vs heater size (diameter) and configuration. Tubular heaters are used throughout sodium facilities and sodium-cooled fast breeder reactors for preheating sodium lines, tanks, valves, and various components. The importance of ensuring that a quality heater is available for use in order to minimize failures (which may perturb test programs or plant operation) is vital to industry.

ETEC's accelerated life test facility is a wire-screen-enclosed 10 x 25 ft (3 x 7.5 m) area located in Building 057. Within the enclosed area are nine oven-like test boxes in which the heaters are installed. A typical test heater installation is shown in Figure VI-1 with the enclosure top removed. Each heater is supported over its length by several small-diameter wires to reduce "sag" at elevated temperature while minimizing thermal loss and hot-spot formation. The tubular heaters shown are being tested in the straight configuration. The small beaded wires shown attached to the heater surface are thermocouples, which are used to measure heater surface temperature.

Heaters are tested in both straight and bent configurations ("U" or hairpin shape). During the past year, much of the testing was accomplished on the 3/8-in.-diameter (1.27-cm) heaters tested in the straight configuration.

The accelerated thermal life test is the primary test being used to evaluate heater quality and reliability. In addition, a comparison of three manufacturers' heaters is being made to evaluate the variation in heater life expectancy of each.

Figure VI-1. Typical Heater Test Installation

All of the tubular heaters being evaluated and tested were manufactured to RDT Standard P 43-T in one of two grades (Grade I or Grade II). After the heaters are fully X-rayed, they are installed into the enclosures shown in Figure VI-1. The heaters are connected to a three-phase 480-V variable voltage supply. Voltage to each heater is increased until its sheath temperature attains 1700°F ± 25 (920°C ± 14). A rigorous on-off power cycle is started. The cycle consists of 5 min at full power and 10 min with the power off. During the "on" cycle, the heater sheath temperature will achieve 1700°F ± 25 (920°C ± 14) before the power goes off. During the "off" cycle, the heater sheath typically cools to ∿900-1000°F (482.2-593.3°C) before power is applied again. After each 500-1000 thermal cycles, the heaters are permitted to cool to ambient temperature. At this time, several parameters such as coil resistance and insulation resistance are measured. These parameters are monitored periodically for indications of heater degradation. The evaluation heaters are continuously subjected to this thermal cycling until heater failure occurs. When a heater fails, it typically trips the ground fault interrupter protection system. The heater is then removed from the enclosure, X-rayed to determine the location of the failure, and dissected for visual examination; then the failed area is photographed.

B. TEST RESULTS

In the past year, ten tubular heaters were tested until failure occurred. A summary of the accelerated life test results, based on the number of accumulated thermal life test cycles, is presented in Table VI-1. The heaters whose serial numbers are underlined are those which have failed during the past year.

During the past 12 months, the accelerated life testing was accomplished on the 3/8-in.-diameter (0.953-cm) heaters. The Grade I Rama and Chromalox heaters appear to have similar life expectancy based on the 3/8-in.-diameter (0.953-cm) heaters tested. This is significantly different from the 1/2-in.-diameter (1.27-cm) heaters, where the Chromalox heater displayed a greater expected life. The

TABLE VI-1

HEATER ACCELERATED LIFE TEST MATRIX

Diameter (in.)	Grade	Rated Voltage (V)	MgO Density (g/cm^3)	Shape	Heater Manufacturer					
					Rama		Hesco		Chromalox	
					S/N	Cycles	S/N	Cycles	S/N	Cycles
1/2	I	480	>3.0	Straight	74-146	762	74-134	5,309	75-128	36,957
					74-147	3,071*	74-135	5,315	75-129	31,159
					74-148	766	74-136	5,208	75-130	36,700
	II	480		Straight	75-164	8,371	75-171	9,627	75-134	6,980
					75-165	15,092†	75-172	9,722	75-136	11,762
					75-166	15,092§	75-173	9,609	75-137	12,826
	I	480		S-Bend	74-149	4,878	74-137	5,039	75-134	25,055
					78-143	3,745	74-138	7,387	75-132	8,497
	I	480		Hairpin Bend	78-141	10,346	74-139	4,512	75-133	8,359
					78-142	15,886	-	-	75-131	15,029
			<3.0		75-157	6,622	75-178	1,709	75-142	15,703
					75-158	1,776	75-179	1,654	75-143	6,618
3/8	I	480	>3.0	Straight	76-17	15,980	76-59	3,925	76-101	13,160
					76-18	10,126	76-60	10,646	76-102	11,428
					76-19	16,649	76-61	6,956	76-103	In Test
	II	480		Straight	76-38	13,746	76-80	7,076	76-122	77
					76-39	7,720	76-81	280	76-123	33,691
					76-40	2,802	76-82	13,140	76-124	380
	I	480		Hairpin Bend	76-20	9,547	76-63	12,836	76-105	13,350
					76-21	2,703	76-64	57	76-106	15,145
					76-22	2,487	76-65	1,017	76-107	27,638

*Test terminated: No failure
†Test terminated: 70% resistance change
§Test terminated: 117% resistance change

Test Conditions

Cycle = 5 min "on" and 10 min "off"
Maximum sheath temperature: 1700°F
Periodic parameter checks

Grade II Rama heaters (3/8-in or 0.953-cm diameter) and the hairpin Rama heaters indicate a significantly shorter average life than the straight Grade I Rama heaters. The Grade II Chromalox heaters demonstrate a wide dispersion of test results. The Chromalox Grade I heaters in the hairpin-bend configuration indicate a longer average life than those in the straight configuration. This is contrary to much of the previous test results on the 1/2-in.-diameter (1.27-cm) heaters. The Hesco-manufactured heaters exhibited the poorest expected life of the three manufacturers' products tested. Their performance indicates a poorer expected average life in the 3/8-in.-diameter (0.953-cm) heater whether tested in the straight or hairpin-bend configuration.

In summary, the following conclusions seem to be emerging from these tests:

1) The best grade (Grade I) of 1/2-in.-diameter (1.27-cm) Chromalox heater still has more than 100% longer life expectancy than any other heater, independent of manufacturer, grade, or size (diameter) tested thus far.
2) Heaters that have a bend radius of at least four times the heater diameter in the heated section exhibit a reduced life expectancy.
3) In general, the 1/2-in.-diameter (1.27-cm) heaters appear to have a longer average expected life than the 3/8-in.-diameter (0.953-cm) heaters.

VII. MINERAL-INSULATED HEATER CABLE EVALUATION TEST

K. A. DAVIS

A. INTRODUCTION

The ETEC effort to evaluate the applicability of mineral-insulated (MI) heater cable to sodium heat transfer systems was begun in 1978. Interest in the use of MI cable was stimulated by reports of widespread use in some foreign countries and satisfactory operation in one U.S. sodium heat transfer system. The testing program was expanded in 1979 when the use of MI cable was proposed for many systems in the Clinch River Breeder Reactor Plant. This proposal was based upon the belief that the material and installation cost of MI cable and the ease of application on certain components might be more advantageous than the ordinarily used tubular heaters (heaters in which the element wire is in the form of a helix).

The initial types of tests were: (1) accelerated life, (2) prototype pipe, and (3) bend. As initially planned, these have been completed, and most of the results were in last year's report. During 1981, more accelerated life and prototype pipe tests were added and, in addition, a CRBRP prototype verification test was started.

B. TEST DESCRIPTION

1. Test Facility

The accelerated life tests were performed in an existing facility which provided for each heater: (1) a support in an insulated enclosure, (2) an electrical power supply controlled by a circuit to allow thermal cycling of the heater, and (3) instrumentation for temperature control, recording, cycle counting, and failure indication.

The prototype pipe tests were performed in a facility constructed for this series of tests. Initially it consisted of 24 test stands. Half of these contained 203-mm-diameter (8-in. nominal) pipes and the other half contained 33.4-mm-diameter (1-in. nominal) pipes. The test heaters were mounted on these pipes and the assemblies insulated with blanket-type insulation. The facility included an electrical power supply with controllers to maintain the temperature of the pipes at 516°C (960°F) and a data logger for temperature recording. At mid-year, when the tests on many of the test stands were completed and the facility had to be moved into another building, only 12 stands (those for the 8-in. pipes) were assembled in the new building.

The facility for the prototype verification tests was constructed adjacent to the prototype pipe test after the move to the new building. As initially planned, this facility was to consist of a system of 60.3-mm-diameter (2-in. nominal) pipe with horizontal and vertical sections including two elbows, a bellows sealed valve, and an insulated pipe hanger. Due to a priority conflict, the valve was withdrawn and the facility was constructed without it. The facility included an electrical power supply with controllers to provide specified temperatures, a data logger for temperature recording, and power meters.

2. Test Articles

The test articles in operation during the previous year and into 1981 are described as follows:

1) ARI cable with improved ARI-designed and -installed termination consisting of a brazed hot-element-to-cold-element splice, a long cold element, and a brazed cold-element-to-flexible-lead splice, with these transition pieces enclosed and potted
2) ARI cable with ETEC-designed and -installed termination consisting of a brazed hot-element-to-cold-element splice enclosed in a commercial hermetic seal, a short cold element, and a brazed cold-element-to-flexible-lead splice

3) ARI cable with ETEC-designed and -installed termination consisting of a hot-element-to-flexible-lead brazed splice with impregnation of the mineral insulation in the end zone by a moisture-inhibiting compound of silicone to form a seal.

In addition, the test articles which subsequently became available and were added to the test program during 1981 are described as follows:

4) Pyrotenax cable (France) with integral termination consisting of a hot-element-to-cold-element transition achieved by a change in wire diameter (and, therefore, without a splice), a long cold element, and a brazed cold-element-to-flexible-lead splice in a sealing gland

5) Vacuumschmelze cable (Germany) with integral termination consisting of a hot-element-to-cold-element transition achieved by a change in wire diameter formed by a tight-fitting metal sleeve over the wire, a long cold element formed by this sleeve, and a brazed cold-element-to-flexible-lead splice in a sealing gland.

The test articles for the verification test were the heaters and the insulated pipe hanger. Two types of heaters were used: the ARI improved type described in Item 1 and the ARI cable with the ETEC-installed termination described in Item 3 supplemented with a GE-designed stress relief device at the splice. The insulated pipe hanger is a type designed for use in CRBRP. It consists of a split cylinder of Maramet with lengthwise slots for passing heaters and gas (to facilitate sodium leak detection) held by a stainless steel band, forming a body supported by three conventional pipe hanger assemblies.

3. Test Method

The program in effect during 1981 involved three types of tests: (1) accelerated life, (2) prototype pipe, and (3) prototype verification.

The accelerated life test used the thermal cycle method, as has been used for the tubular heaters. In this method, the heater, mounted on a support in an enclosure, is thermally cycled by the application of electrical power for 5 min to raise the sheath temperature to 927°C (1700°F), followed by a 10-min interval without power so that the sheath temperature decreases substantially. The cycling is continued until heater failure, as shown by an open circuit or a low element-to-sheath resistance. In the initial testing, the heaters were wound on a 25.4-mm-diameter (1-in.) tube to form a helix. In later tests, the heaters were mounted on 1.07-m-diameter (42-in.) supports to evaluate the effect of the larger bend radius in prolonging life.

To provide an accelerated life test less severe than that described above, a series of tests was devised late in the year to use the same apparatus and method but to raise the sheath temperature only to 816°C (1500°F) and to mount the heaters on the larger diameter supports.

In the prototype pipe test, the heaters were installed on the test pipes in a manner simulating the installation methods originally proposed for the CRBRP. These heaters were wrapped around the pipes to form a helix. They were powered to maintain the test pipes at 515°C (960°F) throughout the life of the heater. The temperature of each test pipe was monitored to verify proper operation. Heater failure was detected by a temperature decay, or ground fault interrupter trip, indicating possible failure, followed by a continuity and insulation resistance test. The heaters added to the test after the original group were mounted by a different method, believed to be an improvement. In this method, known as the serpentine configuration, the heater is formed on a fixture to provide a wave pattern running lengthwise over 240° of the lower surface of the pipe. The heater thus formed is pressed into place on the pipe.

The prototype verification test was formulated to demonstrate the adequacy of the presently planned designs for MI cable use on CRBRP. The test consists of applying electrical power to the heater to raise the pipe temperature at

specified rates to 438°C (820°F) and measuring the power required and the temperatures at various points in the system. Upon completion of the various temperature ramp and hold tests, the system is to operate at steady state at 438°C for 4000 h. In considering the possible failure of the heating system to meet the test conditions, that is, to achieve the desired heating rate and final sustained temperature, a secondary heater system having a 30% greater power rating was built into the verification test apparatus. If the test data indicate the need, the basic system will be turned off electrically and the test will be performed using the secondary heater system.

C. RESULTS

The results of the accelerated life tests performed during 1981 are presented in Table VII-1.

As shown, the two French heaters, which were wound onto a 25.4-mm-diameter (1-in.) support, lasted for an average of 9366 cycles, which is much greater than any of the 12 U.S. cables tested previously on the 25.4-mm support. The results shown for the cables wound onto the 1.07-m-diameter (42-in.) support were contrary to expectations, since their average cycle capability was only 1786 cycles. The reason for the test on the larger diameter support was to demonstrate that in the absence of cracks in the insulation as the result of short-radius bends, the heater operating life is longer. Such results, as expected, were demonstrated last year on tests of ARI. The insulation compaction density, which is a factor in the cracking phenomenon, was very nearly the same for the two groups of heaters. The insulation purity, also a possible factor, was lower in the French heaters.

The German heaters that were mounted on the large-diameter supports also had a low thermal cycle capability. No tests of these heaters were performed on the small-diameter support because the prototype pipe test had shown that these heaters have a very short operating life and are unsatisfactory. These heaters have a relatively low compaction density and purity.

TABLE VII-1

MI HEATER CABLE ACCELERATED LIFE TEST

Heater Description				Heater Mounting		Test Results	
Serial No.	R/L [Ω/m (Ω/ft)]	L [m(ft)]	Termination	Support Diameter [mm(in.)]	Helix Pitch [mm(in.)]	Operating Cycles	Comments
TESTS WITH SHEATH TEMPERATURE AT 927°C (1700°F)							
Pyrotenax Cable (France), Factory-Installed Termination							
047	2.82 (0.86)	10 (32.8)	D	25.4 (1.0)	5.1 (0.20)	10152	Failed by cable short
048	2.82 (0.86)	10 (32.8)	D	25.4 (1.0)	5.1 (0.20)	8580	Failed by cable element open
049	2.82 (0.86)	10 (32.8)	D	1067 (42)	25.4 (1.0)	2105	Failed by cable element open
050	2.82 (0.86)	10 (32.8)	D	1067 (42)	25.4 (1.0)	1468	Failed by cable element open
Vacuumschmelze Cable (Germany), Factory-Installed Termination							
059	2.49 (0.76)	10 (32.8)	E	25.4 (1.0)	4.8 (0.19)	2272	Failed by cable element open
060	2.49 (0.76)	10 (32.8)	E	25.4 (1.0)	4.8 (0.19)	1620	Failed by cable element open
TESTS WITH SHEATH TEMPERATURE AT 816°C (1500°F)							
ARI Cable (USA), Field-Installed Termination, EBR-II Type							
075	2.40 (0.73)	6.25 (20.5)	C	1067 (42)	25.4 (1.0)	4662	Operating as of Dec. 31, 1981
076	2.40 (0.73)	6.25 (20.5)	C	1067 (42)	25.4 (1.0)	4662	Operating as of Dec. 31, 1981
078	2.40 (0.73)	6.25 (20.5)	C	1067 (42)	25.4 (1.0)	2531	Operating as of Dec. 31, 1981
079	2.40 (0.73)	6.25 (20.5)	C	1067 (42)	25.4 (1.0)	2531	Operating as of Dec. 31, 1981
080	2.40 (0.73)	6.25 (20.5)	C	1067 (42)	25.4 (1.0)	4062	Operating as of Dec. 31, 1981
081	2.40 (0.73)	6.25 (20.5)	C	1067 (42)	25.4 (1.0)	2531	Operating as of Dec. 31, 1981

Terminations:

Type C – ETEC-installed using silicone seal. Flexible lead brazed directly to the hot element wire.

Type D – Integral hot-to-cold transition. Heater manufactured by Pyrotenax (France).

Type E – Integral hot-to-cold transition. Heater manufactured by Vacuumschmelze (Germany).

The tests at the lower sheath temperature of 816°C (1500°F), using the ARI cable with the field-installed terminations, were started late in the year. Since these heaters are to be tested at a lower sheath temperature but otherwise under the same conditions as those tested last year at 927°C (1700°F), which averaged an 8634-thermal-cycle capability, a much greater number of cycles is expected. The results of the tests are presented in Table VII-1.

In the prototype pipe test, nine heaters of the original group of 24 remained in operation at the beginning of the year. Since those of the original group which failed did so within a relatively few hours of startup, and these nine heaters had operated uneventfully for thousands of hours, the test was considered complete and was ended on April 15. At that time, these heaters had operated 12,784 h at 516°C (960°F). All of these heaters were made of ARI cable. One was terminated through hermetic seals, and the other eight used a simple termination consisting largely of a flexible lead brazed directly to the heater element wire (Type C in Table VII-2).

The four French heaters (Type D in Table VII-2) in the prototype pipe test are continuing to perform satisfactorily. The operation of one of these was interrupted three times by a failure of the splice between the flexible lead and the cold conductor. By the end of the year, this heater had operated 7068 h and the others had operated 8568 h.

The four German heaters (Type E in Table VII-2) in the prototype pipe test failed within a relatively few hours of startup. In all cases, the failure was a brittle fracture of the element wire without any apparent insulation failure. A comparison of these heaters with others (French and U.S.) having a much longer operating life showed that the most obvious difference was that the German heaters had much lower insulation compaction density and purity. These factors ordinarily are associated with insulation breakdown failure and not element fracture as was observed. The results of this test are presented in Table VII-2.

The prototype verification test has been in operation such a short time that no significant results can be presented in this report.

TABLE VII-2

PROTOTYPE PIPE TEST

Serial No.	R/L (Ω/ft)	Length (ft)	Termination Type	Mandrel Diameter (in.)	Pipe Diameter (in.)	Pitch (in.)	Standoff (in.)	End		Cable		Operating Time (h)	Notes
								O		O			
27	0.73	52.5	C	1.25	1.315	1.5	0					12,784	R
28	0.73	52.5	C	1.75	1.315	2.1	0.25					12,784	R
19	0.18	213	C	1.25	1.315	0.375	0					12,784	R
18	0.18	213	B	1.75	1.315	0.50	0.25	X				0	F
20	0.18	213	C	1.75	1.315	0.50	0.25					12,784	R
30	0.73	44	B	----	8.625	5.0	0					12,784	R
31	0.73	44	C	----	8.625	5.0	0					12,784	R
32	0.73	44	C	----	8.625	5.25	0.25					12,784	R
15	0.18	178	C	----	8.625	1.2	0					12,784	R
16	0.18	178	C	----	8.625	1.3	0.25					12,784	R
41	0.73	50	A'	8.625	8.625	6.13*	0.25					8,568	T
42	0.73	50	A'	8.625	8.625	6.13*	0.25					1,464	F
43	0.86	32.8	D	8.625	8.625	9.22*	0.25					8,568	T
44	0.86	32.8	D	8.625	8.625	9.22*	0.25					8,568	T
45	0.86	32.8	D	8.625	8.625	9.22*	0.25					8,568	T
46	0.86	32.8	D	8.625	8.625	9.22*	0.25					7,068	T
55	0.76	32.8	E	8.625	8.625	9.22*	0.25			X		149	F
56	0.76	32.8	E	8.625	8.625	9.22*	0.25			X		40	F
57	0.76	32.8	E	8.625	8.625	9.22*	0.25			X		38	F
58	0.76	32.8	E	8.625	8.625	9.22*	0.25			X		198	F

Key:

O = open circuit; S = short circuit.
* = serpentine configuration. Dimension refers to "wavelength." All others have helix configuration.
' = improved Type A.
Type A = factory installed.
Type B = ETEC installed, ceramic seal.
Type C = ETEC installed, silicone seal.
Type D = integral hot-to-cold transition. Heater manufactured by Pyrotenax (France).
Type E = integral hot-to-cold. Heater manufactured by Vacuumschmelze (Germany).
F = failed at operating time shown.
R = satisfactorily completed full term of test, then removed from test at the number of hours shown.
T = testing is in progress, with the number of hours shown as of Dec. 31, 1981.

VIII. PROXIMITY TRANSDUCERS

V. DE VITA

A. INTRODUCTION

As a continuing development and test program to assess the performance of an ultrasonic proximity measurement system, this year's effort focused on static measurements in sodium. The design features and assembly techniques were finalized during the previous year's activity, which also included static testing in water. This year's sodium testing period, covering a span of 10 months, evaluated basic performance characteristics including linearity, resolution limitations, measurement range, sodium temperature compensation, sodium temperature limits, repeatability, and reliability. No dynamic testing in sodium was conducted, but it is planned for next year.

B. TEST DESCRIPTION

1. Facility

The high-bay area in Building 057 was used for the static sodium testing. The testing utilized the fixture from Rig 2 in exactly the same manner as reported in previous annual reports on the ultrasonic proximity transducer, except that the mounting bracket was modified to adapt to the ultrasonic transducer configuration.

2. Test Article

a. Transducer

An isometric drawing of the transducer assembly is shown in Figure VIII-1. As described in the previous year's report, the design features and assembly techniques are a result of first testing in water. The front plate thickness is

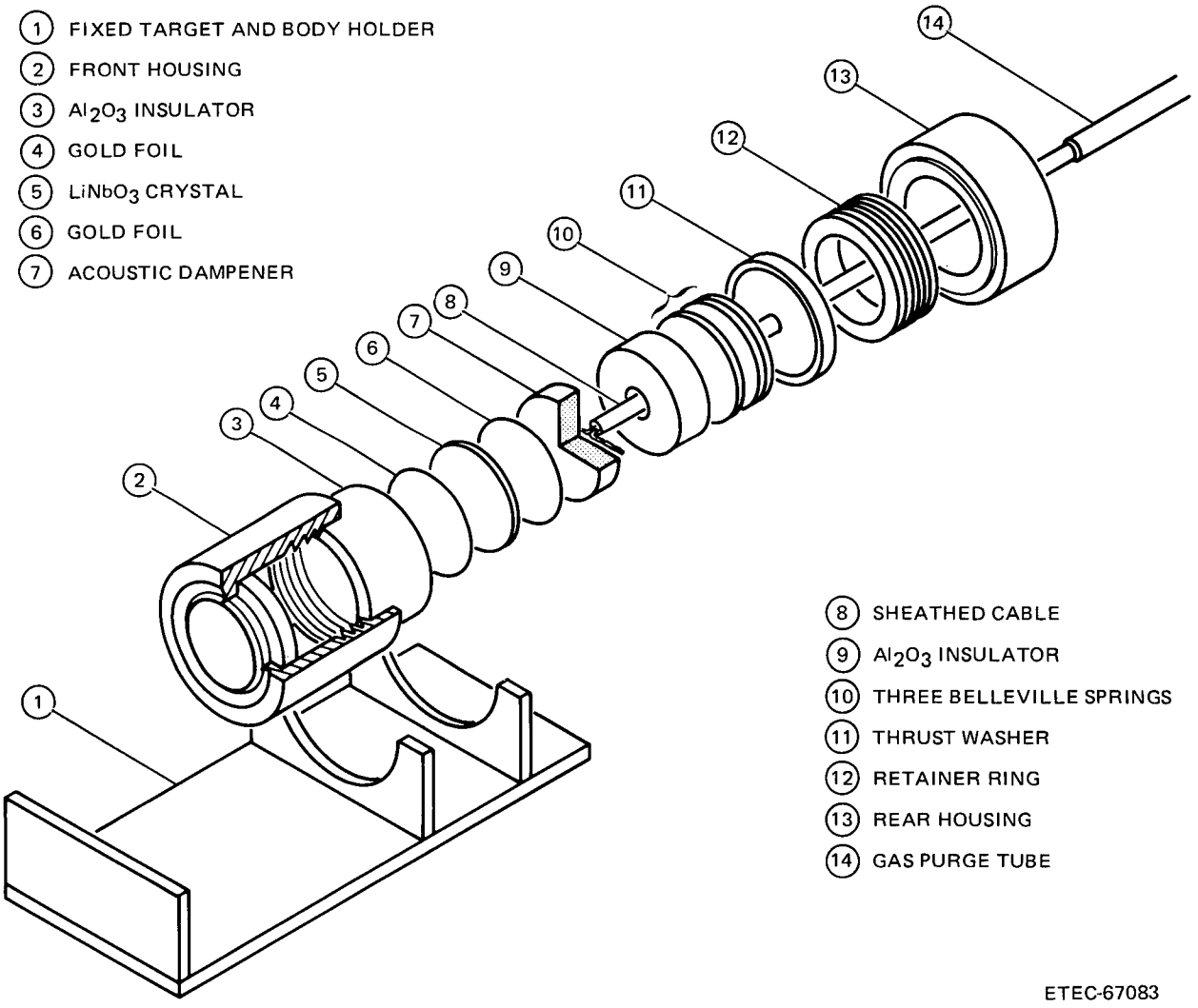

Figure VIII-1. Assembly Drawing of Ultrasonic Transducer

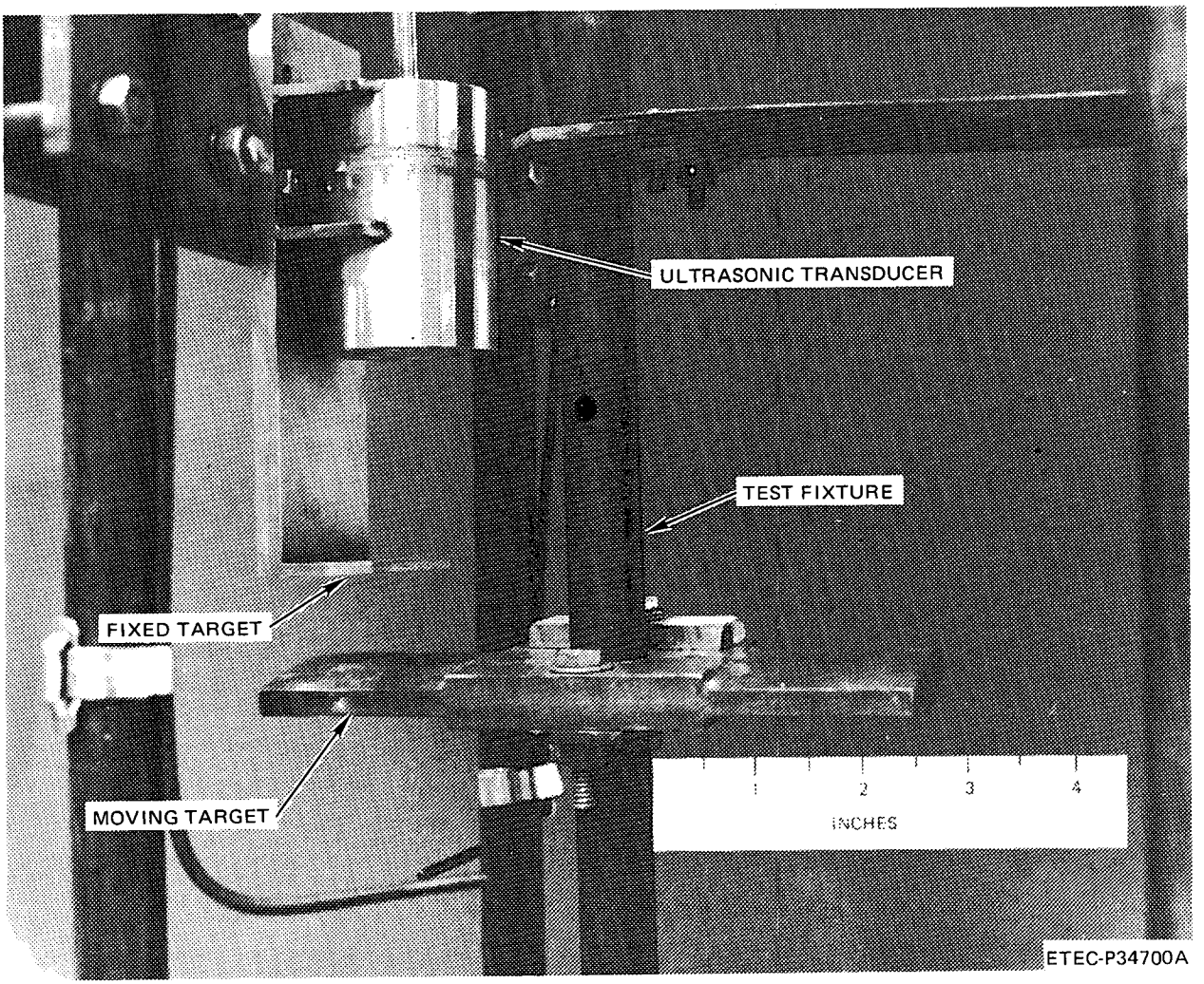

Figure VIII-2. Ultrasonic Transducer Mounted in Test Fixture

an even multiple of wavelengths, at 5 mHz, for maximum pulse transmission. Figure VIII-2 shows the test article installed in the test fixture. The moving target, part of the test fixture, travels vertically. The moving target is coupled to a micrometer and dial indicator, located outside the top lid. The reflected surface of the moving target is machined to a radius of 6 in. (15.2 cm), simulating the diameter of the FFTF pump shaft.

b. Electronics

The transducer and electronic signal conditioning module are separated by ~60 ft (18.29 m), 30 ft (9.15 m) of stainless steel sheathed cable, 5 ft (1.5 m)

of which is immersed in liquid sodium, and 30 ft (9.15 m) of soft RG-62/μ coaxial cable. The same electronic module generates the excitation (transmitted) pulses and conditions the reflected (received) pulses. The flow of the transmit/receive functions is as follows: A free-running pulse oscillator generates a 250-V narrow-width pulse at a rate of 5000 pulses per second. Synchronous with the pulse that is transmitted to the ultrasonic transducer crystal is an internal pulse that simultaneously gates a 50-mHz oscillator. The oscillator is gated off synchronous with the return of the reflected fixed pulse. The number of pulses is counted in this gated time period and compared to a preset reference counter. If the difference of counted pulses is greater than 1 count, then within a closed feedback loop an offset voltage is produced that varies the frequency of the 50-mHz oscillator in order to produce no difference in counted pulses when compared to the preset reference counter. This is the compensation technique used for variations in the gap measurement due to velocity of sound changes and dimensional changes in the fixed target due to thermal expansion. The automatic gain control (AGC) network follows the amplitude of the reflected fixed target and continually varies the gain to maintain a constant fixed-target level. The threshold level for the start of the timing gate is then adjusted for a fixed ratio with respect to the peak level. Simultaneous with the start of the timing gate is the restart of the 50-mHz oscillator, which continues until shut off by the reflected moving-target pulse. The number of pulses is again compared to a second preset counter. The overflow of pulses is then a direct measure of the gap (in mils). One count is equivalent to a displacement of 1 mil in the digital form. But in the digital-to-analog conversion, a significant increase in resolution is generated. The "zero" gap is arbitrarily set and lies anywhere between the fixed target and moving target. The "zero" in this measurement is set at $\sim$1.1 in. (2.79 cm) from the front edge of the fixed target. The position of the moving target from 1.100 in. (2.79 cm) to 1.350 in. (3.43 cm) generates an output voltage between 0 and 10 V dc.

C. TEST RESULTS

Figure VIII-3 displays the signal response of the fixed and moving targets in water prior to installation in sodium. By design, the moving-target pulse is

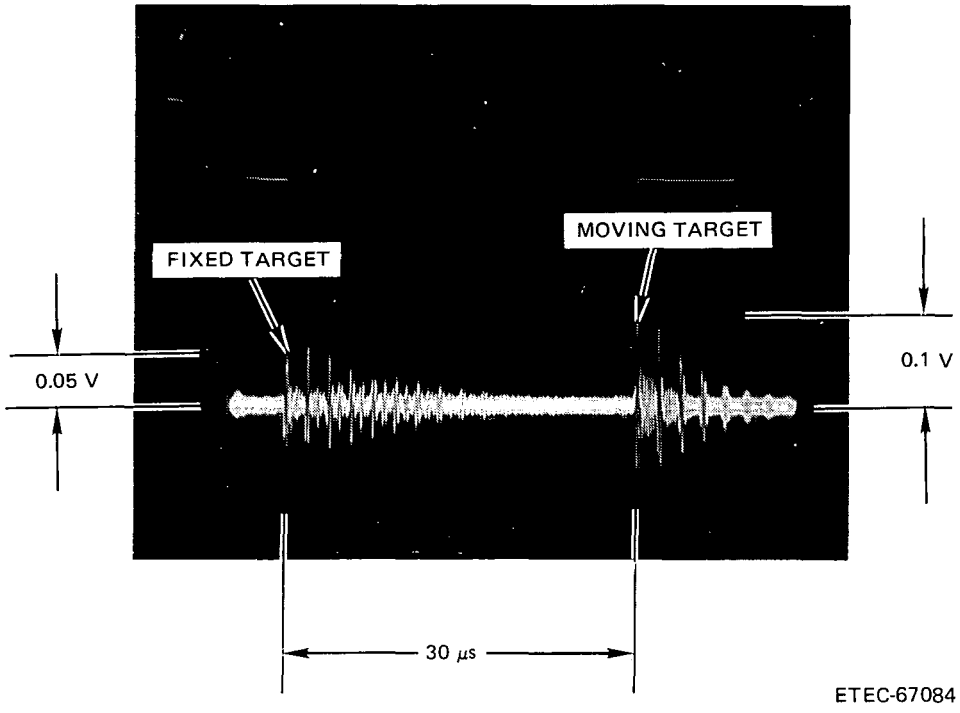

Figure VIII-3. Target Reflections in Water Medium

larger in amplitude than the fixed-target pulse. Also, note the trailing pulses from both targets following the initial reflection. This is due to reverberations from the front plate, which is 0.246 in. (0.625 cm) thick.

After insertion into the Rig 2 sodium tank, the first indications of reflected signals were not observed until the temperature reached 800°F (426.7°C). This established the wetting temperature needed for future pump installations. Figure VIII-4 shows the change in character of the signal in liquid sodium. Note the more rapid decay of the trailing pulses from both targets following the initial reflection when compared to Figure VIII-3. This is a result of a reduction of the mismatch in acoustic impedance between stainless steel-water and stainless steel-sodium.

Improvements in electronic signal enhancement techniques were implemented and evaluated. Figures VIII-5a and -5b show two signals simultaneously. Figure VIII-5a shows a typical cycle, which includes the excitation and the fixed- and moving-target reflections. Figure VIII-5b displays a closer view of a typical moving-target reflection; the upper trace is a typical reflected signal that

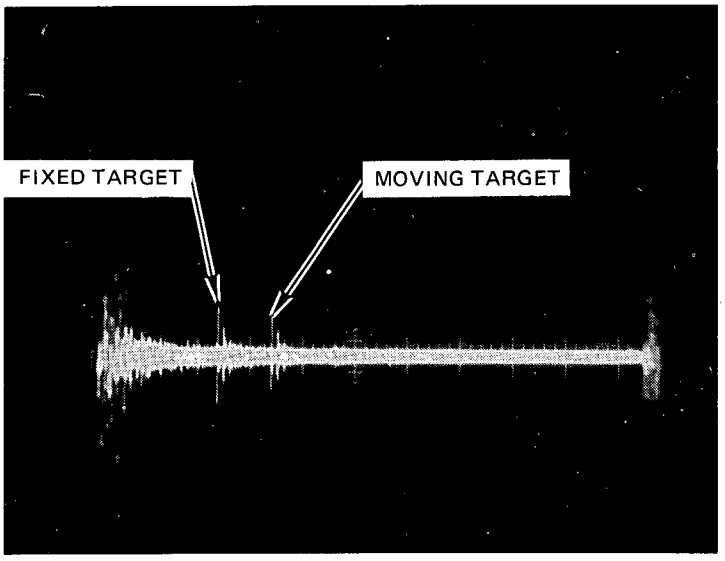

Figure VIII-4. Target Reflections in Sodium at 800°F (426.7°C)

has only been amplified. Note the level of acoustic background noise. The lower trace is the output of the same pulse that has been split by a quadrature detector, each output squared and then summed. Note the absence of any negative going signal, due to the squaring function; more important is the significant reduction of the background noise level despite an increase in amplitude of the reflected signal. With this circuitry and threshold level voltage adjusted for both fixed and moving targets, testing from 400 to 1050°F (204.4 to 565.5°C) was performed. Displacement vs the ultrasonic output, in volts, was conducted at 400, 500, 600, 700, 800, 900, 1000, and 1050°F (204.4, 260, 315.5, 371.1, 426.7, 482.2, 537.8, and 5.65.5°C). Figure VIII-6 is the typical output plot observed at all temperatures. Nonlinearity errors over a 250-mil (0.64-cm) range is, typically, the equivalent of ±0.5 mil (0.0013 cm). Figure VIII-7 demonstrates that the resolution, despite the wide range of 250 mils (0.64 cm), is 0.1 mil (2.5×10^{-4} cm).

With the fixture positioned at a constant 40-mil (0.1-cm) reference gap, the output was plotted at each test temperature (Figure VIII-8). The plot shows an apparent shift in output vs temperature. But it has been shown, through the aid

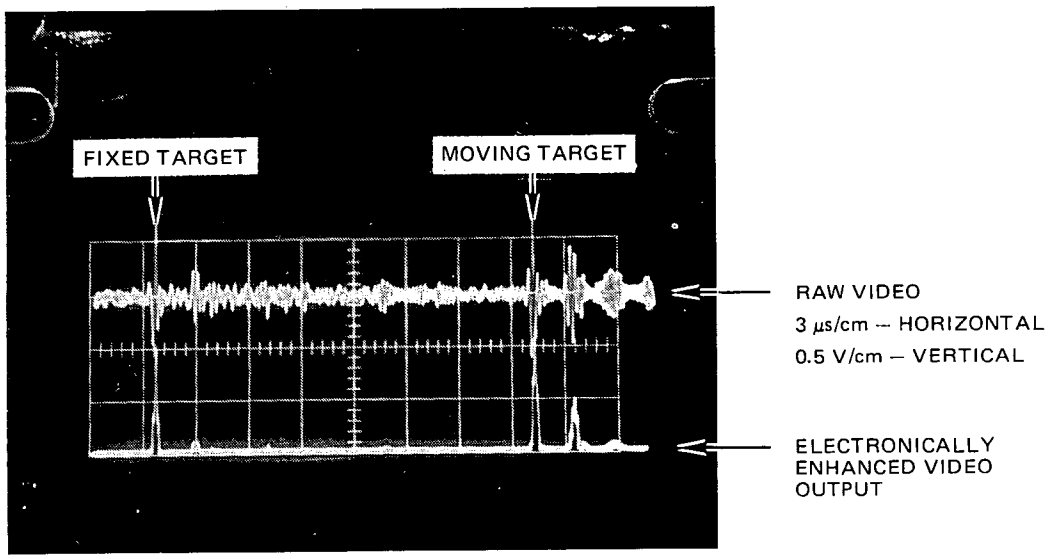

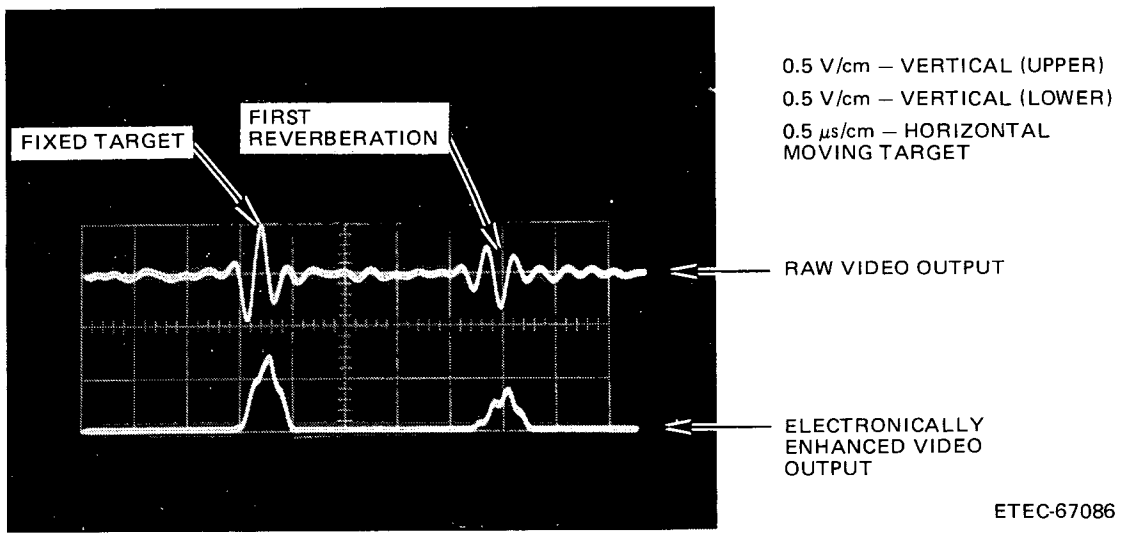

Figure VIII-5. Electronically Enhanced Video Outputs

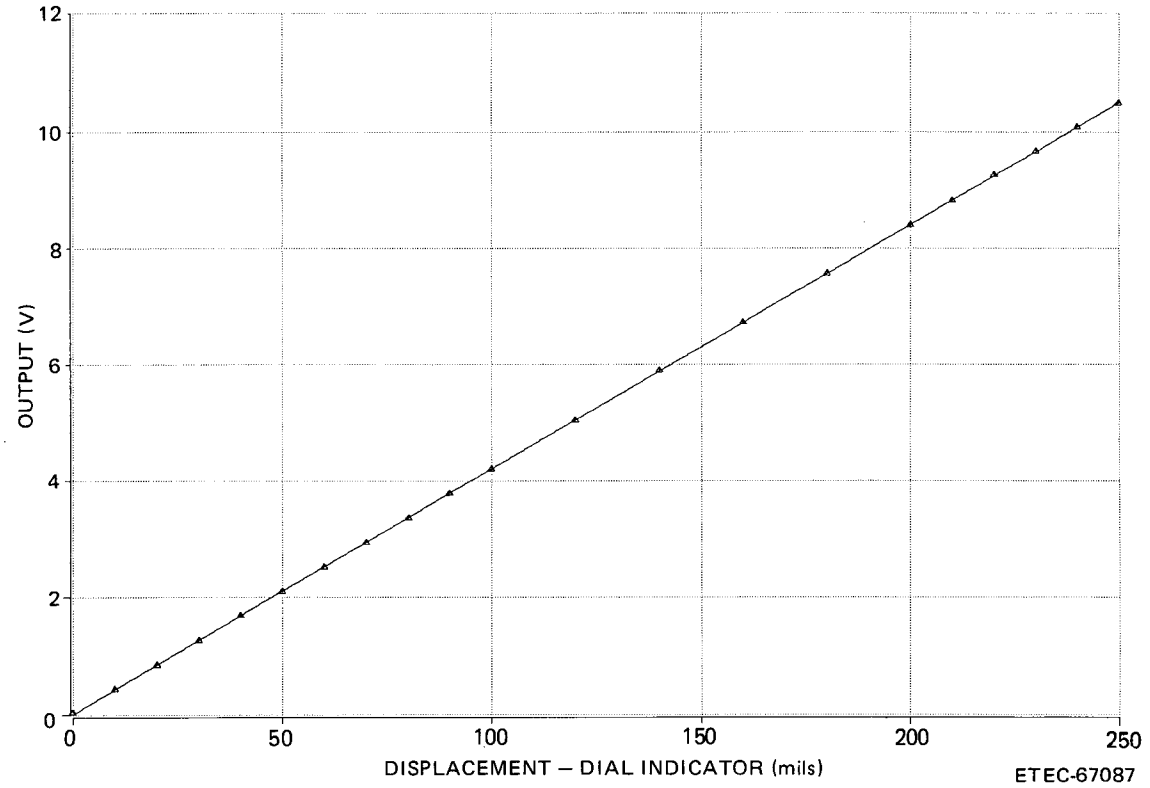

Figure VIII-6. Ultrasonic Proximity Calibration, 600°F, December 14, 1981

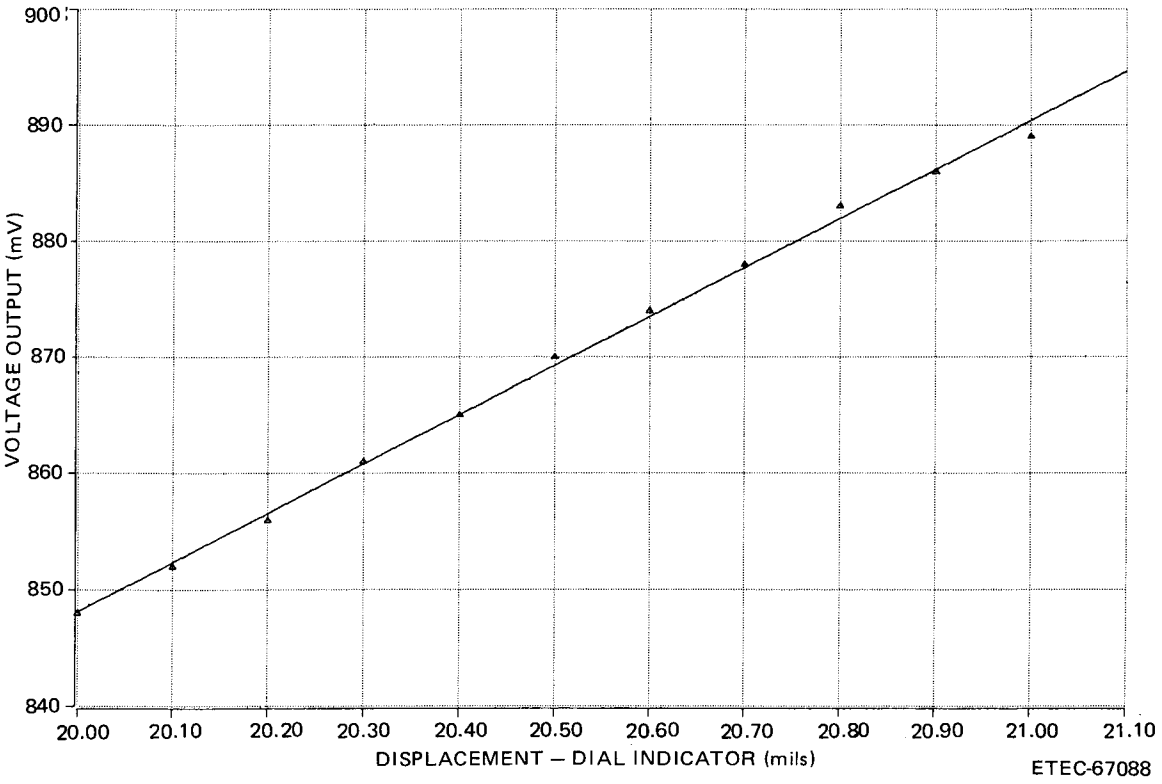

Figure VIII-7. Ultrasonic Proximity Calibration, 600°F, December 11, 1981

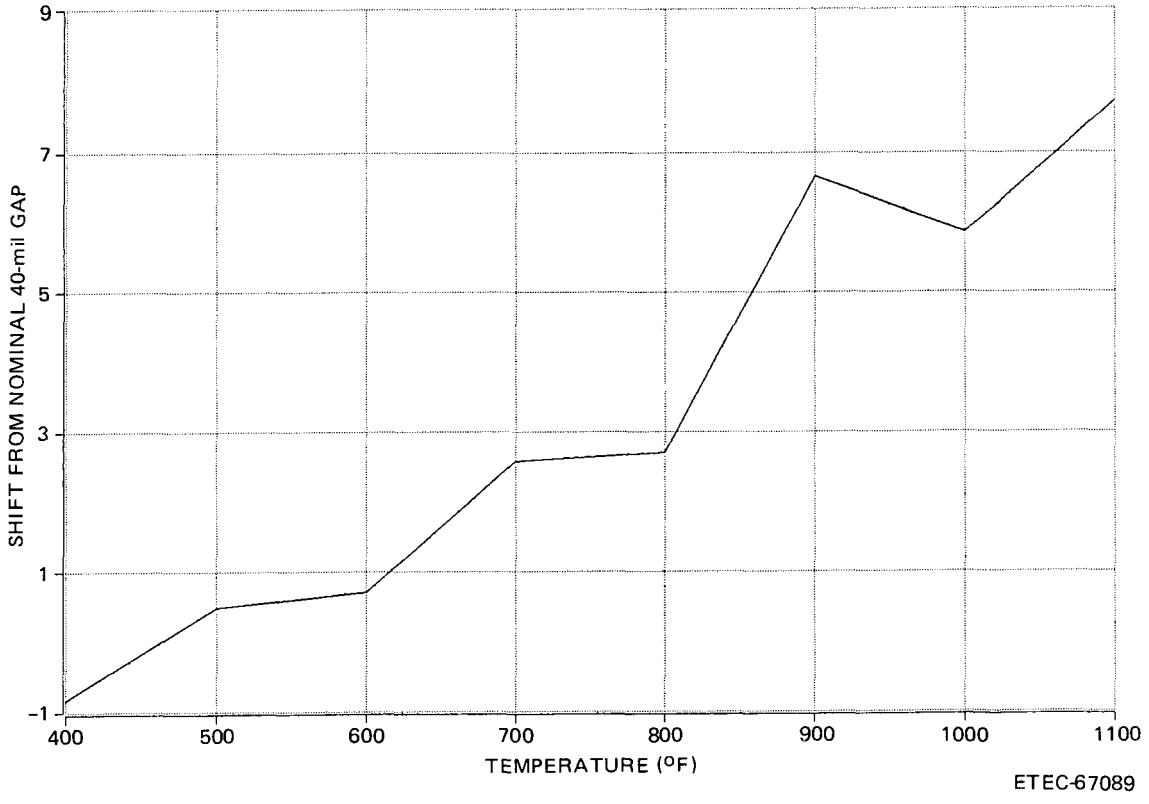

Figure VIII-8. Ultrasonic Proximity Calibration, 400-1100°F

of a very stable and high-resolution time interval counter, that, in fact, the test fixture gap was shifting over this temperature range. The ∿5-mil (∿0.013-cm) shift is not unrealistic, consdering that the length of test fixture exposed to the elevated temperatures is 33 in. (83.8 cm).

The stability of the start and end of the basic timing gate over the 400-1050°F (204.4-565.5°C) temperature range is shown in Figures VIII-9 and -10. These figures show simultaneous traces of the reflected fixed-target pulse with the start of the basic time measurement gate and the reflected moving-target pulse with the end of the basic time measurement gate. Because the AGC circuitry maintains the fixed-target pulse amplitude at a constant level over the active temperature range, the start of the basic time measurement pulse is constant with respect to the pulse peak amplitude. A similar technique is used for the moving-target pulse by designing the threshold level at a fixed ratio of the moving-target pulse amplitude. The stability of the start and end of the timing gate with respect to the main and synchronous pulse is 2 ns when measured in terms of 1 sigma. This is the equivalent of 0.1 mil (25×10^{-6} cm).

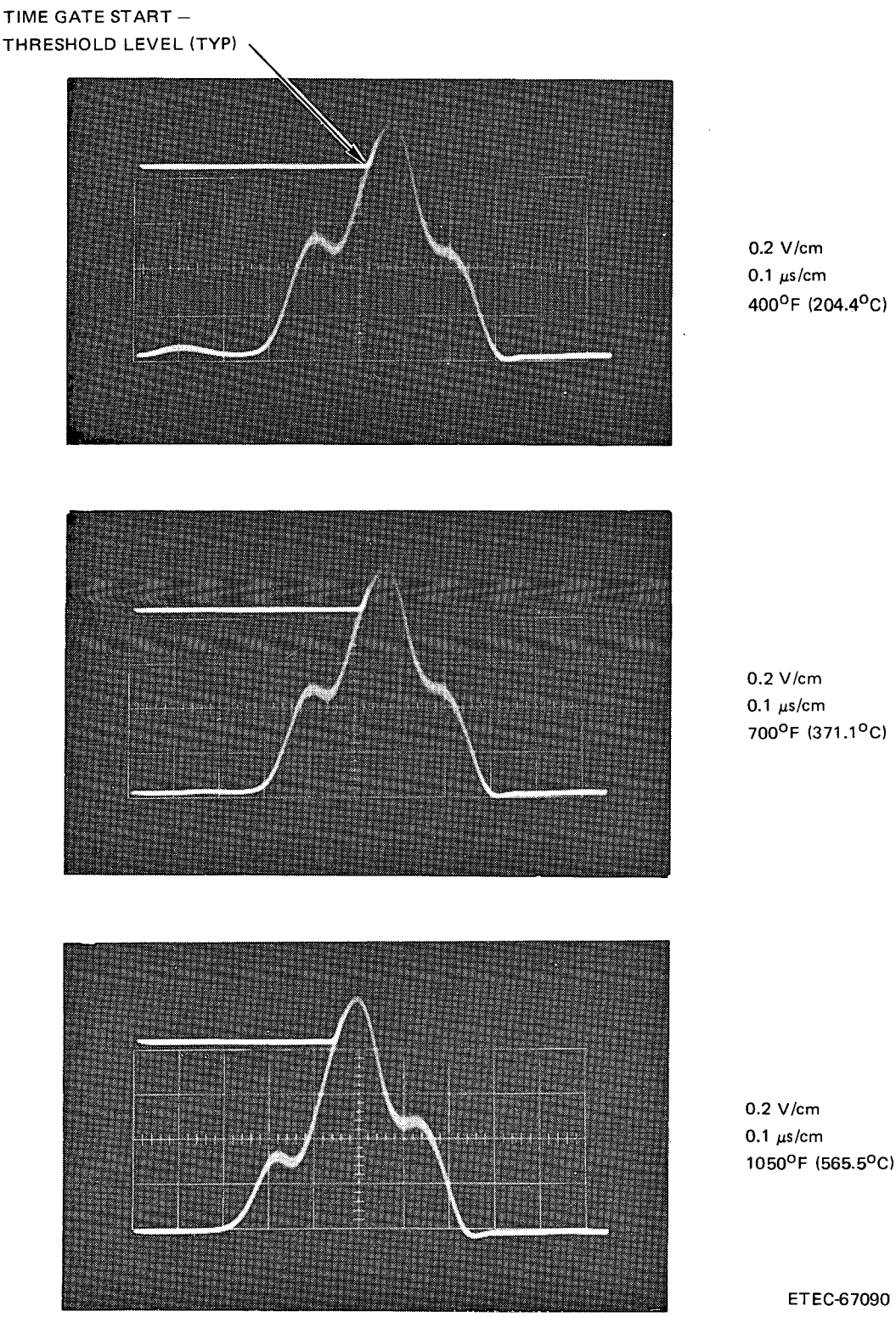

Figure VIII-9. Fixed-Target Reflection

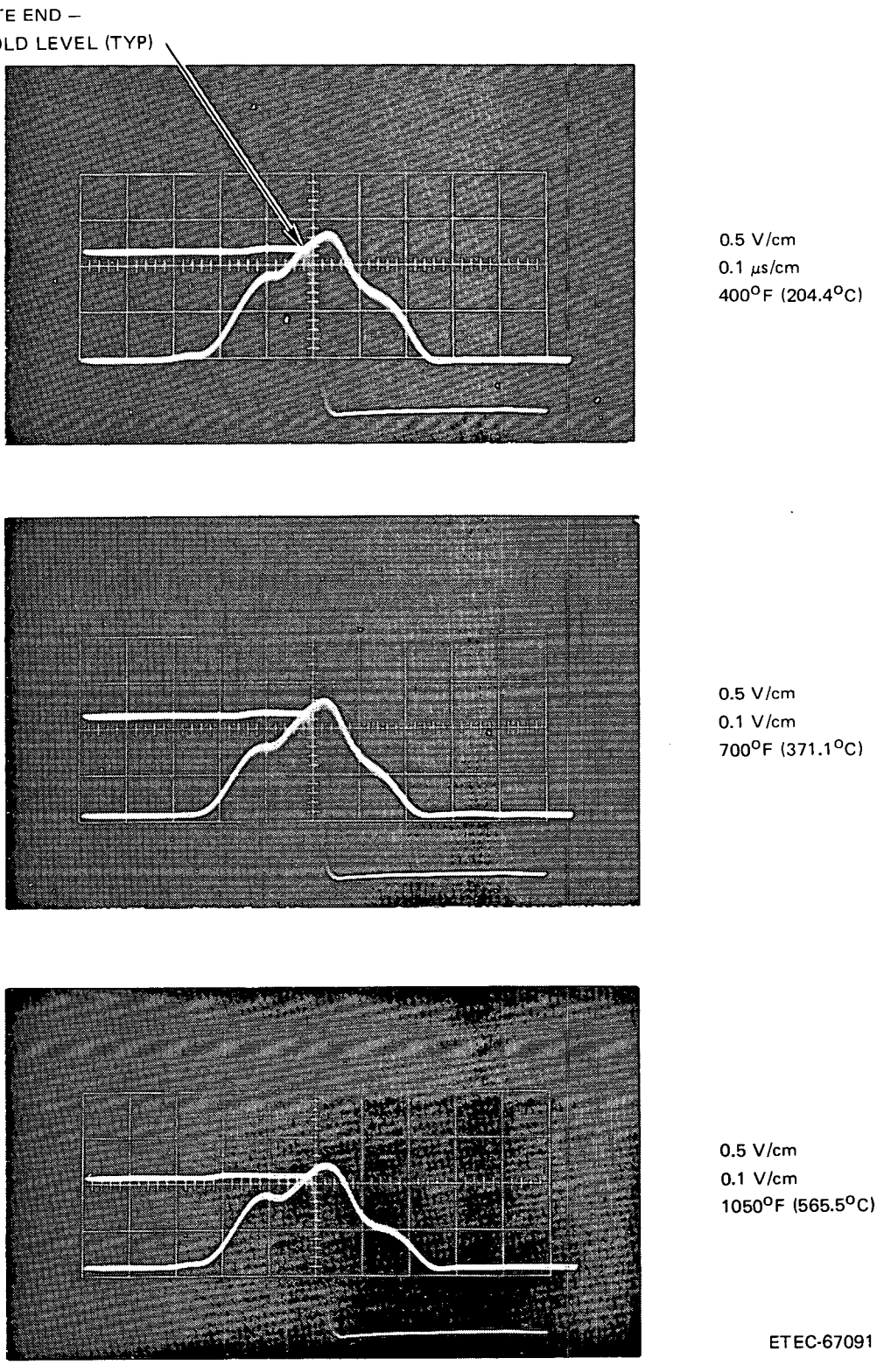

Figure VIII-10. Moving-Target Reflection

A very recent modification in the signal enhancement circuit was implemented to further improve the measurement stability. The modification essentially eliminated the first and third lower-level peaks from the target reflections (Figures VIII-9 and -10). Figures VIII-11 and -12 show the results of the modification measured at 1050, 1000, and 900^{o}F (565.5, 537.8 and 482.2^{o}C). Evaluation over the entire temperature range is in progress at this writing. Initial results have confirmed the justification for the modification.

Next year's planned testing will include a modification to the test rig to include (1) a mechanical "zero" stop, (2) up to 30 ft (9.1 m) of sheathed cable immersed in liquid sodium, and (3) an added 200 ft (61 m) of soft coaxial cable in the transmit/receive line.

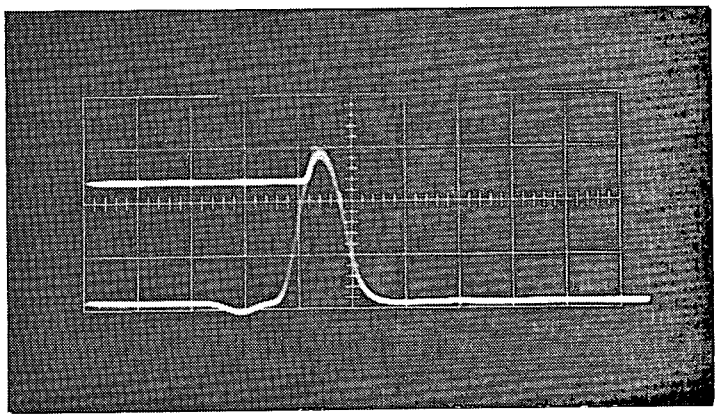

1050°F

GATE START = 1.0 V/cm
FIXED-TARGET PULSE = 0.2 V/cm
HORIZONTAL = 0.1 μs/cm

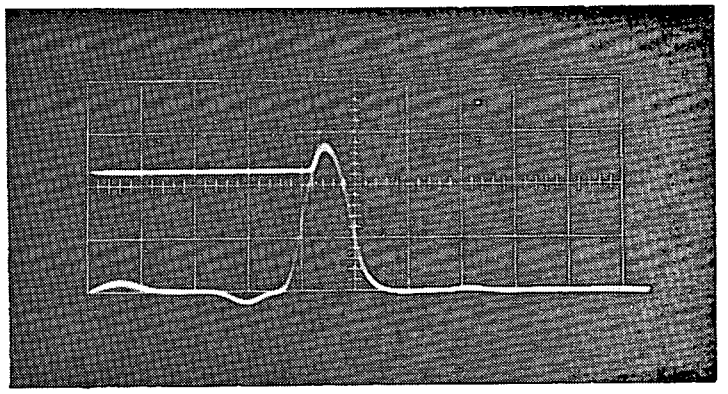

1000°F

GATE START = 1.0 V/cm
FIXED-TARGET PULSE = 0.2 V/cm
HORIZONTAL = 0.1 μs/cm

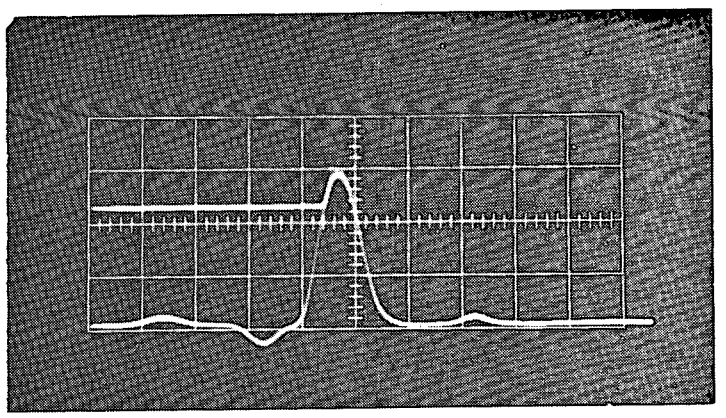

900°F

GATE START = 1.0 V/cm
FIXED-TARGET PULSE = 0.2 V/cm
HORIZONTAL = 0.1 μs/cm

ETEC-67092

Figure VIII-11. Fixed-Target Reflections

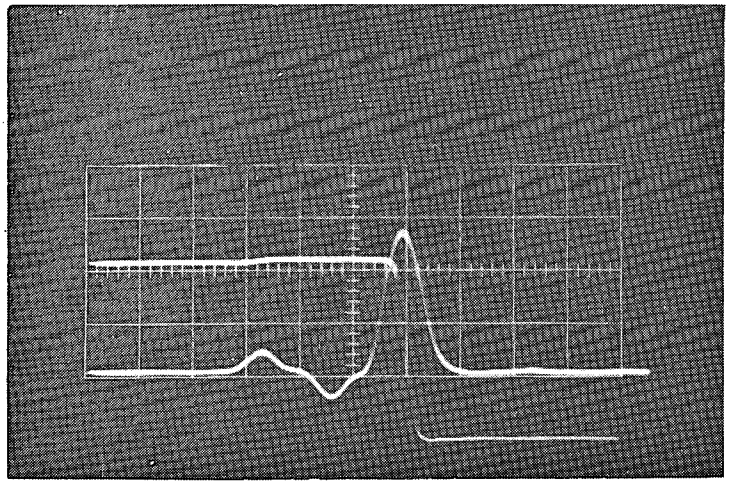

1050°F

GATE END = 1.0 V/cm
MOVING-TARGET PULSE = 0.2 V/cm
HORIZONTAL = 0.1 μs/cm

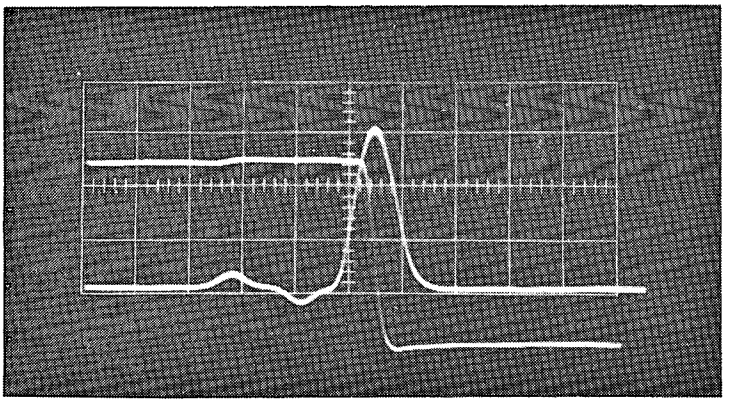

1000°F

GATE END = 1.0 V/cm
MOVING-TARGET PULSE = 0.2 V/cm
HORIZONTAL = 0.1 μs/cm

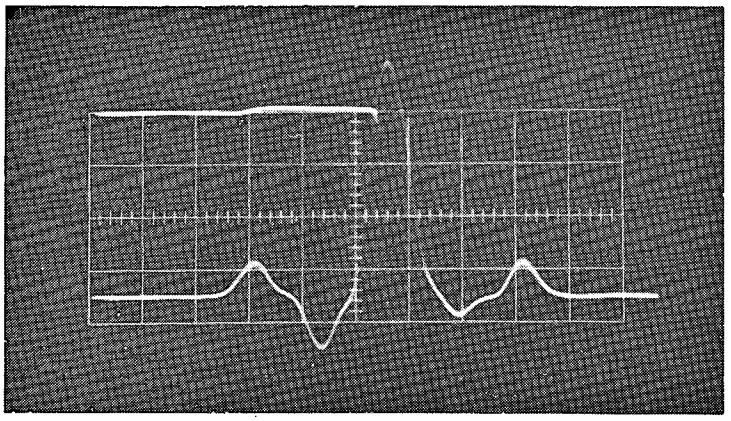

900°F

GATE END = 0.5 V/cm
MOVING-TARGET PULSE = 0.2 V/cm
HORIZONTAL = 0.1 μs/cm

ETEC-67093

Figure VIII-12. Moving-Target Reflections

IX. INSERVICE INSPECTION

V. DE VITA

A. INTRODUCTION

Several types of approach for inservice volumetric inspection of austenitic stainless steel, sodium-wetted pipe welds are actively being investigated by ANL, ORNL, and HEDL. The ultrasonic method is being developed by HEDL. This test program was conducted at HEDL's request using HEDL-developed equipment and personnel. The purpose of the test was to assist them in finalizing the design and development of their ultrasonic scanning equipment (USE) and inspection procedures prior to a volumetric inspection of a secondary system pipe weld at FFTF.

B. OBJECTIVES

The major test objectives were to:

1) Collect and analyze data for finalizing the transducer system for the FFTF test.
2) Collect and analyze data for separating noise signals from defect signals during austenitic stainless steel weld inspections.
3) Collect documented calibration data for sizing and locating weld flaw indications reported during later inspections at FFTF.
4) Develop procedures for installation of USE on 400^{o}F sodium pipe incorporating the following considerations:
   a) Personnel safety
   b) Equipment safety.
5) Evaluate integrity of developed scan procedures to accurately gather, manipulate, and store weld examination data.
6) Evaluate USE system capability to gather repeatable data with mechanical and electrical reliability at elevated pipe temperature conditions.

7) Evaluate USE data gathering and processing capability from a remotely positioned instrumentation trailer.

8) Train HEDL technology and engineering personnel in the operation and manipulation of the USE and computer scan procedures under field conditions.

C. EQUIPMENT DESCRIPTION

The pipe weld inspection system consists of a mechanical scanning section, a couplant cart, scan equipment positional control electronics, ultrasonic data acquisition electronics, a central computer for master control and data analysis, and a remote instrumentation van.

The mechanical scanning equipment consists of a pipe clamp assembly and the ultrasonic scanning mechanism (USM). The USM is mounted on a circumferential track that is part of the pipe clamp assembly. It has six degrees of freedom, all under computer control. The primary purpose of the USM is to position the ultrasonic transducer assemblies in controlled, measured positions with respect to the test weld and to manage the coolant and electrical control/instrumentation lines such that a full 360-degree scan of the weld can be made. Figure IX-1 shows the mechanical scanning equipment installed on the test pipe section.

The couplant cart delivers a stream of 130^{o}F constant-temperature silicone oil couplant to each ultrasonic transducer mounted on the USM. The primary purpose is to establish an ultrasonic signal path between the test weld and the transducer. The secondary purpose is to provide coolant to the ultrasonic transducer and maintain the transducer at a constant operating temperature. The cart was installed as close to the test weld as practical.

A block diagram/schematic of the total system is shown in Figure IX-2.

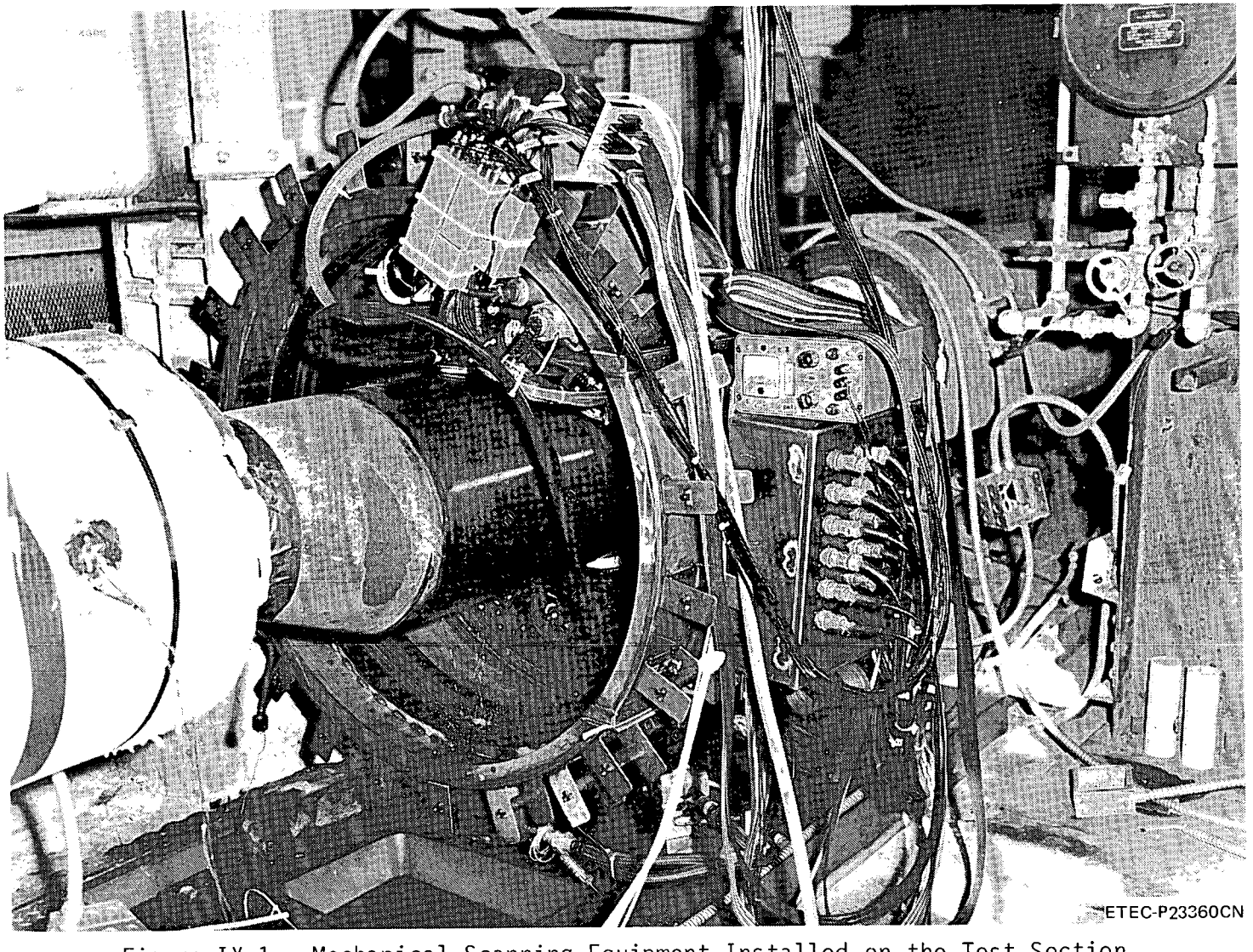

Figure IX-1. Mechanical Scanning Equipment Installed on the Test Section

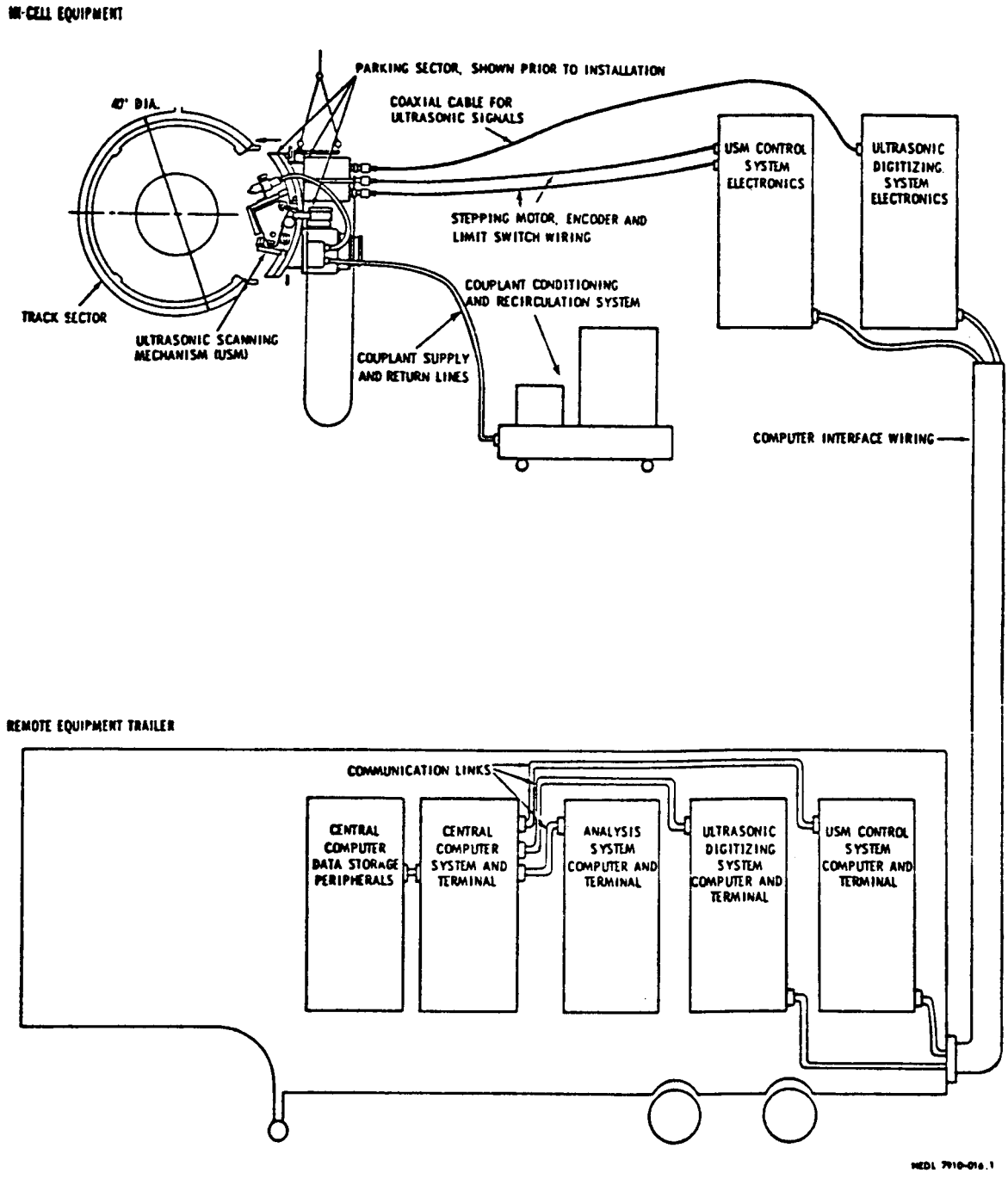

Figure IX-2. Ultrasonic Scanning Equipment

D. TEST DESCRIPTION

The 16-in.-diameter pipe test section containing the circumferential butt welds with the calibration defects was adapted to fit into a 10-in.-diameter sodium line in SCTI. This was accomplished with the use of 16-in. to 10-in. eccentric reducers at each end of the test section. Eccentric reducers were used to ensure that a gas bubble did not exist between the inside surface of the test article welds and the sodium.

After the test section was welded into the sodium, HEDL was informed. The mechanical scanning system was then installed on the test section by HEDL personnel with assistance from ETEC. The couplant cart, the electronic racks, the van, and all the interconnecting wire between equipment were installed. These operations were performed at this time to:

1) Ensure that the space envelope available in the area of the test specimen was adequate to allow proper scanner operation and full freedom for all scanner motions.
2) Allow a training exercise for the personnel who will be involved in installing USE on the test specimen at elevated temperature.
3) Obtain additional baseline ultrasonic data at room temperature for comparison to data that will be acquired at elevated temperature.

After completion of this checkout, the mechanical scanning equipment was removed and electrical heaters were installed on the test section. The section was then thermally insulated. The sodium loop, including the test article, was preheated to $400^{o}F$, and the loop was filled with sodium and circulation established. The loop temperature was raised to $900^{o}F$ to obtain internal wetting of the test section. The system temperature was then lowered to $400^{o}F^{+50}_{-10}$, and a flow rate of ~1000 gal/min was established. These conditions simulate the expected secondary system refueling conditions. The thermal insulation and electrical heaters were then removed from the test section, and the test section was turned over to HEDL to commence the test. HEDL installed the mechanical scanning system on the test section (in the heated condition), connected equipment to the related

hardware, established couplant flow, and initiated ultrasonic weld inspection. HEDL personnel operated all the equipment during the testing and gathered all data on system performance on equipment furnished by HEDL. Data analysis and performance reports are a HEDL responsibility. No data are provided herein; however, it can be stated that the field installation and application of the equipment were verified.

The testing proceeded in a timely and orderly fashion except that a sodium leak that developed in the H-1 sodium heater economizer at SCTI forced a disruption in testing because it required that the loop be drained of sodium while repair was accomplished.

X. SELF-ACTUATED SHUTDOWN SYSTEM — ARTICULATED CONTROL ASSEMBLY (SASS-ACA) TEST PROGRAM

R. L. BRYAN

A. INTRODUCTION

Several self-actuated shutdown systems for future liquid metal fast breeder reactors (LMFBRs) are being developed. One of the candidate concepts consists of an articulated absorber comprised of three sections of stainless steel rods with enriched B_4C pellets. The test unit being tested as a proof-of-principle was designed and built by Westinghouse — Advanced Reactors Division (WARD). The assembly is supported by an electromagnet in which a portion of the magnetic circuit is made of an alloy with a selected Curie temperature. The Curie temperature of this alloy was selected to provide a sharp decrease in magnetic saturation at $1050^{o}F$ ($565.5^{o}C$) — the target temperature for inherent release of the absorber assembly. The test unit is being tested in sodium.

The test program consists of testing a full-scale test unit of an articulated rod secondary shutdown system with inherent insertion. Test program objectives include: (1) injection characterization, (2) pretest characterization, (3) inherent release, (4) drop time, (5) withdrawal load, (6) performance after an extended dwell, and (7) performance with a bowed guide tube.

B. DESCRIPTION

1. Facility

The Static Sodium Test Facility (SSTF) provides the capability for sodium fill, drain, purification, and sampling to enable research and development testing, acceptance testing of prototype units, friction and wear experiments, and calibration of instruments in support of the Fast Flux Test Facility (FFTF), Clinch River Breeder Reactor (CRBR), LMFBR projects, and other national energy programs.

The facility consists of six test rigs identified as 032-R1 through 032-R6. Each test rig performs a different function.

The SSTF sodium systems consists of a supply-storage vessel that provides sodium for test vessel(s) in each rig and a sodium purification system capable of filtering cold trapping and sampling of the sodium in the various test vessels.

Test Rig 032-R2 provides three vessels (T-2, T-4, and T-5), each with flanged-head access. T-2 is 12 in. (30 cm) in diameter by 8 ft 5 in. (2.6 m) high and serves primarily as a sodium expansion tank for 032-R2 when the test rig is isolated from 032-R1. T-4, the smallest test vessel, is 12 in. (30 cm) in diameter by 5 ft 10 in. (1.8 m) high. T-5, the largest test vessel, is 36 in. (91 cm) in diameter by 10 ft (3 m) high. The vessels are capable of operating independently of each other or in parallel, and statically or under flow-through conditions. 032-R2 also possesses its own sodium purification system for use when the rig is isolated from 032-R1.

The SASS-ACA Phase I processes and instrumentation are shown schematically in Figure X-1. The sodium system consists of two vessels (T-11 and T-12), test article housing, and associated sodium piping and argon systems, which tie into 032-R2. T-11 surge tank is 26 in. (66 cm) in diameter by 8 ft 3 in. (2.5 m) high and serves as a surge and supply tank for the SASS-ACA sodium inventory. T-12 injection tank is 18 in. (45.7 cm) in diameter by 5 ft 2 in. (1.6 m) high and serves as the supply tank for the sodium injection tests.

2. Test Article

The Phase I test unit (Figure X-2) consists of three bundles of absorber pins connected in a linear assembly by ball-and-socket joints that allow limited motion ($\sim 10^{o}$). The assembled articulated absorber fits within a cylindrical guide tube (Figure X-3). In the withdrawn, or parked, position, the assembly is held by a magnetic latch; the magnetic circuit consists of an electromagnet, a ferromagnetic cylinder fixed to the end of the absorber assembly, and a special ferromagnetic ring (Figure X-4) fixed to the upper end of the guide tube. When

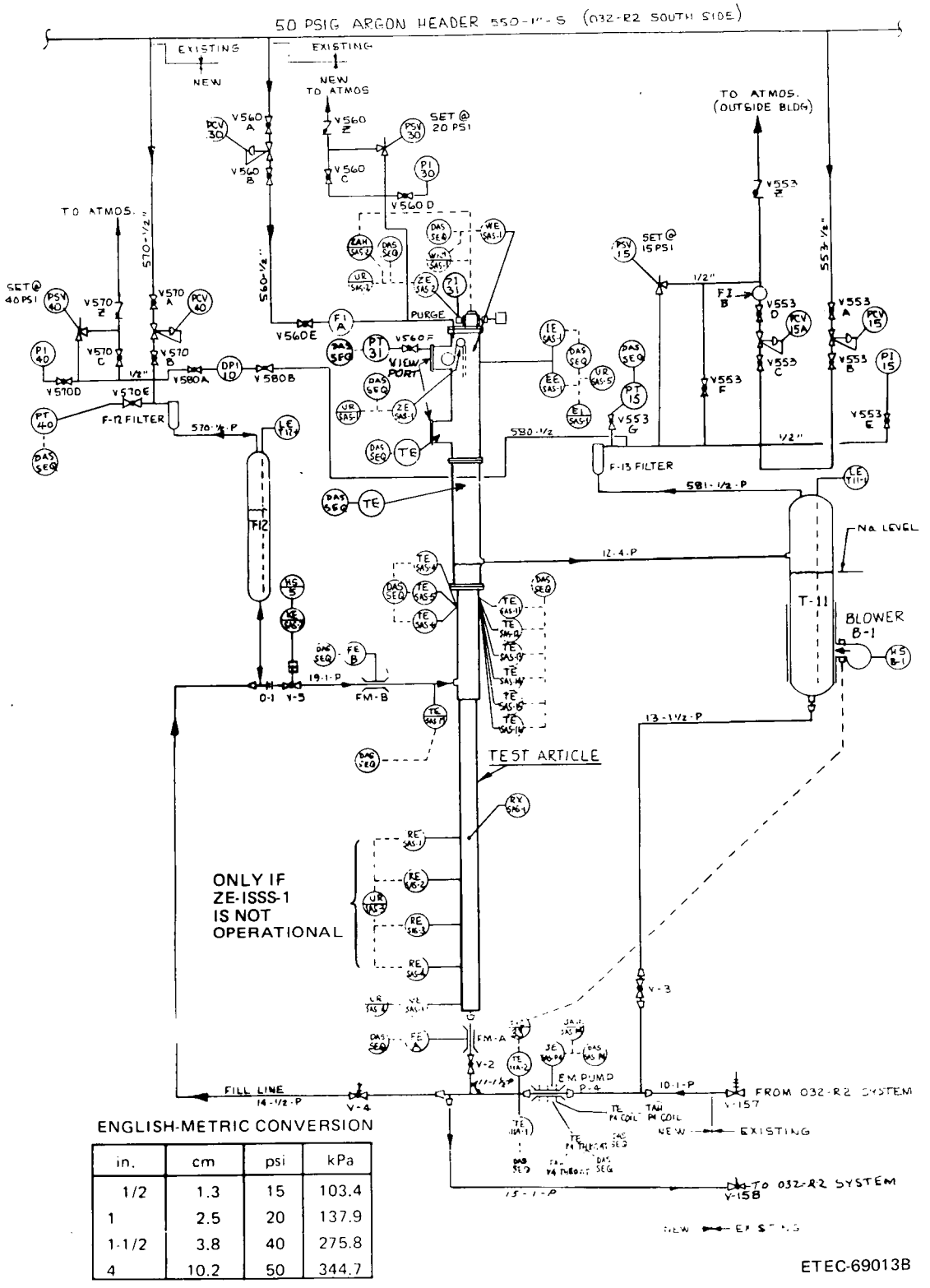

ENGLISH-METRIC CONVERSION

in.	cm	psi	kPa
1/2	1.3	15	103.4
1	2.5	20	137.9
1-1/2	3.8	40	275.8
4	10.2	50	344.7

Figure X-1. Phase I Processes and Instrumentation Diagram

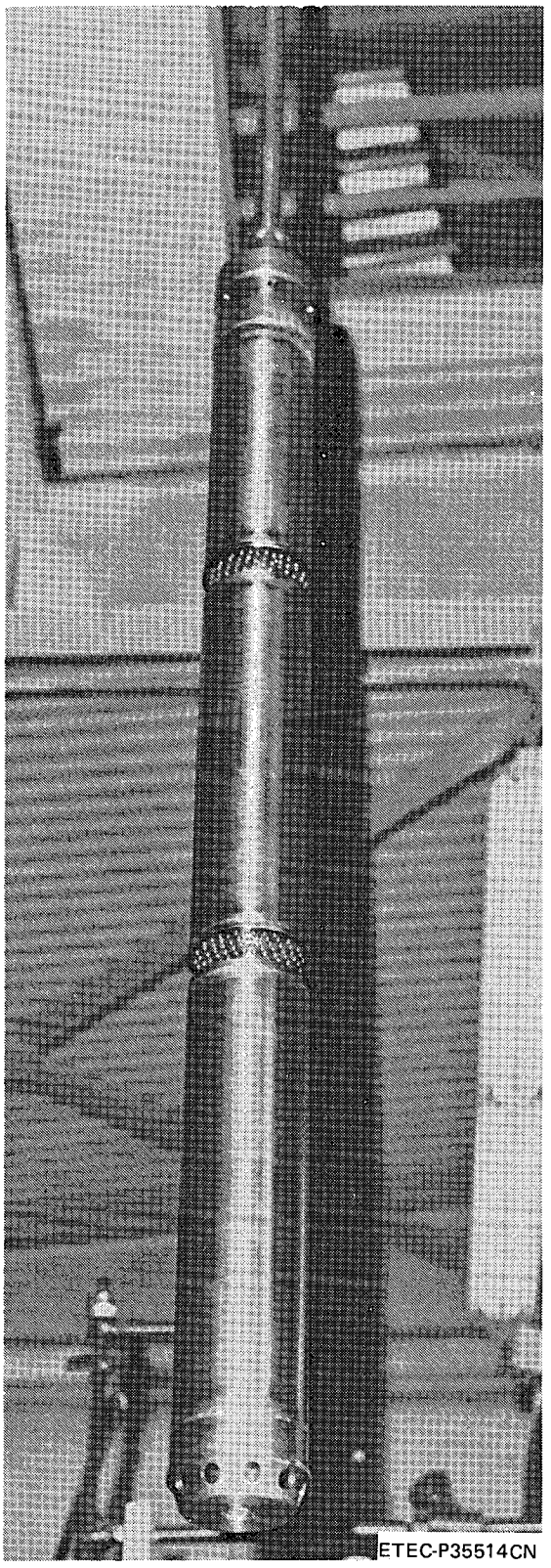

Figure X-2. Phase I Test Unit

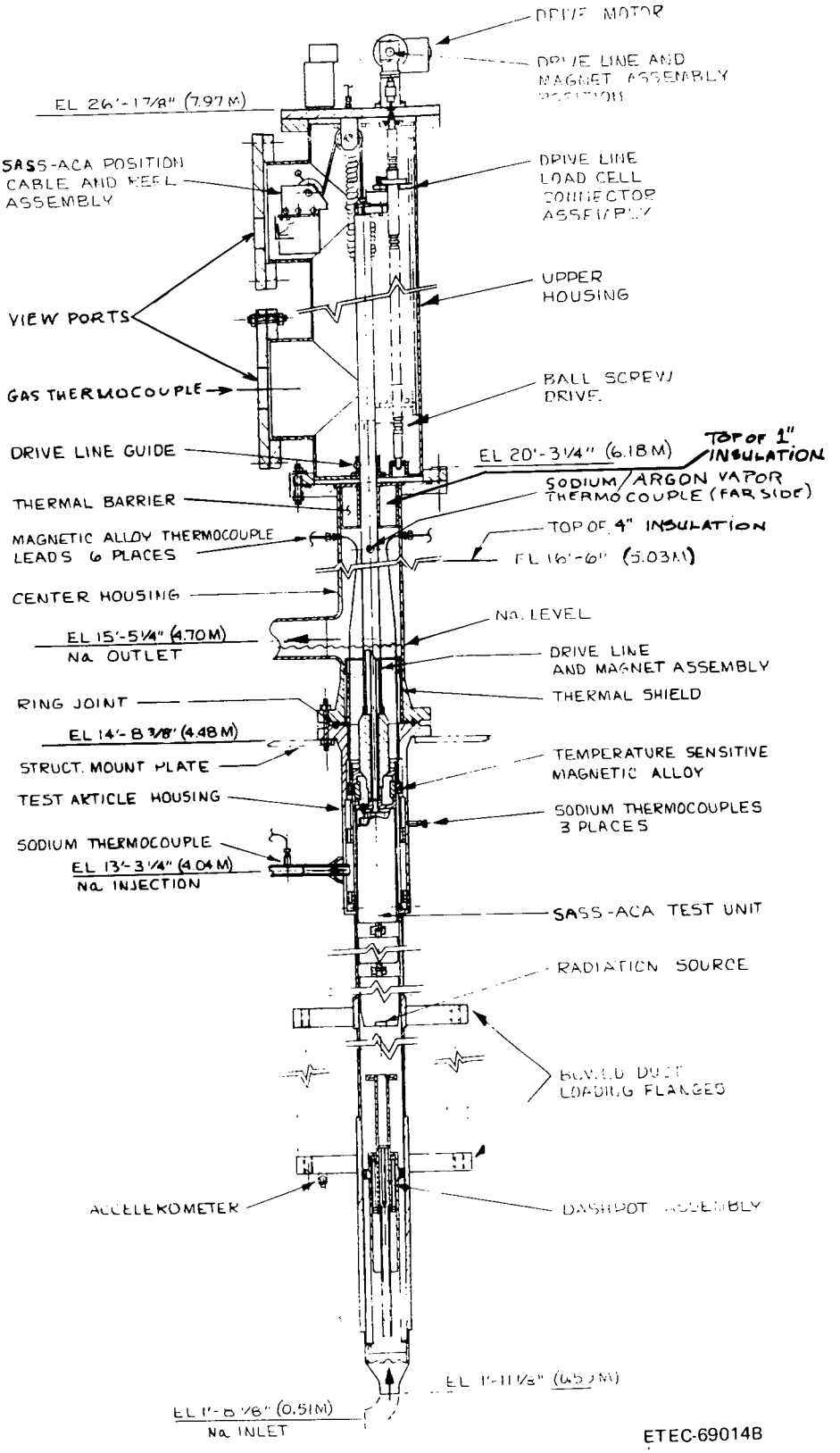

Figure X-3. Phase I Test Unit Cross Section

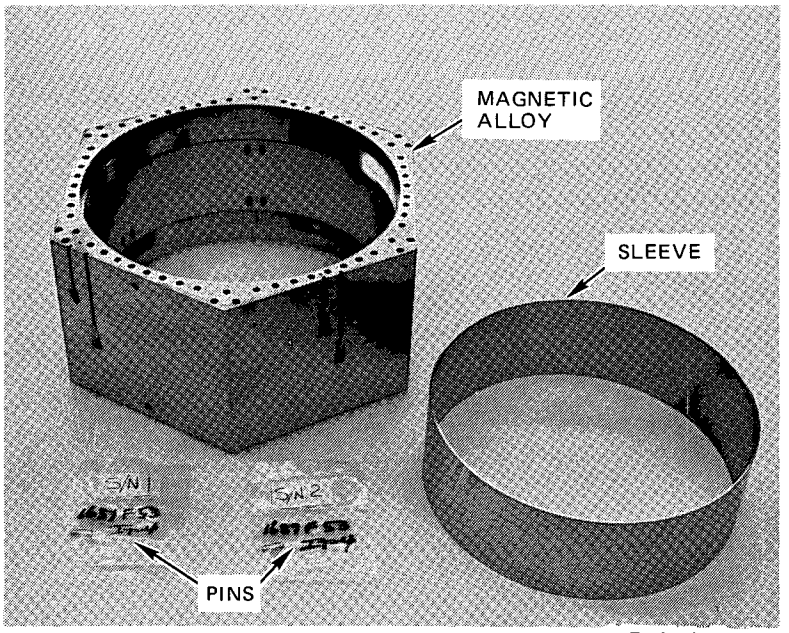

Figure X-4. Phase I Temperature-Sensitive Magnetic Alloy and Sleeve

the magnetic circuit is interrupted, the absorber assembly is dropped in the guide tube of 48-in. (121.9-cm) nominal length. The free fall of the articulated absorber assembly is stopped by a piston-dashpot assembly mounted in the lower end of the guide tube. To withdraw the articulated absorber assembly, the electromagnet is lowered into the guide tube until it contacts the top of the absorber assembly. The electromagnet is then driven onto the absorber assembly with a predetermined force. The absorber assembly is latched to the electromagnet by a magnetic circuit that includes the same elements as latched in the parked position except that the guide tube, which is 2-1/4 Cr - 1 Mo steel, substitutes for the special ferromagnetic material fixed in the upper end of the guide tube. The assembly is raised until the parked position is reached.

The special ferromagnetic material fixed to the upper end of the guide tube has a Curie point of $\sim$1050^{o}F (565.5^{o}C), at which the material becomes paramagnetic. Therefore, the absorber assembly can be released either by deenergizing the electromagnet or by raising the temperature of the special material to the 1050^{o}F (565.5^{o}C) limit.

Instrumentation is provided to measure sodium immersion temperature, sodium flow, argon flow, positions, argon pressure, load cell, current, voltage, argon and sodium vapor temperatures, and argon differential pressure.

Phase I internal sodium temperature is measured by ten immersion temperature elements, six of which are installed in the temperature-sensitive magnetic alloy. The other four temperature elements are installed upstream of the temperature-sensitive magnetic (TSEM) alloy with one in the injection line and three in the test article housing to measure sodium injection temperatures.

Phase I sodium flow is measured by two flowmeters, one in the injection line and one in the test article inlet line.

SASS-ACA release is indicated by the load cell, electromagnet current, and position indicator rod and cable attached to the upper bundle of the test unit. Position during drop is monitored by the position indicator rod and four radiation detectors. SASS-ACA insertion is indicated by the load cell, accelerometer, radiation detector, and position indicator rod. The radiation detectors are optional instrumentation.

3. Test Method

The tests are being performed in two phases: Phase I — straight guide tube — and Phase II — redesigned electromagnet, lifting socket, TSEM alloy, test facility, and bowed guide tube. In Phase I, initial tests determined the thermal time constant of the temperature-sensitive magnetic alloy, the absorber drop time, and absorber withdrawal load. The effects of a 6-month dwell upon inherent release and drop time were also determined. In Phase II, the characteristics determined in the Phase I tests will be determined for the redesigned test articles. The effect of two increasing bows in the guide tube upon drop time and withdrawal load will be determined also in Phase II.

Once the Phase II control assembly and drive line has been installed in the test loop, chracterization tests will be performed to do the following:

1) Measure coil resistance and lead resistance to ground.
2) Measure the weight of absorber and magnitude of drag forces with the load cell by raising the absorber ∿6 in. without sodium in the system.
3) Prior to sodium fill and at 400°F (204.4°C), measure coil current decay time when the current is switched off. The drive line should be preloaded on the absorber (in the down position). Repeat with 400°F (204.4°C) sodium in the loop.
4) Perform a full withdrawal with sodium at zero flow and 850°F (454.4°C).
5) With the sodium at 850°F (454.4°C), withdraw the control assembly to the parked position and determine the release current of the system.
6) Perform current characterization and demagnetization tests at 850°F (454.4°C).

Upon completion of the pretest characterization tests, the Phase II tests will be performed and will include the following:

1) Inherent Release — Increase temperature of temperature-sensitive alloy through 1050°F (565.5°C) to determine insertion time and temperature/time for assembly release while varying control assembly flow, injection flow, control assembly position, and electromagnet holding force.
2) Drop Time and Withdrawal Loads — Measure drop time after interrupting power to magnet at 0, 25, 50, 75, and 100% of sodium flows. Control-assembly withdrawal loads will be measured at each flow.
3) Bow the guide tube 0.5 in. (1.27 cm) and repeat the tests defined in Step 2.

4) Dwell Test – Maintain the assembly in the withdrawn position at 850°F (454.4°C) in flowing or stagnant sodium for 6 months. Sodium flow periods will be the maximum possible during this test.

5) Post-Dwell Tests – Repeat the Inherent Release Test (Step 1) and Drop Time and Withdrawal Load Test (Step 2).

6) Bow the guide tube 0.75 in. (1.91 cm) and repeat the tests defined in Step 2.

C. TEST RESULTS

During the bulk of the year, effort was concentrated on facility and test article modifications for Phase II testing. An overview schedule for the year is presented in Figure X-5. The test article assembly was cleaned with water at the

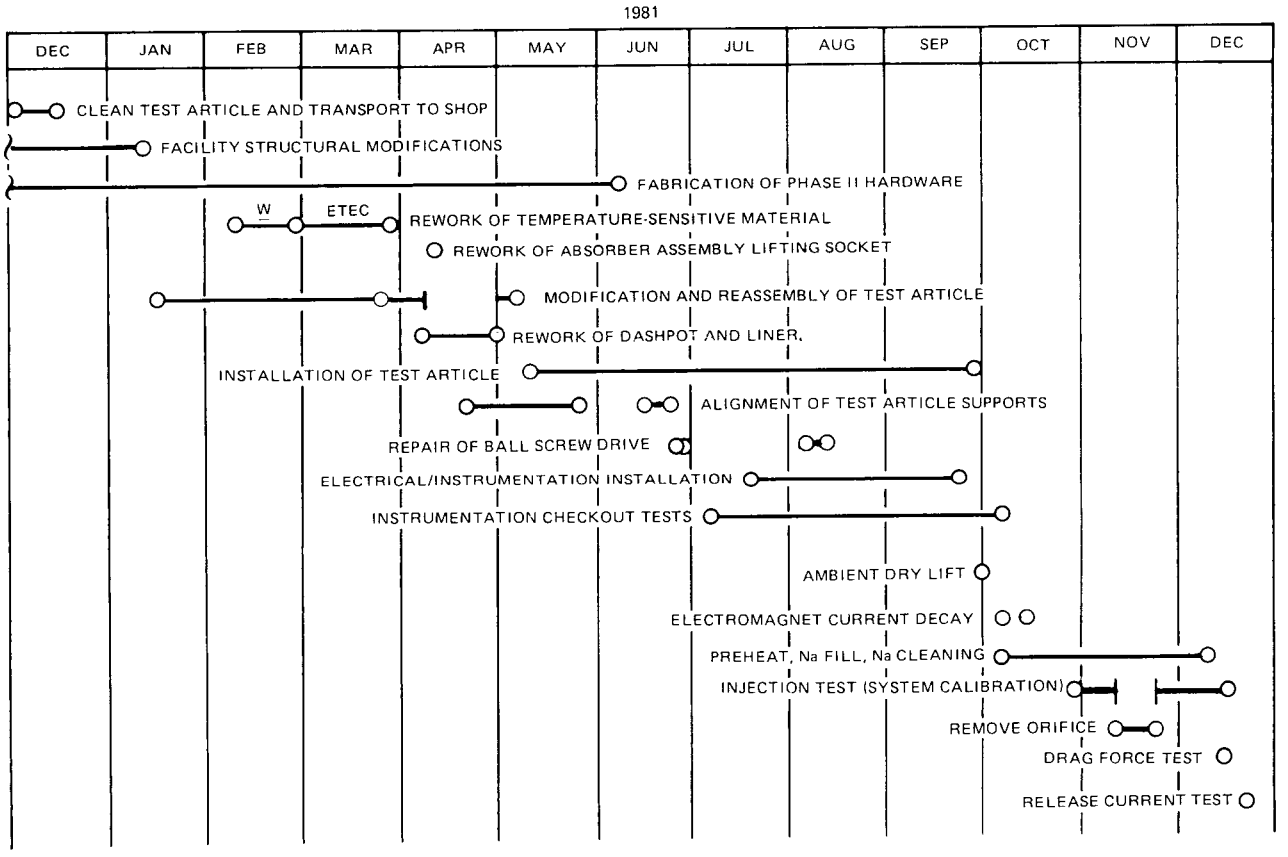

Figure X-5. Facility Modification Schedule for Phase II Program

cleaning facility (CHCF) in December 1980 and purged with nitrogen from December 12-15, 1980. After completion of nitrogen drying, the assembly was transported to the machine shop on December 15, 1980, for Phase II modifications. The SASS-ACA (absorber) was cleaned and stored pending WARD modification for Phase II testing.

The WARD Phase II TSEM was received at ETEC on January 27, 1981. Dimensional checks of the TSEM and mating parts for test article assembly indicated that the TSEM dimensions were out of tolerance (per WARD drawing) and would not permit assembly. The TSEM was returned to WARD for rework.

The reworked TSEM piece was measured, and the measurements showed that the TSEM was out of round by 0.012 in. on the internal diameter (ID). WARD requested that ETEC make the TSEM internal diameter round by pressing on the TSEM flats. Tooling was fabricated, and the TSEM was corrected to a nominal 5.7982-in. ID with a maximum out-of-round condition of 0.0008 in. on the ID.

TSEM fitup and installation on the lower guide tube of the test article assembly was completed on March 25, 1981, except for welding the six additional pins in place. During this fitup process, it was observed that the internal diameters of the lower guide tube, the insert, and the upper guide tube were not matched, although the parts were within drawing tolerances. During Phase I testing, the drag load of the SASS-ACA increased considerably due to variation of the internal diameters at this same position. Changes to drawings were made to permit matching of the internal diameters per agreement with WARD to prevent a repetition of this increased drag load during Phase II testing. The TSEM pins were welded and the internal diameters matched.

Radiography of the dashpot/bottom head assembly indicated that the center ring and two 120^{o} spacers were positioned incorrectly. The dashpot/bottom head assembly was cut and the dashpot/bottom head removed from the test article assembly. The dashpot assembly was removed from the bottom head and examined. The dashpot assembly center ring and spacers were installed and tack welded in place and the spacers tack welded to the dashpot liner. A new spring (free length

25-1/32 in. (63.58 cm)) was installed. The dashpot/bottom head was welded on the test article assembly on April 21-22, 1981. Radiography of this weld showed that the weld was acceptable.

Test article installation commenced in mid-May, and in mid-June, while installing the upper housing and lowering the drive line, some of the ball screw bearings and retainer clips fell to the bottom of the upper housing. The component was repaired and reassembly completed in late June. Installation of the test article was completed by the end of September.

The ambient dry lift was performed September 30, followed by the current decay test, preheat, sodium fill, sodium cleaning, and another current decay test. All test data were within tolerance requirements. Typical data for the ambient dry lift test and the current decay test are presented in Figures X-6, X-7, and X-8.

Injection tests were then performed to verify that the injection system was capable of delivering the flow rates required to perform the test transients. Evaluation of the data revealed that the system resistance was higher than expected. To correct this problem, an orifice in the injection supply line was removed, and higher supply pressures were used to obtain the flow rates. A procedure was also developed for setting the flow balancing valves. Additional heater controllers were also installed to provide better temperature control of the injection stream.

The Phase II test program continued in December with performance of the drag force test to characterize fluid resistance on the absorber and of a release current test to check the electromagnet coil holding capability. The inherent release tests should commence in January 1982. The testing should be interrupted in May/June 1982 for tube bowing operations. The 6-month dwell test with bowed duct is scheduled to start July 28, 1982.

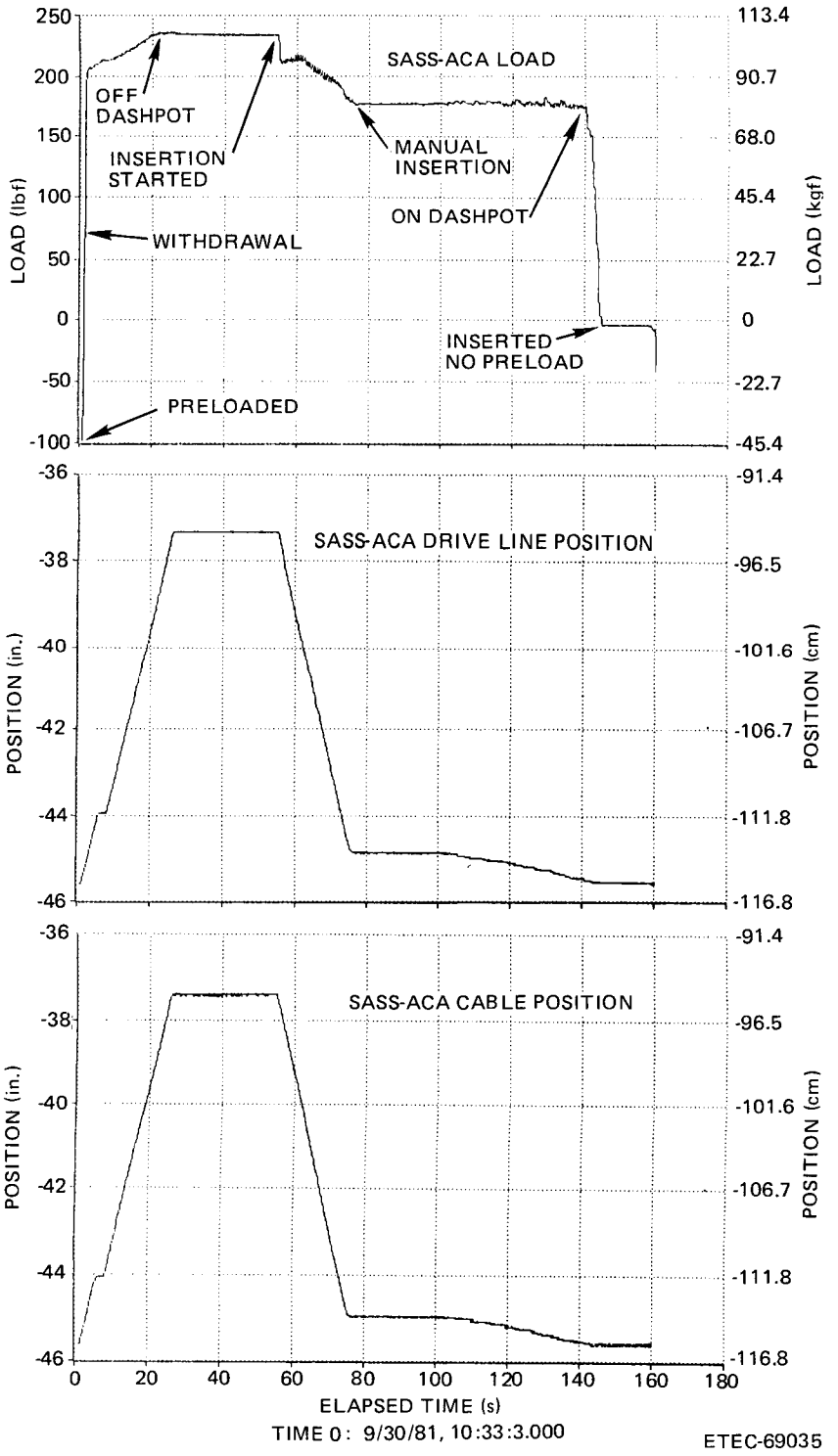

Figure X-6. SASS-ACA Phase II Test 1, Ambient Dry Lift

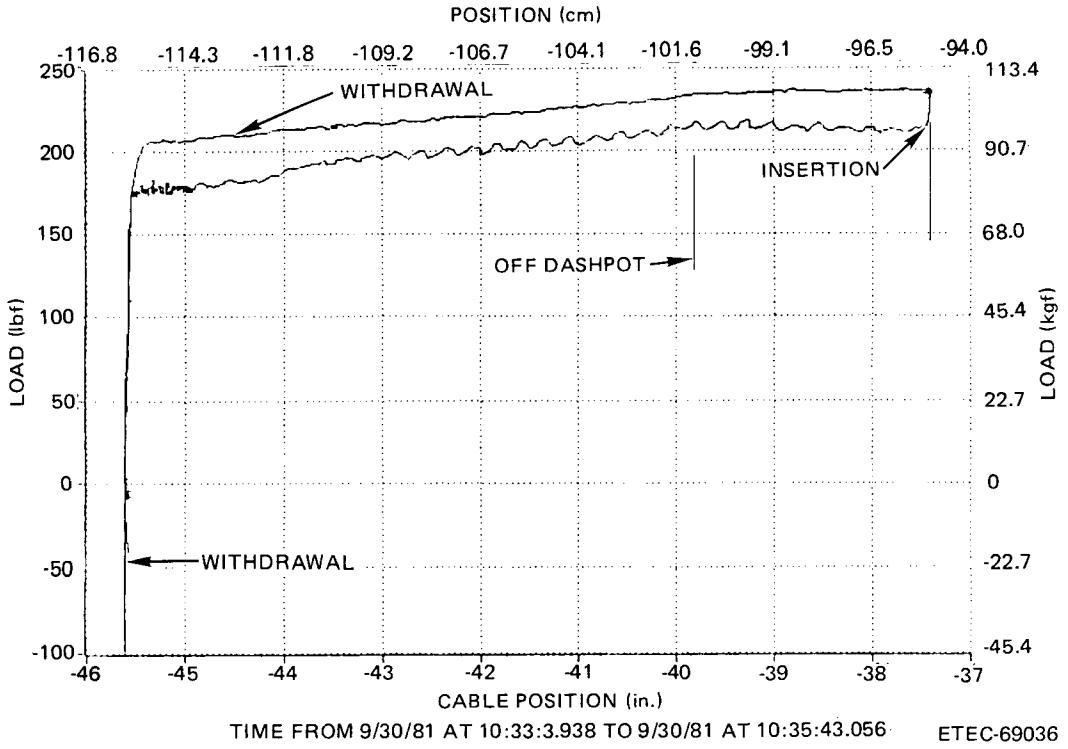

Figure X-7. SASS-ACA Phase II Test 1, Ambient Dry Lift, Load-Cable Position Comparison

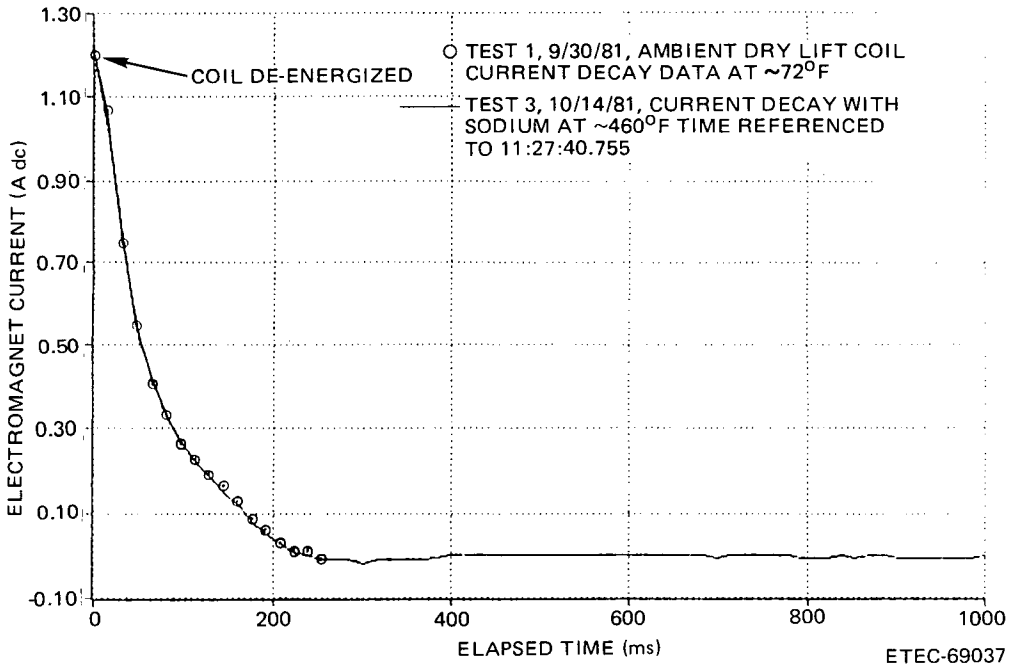

Figure X-8. SASS-ACA Phase II Test 1, Ambient Dry Lift, and Test 3, Current Decay with Sodium, EM Coil Current Decay Comparison

XI. STRAIN GAGES

G. J. TWA AND C. M. NIGHTINGALE

A. INTRODUCTION

The strain gage program fulfills three major functions: (1) general testing of different types of strain gages for use at ETEC, (2) development and evaluation of installation techniques in support of ETEC test programs, and (3) improvement in understanding strain gage data obtained by the various test programs. Testing in support of all three of these functions has been performed during this calendar year.

Four CERL-Planer capacitance gages were tested to determine their usefulness in future steam generator test applications. Evaluation of Hitec gage installation techniques for the ORNL Thermal Ratchetting Test ended early in the year when the gages failed after 4000 h at 900^{o}F.

The major portion of the work involved attempts to precalibrate Ailtech resistance gages in support of the B&W steam generator tests at ETEC. The three methods employed were: (1) bonding, (2) edge-welding, and (3) clamping.

B. AILTECH SG425 PRECALIBRATION TECHNIQUES

Attempts were made to precalibrate eight Ailtech Model SG425 resistance strain gages, employing the following techniques:

1) Bonding – A thin film (0.001-in., 0.025-mm) of Micro-measurements M-Bond GA61 epoxy was used to install the gages on calibration bars made of 2-1/4 Cr - 1 Mo steel. Load cycles were performed at 80, 200, 300, and 400^{o}F, followed by a slow cooldown to room temperature.
2) Edge-Welding – Attachment welds were placed in a single row along the edge of the flange, as shown in Figure XI-1, leaving room for the normal facility installation. Several sequences of load cycles at 80, 300, 600, and 900^{o}F followed by slow cooldowns were performed.

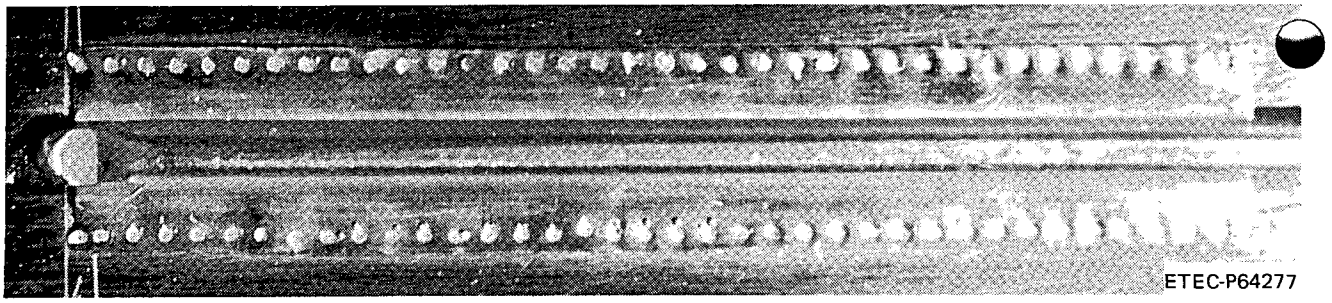

Figure XI-1. Ailtech SG425 Edge-Welding Technique

3) Clamping – A very successful method for determining apparent strain involved clamping the gage in a stainless steel fixture shown in Figure XI-2. No load cycles were performed. Gages were slow-cooled from 900°F to room temperature, then tube-welded and temperature cycled again.

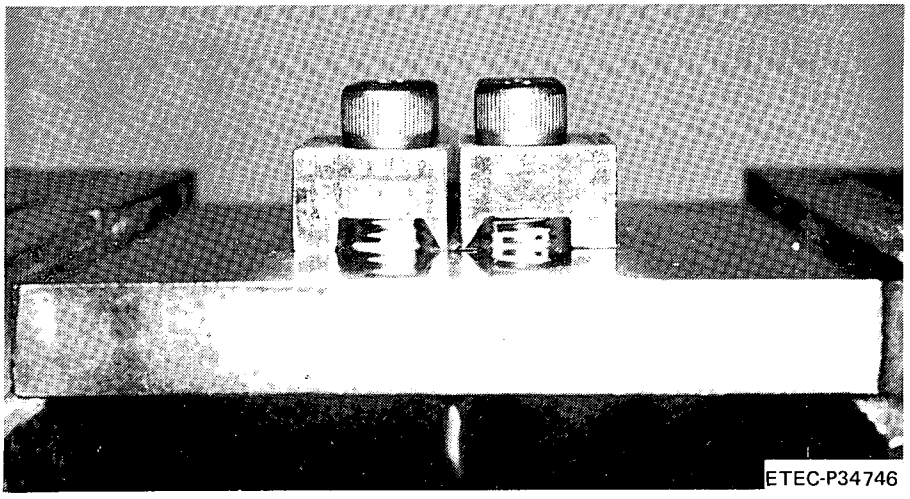

Figure XI-2. Stainless Steel Apparent Strain Precalibration Fixture

4) Tube-Welding – Data obtained using the typical facility installation technique served as a reference for the three precalibration methods described above. Welds were placed as close as possible to the strain tube at intervals of ∿0.030 in. (0.762 mm). The testing sequence was similar to that performed for the edge-welded gages.

In Figure XI-3, the gage factors for all of the gages tested were averaged, and the percent change from the manufacturer's room-temperature value (4.89) was plotted against temperature. The gage factor is a dimensionless quantity related to the change in gage resistance per change in applied strain. As seen in Table XI-1, neither the manufacturer's data nor the edge-welded tests alone could satisfactorily predict the gage factors seen when the gages were tube-welded. The maximum error based on Ailtech's predicted values was almost 10%, while use of the edge-welded data to predict gage factor exceeded 8%. However, by using an epoxy-bond calibration at room temperature and the manufacturer's data for change in gage factor with temperature, errors of less than 4% were obtained for temperatures up to 900°F.

TABLE XI-1

PERCENT DIFFERENCES BETWEEN PREDICTED AND OBSERVED GAGE FACTORS

Strain Gage (S/N)	Bonded + Ailtech		Ailtech Alone		Edge-Welded Alone	
	Error	%[a]	Error	%	Error	%
4078-1	0.11	2.36	0.24	6.12	0.18	3.87
4078-3[b]	0.13	3.12	0.25	5.99	0.24	5.75
4078-4	0.17	3.35	0.17	3.35	0.23	4.53
4078-5	0.13	2.91	0.43	9.63	0.14	3.38
4078-6	0.12	2.80	0.13	3.03	0.18	3.81
4078-7	0.07	1.49	0.10	2.31	0.19	4.04
4078-8	0.07	1.53	0.32	7.31	0.15	3.28
4078-9[c]			0.35	8.61	0.35	8.61

[a]Percent of tube-welded gage factor at the temperature of maximum error.
[b]Gage 4078-2 failed following epoxy-bonding test.
[c]Gage 4078-9 replaced Gage 4078-2 and was not tested in the epoxy-bonded configuration.

Neither Method 1 nor Method 2 was adequate in predicting the tube-welded apparent strain. However, the clamping fixture produced curves that, when zero corrected at ambient temperature, differed by no more than 10 με from curves of tube-welded gages at 800°F. One set of apparent strain curves is shown in Figure XI-4, not corrected to zero at room temperature. A second Ailtech SG425 gage

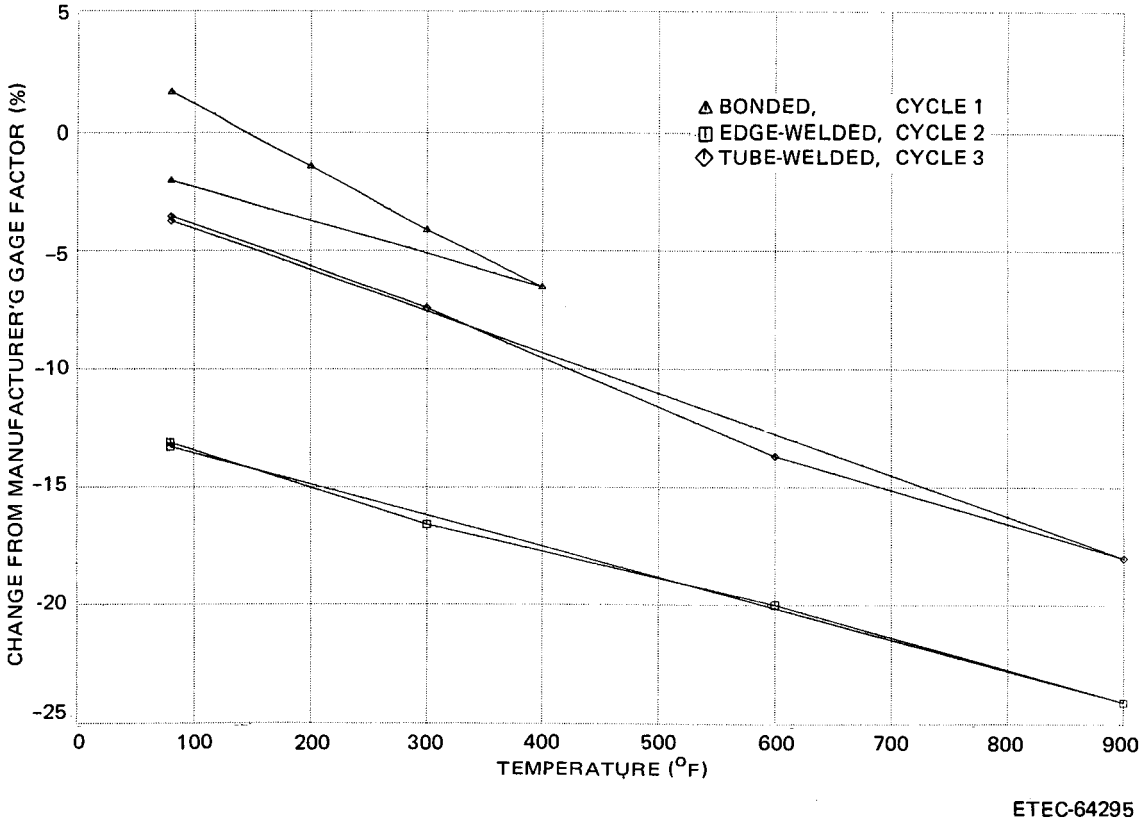

Figure XI-3. Ailtech SG425 Average Gage Factors from Three Installation Techniques

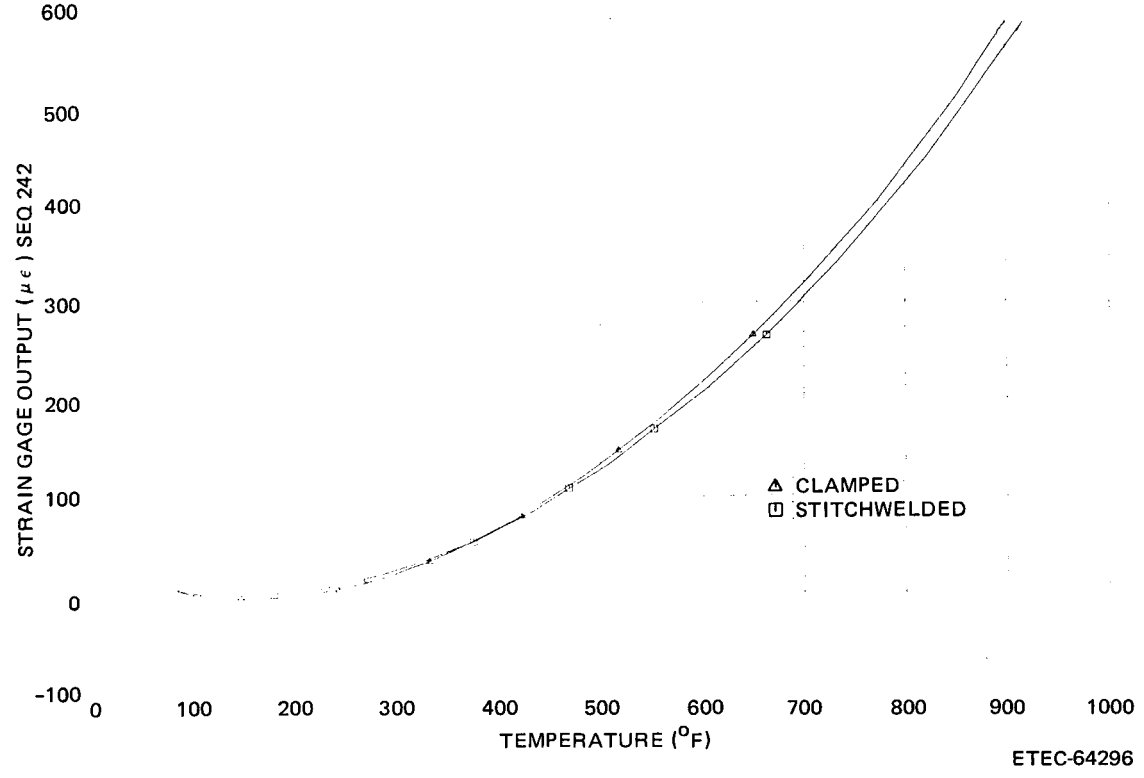

Figure XI-4. Apparent Strain Clamping Fixture Test Data

was tested with an error at 800°F of less than 50 με. A test program involving fixture made of 2-1/4 Cr - 1 Mo steel was initiated at the end of the year.

The tube-welded gages were then baked at 900°F and had completed 5525 h at the end of the year. Four of the gages are shown in Figure XI-5. Table XI-2 summarizes the stability test data.

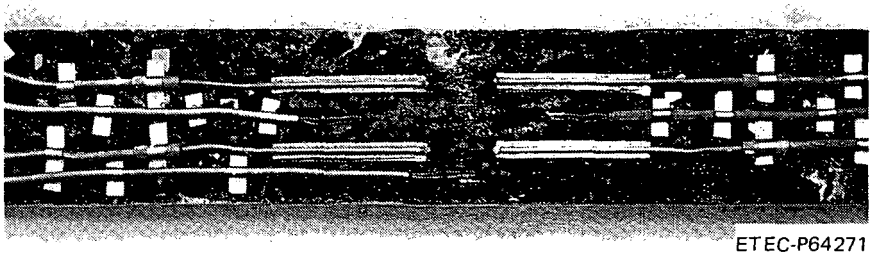

Figure XI-5. Ailtech SG425 Gages after 5500 Hours at 900°F

TABLE XI-2

AILTECH SG425 900°F STABILITY TEST DATA

Gage	Status	Total Drift (με)	Sensitivity[a] (% change from original)
4078-1	Operable[b]	+170	-4.88
4078-3[c]	Failed at 0 h	-	-
4078-4	Failed at 1103 h	+98[d]	+2.38[d]
4078-5	Operable	+161	0.00
4078-6	Failed at 2974 h	+140	0.00
4078-7	Failed at 2974 h	+50	0.00
4078-8	Operable	+165	-4.88
4078-9[c]	Failed at 1103 h	+1151	+2.50

[a]Sensitivity = mV/με from first-order curve fit.
[b]An "Operable" gage still responds to load-cycling.
[c]Gage 4078-9 replaced Gage 4078-2, which failed following the bond test.
[d]"Total Drift" and "% Change in Sensitivity" reflect values at time of failure.

C. AILTECH MG425 PRECALIBRATION TECHNIQUES

A duplicate of the test described in Section B was performed for eight Ailtech Model MG425 gages. A typical gage is shown in Figure XI-6. The only differences between the two programs were:

1) A double row of spot welds was made along the edge of the flange in an attempt to improve the strain transfer of the edge-weld technique. Instead, the mortality rate of the gages increased, possibly because less of the flange remained for successful tube-welding.
2) No tests had been performed in the clamping fixtures at the end of the year.

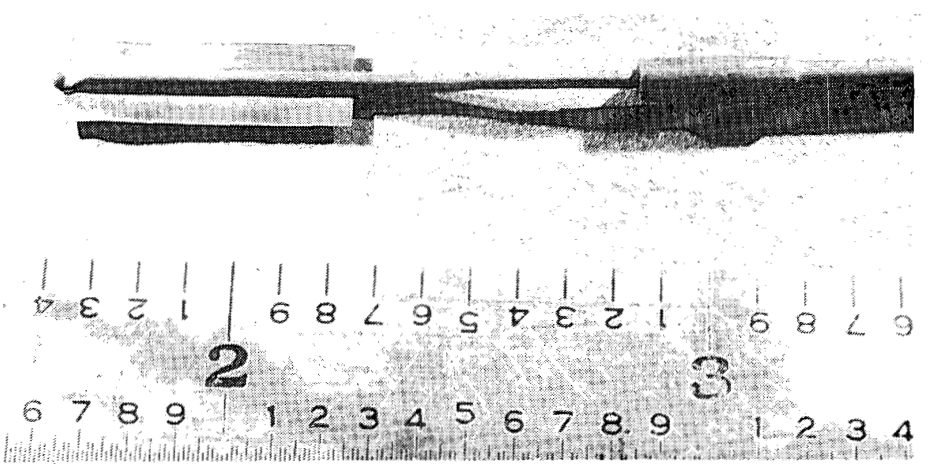

Figure XI-6. Ailtech MG425 Resistance Strain Gage

Only preliminary analysis of the data has been performed. Figure XI-7 summarizes the gage factor data from load-cycling at temperatures up to 900°F. Gage factors from all eight MG425 gages were averaged and plotted against temperature.

Several observations are listed below:

1) The slope of the curve of bonded gage factor vs temperature approximates the slope predicted by Ailtech.

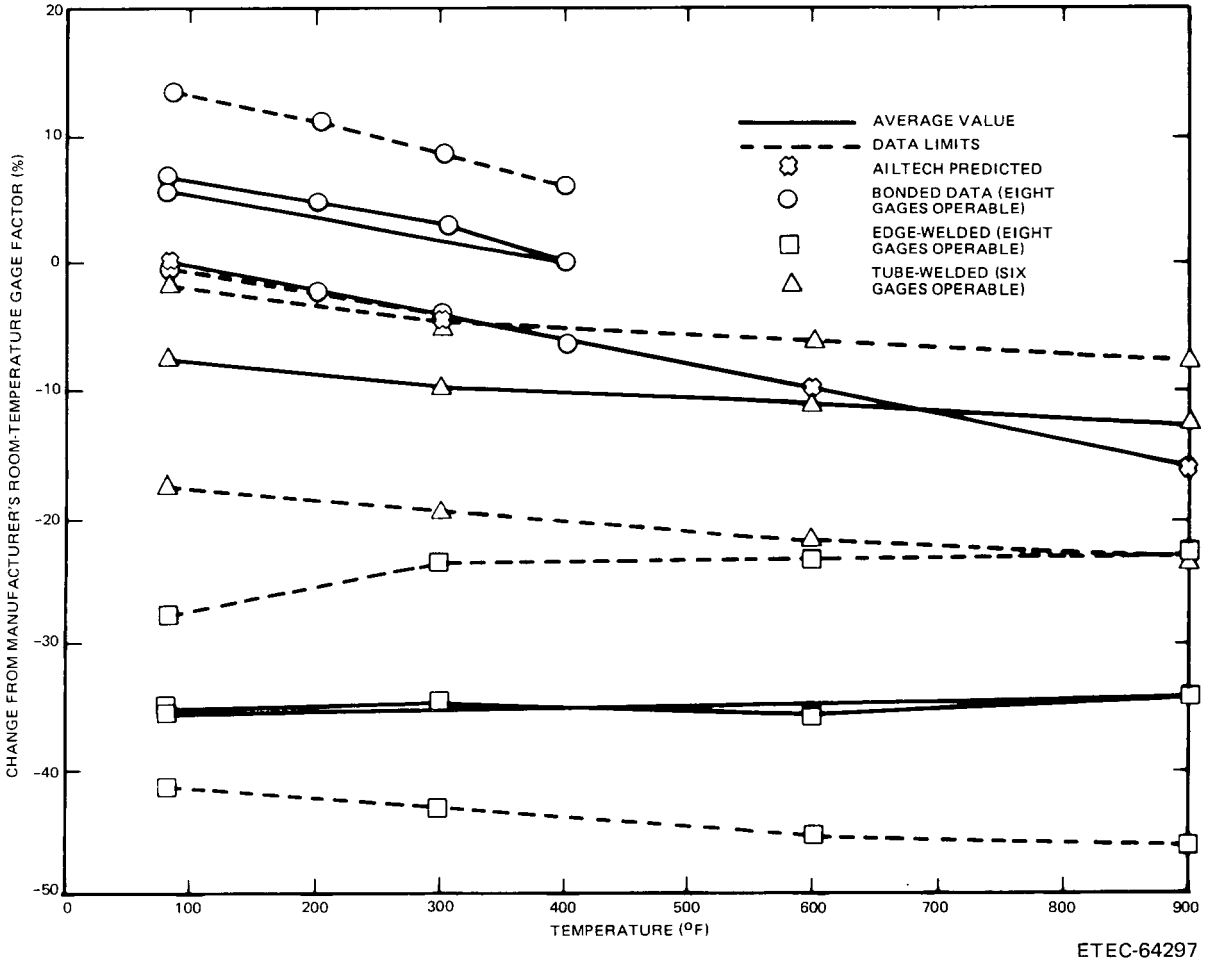

Figure XI-7. Ailtech MG425 Average Gage Factors from Three Installation Techniques

2) The edge-welded data are shifted negatively from the tube-welded gage factors. The difference shown in the average gage factors at room temperature is -30% of the tube-welded value.
3) Both the edge-welded and tube-welded data show very little change in gage factor with temperature.
4) The average gage factor from the room-temperature load cycling of the bonded gages is shifted ∿13% above that of the tube-welded gages.
5) The apparent strain curves from the three methods (bonding, edge-welding, and tube-welding) were very different.

D. CERL-PLANER CAPACITANCE GAGE

Four CERL-Planer Model C4 capacitance strain gages were tested this year. Figure XI-8 illustrates the basic working principles of the gage. Two stainless steel ribbons of differing lengths are welded to the specimen at Points A and B. A change in the distance between A and B produces a change in the distance between capacitor plates attached to the ribbons. The resulting change in gage capacitance is measured and can be related to strain by a third-order function.

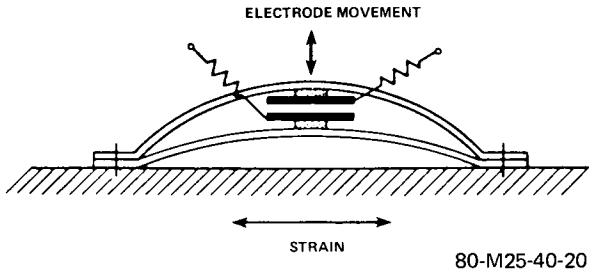

Figure XI-8. Diagram of CERL-Planer Capacitance Strain Gage

Testing was completed in two phases:

1) The gages were clamped in the Hitec-made fixture shown in Figure XI-9 and calibrated at room temperature. Figure XI-10 contains the calibration curve for Gage 4214 over the range -5000 to +5000 microstrain (the full range of the gage). The manufacturer's data are also shown.
2) The gages were spot-welded to 2-1/4 Cr - 1 Mo steel bars and load- and temperature-cycled at temperatures as high as 1200^{o}F. Early in the test sequence, one end of Gage 4211 came loose from the bar due to severe oxidation of the 2-1/4 Cr - 1 Mo steel. All gages displayed abrupt changes in output as the bars were being heated and cooled. During the second series of load cycles (at temperatures of 80, 400, 800, and 1200^{o}F), Gages 4213 and 4214 became even more erratic and at 1200^{o}F failed to respond to load. Following cooldown, the gages were inspected; however, no problems could

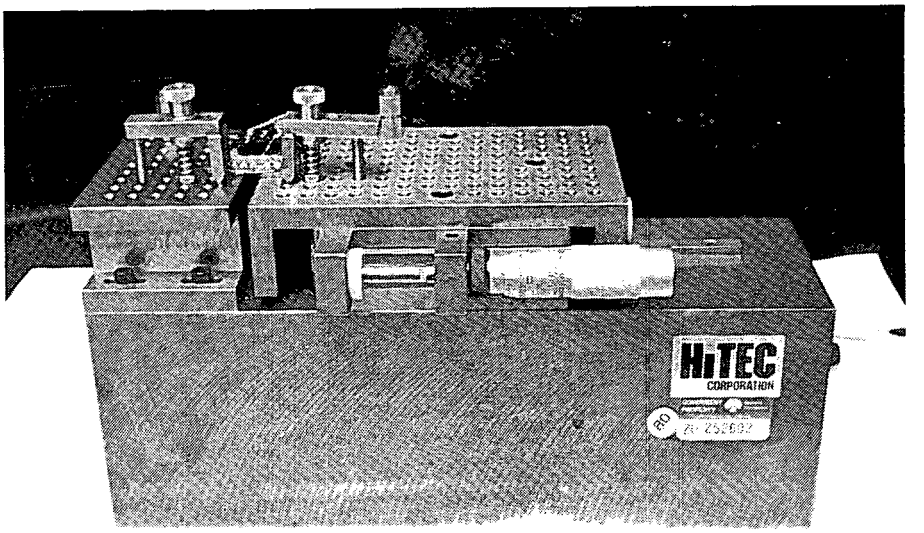

ETEC-P34630

Figure XI-9. Hitec Room-Temperature
Strain Calibrating Fixture

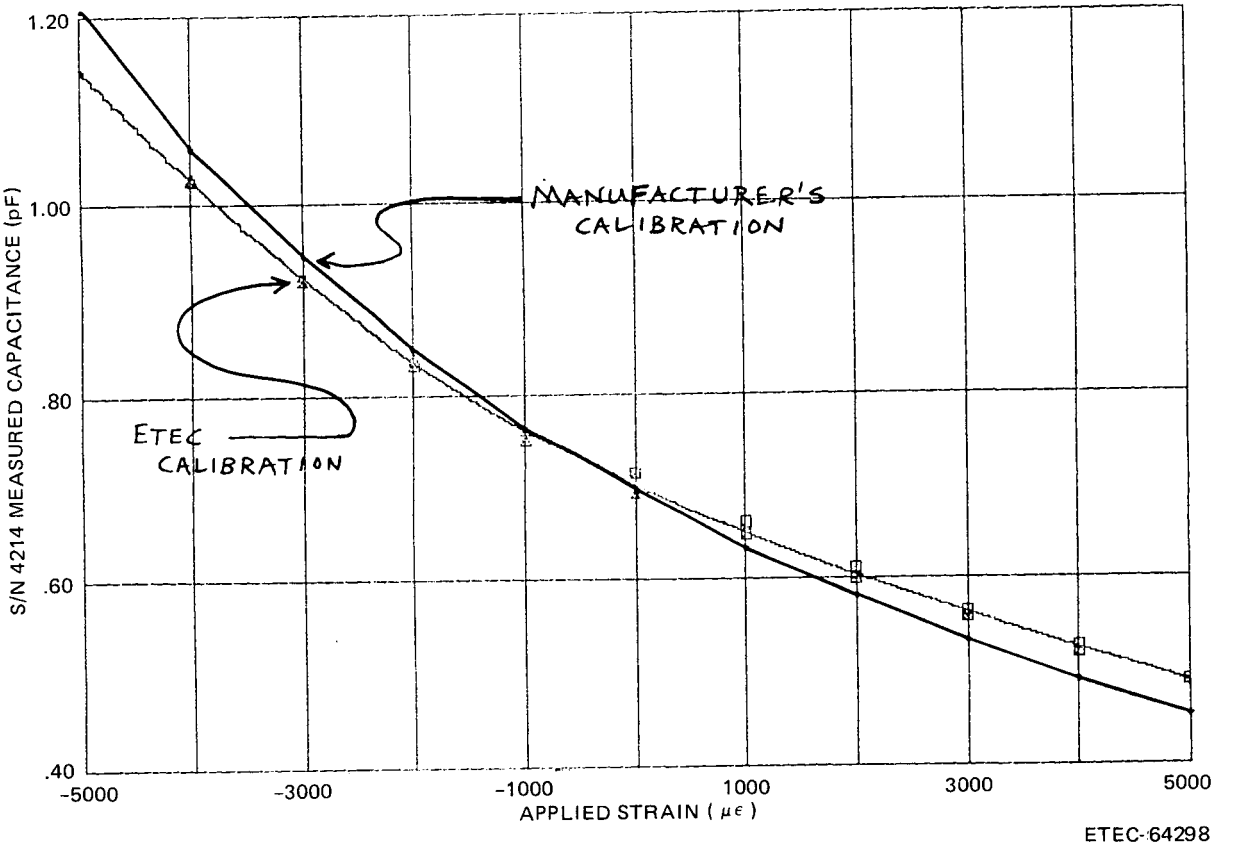

ETEC-64298

Figure XI-10. Room-Temperature Calibration Data
Compared to Manufacturer's Data

be found in the attachment welds or in the lead wires. The bars were heavily oxidized, as can be seen in Figure XI-11. Testing of the remaining gage was discontinued.

E. ORNL STABILITY TEST

A test involving two Hitec 1-in. capacitance gages installed using the method employed for the ORNL Thermal Ratchetting Test was in progress at the beginning of the year. During January, two gages completed 4000 h at 1100°F, at which time sudden unexplained zero shifts were observed. Since the ORNL test was not expected to exceed 4000 h, the stability test was terminated.

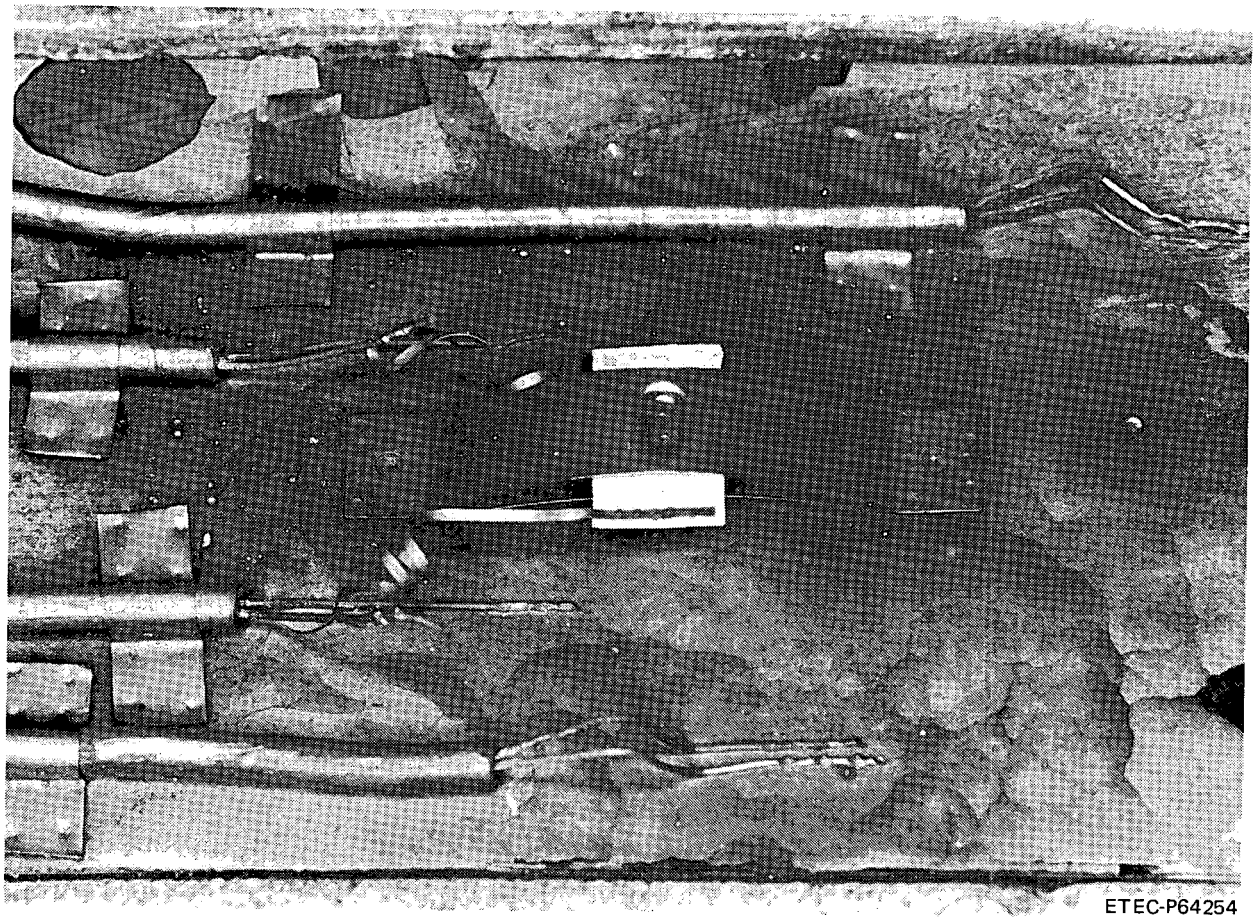

Figure XI-11. Croloy Calibration Bar with CERL-Planer Gage

XII. TRANSITION JOINT LIFE TEST PROGRAM

R. C. SOUCY

A. INTRODUCTION

Three identical test articles were used in the Transition Joint Test Program. Each test article is a pipe section 79 in. (200 cm) long, 18 in. (457 mm) in outside diameter, and with a 1-in. (25.4-mm) wall thickness, made from a combination of 2-1/4 Cr - 1 Mo, Alloy 800H, and 316H SS pipe subsections joined by circumferential welds. These test articles represent full-sized prototype Clinch River Breeder Reactor Plant (CRBRP) intermediate heat transfer system transition joints.

Each test article was equipped with clamshell ovens and hydraulic actuators mounted between load rings to provide for the application of constant axial load and high-temperature isothermal hold periods. The transient test articles were fitted with inlet and outlet flanged connections to allow the in-flow and exhaust of nitrogen gas to provide rapid downtransient conditions.

Instrumentation was installed on the test articles to measure applied loads, temperatures, and strains to record the effects of thermal shock and external mechanical loads on the tri-metallic weld seams.

Three test articles were provided to allow the performance of three transient test series and one isothermal test series. These tests simulated loading and thermal cycling conditions required for CRBRP operation accelerated to induce failure at the tri-metallic weld seams within an expected 1-year period.

Transient Test Article 1 (TRTA-1) and the isothermal test article (ISOTA) were tested to completion last year and covered in a previous report.

This report deals with the performance and results of the test series completed for Transient Test Article 2 (TRTA-2) and Transient Test Article 3 (TRTA-3).

Test results will be used to determine the mode of failure in the test article, evaluate the effects of accumulative creep and thermal fatigue, and evaluate the service life of the tri-metallic joint as compared to the bi-metallic design.

B. TEST DESCRIPTION

1. Test Facility

The Thermal Transient Facility (TTF) provides a single-pass gas flowdown system designed to supply a preprogrammed flow of nitrogen gas, at essentially constant pressure and temperature through a thermally preconditioned test article. Thermal transients are simulated by flowing nitrogen gas from high-pressure gas storage, through flow control valves, past the test article, through back-pressure control valves, and out of the exhaust stack to the atmosphere. In addition, the facility is designed to hold the selected test article in a fixture capable of imposing prescribed mechanical loads on specific portions of the test article, thus simultaneously subjecting the test article to expected plant mechanical and thermal transient stresses. The system flow diagram is shown in Figure XII-1.

Capability to perform both upramp and downramp transients is provided. For downramp testing, ambient-temperature gas is discharged through a heated test article to cool it at a precalculated rate. The test article can be preheated from ambient to any temperature up to 1200^{o}F (649^{o}C) and held within 25^{o}F (13.9^{o}C) of the selected temperature. Components can be tested up to and including failure by subjecting the test article to repetitive transients at design conditions or in excess of design conditions.

Control of the test is entirely by digital computer. Transient rates are directly controlled by temperature feedback from thermocouples located on the test article. Alternatively, the transient can be controlled by a preprogrammed time-varying nitrogen flow rate determined by a polynomial equation of flow vs time generated by the computer. A similar equation can be generated for system

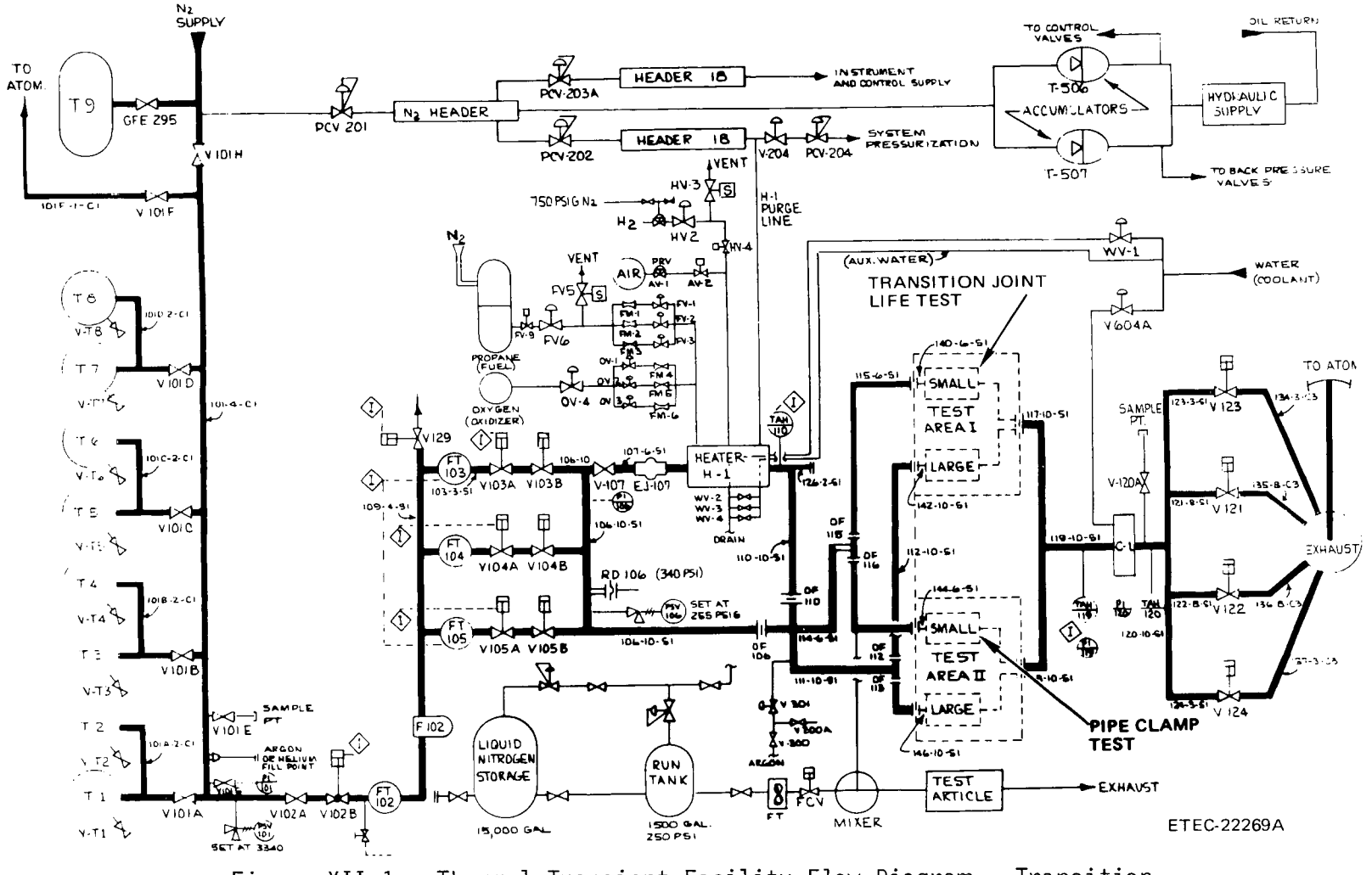

Figure XII-1. Thermal Transient Facility Flow Diagram — Transition Joint Life Test at Test Area I

pressure control. All data during a test are processed by the computer. It compares measured temperature or flow to the demand values and sends signals to the servo valve controllers to bring the two values together. The control signal is updated 50 times per second.

Instrumentation to measure pressure, flow, temperature, and strain for the facility equipment and piping is provided. The test area is equipped with a support fixture and floor structure providing reaction points for applying mechanical loads. Hydraulic fluid or high-pressure gas is available so that constant loads can be imposed on the test article.

The facility is located at the Energy Technology Engineering Center (ETEC) in the Santa Susana Mountains of Southern California. An existing building (013) was modified to house the test stations and the gas process system. Utilities and supporting facilities such as power, water, and natural gas are available at the site. A special high-pressure gas supply system is provided to allow tie-in to the Santa Susana 5000-psig nitrogen distribution system.

2. Test Article

Two identical test articles were provided to allow the performance of two transient test series.

Each test article is a pipe section 79 in. (200 cm) long, 18 in. (457 mm) in outside diameter, and with a 1-in. (25.4-mm) wall thickness, made from a combination of 2-1/4 Cr - 1 Mo, Alloy 800H, and 316H SS pipe subsections joined by circumferential welds. The entire assembly consists of six metal subsections, including the tri-metallic joint, the bi-metallic joint, extension pieces required for test article support, and nitrogen connections as shown by the schematic in Figure XII-2.

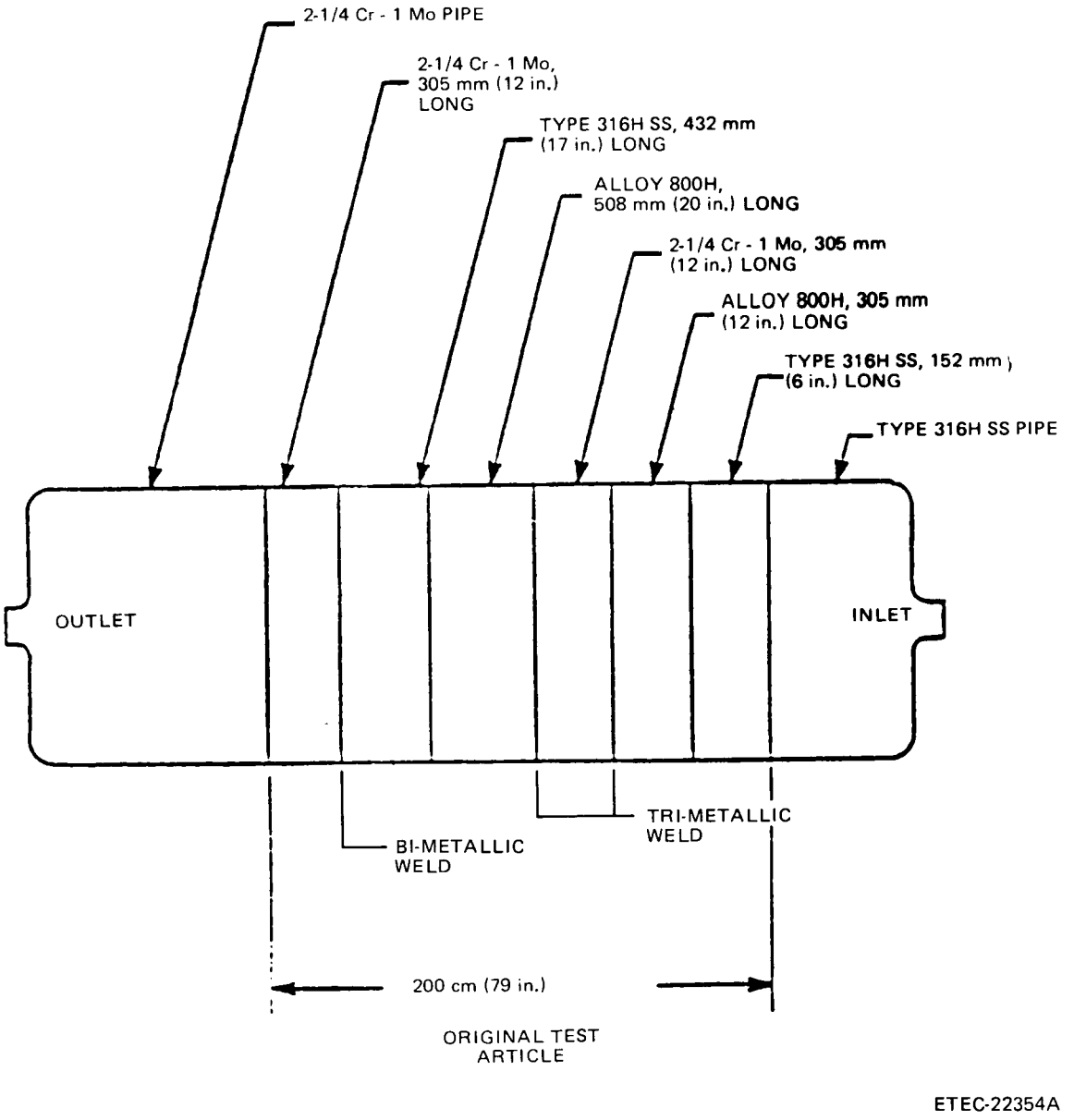

Figure XII-2. Test Article Schematic

The test article was designed to simultaneously test several dissimilar metal welds. The dissimilar metal combinations in the test article are the same as those in the reference design for the CRBR transition joints, with the addition of a weld of 2-1/4 Cr - 1 Mo to 316H SS, which is typical of a conventional bi-metallic weld. This weld served as a reference from which to measure the additional life resulting from the tri-metallic design.

Each test article was fitted with brackets and load rings mounted on extension assemblies welded to each end of the test article pipe sections to provide test article support and a fixture for the location of hydraulic actuators mounted between the load rings to allow for the application of constant axial load. The test articles were provided with clamshell ovens fitted with electrical heaters and equipped with temperature-indicating controllers to allow a controlled heatup capability and the maintenance of high-temperature isothermal conditions.

The transient test articles were fitted with inlet and outlet flanged connections to allow the in-flow and exhaust of nitrogen gas to provide rapid down-transient conditions. A centerbody was located within the test article pipe section to improve nitrogen flow heat transfer.

The overall transient test article assembly (TRTA-2) is shown in Figure XII-3. The overall assembly of the third transient test article (TRTA-3) is shown in Figure XII-4.

After installation at the TTF, each test article was instrumented with internal and external thermocouples. A typical test article configuration is shown in Figure XII-5, along with the location of internal thermocouples for both test articles.

Nine internal thermocouples, brazed and percussion-welded, were installed on TRTA-2, where three were located between each of the first four weld seams. Twenty-four external thermocouples, mounted with marimet blocks, were installed on the test article, six located adjacent to each of the first four weld seams.

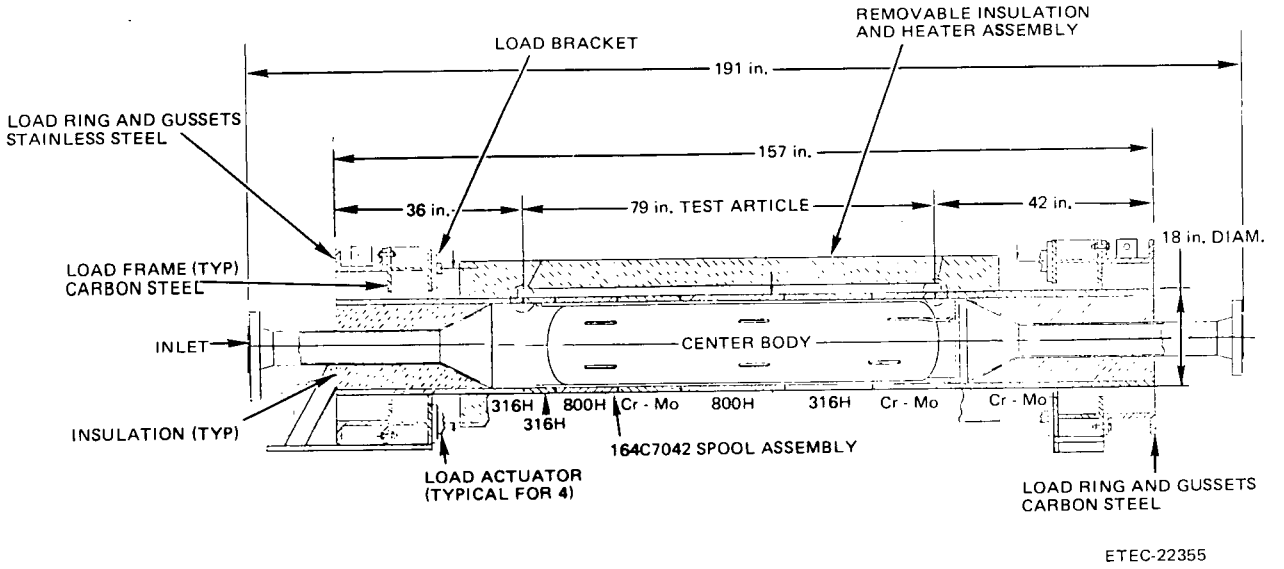

Figure XII-3. Thermal Transient Test Article Assembly — Test Articles 1 and 2

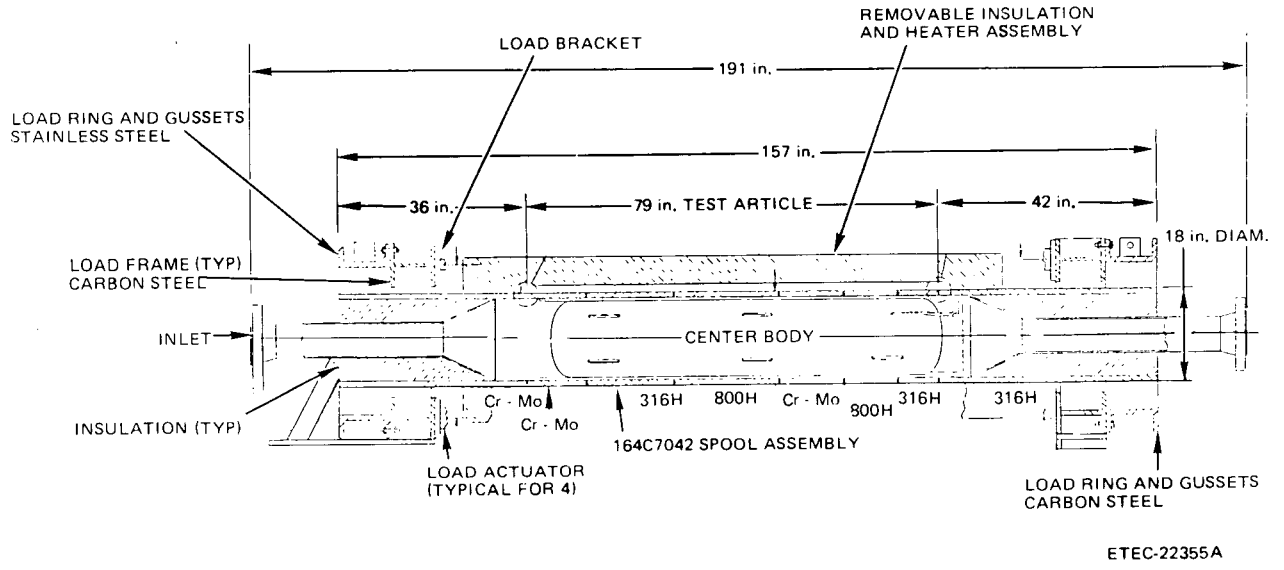

Figure XII-4. Thermal Transient Test Article Assembly — Test Article 3*

*Test Article 3 was removed from the ISOTA assembly and installed in TRTA-3

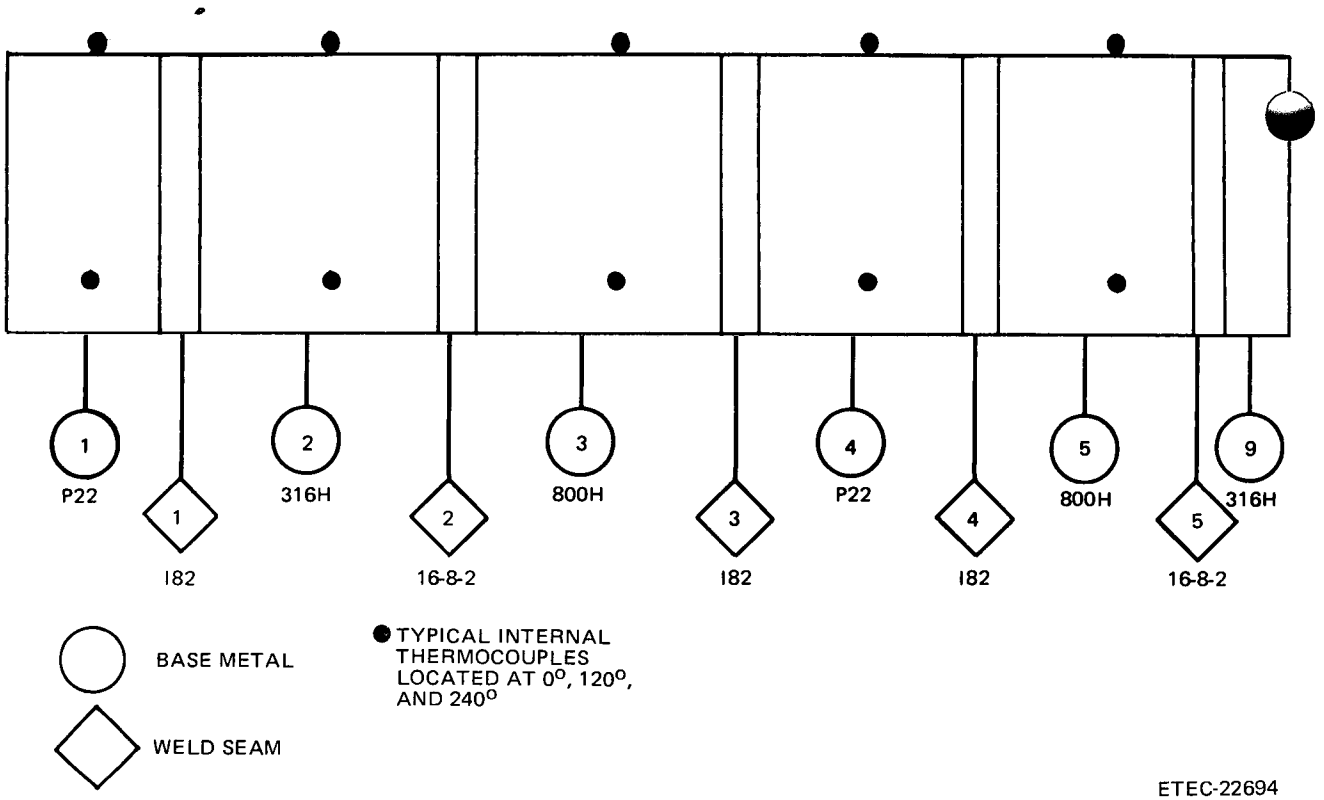

Figure XII-5. Configuration and Internal Thermocouple Arrangement (TRTA-2 and TRTA-3)

Sixteen additional percussion-welded external thermocouples were added on TRTA-2 during March 1980 to supplement temperature measurements. One was located adjacent to each of the nine internal thermocouples and the others adjacent to Welds 1, 3, and 4.

Six internal and six external percussion-welded thermocouples were added on TRTA-2 during January 1981 to measure temperature in base-metal Sections 1 and 5 as shown in Figure XII-5.

TRTA-3 was fabricated from the isothermal test article and installed in the reverse position with the bi-metallic joint at the upstream location. This test article was fitted with fifteen percussion-welded internal thermocouples, three located between each weld seam and 15 percussion-welded external thermocouples, one located adjacent to each internal thermocouple. Twenty-four external thermocouples, mounted with marimet blocks, were installed on the test article, six located adjacent to each of the first four weld seams.

3. Test Methods

a. Thermal Transient Test

Figure XII-6 shows the time-temperature-load diagram for the transient test articles, and Table XII-1 shows the axial loads, hold temperatures and times, thermal transient rates, and the tolerance of each parameter.

Transient test articles were heated from ambient to a 1100°F (593°C) hold temperature at the maximum practical rate, as shown in Table XII-1. The temperature of the article was maintained at a nominal 1100°F (593°C) for each transient test article, with a nominal 66-h hold time per cycle. The estimated time per complete cycle was 72 h (3 days). Each unit was subjected to a three-step thermal transient as shown in Figure XII-6.

The nitrogen flow and transient rate for TRTA-2 and TRTA-3 were directly controlled by temperature feedback from internal thermocouples located in the tri-metallic joint Cr-Mo section. Upon reaching ambient temperature, the test article was again heated to the hold temperature and the cycle repeated. The nominal axial load of 400,000 lb (1.78×10^6 N) for each article was maintained during the hold times and during transients but removed during nondestructive examination. In this case, removal of loads was performed after the test article had reached ambient temperature. The TRTA-2 axial load was reduced to 100,000 lb (0.45×10^6 N) for Cycles 27-46.

An external enclosure fabricated from flexible plastic was installed on TRTA-2, Phase II, Cycle 12 on September 11, 1980, and TRTA-3 Cycle 1 on October 17, 1980, to provide a nitrogen cover gas atmosphere to prevent severe oxidation of the test article Cr-Mo surfaces. Belts of titanium oxygen getter meterial were installed on TRTA-2 and TRTA-3 to supplement the Cr-Mo protection system. Following Cycle 6, TRTA-3 was fitted with a new butyl rubber cover gas enclosure designed to provide a more leaktight system and improve the protection of the Cr-Mo surfaces. Figure XII-7 shows the butyl rubber enclosure installed on TRTA-3.

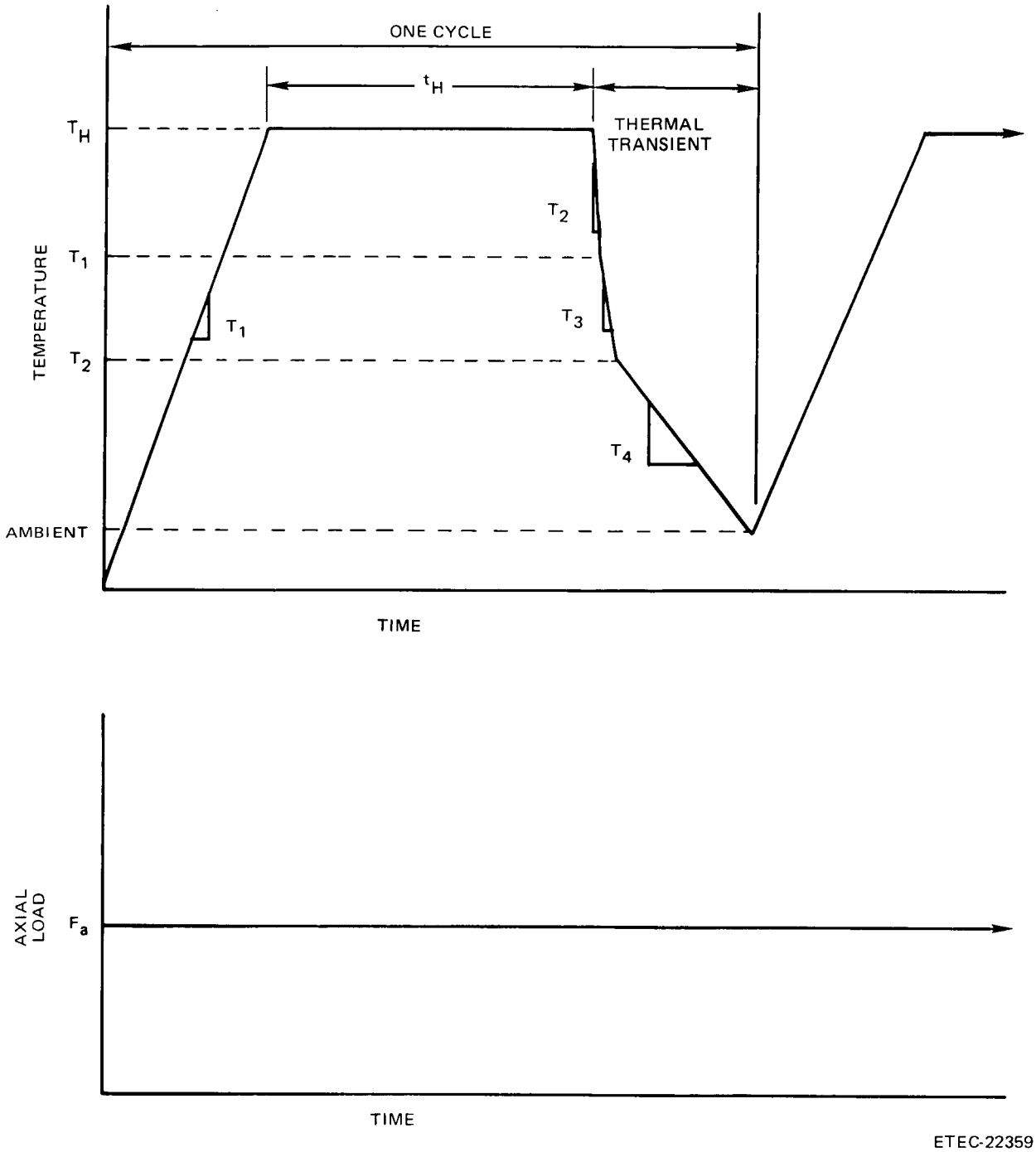

Figure XII-6. Schematic of Test Conditions
(Symbols are identified in Table XII-1)

TABLE XII-1

TRANSITION JOINT LIFE TEST CONDITIONS

Test Condition	Symbol	Test Article Identities
		TRTAs 1, 2, and 3
Hold temperature	T_H	$593^oC \pm 5.5$ $1100^oF \pm 10$
Hold time	t_H	66 h ± 1
External load[a]	F_a	1.78×10^6 N ± 10[b] 4×10^5 lb ± 2250
Cycles/time to failure		120/7900 h[c]
Cooldown rate and range		
593-426°C	$\dot{T}_2$	$-5.6^oC/s \pm 0.6$
1100-800°F		$-10^oF/s \pm 1$
426-288°C	$\dot{T}_3$	$-2.2^oC/s \pm 0.6$
800-500°F		$-4^oF/s \pm 1$
288°C-ambient[d]	$\dot{T}_4$	$-0.11^oC/s$ min
550°F-ambient[d]		$-0.2^oF/s$ min
Heatup rate	$\dot{T}_1$	$112^oC/h \pm 5.5$ $200^oF/h \pm 0$
First intermediate temperature	T_1	465^oC 800^oF
Second intermediate temperature	T_2	288^oC 550^oF

[a]Maximum loading-unloading rate 200 kN/s (45 kip/s)
[b]Maximum bending moment shall be 5000 ft/lb (6780 J)
[c]Estimated
[d]Maximum bending moment shall be 7000 ft/lb (9490 J)

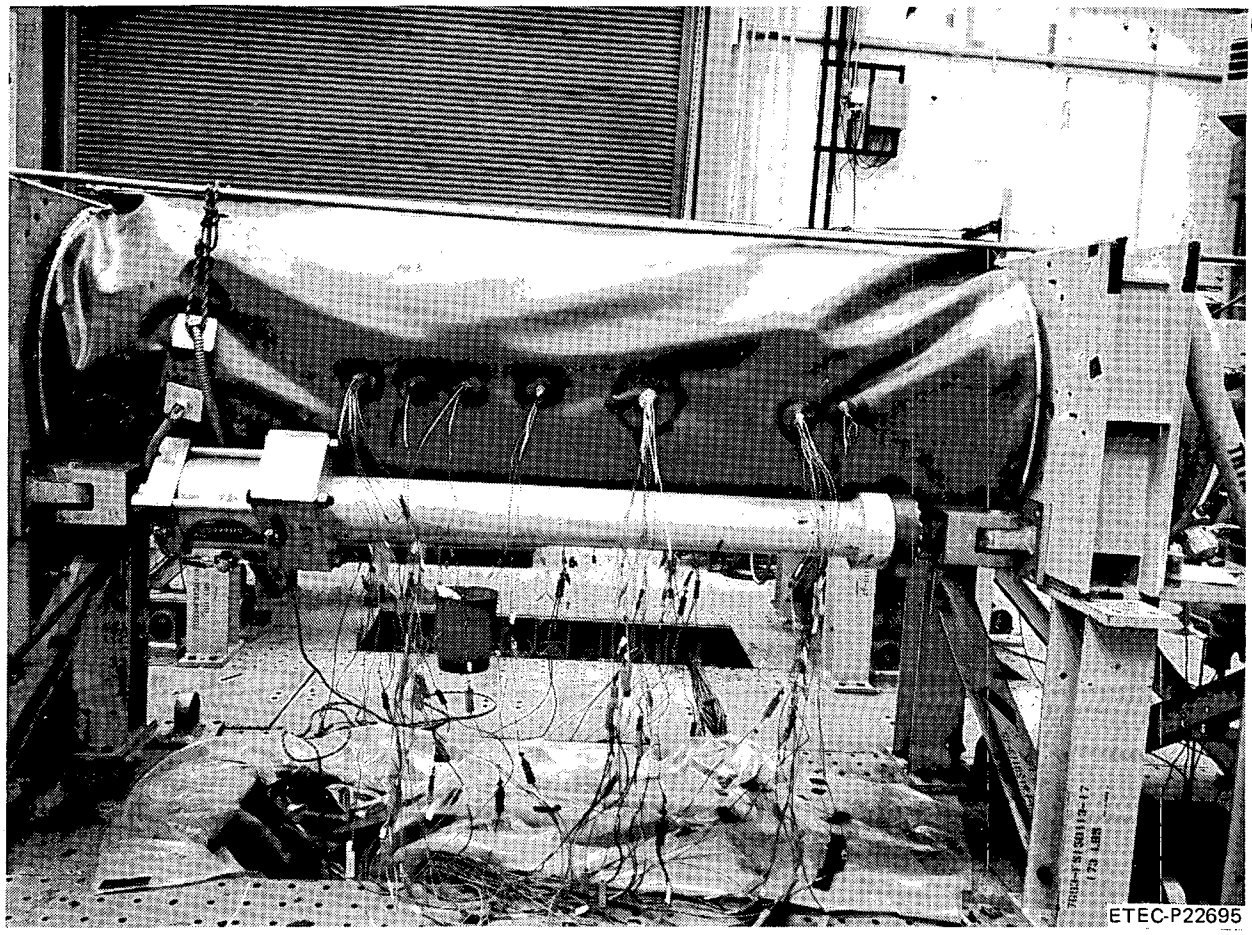

Figure XII-7. TRTA-3 Cover Gas Enclosure

b. Inservice Inspection

GE performed periodic inservice inspections (ISI) on both test articles to detect crack initiation and monitor crack growth by ultrasonic examinations (UT) and liquid penetration examinations (LP) on Weld Joints 1, 2, 3, and 4. Prior to any ISI, ETEC dismantled the test article and removed obstacles to allow proper access to each weld joint. These inspections were performed as indicated by the time history shown in Tables XII-2 through XII-4.

TABLE XII-2

TRTA-2 PHASE I TIME HISTORY

Test Procedure	Cycle Number	Start Date	End Date	Calendar Day (End)
013-STP-14		05-17-79	05-22-79	142
013-STP-16		05-22-79	05-30-79	150
013-STP-17		05-31-79	05-31-79	151
013-SPT-18		06-01-79	06-01-79	152
013-STP-17		06-07-79	06-12-79	163
013-STP-14		06-28-79	07-05-79	186
013-STP-14		08-07-79	08-07-79	219
013-STP-14		08-23-79	08-23-79	235
Shutdown and Hold		08-23-79	10-12-79	285
013-STP-14		10-12-79	10-24-79	297
013-STP-17		10-24-79	10-24-79	297
013-STP-18		10-26-79	10-26-79	299
TP-42-PA-005	1	10-26-79	10-29-79	302
TP-42-PA-005	2	10-30-79	11-02-79	306
TP-42-PA-005	3	11-02-79	11-05-79	309
TP-42-PA-005	4	11-09-79	11-12-79	316
TP-42-PA-005	5	11-13-79	11-16-79	320
TP-42-PA-005	6	11-16-79	11-19-79	323
TP-42-PA-005	7	11-27-79	11-30-79	334
TP-42-PA-005	8	11-30-79	12-03-79	337
TP-42-PA-005	9	12-03-79	12-06-79	340
TP-42-PA-005	10	12-06-79	12-09-79	343
TP-42-PA-005	11	12-09-79	12-12-79	346
TP-42-PA-005	12	12-12-79	12-15-79	349
TP-42-PA-005	13	12-15-79	12-18-79	352
TP-42-PA-005	14	12-18-79	12-21-79	355
TP-42-PA-005	15	01-02-80	01-05-80	005
TP-42-PA-005	16	01-05-80	01-08-80	008
TP-42-PA-005	17	01-08-80	01-11-80	011
TP-42-PA-005	18	01-11-80	01-14-80	014
TP-42-PA-005	19	01-14-80	01-17-80	017
TP-42-PA-005	20	01-17-80	01-20-80	020
TP-42-PA-005	21	01-20-80	01-23-80	023
TP-42-PA-005	22	01-23-80	02-26-80	026
TP-42-PA-005	23	01-26-80	01-29-80	029
TP-42-PA-005	24	01-29-80	02-01-80	032
TP-42-PA-005	25	02-01-80	02-04-80	035
ISI-Shutdown		02-04-80	05-06-80	127

TABLE XII-3

TRTA-2 PHASE II TIME HISTORY
(Sheet 1 of 2)

Test Procedure	Cycle Number	Start Date	End Date	Calendar Day (End)
TP-42-PA-005	1	05-16-80	05-19-80	140
TP-42-PA-005	2	05-19-80	05-22-80	143
TP-42-PA-005	3	05-27-80	05-30-80	151
TP-42-PA-005	4	06-20-80	06-23-80	175
TP-42-PA-005	5	06-24-80	06-27-80	179
TP-42-PA-005	6	06-27-80	06-30-80	182
TP-42-PA-005	7	06-30-80	07-03-80	185
TP-42-PA-005	8	08-05-80	08-08-80	221
TP-42-PA-005	9	08-08-80	08-11-80	224
TP-42-PA-005	10	08-11-80	08-14-80	227
ISI		08-14-80	09-02-80	246
TP-42-PA-005	11	09-02-80	09-05-80	249
TP-42-PA-005	12	09-11-80	09-14-80	258
TP-42-PA-005	13	09-14-80	09-17-80	261
TP-42-PA-005	14	09-17-80	09-20-80	264
TP-42-PA-005	15	09-29-80	10-02-80	276
TP-42-PA-005	16	10-28-80	10-31-80	305
TP-42-PA-005	17	11-01-80	11-04-80	309
TP-42-PA-005	18	11-04-80	11-07-80	312
TP-42-PA-005	19	11-07-80	11-10-80	315
TP-42-PA-005	20	11-10-80	11-13-80	318
ISI and Shutdown		11-13-80		
TP-42-PA-005	21	01-13-81	01-13-81	13
TP-42-PA-005	22	01-14-81	01-14-81	14
TP-42-PA-005	23	01-15-81	01-15-81	15
TP-42-PA-005	24	01-16-81	01-16-81	16
TP-42-PA-005	25	01-19-81	01-19-81	19
ISI		01-23-81		
TP-42-PA-005	26	02-04-81	02-23-81	54
ISI		02-25-81		
TP-42-PA-005	27	03-06-81	03-09-81	68
TP-42-PA-005	28	03-10-81	03-13-81	72
TP-42-PA-005	29	03-13-81	03-16-81	75

TABLE XII-3

TRTA-2 PHASE II TIME HISTORY
(Sheet 2 of 2)

Test Procedure	Cycle Number	Start Date	End Date	Calendar Day (End)
TP-42-PA-005	30	03-16-81	03-19-81	78
TP-42-PA-005	31	03-20-81	03-23-81	82
TP-42-PA-005	32	03-23-81	03-26-81	85
TP-42-PA-005	33	03-27-81	03-30-81	89
TP-42-PA-005	34	03-30-81	04-02-81	92
TP-42-PA-005	35	04-03-81	04-06-81	96
TP-42-PA-005	36	04-07-81	04-10-81	100
ISI		04-14-81		
TP-42-PA-005	37	04-24-81	04-27-81	117
TP-42-PA-005	38	04-27-81	04-30-81	120
TP-42-PA-005	39	05-01-81	05-04-81	124
TP-42-PA-005	40	05-04-81	05-07-81	127
TP-42-PA-005	41	05-08-81	05-11-81	131
TP-42-PA-005	42	05-12-81	05-15-81	135
TP-42-PA-005	43	05-15-81	05-18-81	138
TP-42-PA-005	44	05-19-81	05-22-81	142
TP-42-PA-005	45	05-23-81	05-26-81	146
TP-42-PA-005	46	05-26-81	05-29-81	149
ISI		06-03-81		
TP-42-PA-005	47	06-16-81	06-19-81	170
TP-42-PA-005	48	06-19-81	06-22-81	173
TP-42-PA-005	49	06-26-81	06-29-81	180
TP-42-PA-005	50	06-29-81	07-02-81	183
TP-42-PA-005	51	07-03-81	07-06-81	187
ISI		07-09-81		
TP-42-PA-005	52	07-17-81	07-20-81	201
TP-42-PA-005	53	07-20-81	07-23-81	204
TP-42-PA-005	54	07-24-81	07-27-81	208
TP-42-PA-005	55	07-27-81	07-30-81	211
TP-42-PA-005	56	07-31-81	08-03-81	215
ISI		08-12-81		

TABLE XII-4

TRTA-3 TIME HISTORY
(Sheet 1 of 2)

Test Procedure	Cycle Number	Start Date	End Date	Calendar Day (End)
TP-42-PA-013	1	10-17-80	10-20-80	294
TP-42-PA-013	2	11-04-80	11-07-80	312
TP-42-PA-013	3	11-07-80	11-10-80	315
TP-42-PA-013	4	11-10-80	11-13-80	318
TP-42-PA-013	5	11-14-80	11-17-80	322
TP-42-PA-013	6	11-17-80	11-20-80	325
TP-42-PA-013	7	12-09-80	12-12-80	347
TP-42-PA-013	8	12-12-80	12-15-80	350
TP-42-PA-013	9	12-15-80	12-18-80	353
TP-42-PA-013	10	12-19-80	12-22-80	357
ISI		01-07-81		
TP-42-PA-013	11	02-24-81	02-27-81	58
TP-42-PA-013	12	02-27-81	03-02-81	61
TP-42-PA-013	13	03-03-81	03-06-81	65
TP-42-PA-013	14	03-06-81	03-09-81	68
TP-42-PA-013	15	03-10-81	03-13-81	72
TP-42-PA-013	16	03-13-81	03-16-81	75
TP-42-PA-013	17	03-17-81	03-20-81	79
TP-42-PA-013	18	03-20-81	03-23-81	82
TP-42-PA-013	19	03-23-81	03-26-81	85
TP-42-PA-013	20	03-27-81	03-30-81	89
ISI		04-02-81		
TP-42-PA-013	21	04-13-81	04-16-81	106
TP-42-PA-013	22	04-17-81	04-20-81	110
TP-42-PA-013	23	04-20-81	04-23-81	113
TP-42-PA-013	24	04-24-81	04-27-81	117
TP-42-PA-013	25	04-27-81	04-30-81	120
TP-42-PA-013	26	05-01-81	05-04-81	124

TABLE XII-4

TRTA-3 TIME HISTORY
(Sheet 2 of 2)

Test Procedure	Cycle Number	Start Date	End Date	Calendar Day (End)
TP-42-PA-013	27	05-05-81	05-08-81	128
TP-42-PA-013	28	05-08-81	05-11-81	131
TP-42-PA-013	29	05-12-81	05-15-81	135
TP-42-PA-013	30	05-15-81	05-18-81	138
ISI		05-20-81		
TP-42-PA-013	31	06-12-81	06-18-81	169
TP-42-PA-013	32	06-19-81	06-22-81	173
TP-42-PA-013	33	06-26-81	06-29-81	180
TP-42-PA-013	34	06-29-81	07-02-81	183
TP-42-PA-013	35	07-03-81	07-06-81	187
ISI		07-09-81		
TP-42-PA-013	36	07-21-81	07-24-81	205
TP-42-PA-013	37	07-24-81	07-27-81	208
TP-42-PA-013	38	07-28-81	07-31-81	212
TP-42-PA-013	39	07-31-81	08-03-81	215
TP-42-PA-013	40	08-03-81	08-06-81	218
ISI		08-12-81		
TP-42-PA-013	41	08-28-81	08-31-81	243
TP-42-PA-013	42	08-31-81	09-03-81	246
TP-42-PA-013	43	09-05-81	09-08-81	251
TP-42-PA-013	44	09-08-81	09-11-81	254
TP-42-PA-013	45	09-11-81	09-14-81	257
TP-42-PA-013	46	09-14-81	09-17-81	260
TP-42-PA-013	47	09-18-81	09-21-81	264
TP-42-PA-013	48	09-21-81	09-24-81	267
TP-42-PA-013	49	09-25-81	09-28-81	271
TP-42-PA-013	50	09-28-81	10-01-81	274
Shutdown		10-01-81		

C. TEST RESULTS – TRANSIENT TESTING

1. TRTA-2

TRTA-2 resumed the second phase of transient testing on January 13, 1981. Five cycles were completed, with short hold periods of 1 h, and the test article was shut down following Cycle 25 for GE to perform an inservice inspection on January 23, 1981.

Crack propagation was investigated by local grinding and removal of boat samples from Welds 1, 3, and 4. Results indicated that maximum crack depths ranged between 120 and 160 mils.

TRTA-2 testing was resumed on February 4, 1981, by starting Cycle 26 with an extended hold period of 330 h, followed by a slow cooldown of 200°F/h and a second inservice inspection. Boat samples removed from Welds 3 and 4 indicated that crack depths had not increased.

Transient testing was continued at a reduced axial load of 100,000 lb (0.45×10^6 N) for ten cycles, through Cycle 36, followed by an inspection April 14, 1981, to determine the extent of crack growth. Ultrasonic examination indicated maximum crack depth was ∿200 mils at Weld 4. Ten more cycles were performed, through Cycle 46, at a load of 100,000 lb (0.45×10^6 N), followed by inspection on June 3, 1981. Results indicated that crack depths did not change at Welds 1, 3, and 4.

The final series of ten transient cycles was performed at the normal axial load of 400,000 lb (1.78×10^6 N) through Cycle 56. Inspection by GE on August 12, 1981, following 81 cycles (Phase I and Phase II) indicated that crack propagation was more than half the wall thickness and that testing was considered complete. ETEC dismantled the test article into weld area sections and returned the test article sections to GE for metallographic examination.

A typical downtransient temperature profile utilizing internal thermocouple control at the Cr-Mo section is shown in Figure XII-8.

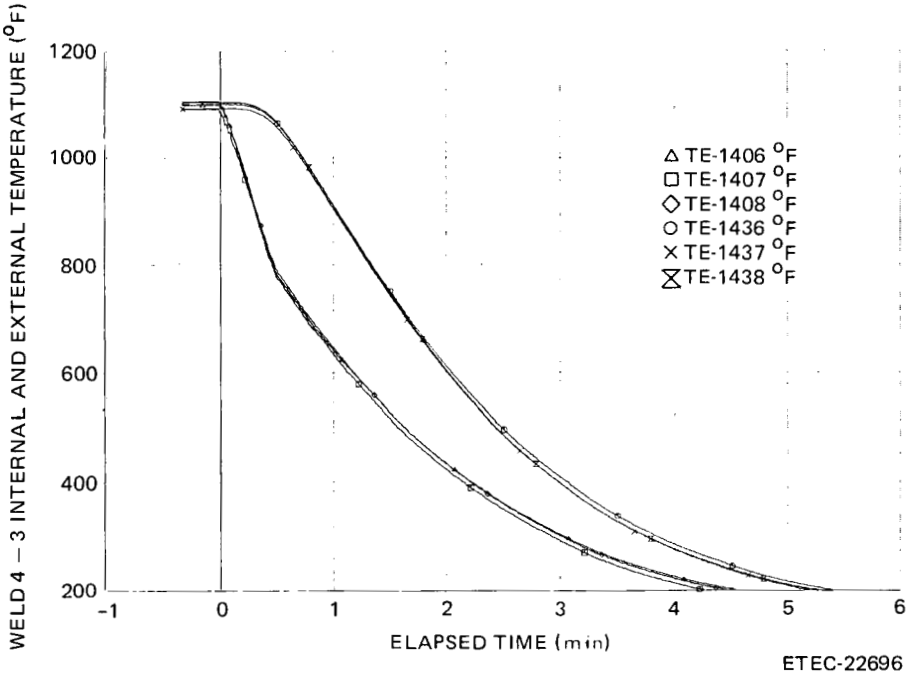

Figure XII-8. Downtransient Temperature Profile, TRTA-2, Phase II, Cycle 41

A time history of the test series is shown in Tables XII-2 and -3.

2. TRTA-3

TRTA-3 completed transient Cycle 10 and was shut down for GE to perform an inservice inspection on January 7, 1981. Surface inspection of the test article showed a light film of oxidation on the Cr-Mo surfaces; UT examination did not reveal any cracks in the weld joints.

The test article was fitted with bulkhead end plates to support a new butyl rubber enclosure required to reduce leakage and maintain a more positive pressure on the nitrogen cover gas system.

Transient testing was continued for ten cycles, through Cycle 20, and was shut down April 2, 1981, for inspection by GE. No cracks were found in the test article weld joints after UT examination.

The Cr-Mo surfaces appeared to have been protected by the new butyl rubber cover gas enclosure, which maintained a nitrogen pressure of 0.1 in. of water on the test article surface during the series of ten transient cycles. The Cr-Mo surfaces were found to be only lightly oxidized with a thin, adherent oxide film.

Transient testing was continued for ten cycles, through Cycle 30, and was shut down on May 21, 1981, to inspect the oxidation on the Cr-Mo surfaces and to investigate the condition of the adjacent bi-metallic and tri-metallic weld joints. Total oxidation depth on Cr-Mo surfaces for 30 cycles was found to be ∿5 mils. The adjacent weld metal was polished to provide a flat surface to perform dye penetrant examinations, which showed indications of crack initiation on Weld Joints 1, 3, and 4. These indications disappeared when the weld joint areas were polished down an additional 5 mils.

TRTA-3 testing was continued for a series of five transient cycles and was shut down following Cycle 35 on July 6, 1981, to investigate the condition of the weld joints. Dye penetrant examination showed indications of cracks at Welds 1, 3, and 4. These indications disappeared when specified weld joint areas were polished down ∿10 mils at Weld 1, 5 mils at Weld 3, and 5 mils at Weld 4. TRTA-3 was again tested for five cycles and inspected on August 12, 1981, following a total of 40 transient cycles. GE indicated that maximum crack depths ranged from 60 mils at Weld 1 to 15 mils at Weld 4, judging from boat samples removed at these locations.

TRTA-3 was tested for a final ten cycles ending in Cycle 50 and shut down October 1, 1981, to complete transition joint testing. The test article was dismantled and returned to GE for weld joint examination.

Typical reduced data plots of overall temperature profile, load, and down-transient temperature profiles are shown in Figures XII-9, -10, and -11.

A time history of the test series is shown in Table XII-4.

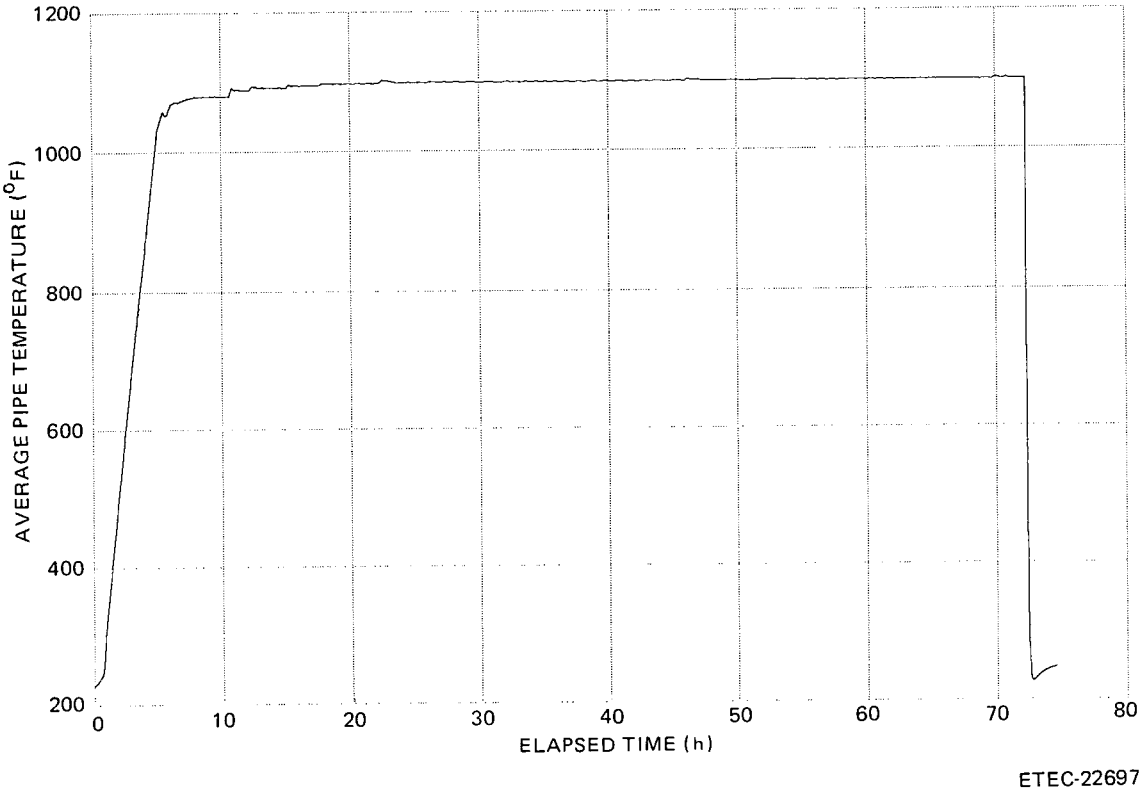

Figure XII-9. Overall Temperature Profile, TRTA-3, Cycle 50

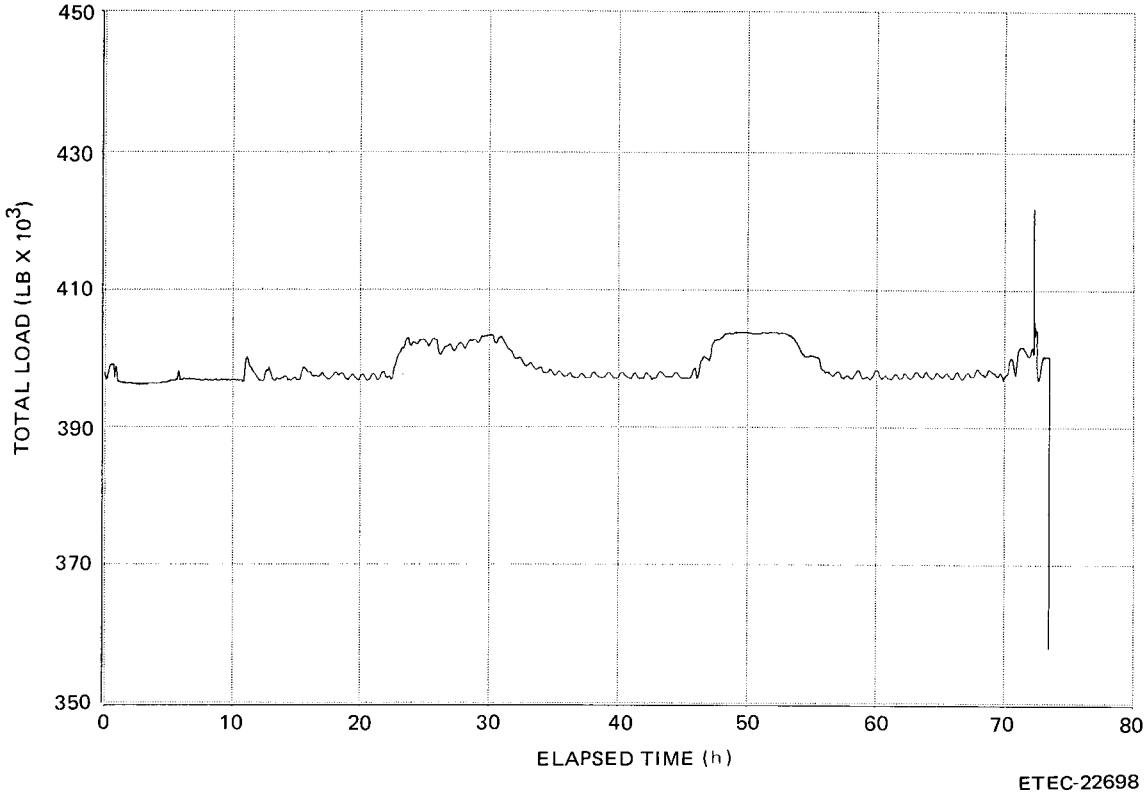

Figure XII-10. Load, TRTA-3, Cycle 50

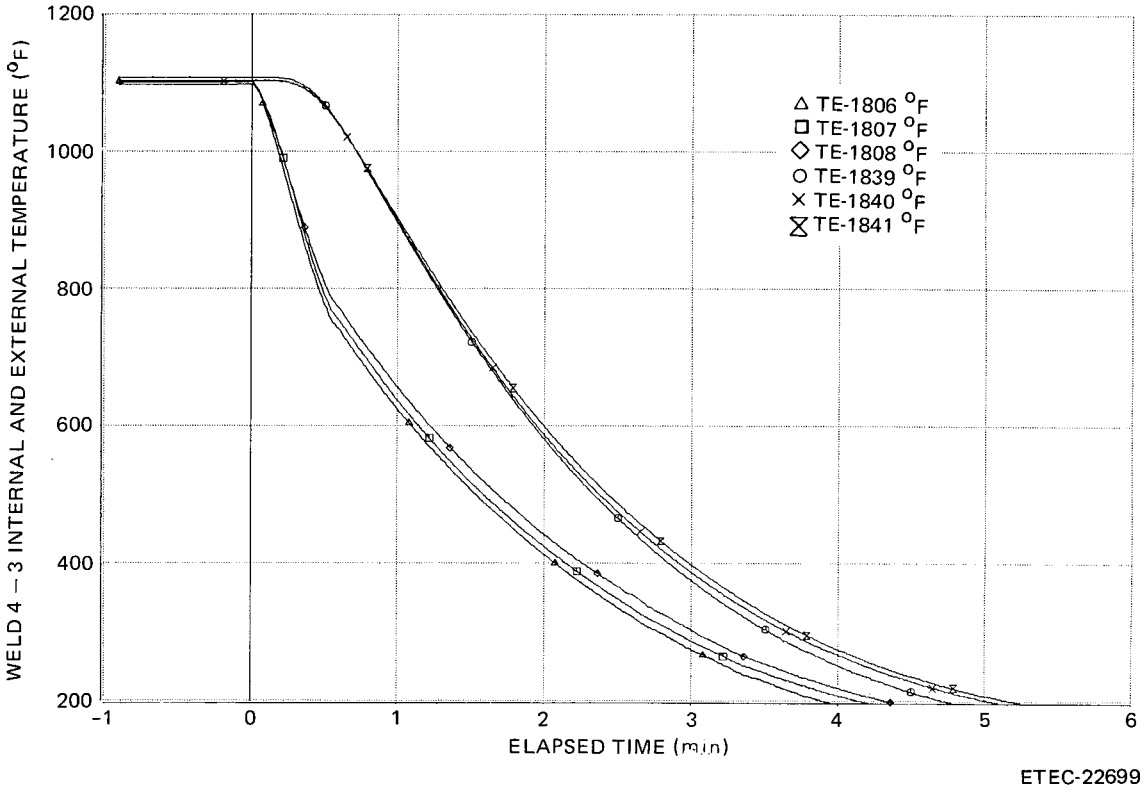

Figure XII-11. Downtransient Temperature Profile, TRTA-3, Cycle 50

XIII. CRBR VALVES

P. ARCHBOLD

A. INTRODUCTION

The test article for this program consists of nine different valve configurations for use in the CRBR program. The complement of valves is listed below:

1) 1-in. (25.4-mm) Hoke bellows seal 90^{o} globe valve, C_v = 12
2) 1-in. (25.4-mm) Hoke bellows seal 90^{o} globe valve, C_v = 3
3) 1/2-in. (12.7-mm) Hoke bellows seal 90^{o} globe valve, C_v = 3
4) 1/2-in. (12.7-mm) Hoke bellows seal 90^{o} globe valve, C_v = 0.5
5) 1-in. (25.4-mm) Powell bellows seal Y-globe valve
6) 2-in. (50.8-mm) Powell bellows seal Y-globe valve
7) 3-in. (76.2-mm) Powell bellows seal Y-globe valve
8) 4-in. (101.6-mm) Powell bellows seal Y-globe valve
9) 6-in. (152.4-mm) Powell swing check valve.

Functional testing of these valves is necessary to verify adequacy of design, materials, and thermal responses when used in a sodium environment. The design of parts of these valves has been modified to meet the CRBRP requirements, and empirical testing is required to assess the design adequacy since current analytical techniques are inadequate to predict the effects of mechanical and thermal cycling on the performance of these valves. Present theoretical analysis is not considered adequate to predict the dynamic response of these valve-operator assemblies to seismic events, and since some of them are "active" safety-related components, dynamic testing is considered to be necessary. The test program is designed to measure flow characteristics and seat leakage before and after mechanical life cycling and thermal cycling in sodium with nozzle loads applied. Seismic testing is to be performed on selected valves from the second, or backup, set of valves.

Testing conducted and reported during CY 1978, 1979, and 1980 on this program consisted of:

1) Operability and gas seat leakage tests at ambient temperature for all four Hoke valves
2) Sodium flow characteristics tests at 400°F (204°C) and 750°F (399°C) for the 1-in. (25.4-mm) Hoke valve (C_v = 12)
3) Mechanical life cycling tests (2000 cycles) at 750°F (399°C) and 925°F (496°C) for the 1-in. (25.4-mm) Hoke valve (C_v = 12)
4) Operability and gas seat leakage tests at ambient temperature for the four Powell Y-globe valves and swing check valve
5) Sodium flow characteristics at 400°F (204°C) and 750°F (399°C) for the 4-in. (101.6-mm) Powell valve
6) Seat leakage tests with externally applied loads at 400°F (204°C) and 1000°F (538°C) with the 4-in. (101.6-mm) Powell valve
7) Mechanical life cycling tests (1000 cycles) at 1000°F (538°C) with the 4-in. (101.6-mm) Powell valve
8) Sodium flow characteristics at 400°F (204°C) and 925°F (496°C) with the 1/2-in. Hoke valve (C_v = 3)
9) Operability and gas seat leakage tests at ambient temperature for the 4-in. (101.6-mm) Powell valve for seismic testing
10) Seismic test at 1000°F (538°C) and 325 psig (2241 kPa) (five OBE tests plus one SSE test) for the 4-in. (101.6-mm) Powell valve
11) Thermal transient tests from 600°F (316°C) to 1015°F (546°C) and from 1015°F (546°C) to 600°F (316°C) for the 4-in. (101.6-mm) Powell valve
12) Flow characteristics in water for 1-in. (25.4-mm), 2-in. (50.6-mm), and 3-in. (75.9-mm) Powell valves
13) Flow characteristics in sodium at 900°F (482°C) for a 6-in. (151.8-mm) Powell check valve.

Testing conducted during the present year (CY 1981) on this program consisted of:

1) Completion of flow characteristics testing in sodium at 900°F (482°C) for a 6-in. (151.8-mm) Powell check valve
2) Seat leakage testing in static sodium at 900°F (482°C) for the 6-in. (151.8-mm) Powell check valve
3) Seat leakage and life cycle testing in static sodium at 600°F (316°C) for the 2-in. (50.8-mm) Powell valve
4) Diagnostic testing on the 4-in. (101.6-mm) Powell valve used in seismic testing.

B. TEST DESCRIPTION

1. Facility

Check valve testing in flowing sodium is accomplished in the Sodium Component Test Installation (SCTI). The valve is mounted in a horizontal attitude in a bypass loop that contains the purification line and P-6 and P-8 EM pumps, as shown in Figure XIII-1. Instrumentation is provided as shown in Figure XIII-2 and is connected to the digital data acquisition system (DDAS). The location of the test article provides convenient platforms and space sufficient to facilitate radiography. The loop is capable of providing 960 gal/min (0.06 m^3/s) of 950°F (510°C) sodium at a pressure of 200 psig (1379 kPa). Testing is performed with Valve V-506 throttled to obtain the desired flow. Flow is bypassed through the 2-in. (5.08-cm) line and the EM pumps, which are electrically connected to provide a negative pressure on the check valve disc for positive closure during life cycle tests. Cycling of the test article is accomplished by cycling Valve V-507 using computer control. With the valve in the closed position, leak rates are measured at ambient temperature and 325 psid (2241 kPa) on both forward and reverse directions.

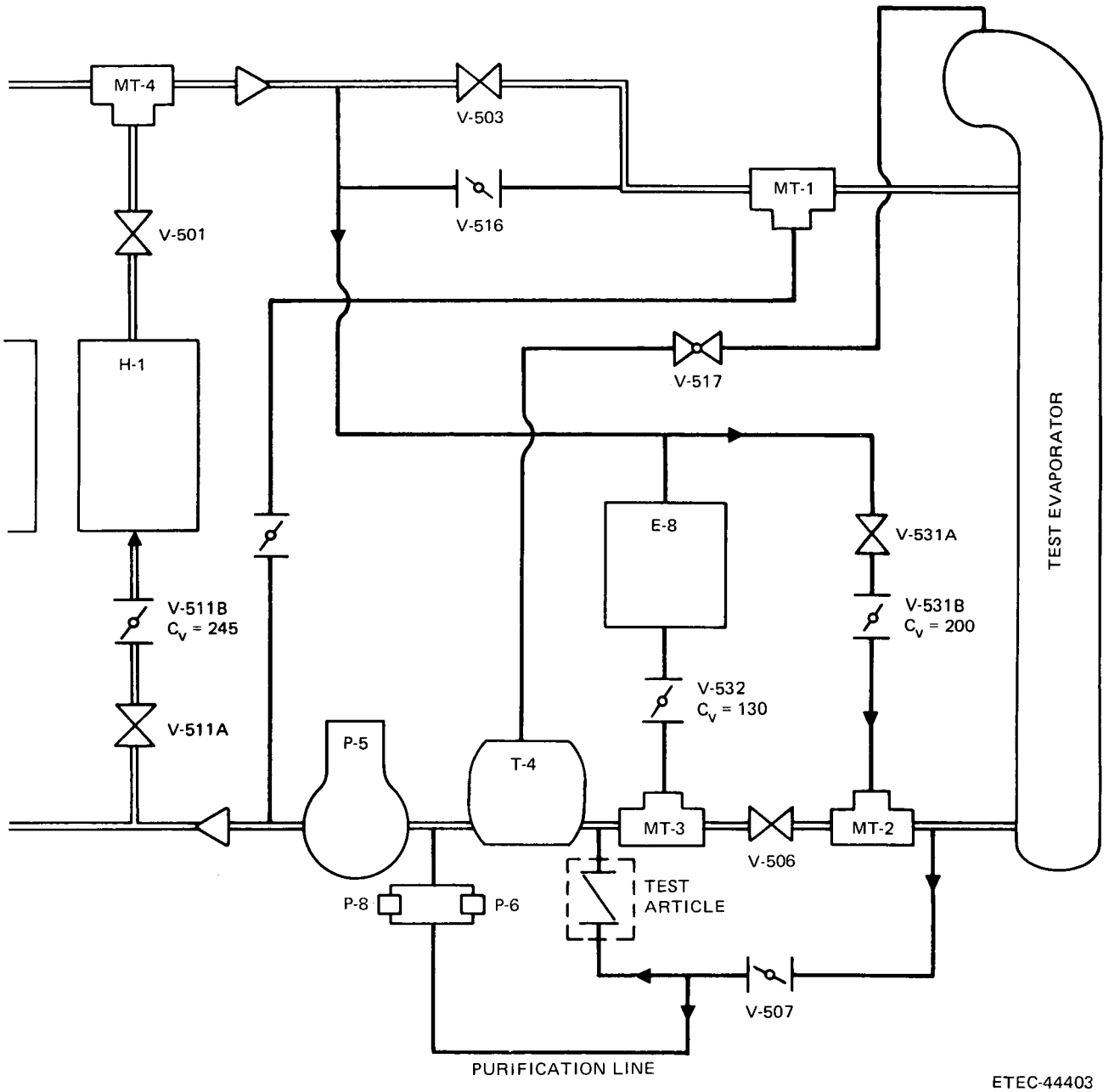

Figure XIII-1. SCTI Check Valve Test

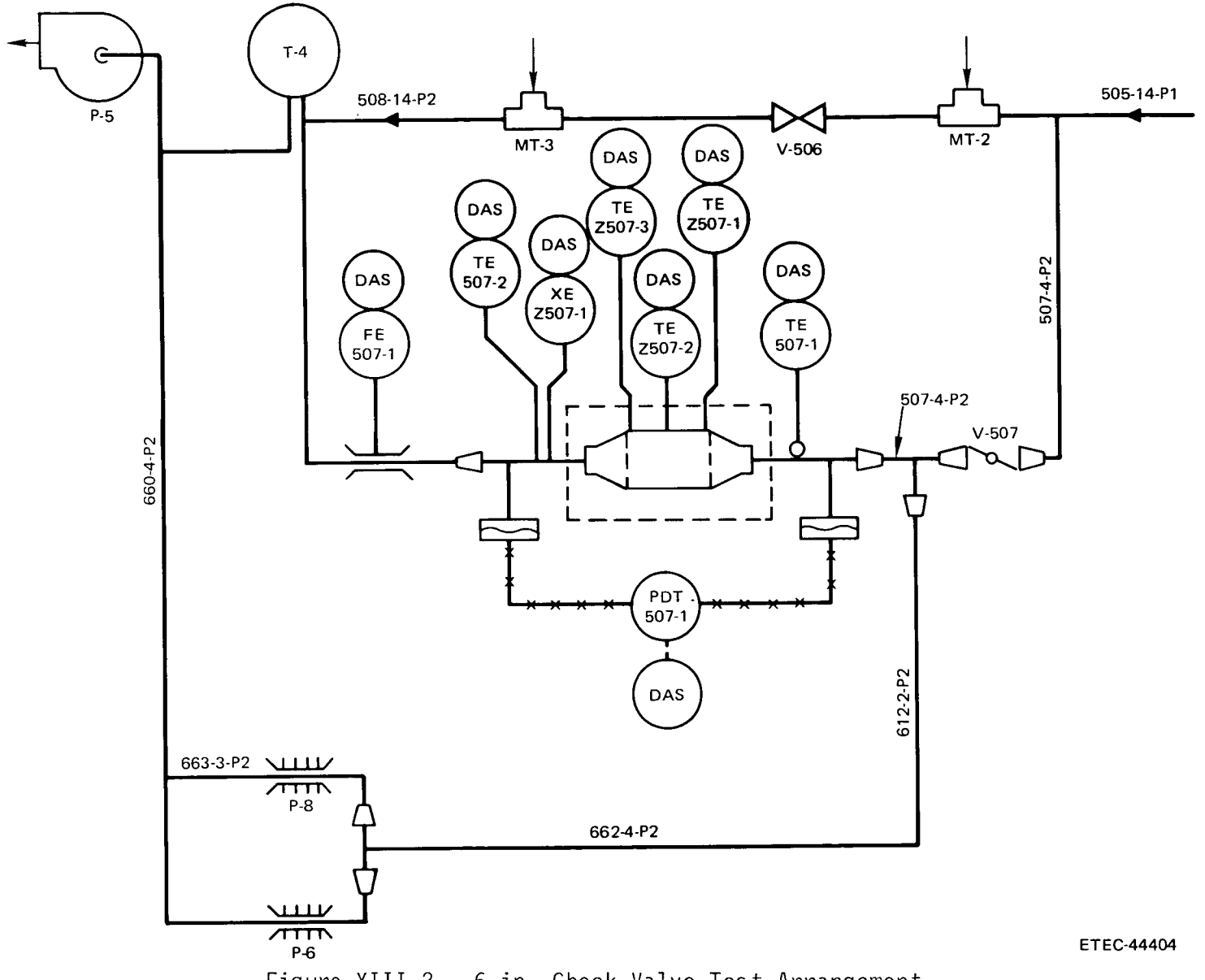

Figure XIII-2. 6-in. Check Valve Test Arrangement

Sodium seat leakage testing and valve cycling in static sodium are accomplished in a static test rig. The static test rig is located in the SCTI, on a platform above Sodium Water Reaction Vessel T-21. The test rig is connected to the SCTI sodium system through sodium fill and drain lines. There is no sodium flow-through capability, and purification of the valve/test rig combination is accomplished by filling and draining the rig several times with purified sodium. The rig is provided with a Fisher Leveltrol to monitor seat leakage on the upstream side of the valve so that there is no problem accounting for changes due to a possible gas bubble trapped in the bonnet area of the valve. The upstream piping is anchored to the rig, and the test valve and downstream piping are supported by a system of constant-load hangers. Simulated pipe loads are applied to the valve by hydraulic actuators that are manually loaded using a self-contained hydraulic system built into the rig. The actuator loads are monitored using calibrated load cells. The output from the load cells is routed to the DDAS in the control room. Preheat and test temperatures are provided by means of strip heaters that are controlled locally at the static test rig control panel SSTI. The test rig has a built-in instrument air system, which is interfaced with the 150-psig (1034-kPa) SCTI instrument air system. Argon is supplied from a K-bottle. Temperature readings, load cell readings, valve position, and liquid level readings are all connected to the SCTI DDAS in the control room.

2. Test Article

The test articles are a series of valves constructed in accordance with the requirements of Section III Division 1 of the ASME Boiler and Pressure Vessel Code. The Powell valves are all Y-pattern globe valves complete with Fisher actuators except for the 4-in. (101.6-mm) seismic test valve, which has a radiation-resistant actuator. Figure XIII-3 is a typical valve arrangement for the Powell series. One 6-in. (152.4-mm) check valve completes the complement of Powell valves and is shown in Figure XIII-4.

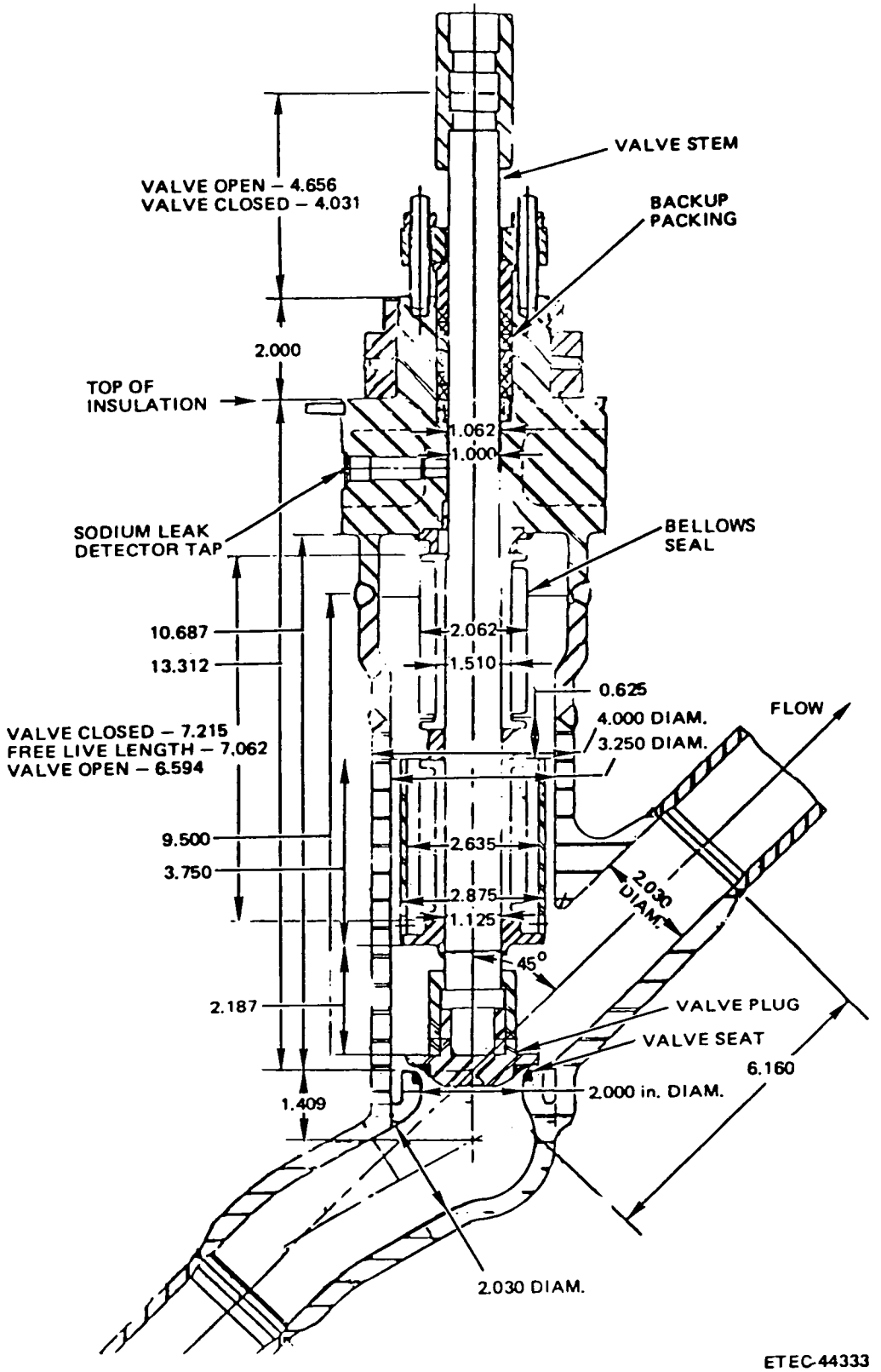

Figure XIII-3. 2-in. Powell Y-Globe Valve

The valves are heated by means of strip heaters formed around the shell and controlled in zones to provide a uniform heat pattern as shown in Figure XIII-5. Thermocouples are installed to provide both control and temperature data. Strain gages are installed to aid in determining whether applied loads react as expected. Mechanical loads are applied to simulate piping loads, etc., using hydraulic cylinders and a load maintainer or hand pump. The loads are monitored by means of load cells attached to the hydraulic cylinders.

3. Test Method

a. Mechanical Cycling

The 6-in. (152.4-mm) Powell check valve was cycled in the SCTI 4-in. (101.6-mm) loop at the design flow rate and a system pressure of ∿50 psi. The valve is cycled from the open to the closed position automatically by using the computer to cycle facility system Valve V-507.

Mechanical cycling in the static test rig is accomplished using the DDAS computer to control the test valve pneumatic controller automatically. This test is performed in static sodium.

b. Seat Leakage Measurements With Applied Loads

Seat leakage measurements are made in the static test rig, which has two test positions. Each position is equipped with a gas system for pressurizing either side of the valve and with a Fisher Leveltrol, located in the upstream piping, to measure the actual leak rate. The sodium level is balanced in the piping, across the valve, and gas pressure is applied to the upstream or downstream side as required. The Leveltrol records the leak rates. Loads can be applied to simulate various piping loads and conditions by means of a hydraulic loading system built into the static test rig. This capability enables evaluation of valve performance under various load conditions.

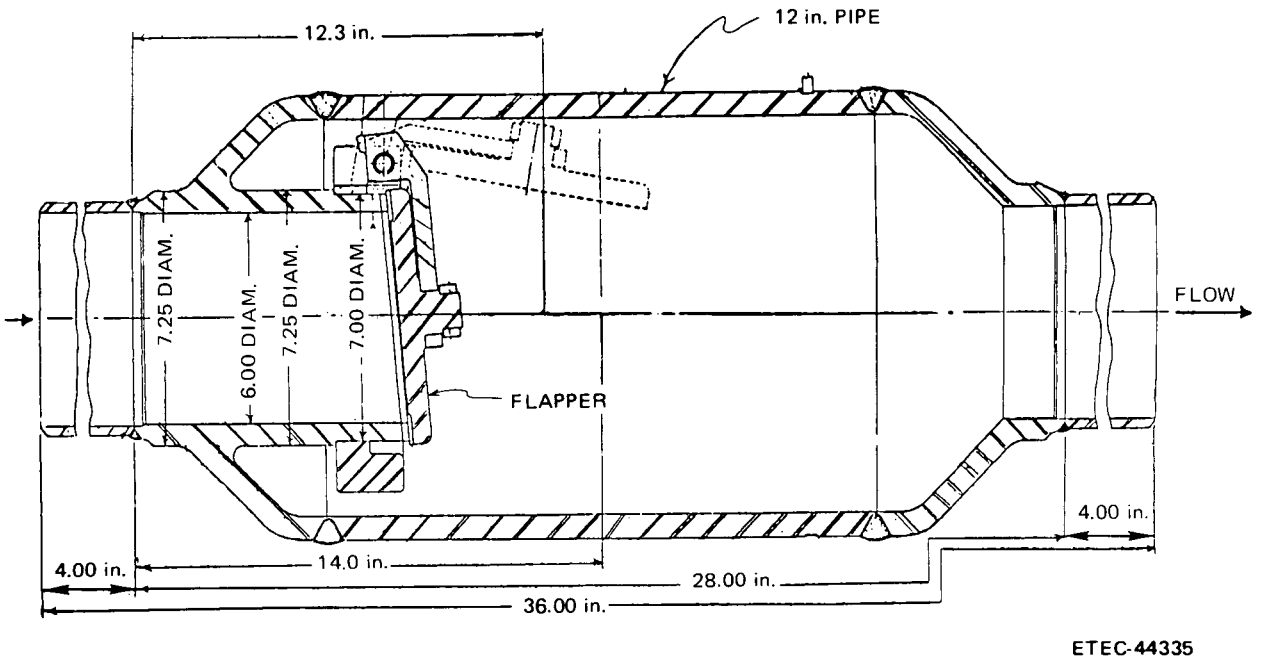

Figure XIII-4. 6-in. Powell Check Valve

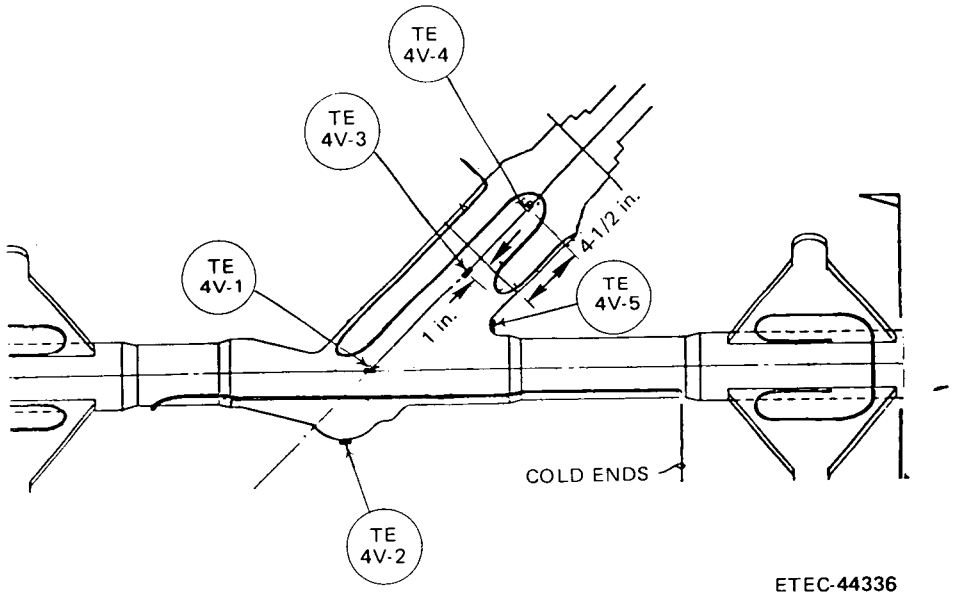

Figure XIII-5. Typical Heater and Thermocouple Installation

4. Test Results

a. Mechanical Life Cycle Operation — 6-in. Check Valve

The 6-in. (152.4-mm) swing check valve was cycled from the open to the closed position 500 times at the design flow rate of 560 gal/min (0.035 m^3/s) at both 400°F (204°C) and 900°F (482°C). These life cycle tests were performed at a maximum system pressure of 50 psig (345 kPa). Sample plots of the results of these tests are shown in Figures XIII-6 and -7, respectively. The valve was cycled by cycling the facility loop Valve V-507 under computer control.

b. Reverse Flow Seat Leakage Test — 6-in. Check Valve

Reverse flow seat leakage testing of the 6-in. (152.4-mm) swing check valve was performed in Position 2 of the static test rig. After the test article and rig piping were purged with argon, the system was preheated to 400°F (204°C), purged again, and filled with sodium at 400°F (204°C). The rig was heated to 950°F (510°C), held for 8 h, then hot-drained to flush out impurities. After refilling with sodium at 400°F (204°C), the rig was reheated to the test temperature of 900°F (482°C) and allowed to stabilize. The pressure across the test article was raised to 100 psi (690 kPa) in the reverse direction, then held for ∿4 h. The leak rate was determined and recorded by the data acquisition system. Since the leak rate was extremely low, this test was repeated, and after 4 h at 100 psig (690 kPa), the incremental leak rate was determined to be 51.46 cm^3/h. This leak rate increased steadily from 22.5 cm^3/h at the end of the first hour to 51.46 cm^3/h at the end of 4 h. The total leakage of sodium for 4 h was 206.3 cm^3. The allowable leak rate at 100 psi (690 kPa) given by Specification N099NV812017 is 93,465 cm^3/h. Figure XIII-8 is a plot of the total leakage vs time for this test.

The valve was then tested with a differential pressure of 1.5 psi (10.35 kPa). During this test, the incremental leakage rate decreased from ∿880 cm^3/h at the start of the test to ∿749 cm^3/h about three-quarters through the test, then increased again to 880 cm^3/h. The total leakage over a period of 44 min was

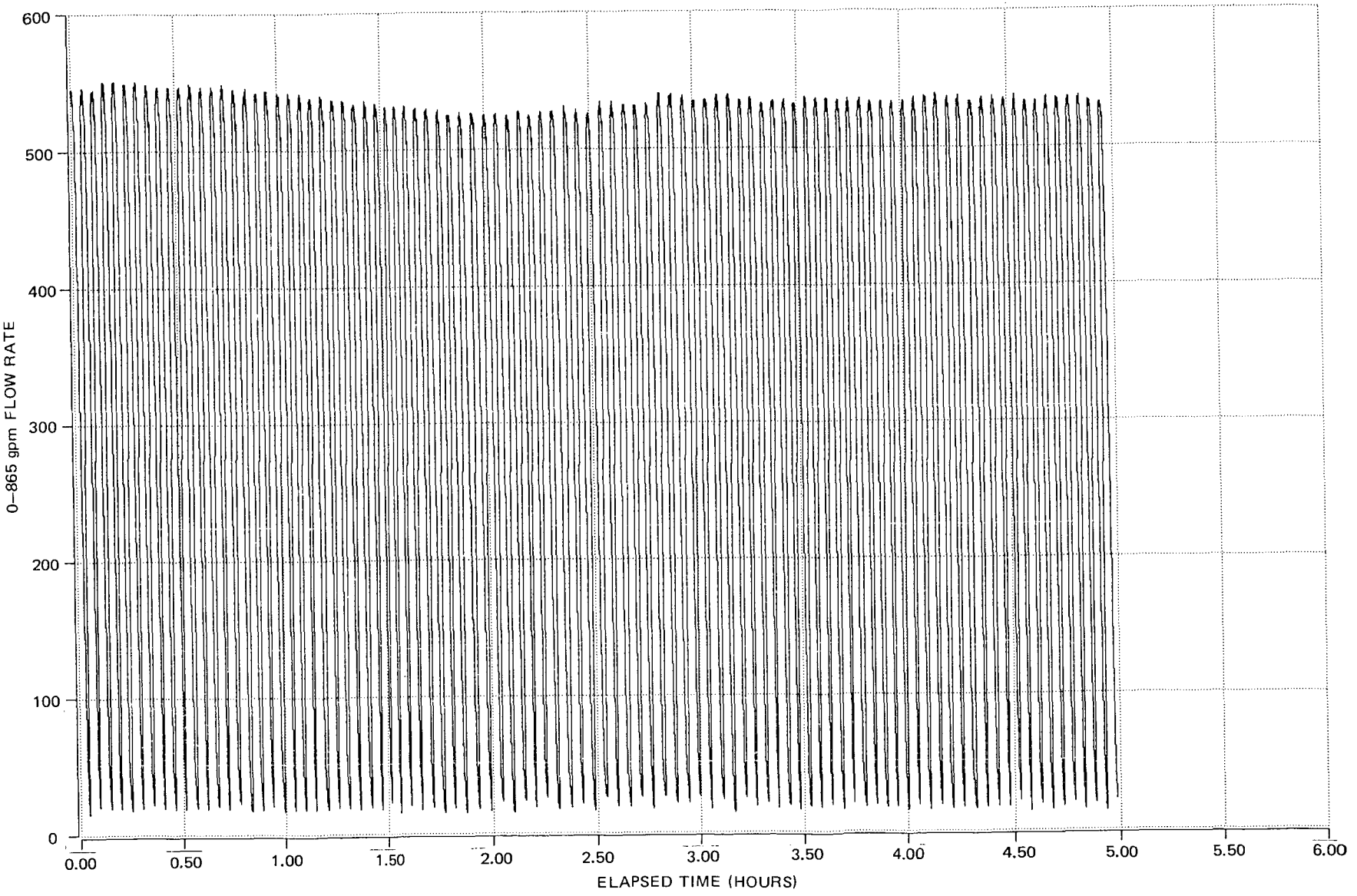

Figure XIII-6. Typical Valve Open/Close Cycles at 400^{O}F (Data Plot)

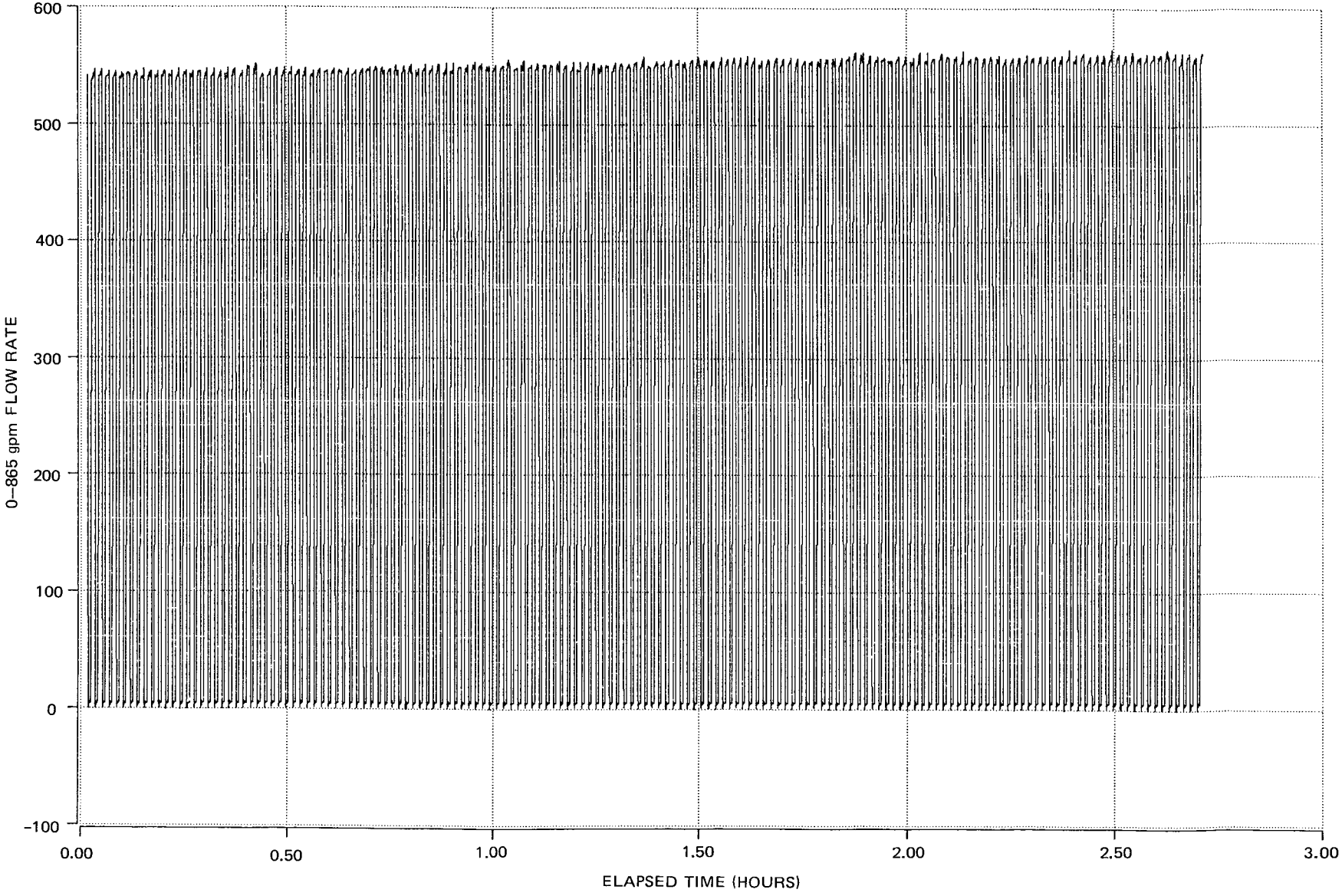

Figure XIII-7. Typical Valve Open/Close Cycles at 900^{O}F (Data Plot)

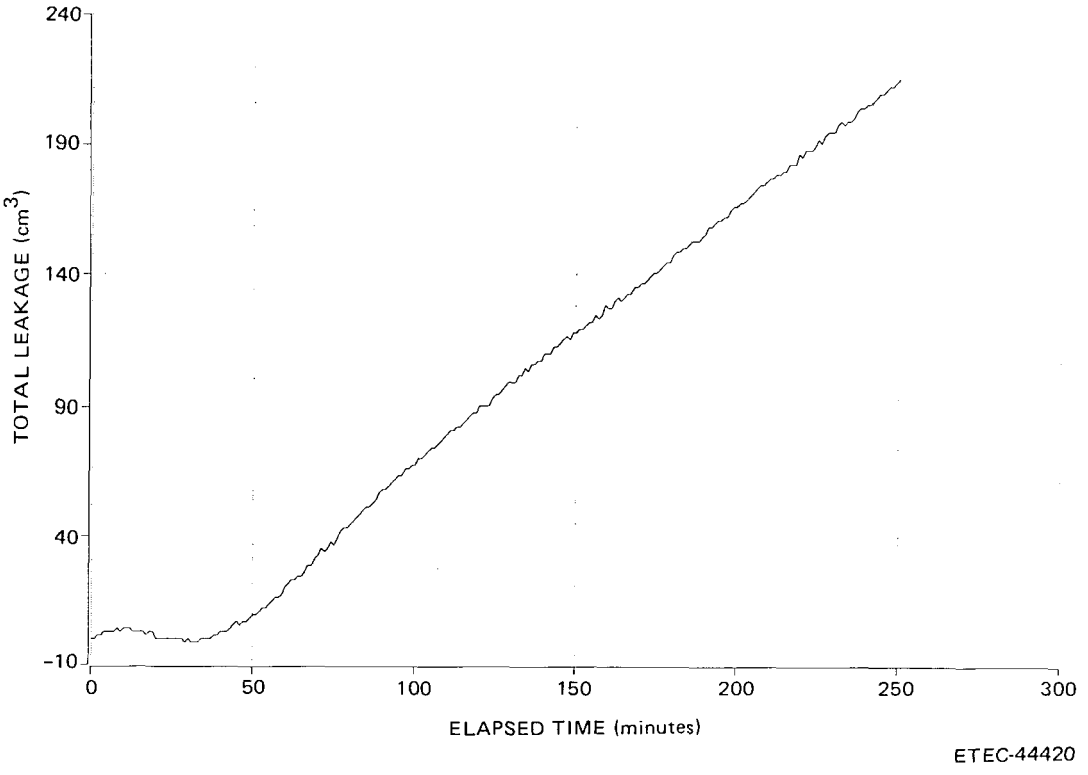

Figure XIII-8. 6-in. Powell Valve Test Program at SCTI — Seat Leakage Test at 100 psi

643.4 cm^3, which is equivalent to an average leak rate of 14.7 cm^3/min. The allowable leak rate specified is 15,576 cm^3/min. Figure XIII-9 is a plot of the total leakage vs time for this test.

c. Seat Leakage and Life Cycle Testing — 2-in. Powell Valve

After checkout of the hydraulic loading system and a period of operator training on the system, a series of tests was initiated to evaluate the load system and determine how the loads were being reacted. Initial tests showed that the reactions obtained were in the right direction but the values were less than predicted. An axial load application was tried but at a load of 360 lb (162 kg), the strain gage readings changed suddenly. The instrumentation was at fault, and after correcting this, the axial load test was satisfactorily completed. The bending test was then repeated, but the results were not satisfactory. Analysis of the data indicated the possiblity that some external load was being experienced. This was eventually determined to be a thermal problem created by exposure of the

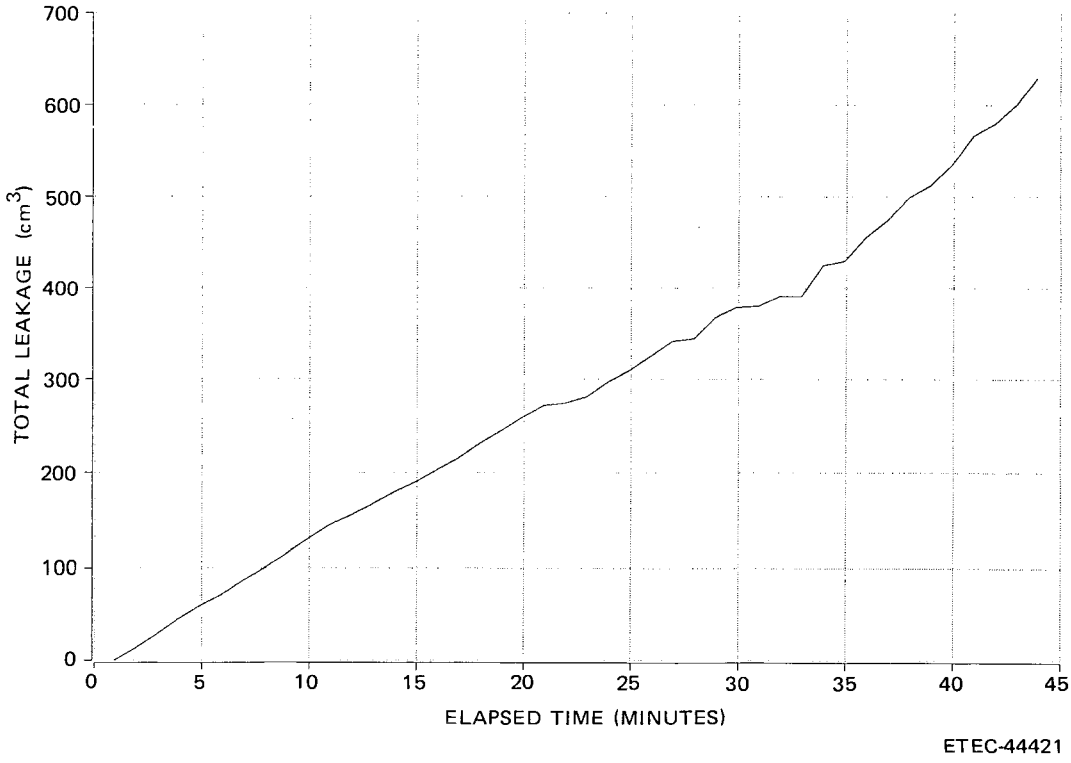

Figure XIII-9. 6-in. Powell Valve Test Program at SCTI — Seat Leakage Test at 1.5 psi

test rig to direct sunlight coming in through an access opening created in the wall for installation of a steam generator. The test rig was shielded from this effect and the strain gage recording equipment was moved to the lower platform. The bending test was repeated, with good results obtained, and the decision was made to complete the load evaluation tests required by Procedure SCTI-SP-410. These tests were completed, and ESG personnel reviewed the data and indicated acceptance of the results of these tests. The test rig was then connected to the SCTI system piping through fill and drain lines, and the test article and rig piping were filled with sodium at 400°F (204°C). After heating to 950°F (510°C) and soaking, followed by a hot drain, then refilling at 400°F (204°C), a seat leakage test was performed. The leak rate proved to be excessive. It was discovered that the manual override mechanism was holding the valve off the seat. The mechanism was centered and the test was repeated. Again the leak rate was excessive, and investigation showed that the test article actuator solenoid valve vent to atmosphere had been plumbed to the test rig system and was restricted.

This created a cushion of pressure on the underside of the actuator piston, which prevented the valve from closing until the pressure could decay. The vent was opened and testing was resumed. The strip chart recording of the leak rate indicated a problem in the Leveltrol, so the system was drained to enable examination of the Leveltrol unit. A thermal baffle in the unit seemed to be causing the problem and was removed. When the system was filled with sodium at 400°F and a leak test performed, the valve seat leakage was out of specification. ESG personnel were contacted and agreed to use the manual override cautiously to see if the valve could be seated. With approximately one half-turn of the handwheel, the valve seated and the leak rate diminished. The valve was then stroked pneumatically and another leak test performed. The leak rate was once more out of specification. ESG was informed and they contacted the Powell Company, who arranged for a Fisher representative to witness testing.

The seat leak test was repeated in the presence of ESG and Fisher representatives. The valve could no longer be seated under either pneumatic control or manual override. Powell then suggested loosening the packing gland nut and retesting. If this did not resolve the problem, they recommended removing the block connecting the valve and actuator stems and checking the alignment. The packing was loosened and the valve was stroked open and closed and monitored to see if there was any obvious change in travel. On the third opening stroke, the valve jammed at approximately half-open position. The valve was closed by actuator spring pressure, and the connecting block between the stems was removed. The stems were observed to be about 1/8 in. (3.175 mm) out of alignment. The packing was removed and the stems were reconnected. X-rays were taken of the valve at the seat location and below the gland area. Although the X-ray pictures were somewhat distorted, there was some indication that the stem might be bent. The connecting block was again removed, and the operation of the actuator was checked. This proved to be smooth, indicating that the problem was not in the actuator. The connecting block was replaced and the valve was partially opened, using the manual override, to enable sodium drain. The handwheel was locked in this position. After the sodium was drained, the valve was removed from the static test rig. Another set of X-rays was taken; then the valve was cleaned and

shipped to ESG for examination. The second set of X-rays was less distorted and gave a more positive indication that the valve stem was bent. The test program was terminated with shipment of the valve to ESG.

d. Diagnostic Testing of 4-in. (101.6-mm) Powell Seismic Valve

In October 1980, representatives from ESG and the Powell Company witnessed some diagnostic testing on the 4-in. (101.6-mm) seismic valve. Both the actuator and the valve body were helium leak checked and found to be intact. The coupling block between the valve and actuator stems was removed and a misalignment between the shafts was observed. Next, the actuator was operated using pneumatic pressure, and it appeared to be functioning normally. The valve stem could only be moved 5/16 in. (8 mm), using a crowbar, and X-rays were taken of the stem from the valve seat to the packing gland area. These pictures indicated a bent stem. The valve was then removed from the test frame assembly and the supports, snubbers, load cells, and spherical bearings were examined. The only damage observed was to the axial load cell, which had suffered a failure in the end plate that functions as a diaphragm. The valve was crated and shipped to Powell Company for further step-by-step examination.

XIV. ANL VALVE QUALIFICATION TEST PROGRAM

P. ARCHBOLD AND W. G. DEWART

A. INTRODUCTION

A number of commercial valves of different sizes and types were purchased as test articles for the ANL Valve Test Program. The purpose of this test program is to demonstrate the functional and performance characteristics of valves designed and modified for sodium usage by commercial suppliers. The tests to be conducted include: (1) nondestructive testing (NDT) inspection, (2) gas seat leakage at ambient conditions, (3) flow characteristics with water, (4) external static pipe loads with contained sodium at pressure and temperature, (5) sodium seat leakage at temperature, and (6) mechanical cycling with sodium to simulate 40-year service life in sodium-cooled reactor systems.

During this reporting period, NDT inspection, gas seat leakage tests, and flow characteristics tests in water were completed on the Velan valves, and sodium tests were completed on both Velan and Westinghouse 6-in. (152-mm) swing check valves.

B. TEST DESCRIPTION

1. Facility

Flow characteristics tests utilizing water are performed in the Hydraulic Test Facility (HTF). Water circulation is supplied by three centrifugal pumps arranged in a parallel configuration. One pump (P-3) is rated at 3000 gal/min (0.189 m^3/s) and 300 ft of head (0.89 kPa); two pumps (P-2 and P-1) are each rated at 750 gal/min (0.045 m^3/s) and 900 ft of head (2.67 kPa). The pumps discharge into either a 10-in. (0.254-m) or an 8-in. (0.203-m) pipe manifold. Testing may be conducted in either the 10-in. or the 8-in. loops.

In the 10-in. (0.254-m) loop, water flows from the pumps through a 10-in. line, through the test article section, through the deaeration tank, and back to the pump suction manifold. A water-cooled heat exchanger provides for temperature control and for removal of heat resulting from pump energy input. This 10-in. loop was used for all of the ANL valve tests.

In the 8-in. (0.203-m) loop, water flows from the pump discharge through an 8-in. line, through a manifold pipe array, through the test article section, and back. The manifold pipe array consists of a 2-in. (0.05-m), a 4-in. (0.1-m), and a 6-in. (0.15-m) pipe run in parallel, with each pipe run containing a flowmeter and a shutoff valve. An airblast heat exchanger is provided in the 8-in. loop for temperature control and removal of heat from the pump energy input.

The primary function of the 7600-gal (29.6-m^3) deaeration tank is to remove entrained gases from the circulating water. An internal antivortex baffle has been installed in the deaeration tank over the outlet nozzle to prevent reentrainment of gas by vortex action. A vacuum system is provided for reducing the pressure of the gas space above the water surface.

The digital data acquisition system (DDAS) records data on disc for on-line data processing and on tape for off-line processing and a more permanent record of the data.

Each flow characteristic parameter recorded on tape and disc is an average of 50 scans taken over every 5 s. A cathode ray tube (CRT) display provides instantaneous values every 2 s for monitoring test data. An X-Y plotter is provided for either on-line or off-line plotting of data. The computer is programmed to calculate the flow coefficient utilizing the equation $Q\sqrt{S/\Delta P}$, where Q is flow (gal/min), S is the specific gravity (water = 1.0 used), and ΔP is the pressure drop across the test article (psid). A schematic of the HTF is shown in Figure XIV-1.

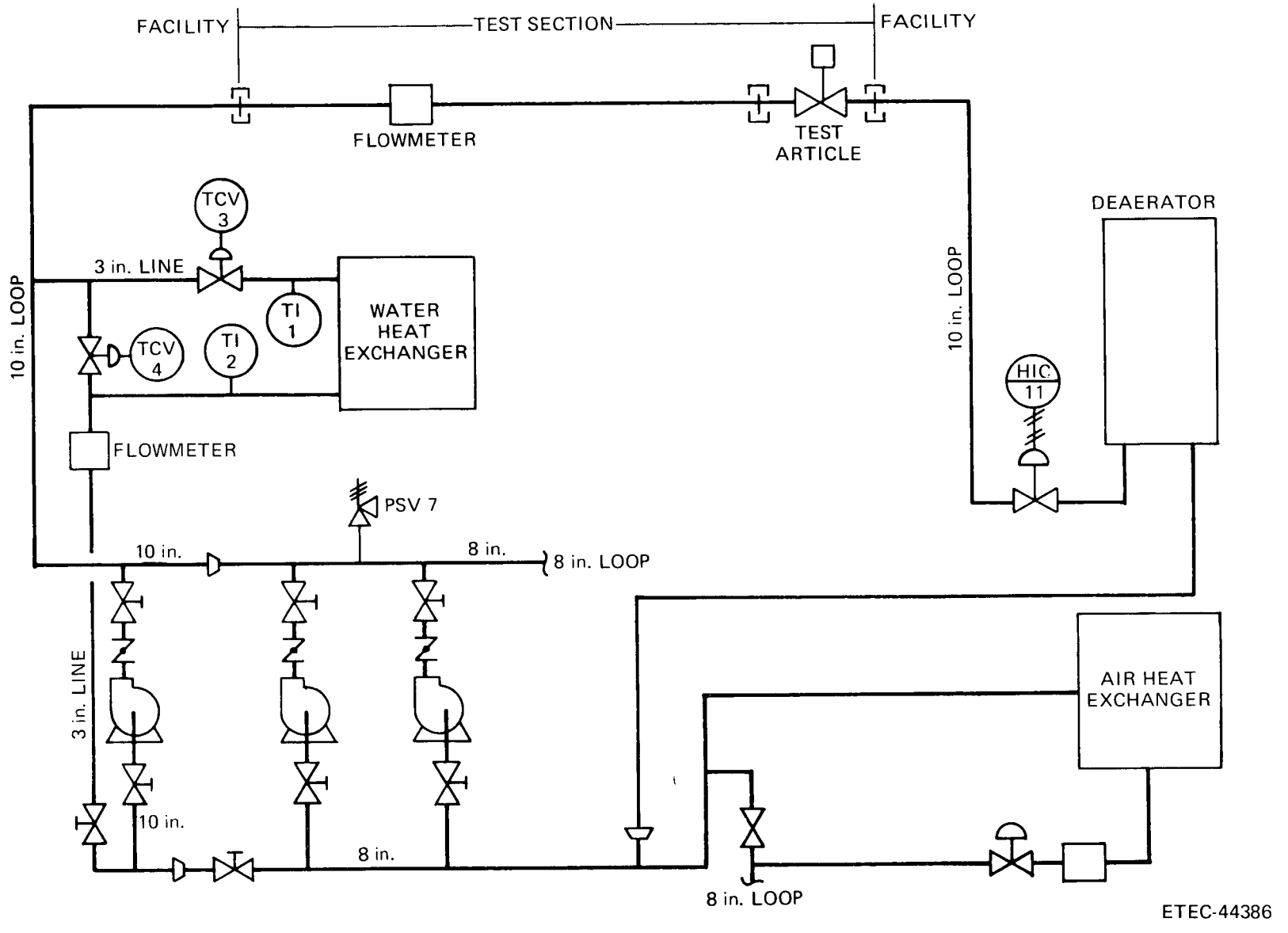

Figure XIV-1. Schematic of HTF Loop

Sodium testing is performed in the Sodium Component Test Installation (SCTI). A 4-in. (0.101-m) test loop is used to test 6-in. (0.152-m) check valves as sho in the schematic diagram, Figure XIV-2. Testing is performed with Valve V-506

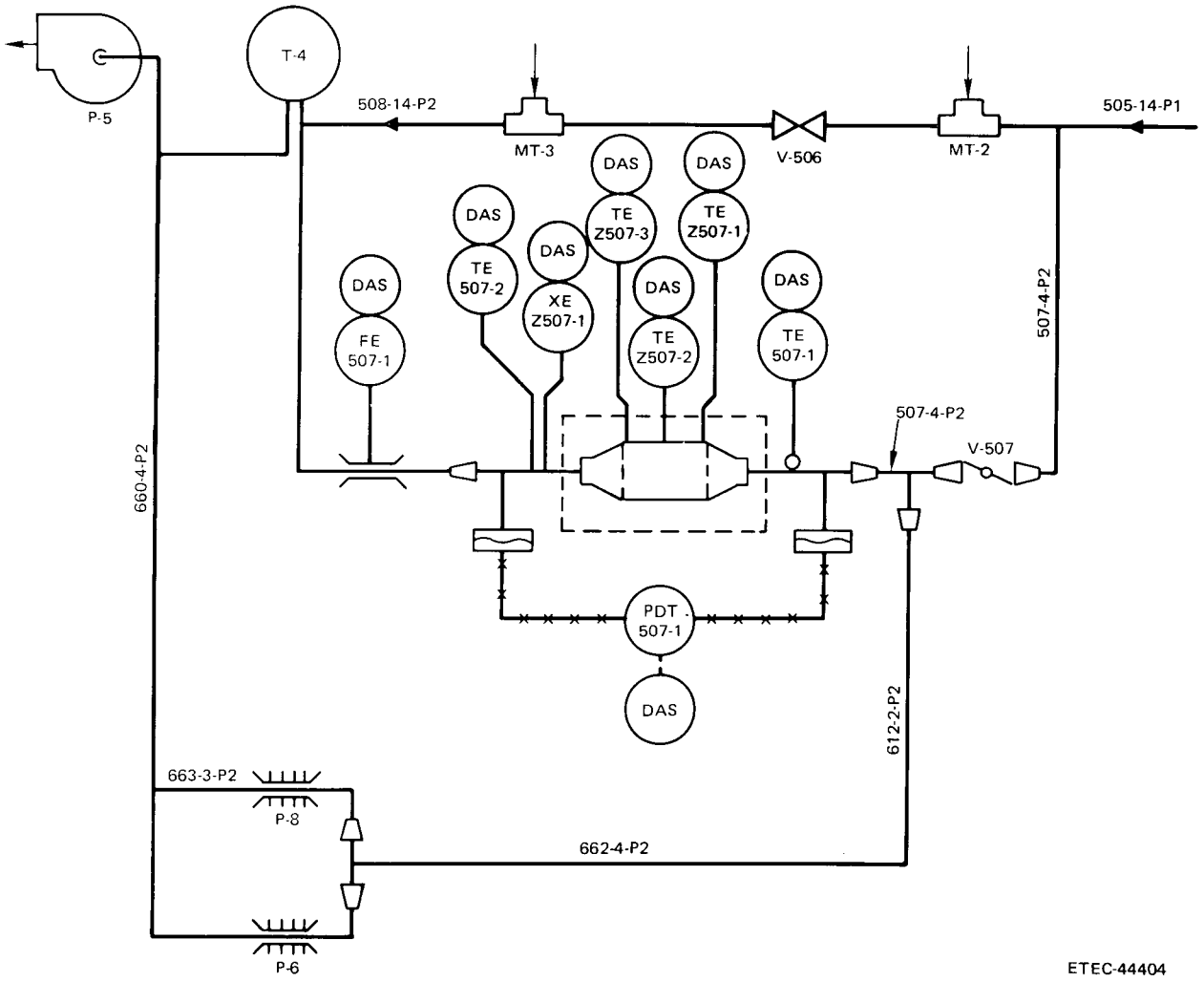

Figure XIV-2. 6-in. Check Valve Test Arrangement

closed, and design flow through the test article is measured at Flowmeter FE507-1. The test article is cycled by cycling Valve V-507. Part of the flow is bypassed through the 2-in. (0.05-m) line and through the electromagnetic (EM) pumps P-6 and P-8. The wiring to the pumps is connected to provide a negative pressure on

the check valve disc to ensure positive closure during life cycling tests. The facility provides 600 gal/min (0.038 m^3/s) of sodium at 950°F (510°C) and 100 psig (689.5 kPa) and the expansion tank, T-4, is set at 20 psig (137.5 kPa) for reverse flow testing. The temperature, facility pressure, differential pressure, and flow rate are recorded continuously by the data acquisition system in the facility control room.

2. Test Article

The test program included commercially available valves in the 1-in. (0.025-m), 2-in. (0.05-m), 4-in. (0.1-m), and 6-in. (0.15-m) sizes of the following types: (1) Y-globe, (2) straight globe, (3) angle globe, (4) offset globe, (5) gate, and (6) swing check. Valves 5261 through 5270 and 5276 through 5285 were tested during this period. Tested in sodium were 6-in. Gate Valves 2444 and 2446 . The complete list of valves is shown in Table XIV-1.

3. Test Method

The test valves are inspected "as received" for visible damage, and the body and bonnet are radiographed in accordance with ANSI B16.34-1977. Bellows are leak checked by the "hood method" per Section V, T-1060, of the ASME Boiler Code.

Seat leakage tests using dry nitrogen are conducted in accordance with ANSI B16.104 under the category Class IV and Test Procedure A. The inlet and outlet nozzles are blanked off with flat plates sealed with rubber gaskets and secured with six tie rods. There is a Swagelok connector at the center of each end plate for either pressurization or measurement of gas leakage. The gas leakage is measured by running a flexible hose from the connector to an array of gas flow-meters or by putting the free end into an inverted graduate filled with water and suspended over a waterbath.

TABLE XIV-1

DESCRIPTION OF VALVES
(Sheet 1 of 3)

ETEC ID Number	Manufacturer's Model Number	Size (in.)	Class	Type	Materials				Seals	
					Body	Stem	Seat Contact Surface	Bellows	Primary	Secondary
5087	Rockwell 15108MML	1	1500	Y-Globe	316SS	17-5PH	Stellite	DNA[a]	Membrane (Inconel 718)	Packing
5088	Rockwell 15108MM	1	1500	Y-Globe	316SS	17-5PH	Stellite	DNA[a]	Membrane (Inconel 718)	Packing
5090	Rockwell 15108MML	2	1500	Y-Globe	316SS	17-5PH	Stellite	DNA[a]	Membrane (Inconel 718)	Packing
5091	Rockwell 15108MM	2	1500	Y-Globe	316SS	17-5PH	Stellite	DNA[a]	Membrane (Inconel 718)	Packing
2611	Valtek Mark 1	1	600	Straight Globe	316SS	316SS	Stellite-6	316SS	Bellows	Packing
2612	Valtek Mark 1	1	600	Straight Globe	316SS	316SS	Stellite-6	316SS	Bellows	Packing
2613	Valtek Mark 1	2	600	Straight Globe	316SS	316SS	Stellite-6	316SS	Bellows	Packing
2614	Valtek Mark 1	2	600	Straight Globe	316SS	316SS	Stellite-6	316SS	Bellows	Packing
2615	Valtek Mark 1	4	600	Straight Globe	316SS	316SS	Stellite-6	316SS	Bellows	Packing
2616	Valtek Mark 1	4	600	Straight Globe	316SS	316SS	Stellite-6	316SS	Bellows	Packing
2617	Valtek Mark 1	6	600	Straight Globe	316SS	316SS	Stellite-6	316SS	Bellows	Packing
2618	Valtek Mark 1	6	600	Straight Globe	316SS	316SS	Stellite-6	316SS	Bellows	Packing
2619	Valtek Mark 1	1	600	Angle Globe	316SS	316SS	Stellite-6	316SS	Bellows	Packing
2620	Valtek Mark 1	1	600	Angle Globe	316SS	316SS	Stellite-6	316SS	Bellows	Packing
2621	Valtek Mark 1	2	600	Angle Globe	316SS	316SS	Stellite-6	316SS	Bellows	Packing
2622	Valtek Mark 1	2	600	Angle Globe	316SS	316SS	Stellite-6	316SS	Bellows	Packing
2623	Valtek Mark 1	4	600	Angle Globe	316SS	316SS	Stellite-6	316SS	Bellows	Packing
2624	Valtek Mark 1	4	600	Angle Globe	316SS	316SS	Stellite-6	316SS	Bellows	Packing
2625	Valtek Mark 1	6	600	Angle Globe	316SS	316SS	Stellite-6	316SS	Bellows	Packing
2626	Valtek Mark 1	6	600	Angle Globe	316SS	316SS	Stellite-6	316SS	Bellows	Packing
2627	Valtek Mark 8	1	600	Y-Globe	316SS	316SS	Stellite-6	316SS	Bellows	Packing
2628	Valtek Mark 8	1	600	Y-Globe	316SS	316SS	Stellite-6	316SS	Bellows	Packing
2629	Valtek Mark 8	2	600	Y-Globe	316SS	316SS	Stellite-6	316SS	Bellows	Packing
2630	Valtek Mark 8	2	600	Y-Globe	316SS	316SS	Stellite-6	316SS	Bellows	Packing
2631	Valtek Mark 8	4	600	Y-Globe	316SS	316SS	Stellite-6	316SS	Bellows	Packing
2632	Valtek Mark 8	4	600	Y-Globe	316SS	316SS	Stellite-6	316SS	Bellows	Packing
2633	Valtek Mark 8	6	600	Y-Globe	316SS	316SS	Stellite-6	316SS	Bellows	Packing

TABLE XIV-1

DESCRIPTION OF VALVES
(Sheet 2 of 3)

ETEC ID Number	Manufacturer's Model Number	Size (in.)	Class	Type	Materials				Seals	
					Body	Stem	Seat Contact Surface	Bellows	Primary	Secondary
2634	Valtek Mark 8	6	600	Y-Globe	316SS	316SS	Stellite-6	316SS	Bellows	Packing
2745	Persta - Type 11, NW50	50MM	17BAR[b]	Offset Globe, Throttling	304SS[c]	318SS[c]	Stellite-6	Inconel 600	Bellows	Packing
2746	Persta - Type 11, NW50	50MM	17BAR[b]	Offset Globe, Throttling	304SS[c]	318SS[c]	Stellite-6	Inconel 600	Bellows	Packing
2747	Persta - Type 11, NW100	100MM	17BAR[b]	Offset Globe, Throttling	304SS[c]	318SS[c]	Stellite-6	Inconel 600	Bellows	Packing
2748	Persta - Type 11, NW100	100MM	17BAR[b]	Offset Globe, Throttling	304SS[c]	318SS[c]	Stellite-6	Inconel 600	Bellows	Packing
2749	Persta - Type 10, NW50	50MM	17BAR[b]	Offset Globe, Shutoff	304SS[c]	318SS[c]	Stellite-6	Inconel 600	Bellows	Packing
2750	Persta - Type 10, NW50	50MM	17BAR[b]	Offset Globe, Shutoff	304SS[c]	318SS[c]	Stellite-6	Inconel 600	Bellows	Packing
2751	Persta - Type 10, NW100	100MM	17BAR[b]	Offset Globe, Shutoff	304SS[c]	318SS[c]	Stellite-6	Inconel 600	Bellows	Packing
2752	Persta - Type 10, NW100	100MM	17BAR[b]	Offset Globe, Shutoff	304SS[c]	318SS[c]	Stellite-6	Inconel 600	Bellows	Packing
2442	Velan B12-1114B-13MS	4	300	Swing Check	316SS	DNA	SA351-CF8	DNA	Gasket	DNA
2443	Velan B12-1114B-13MS	4	300	Swing Check	316SS	DNA	SA351-CF8	DNA	Gasket	DNA
2444	Velan B14-1114B-13MS	6	300	Swing Check	316SS	DNA	SA351-CF8	DNA	Gasket	DNA
2445	Westinghouse 8377 D40	6	345[b]	Swing Check	316SS	DNA	Stellite-165	DNA	Welded	DNA
2446	Westinghouse 8377 D40	6	345[b]	Swing Check	316SS	DNA	Stellite-165	DNA	Welded	DNA
5261	Velan	1	300	Gate	316SS	316SS	Stellite-6	Inconel 600	Bellows	Packing
5262	Velan	1	300	Gate	316SS	316SS	Stellite-6	Inconel 600	Bellows	Packing
5263	Velan	6	300	Gate	316SS	660SS	Stellite-6	Inconel 600	Bellows	Packing
5264	Velan	6	300	Gate	316SS	660SS	Stellite-6	Inconel 600	Bellows	Packing
5265	Velan	3	300	Gate	316SS	660SS	Stellite-6	Inconel 600	Bellows	Packing
5266	Velan	3	300	Gate	316SS	660SS	Stellite-6	Inconel 600	Bellows	Packing
5267	Velan	4	300	Gate	316SS	660SS	Stellite-6	Inconel 600	Bellows	Packing
5268	Velan	4	300	Gate	316SS	660SS	Stellite-6	Inconel 600	Bellows	Packing
5269	Velan	2	300	Gate	316SS	316SS	Stellite-6	Inconel 600	Bellows	Packing
5270	Velan	2	300	Gate	316SS	316SS	Stellite-6	Inconel 600	Bellows	Packing

TABLE XIV-1

DESCRIPTION OF VALVES
(Sheet 3 of 3)

ETEC ID Number	Manufacturer's Model Number	Size (in.)	Class	Type	Materials				Seals	
					Body	Stem	Seat Contact Surface	Bellows	Primary	Secondary
5276	Velan	1	300	Straight Globe	316SS	316SS	Stellite-6	Inconel 600	Bellows	Packing
5277	Velan	1	300	Straight Globe	316SS	316SS	Stellite-6	Inconel 600	Bellows	Packing
5278	Velan	2	300	Straight Globe	316SS	316SS	Stellite-6	Inconel 600	Bellows	Packing
5279	Velan	2	300	Straight Globe	316SS	316SS	Stellite-6	Inconel 600	Bellows	Packing
5280	Velan	3	300	Straight Globe	316SS	660SS	Stellite-6	Inconel 600	Bellows	Packing
5281	Velan	3	300	Straight Globe	316SS	660SS	Stellite-6	Inconel 600	Bellows	Packing
5282	Velan	4	300	Straight Globe	316SS	660SS	Stellite-6	Inconel 600	Bellows	Packing
5283	Velan	4	300	Straight Globe	316SS	660SS	Stellite-6	Inconel 600	Bellows	Packing
5284	Velan	6	300	Straight Globe	316SS	660SS	Stellite-6	Inconel 600	Bellows	Packing
5285	Velan	6	300	Straight Globe	316SS	660SS	Stellite-6	Inconel 600	Bellows	Packing

[a]DNA = does not apply
[b]Maximum working pressure (psi) at 1000°F
[c]ASME alloy closest to actual composition

Water flow characteristics are obtained with the test article installed in the test section of the 10-in. (25.4-cm) loop of the HTF installation using Vitaulic couplings. The valve stroke is measured, and the valve is set in the fully open position. Flow is then established through the valve and the pressure drop is set to 20 ± 0.5 psid by adjusting the downstream control valve (FCV-11). The system is allowed to stabilize at this condition and data are recorded. The pressure drop is then adjusted to 17.5 ± 0.5 psid and allowed to stabilize, and the data are recorded. A further adjustment is made to 15 ± 0.5 psig and after stabilizing, data are recorded. This process is repeated three times for a total of nine data points. The flow is reduced to zero and then gradually increased from zero to full flow by adjusting the FCV-11 valve until it is fully open. The circulating system is then shut down and the following plots are printed out, utilizing the computer and X-Y plotter: (1) C_v vs flow, (2) $\sqrt{\Delta P}$ vs flow, (3) downstream pressure (P-2), (4) C_v vs flow, cavitation run, (5) $\sqrt{g}$ vs flow, cavitation run, (6) $\sqrt{\Delta P}$ vs flow, cavitation run, and (7) downstream pressure (P-2), cavitation run. If the test data are acceptable, the whole procedure is repeated for each 10% increment in valve position from fully open to 10% open.

Sodium testing of the 6-in. check valves is accomplished by closing Valve V-506 in the test loop, shown schematically in Figure XIV-2, and adjusting Valve V-507 to control the flow rate. Back pressure to close the test article clapper is achieved by closing Valve V-507 and reducing the pressure on the upstream side through operation of the P-6 and P-8 EM pumps in the reverse direction. Cycling of the valve is accomplished by cycling Valve V-507 under computer control.

C. TEST RESULTS

1. Results of Receiving Inspection

All of the valves were visually inspected, and no reportable defects were found. All valves showed a bellows leak rate of less than 1×10^{-7} scc of helium

per second, which is the acceptable limit. The seat leakage test was performed at ambient temperature using nitrogen at 50 psig with a seat load of 100 lb per circumferential inch of nominal valve size. All of the globe valves met the leak rate requirements and nine of the ten gate valves were satisfactory.

All of the valves were satisfactory in both radiographic and liquid-penetrant examinations.

2. Flow Characteristics

A total of ten Velan valves were tested in the HTF water flow loop. One valve of each type (globe and gate) of each size was tested between June and August. Table XIV-2 shows the on-line C_v values obtained from these valves. Data from the tests were later reduced off-line; more precise calculations of C_v were made and presented in individual valve test reports. On-line plots were produced

TABLE XIV-2

FLOW CHARACTERISTICS RESULTS

Test Article Type and Size	E-Number	Measured Full-Open C_v	Manufacturer's Quoted Full-Open C_v
Globe 1-in.	E-5276	3.4	8
Globe 2-in.	E-5278	13	24
Globe 3-in.	E-5280	54	45
Globe 4-in.	E-5282	115	95
Globe 6-in.	E-5284	230	230
Gate 1-in.	E-5216	20	27.2
Gate 2-in.	E-5269	119	181
Gate 3-in.	E-5265	398	425
Gate 4-in.	E-5267	1386	760
Gate 6-in.	E-5263	≈4000	2130

and monitored to determine the validity of the tests as performed. Typical plots are shown in Figures XIV-3 through -9. No serious anomalies were observed in any of the data or plots obtained, and no operational difficulties were experienced. The 3-in. (7.62-cm) valves were tested in August, after which the program was suspended because of budget constraints. A typical globe valve is shown in Figure XIV-10.

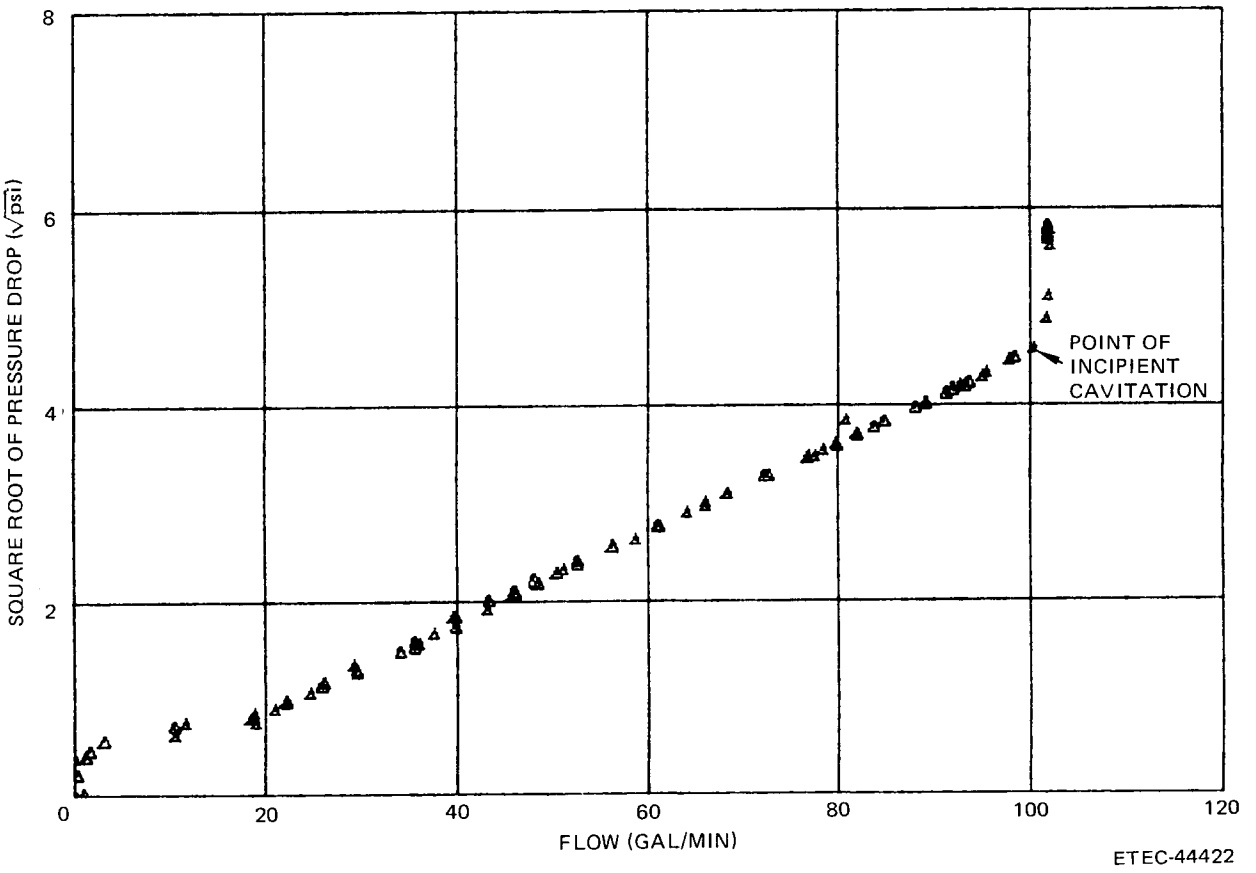

Figure XIV-3. 1-in. Valve Flow Test Curve

3. Sodium Tests

Two 6-in. swing check valves, one Velan (Figure XIV-11) and one Westinghouse (Figure XIV-12) were tested in flowing sodium at 900°F (482°C). Each valve was tested for ~48 h under these conditions and was subjected to 1500 reversing

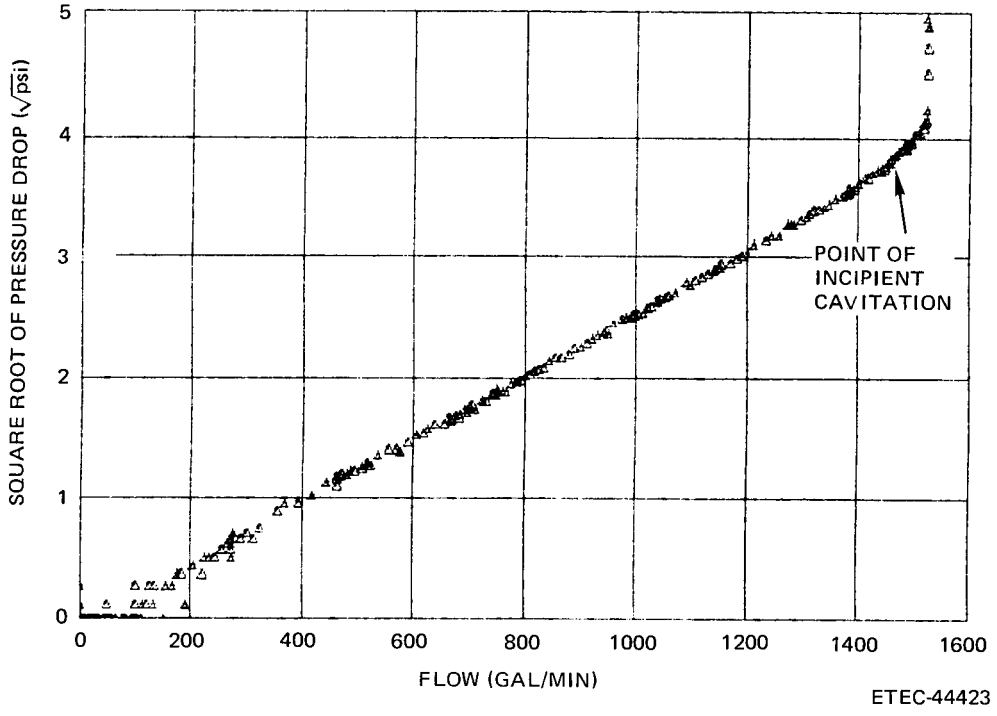

Figure XIV-4. 3-in. Valve Flow Test Curve

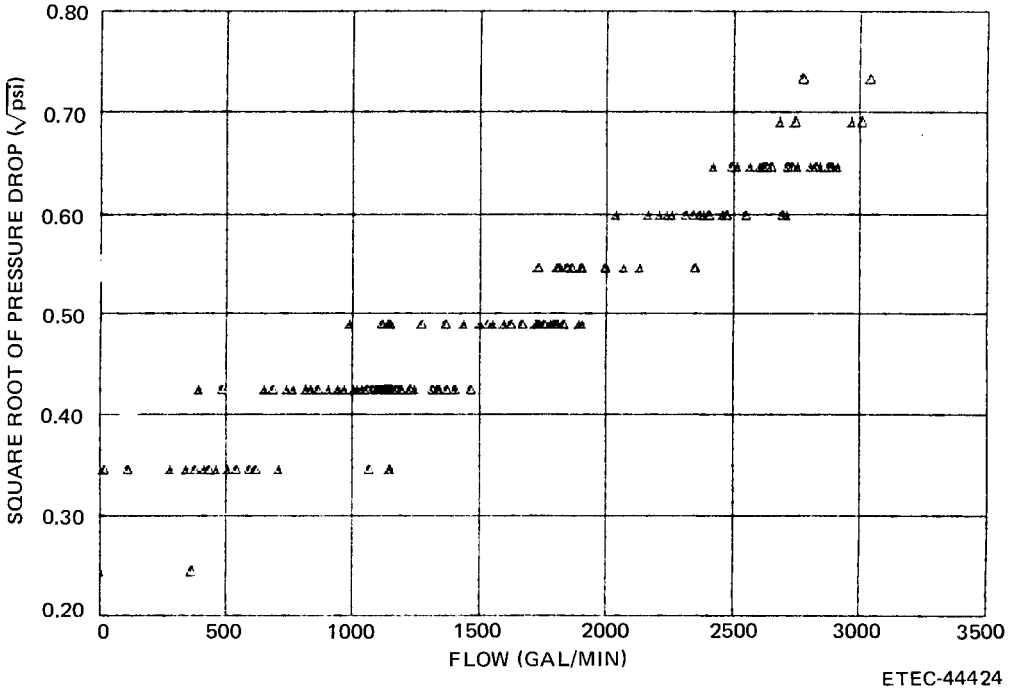

Figure XIV-5. 6-in. Valve Flow Test Curve

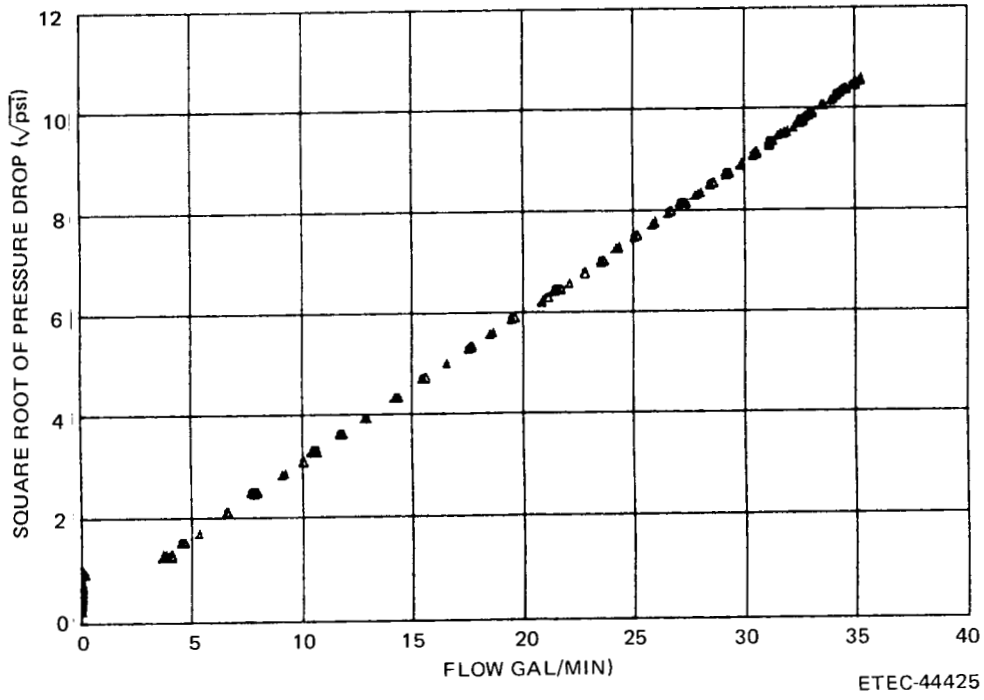

Figure XIV-6. 1-in. Valve Flow Test Curve at 100% Open

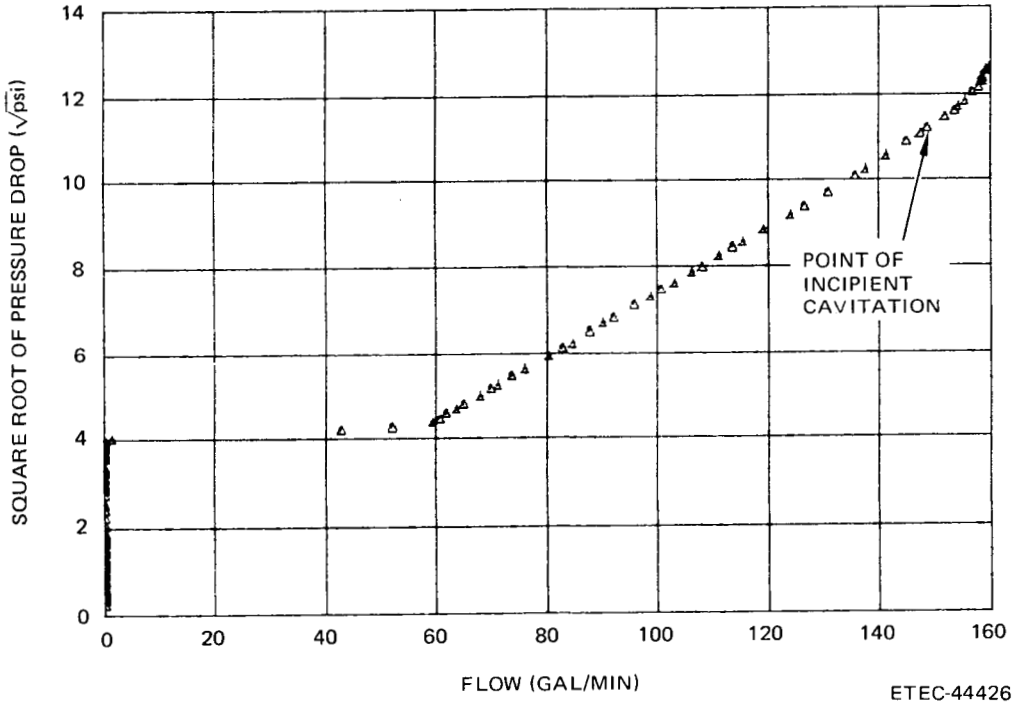

Figure XIV-7. 2-in. Valve Flow Test Curve at 100% Open

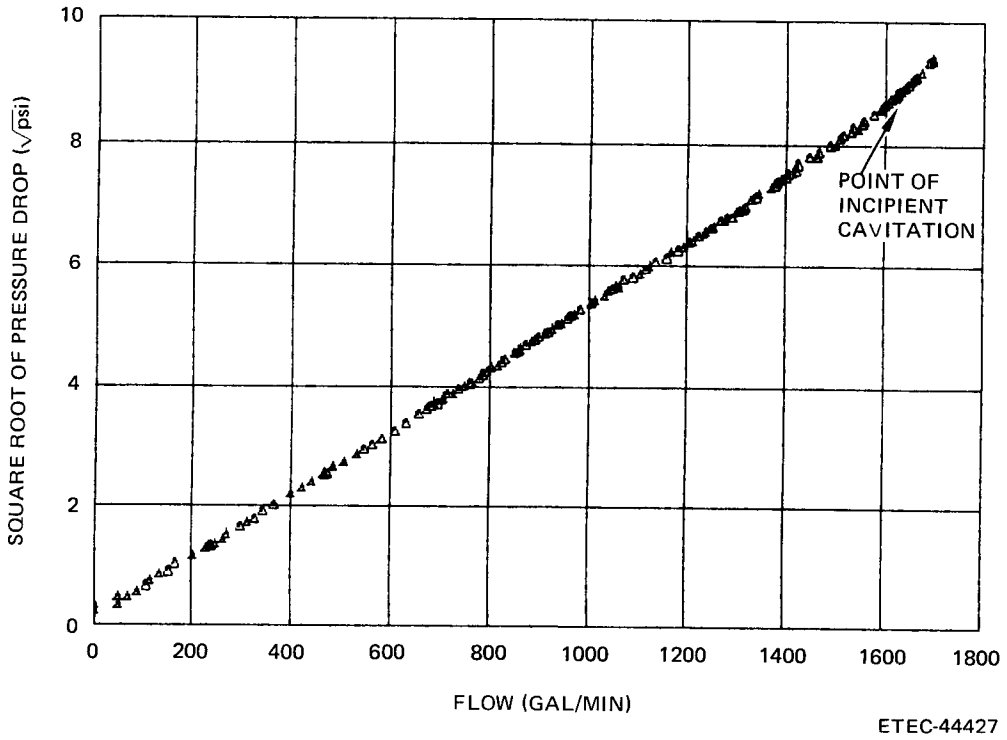

Figure XIV-8. 6-in. Valve Flow Test Curve at 70% Open

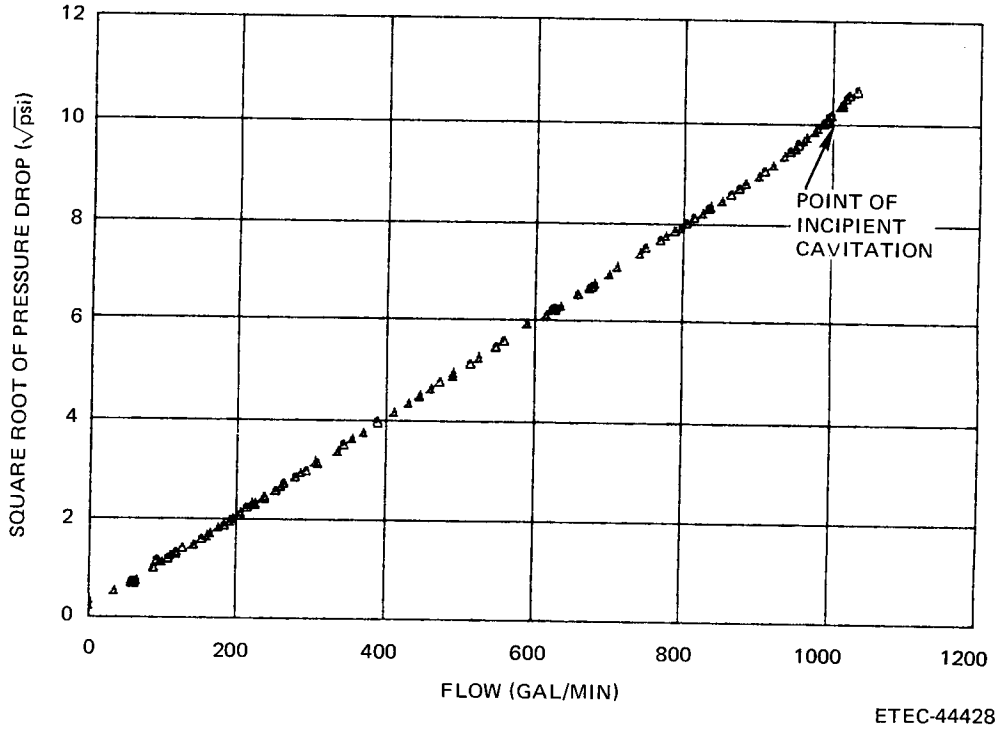

Figure XIV-9. 4-in. Valve Flow Test Curve at 80% Open

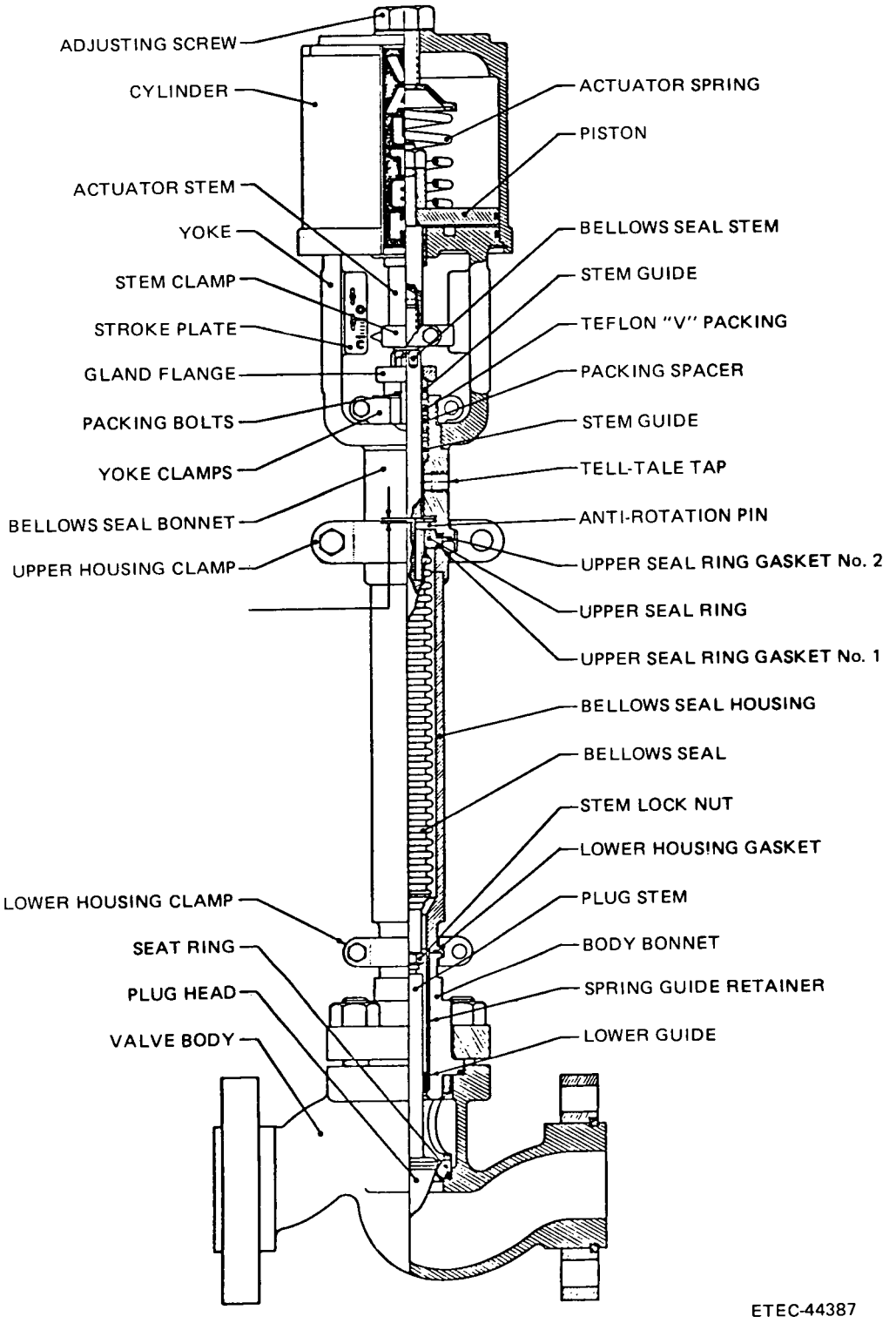

Figure XIV-10. Valtek Bonnet Extension with Bellows Seal

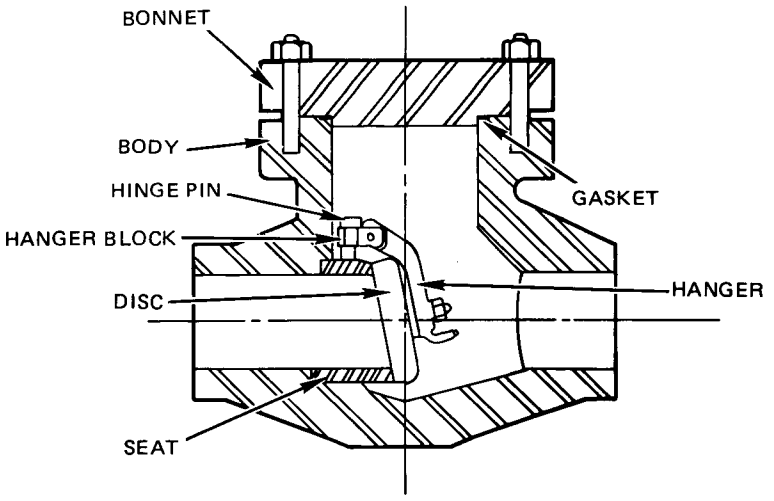

Figure XIV-11. Velan Swing Check Valve

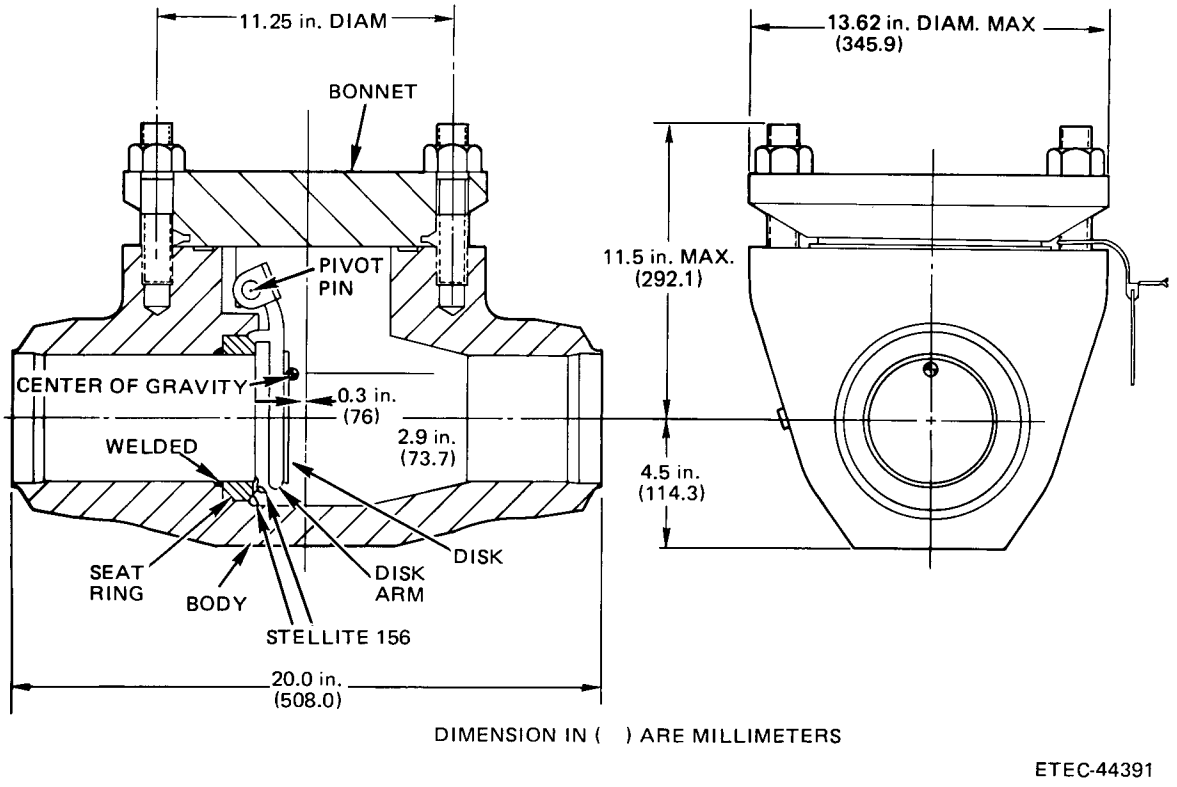

Figure XIV-12. Westinghouse Swing Check Valve

sodium flow cycles. There were no malfunctions or problems experienced with either valve. Figure XIV-13 is a typical plot showing flow rates ranging from 0 to 560 gal/min (0.035 m^3/s) for each cycle and pressure drop of 1 psid (6.895 kPa) with flow opening the flapper and -10 psid (68.95 kPa) with pressure closing the flapper. This was typical for both valves.

Upon completion of the life cycle test, each valve was cleaned, disassembled, examined for wear, checked by radiography and liquid penetrant, and seat leakage tested for comparison against the as-received condition. Using 40X magnification, there was no evidence of wear or self-welding of facing parts on either valve.

Radiography and dye-penetrant examination revealed no change in the body structure. However, the nitrogen seat leakage test showed that though the Westinghouse valve was well within the allowable rate, the Velan valve exhibited a serious leakage problem. The results are as follows:

Valve	Seat leakage at 100 psid (scfh)	
6-in. Swing Check	Before Sodium Test	After Sodium Test
Westinghouse	0.8	7.0
Velan	11.6	500.0
CRBR allowable	-	210.0

Further examination of the Velan valve showed that the seal face of the flapper had a 0.002-in. (0.05-mm) dish distortion from the flat. Figure XIV-14 is a polar plot showing the distortion.

A test was then performed on the Westinghouse valve with a 0.002-in. (0.05-mm) shim placed to simulate the warped condition of the Velan valve flapper. The nitrogen leakage test was repeated, and a leak rate of 400 scfh (11.32 m^3/h) at 100 psid (689.5 kPa) was observed. This was comparable to the leak rate of the Velan valve. From the results of prior water tests, it is known that the maximum available sodium flow of 560 gal/min (0.035 m^3/s) was not opening either of these valves fully, but it is reasonable to expect that fully opened cycles would not have caused significantly greater wear.

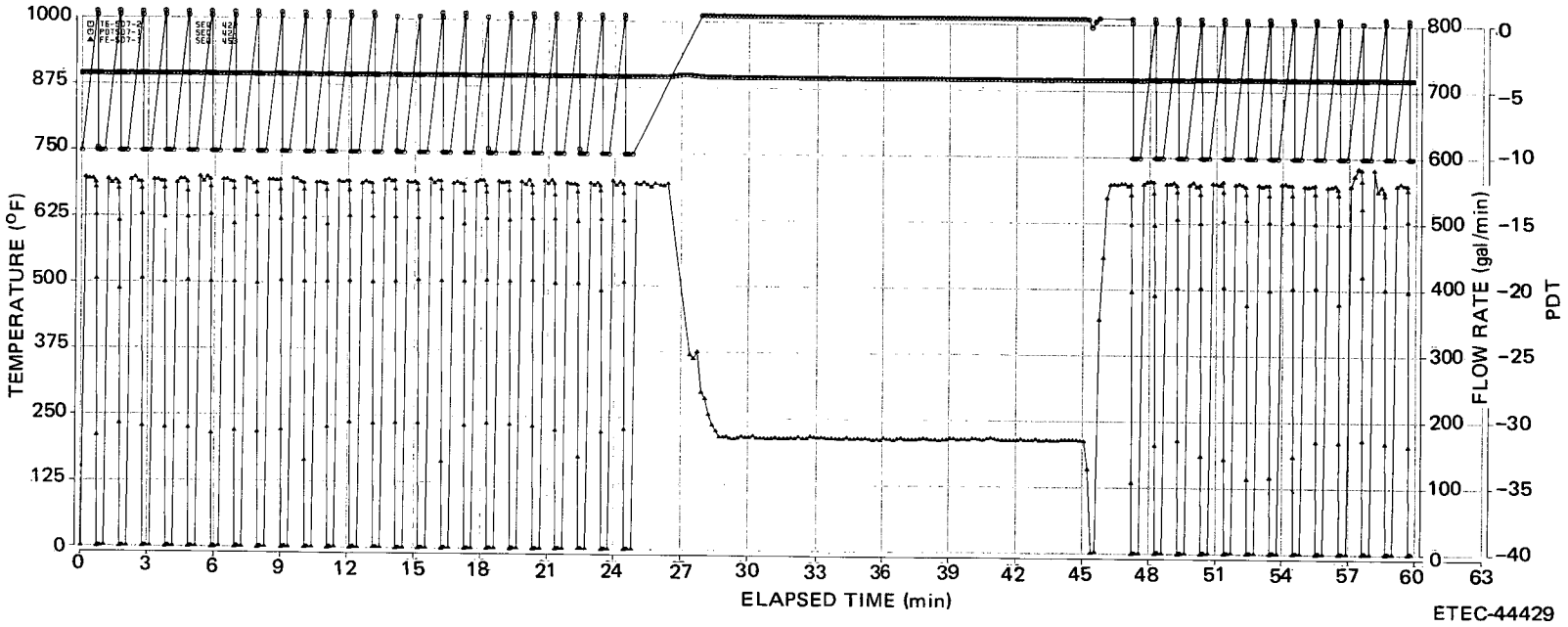

Figure XIV-13. 6-in. Swing Check Valve — SCTI Sodium Test

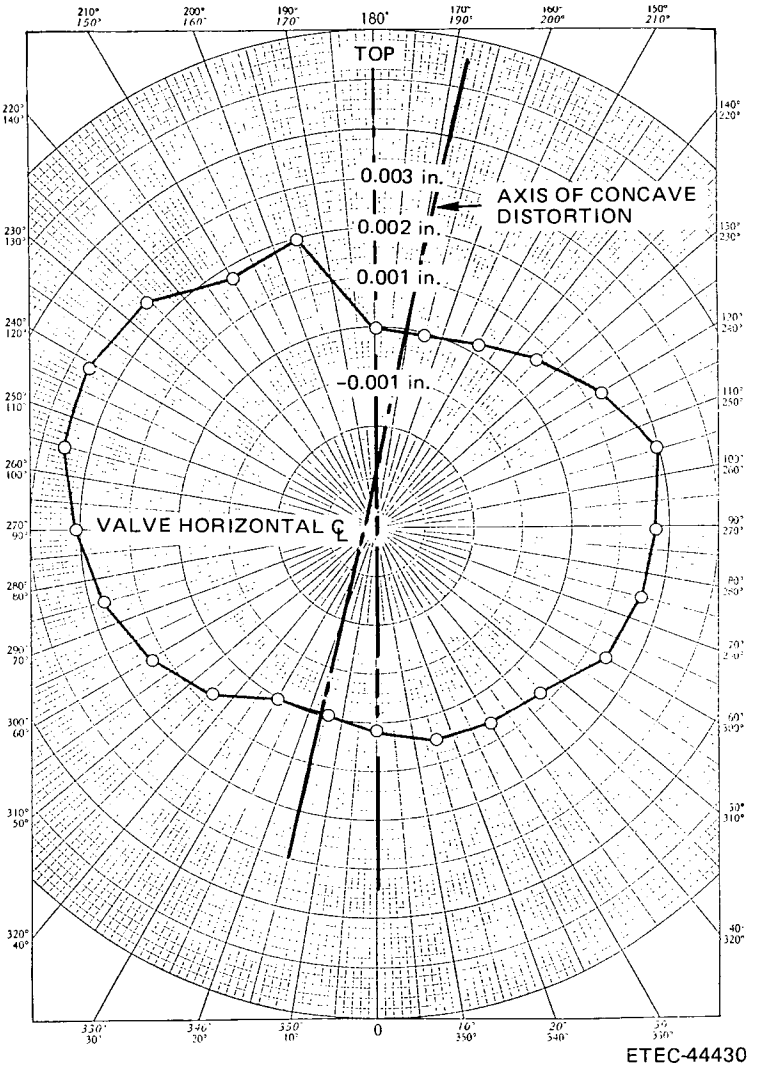

Figure XIV-14. Clapper Flatness, Velan 6-in. Check Valve

Both valves were cleaned with alcohol and flushed with hot water after sodium testing and before gas seat leakage testing.

4. Special Seat Leakage Tests

Twenty-eight valves were tested at various line pressures from 50 to 325 psig with various seat loads to determine the effects of varying these parameters. One valve was tested with three different reworked seats to investigate the effects of seat finish machining techniques and mating taper angles. All globe valves were

purchased with ANSI B16.104 Class IV seat leakage requirements, which is the standard for the control valve industry but not as stringent as is anticipated for the intended service in sodium.

The nitrogen pressurization system and leakage measuring equipment used for the initial receiving inspection and seat leakage tests were utilized for this series of tests. The valve port end plates were redesigned to accommodate the higher test pressures.

The globe valve actuators were pressurized to provide 100, 200, 300, 400, and 600 lb of force per circumferential inch of seat contact except where limited by valve or actuator safe limits. Line pressures were set at 50, 100, 200, and 325 psig.

The gate valve actuators were pressurized to provide a stem-to-disc force in accordance with the following equation:

$$\text{Force} = C\ (0.3\ P_{in}A_{disc} + P_{in}A_{bellows}) + \text{tare}$$

where

P_{in} = 325 psig, P_{out} = 0

A_{disc} = disc seating area

C = 1.0, 1.3, 1.6, or 1.9 as assigned (1.3 is generally used throughout the valve industry)

tare = a measured force that includes actuator and packing friction and bellows spring force less the stem train weight.

Globe valves with gross leakage exhibited only minor leakage reduction when seating force was increased as shown in Figure XIV-15. Globe valves with fine leakage exhibited up to five decades' leakage reduction with increased seating force. Typical results are shown in Figure XIV-16. The effect of increasing line pressure from 50 to 325 psig with 0 psig back pressure was less than a one-decade increase in leakage. All tests were performed with line pressure applied under the plug and atmospheric pressure over the plug.

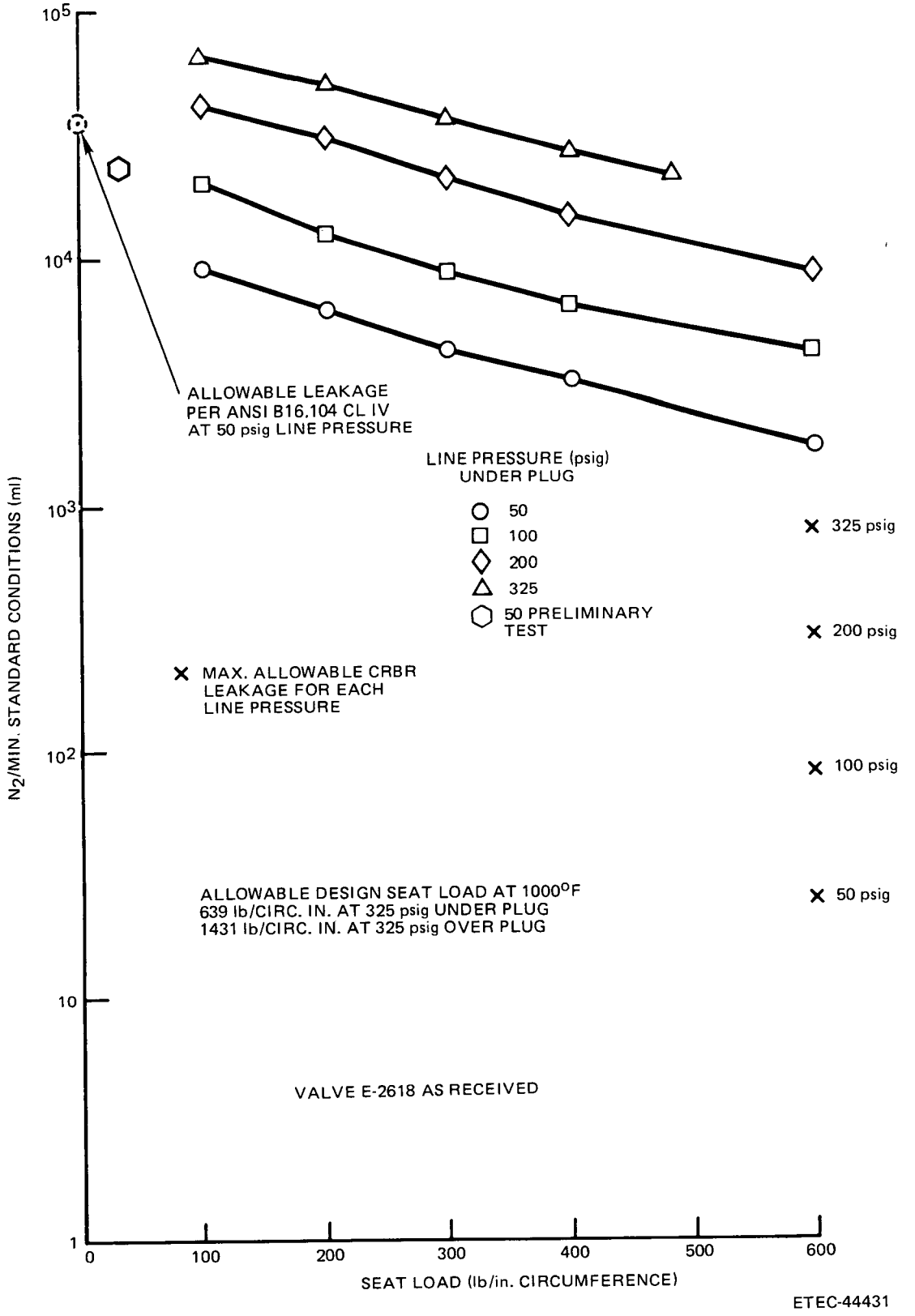

Figure XIV-15. Seat Leakage Test, 6-in. Straight-Pattern Globe Valve (Valve E-2618 as received)

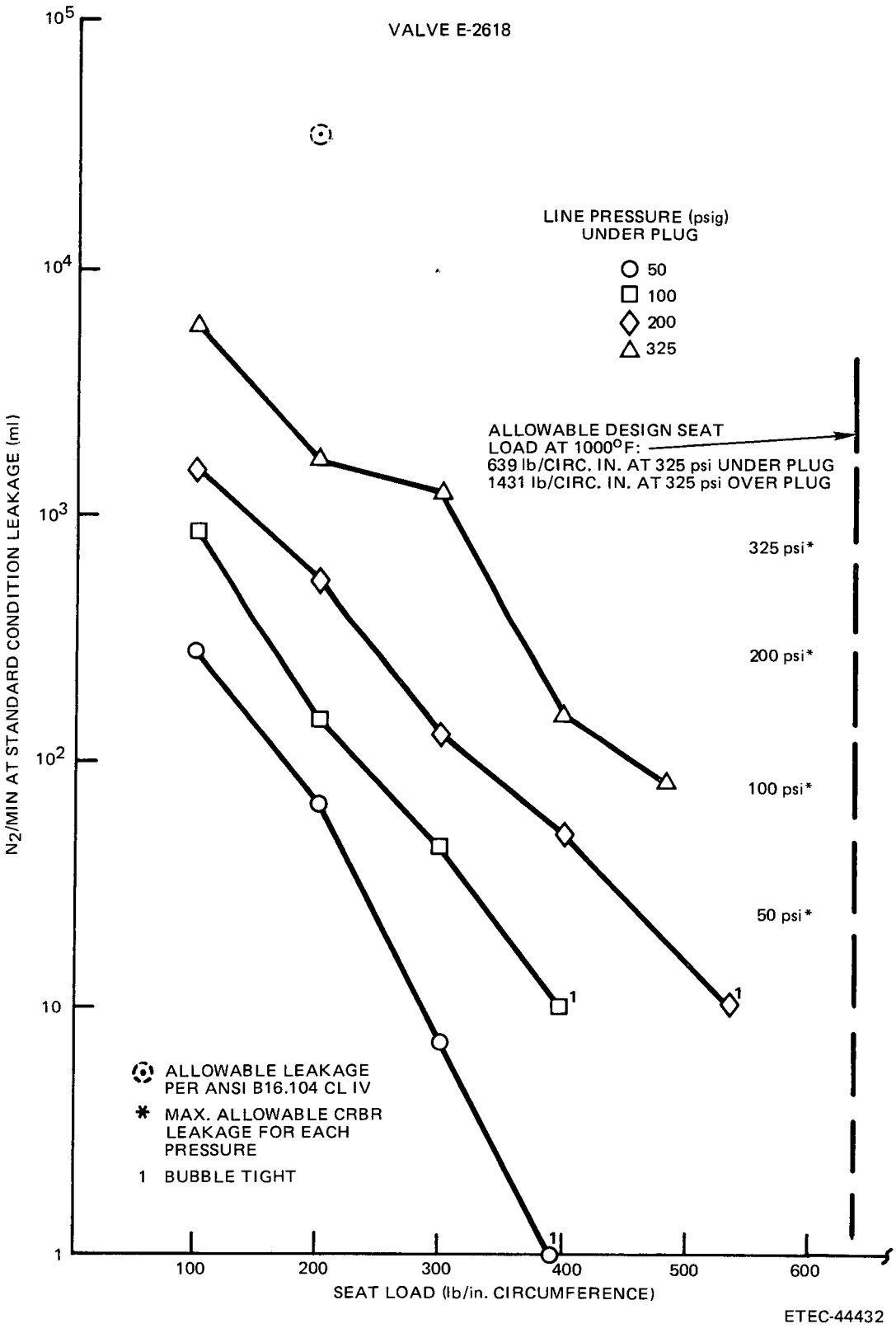

Figure XIV-16. Seat Leakage Test, 6-in. Globe Straight
(E-2618, A-2743, Ground Seat 1)

Gate valves showed very minor leakage change with an increase of seating load and less than a one-decade leakage increase with an increase of pressure from 50 to 350 psid across the seat. Typical results are shown in Figure XIV-17. The small effect on leakage of increased actuator force is attributed to the fact that seat loading is mostly created by the differential pressure acting on the disc area.

Tests performed on the globe valve with refinished seats demonstrated that truing of the conical plug and seat tapers coupled with improved assembly techniques results in significant reduction in seat leakage.

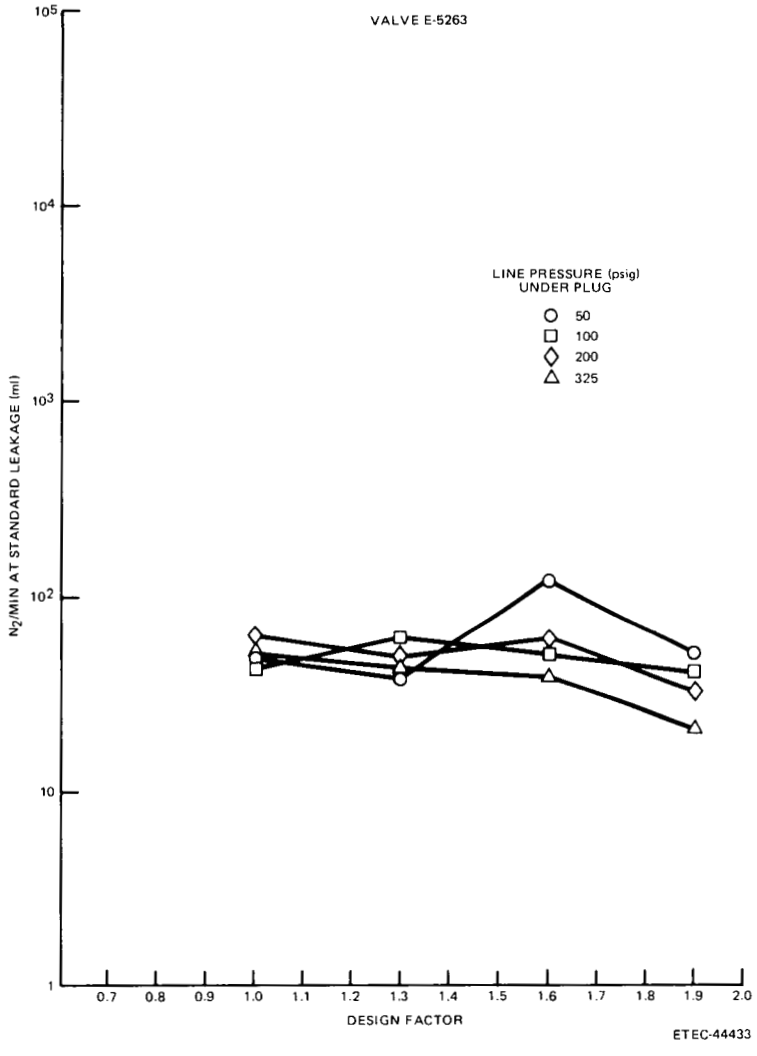

Figure XIV-17. Seat Leakage Test, 6-in. Gate (E-5263)

XV. ORNL PIPE TEST

P. ARCHBOLD
C. M. NIGHTINGALE

A. INTRODUCTION

The test article is a piece of Type 304 stainless steel pipe incorporating both a 0.375-in. (9.53-mm) wall and a 0.5-in. (12.70-mm) wall without structural discontinuities. The purposes of the test are:

1) To provide creep-fatigue failure data on a pipe that is subjected to thermal ratchetting loading
2) To provide thermal ratchetting data on Type 304 stainless steel pipe under severe loading conditions for validation of inelastic analysis procedures and computer codes.

In order to achieve control for the thermal transients without subjecting the test article to spurious trials and test runs, a dummy test assembly having the same dimensions as the final test specimen was used to set up the control systems. This assembly was instrumented with embedded thermocouples in addition to the instrumentation to be provided on the final specimen. The centerbody was designed for use with both test assemblies and included embedded thermocouples for use in the control circuits.

B. TEST DESCRIPTION

1. Facility

The Thermal Transient Facility (TTF) contains the piping and structural supports necessary to produce thermal transients using gaseous nitrogen, under specified mechanical load conditions, for accelerated life tests. The system is

programmed to introduce cold gaseous nitrogen at controlled flow rates for down-ramps. The nitrogen flow is computer controlled for precise transient results. Mechanical loading is accomplished hydraulically with cylinder loads controlled accurately by means of a "load maintainer." The load maintainer takes the hydraulic fluid from the facility pump and can be set up to provide to each cylinder the exact pressure to enable precise load application to the test article. Load cells are used with each load cylinder for monitoring the applied load during test.

Capacitive strain gages are used to measure the strains induced, and thermocouples monitor the temperature distribution across the test article. Heating elements mounted external to the test article are controlled in zones to provide correct temperature distribution, and all parameters are monitored and printed as needed in the facility control room.

2. Test Article

The test article consists of a single 68-in. (1730-mm) length of reference heat 9T2796, Type 304 stainless steel pipe with a 0.5-in. (12.70-mm) wall. The inside diameter is 7.491 in. (190.59 mm), and machined into the outer wall of the specimen is a 12-in. (305.3-mm) gage length having a wall thickness of 0.375 in. (9.53 mm). On either end of the gage length is a 6-in. (152.65-mm) length in which the wall thickness is tapered from 0.5 in. (12.70 mm) to 0.375 in. (9.53 mm) with a 6-in. (152.65-mm) fillet radius to blend the tapers into the gage length. Downstream of the gage length is a uniform 14-in. (356.18-mm) length with a wall thickness of 0.5 in. (12.7 mm) and an inside diameter of 7.491 in. (190.59 mm). The test section is welded into entrance and exit flanges for adapting to the test facility. Extensions are welded to the test article for attachment of the loading mechanism, and transitional sections are welded to these extensions for attaching to the facility piping system.

Figure XV-1 shows the general arrangement of the test article and the location of the thermocouples. The locations of the high-temperature strain gages and the DEMEC-type tabs are shown in Figure XV-2. Table XV-1 provides a listing of the test article instrumentation. The centerbody instrumentation is shown in Figure XV-3. Both percussion-welded and brazed-in thermocouples are provided in order to assure that the control thermocouple selected can provide as rapid a response as possible and produce repeatable transients. The load cells and control instrumentation are capable of measuring and controlling the load within ±1% throughout the test.

3. Test Method

A mechanical axial load of 180,000 lb (0.80 MN) is applied to the test article by means of a load maintainer and three hydraulic actuators in such a manner that the maximum bending moment across any section is less than 2500 ft-lb (3389.5 N-m). The test article is then heated to 1100°F (593°C) at a rate not to exceed 100°F/h (56°C/h). After the temperature stabilizes at 1100°F (593°C), a downramp transient is initiated so that the downramp rate at the inner wall is 60°F/s (33.3°C/s) from 1100°F (593°C) to 500°F (260°C). After stabilizing for approximately 1 h at 500°F (260°C), the test article is heated to 1100°F (593°C) at a rate not to exceed 100°F/h (56°C/h). The temperature is stabilized at this level and held for 16 h. A complete cycle takes 24 h.

At every third cycle, the mechanical load is removed during the low-temperature hold period. To provide elastic loading data for strain gage calibration, an axial load of 76,000 lb (338 kN) is applied and then removed. The full axial load of 180,000 lb (0.8 MN) is then reapplied. All load applications and removals are made at a rate of 60,000 lb/min (267 kN/min). The test histogram is shown in Figure XV-4. At the end of six cycles, twelve cycles, the first month, and every month thereafter, when the test article is at 500°F (260°C) and unloaded, the test article is to be cooled to room temperature and the outer surface examined for cracks using dye penetrant. If cracks become evident, they are to be photographed, an axial load of 20,000 lb (80 kN) applied, and a helium leak test performed. Testing will continue until failure or for a period of 1 year, when a decision will be made on whether to increase the mechanical load.

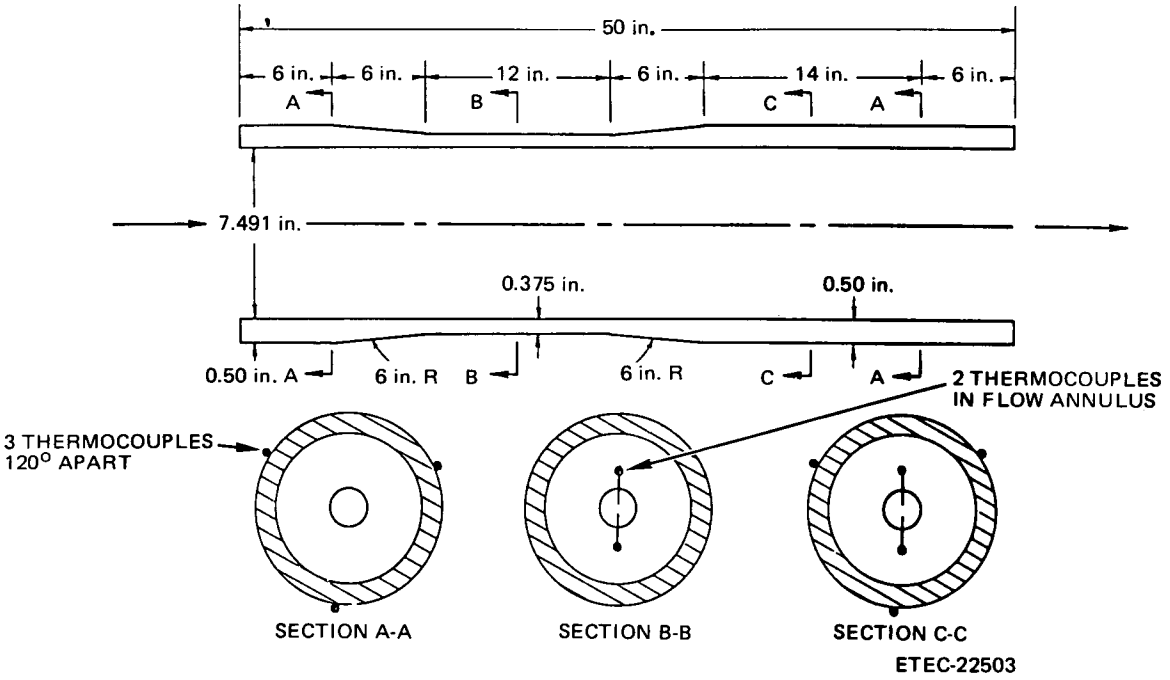

Figure XV-1. Type 304 Stainless Steel Pipe Specimen for Creep-Fatigue Failure and Thermal Ratchetting Test TT-6

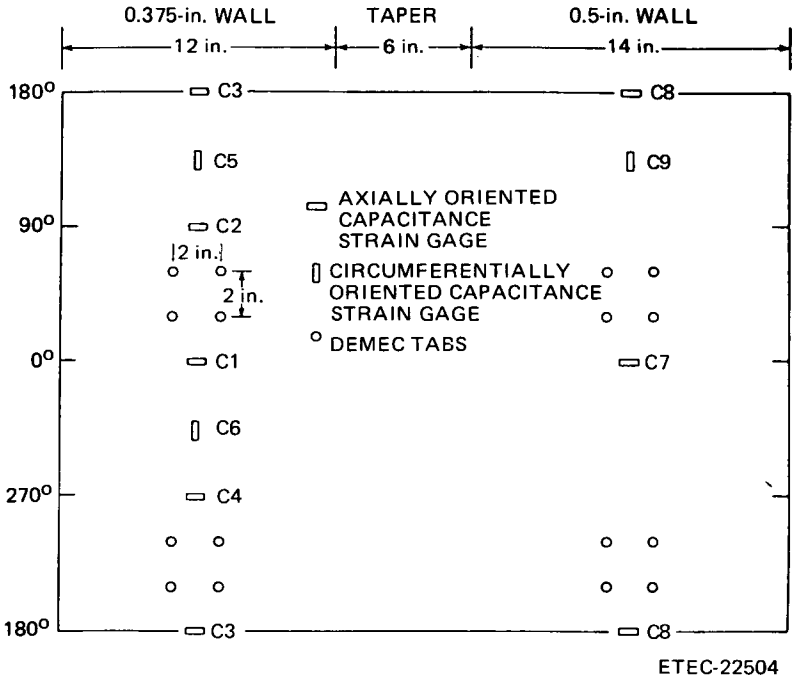

Figure XV-2. Strain-Measuring Instrumentation Used on the TT-6 Test Specimen (pipe shown as though rolled flat)

TABLE XV-1

INSTRUMENTATION FOR SPECIMEN TT-6

Thermocouples*	
Outer pipe surface	9
Capacitive gages†	18
Strain-measuring devices	
Capacitive gages	9
DEMEC tabs	16
TOTAL	52

*All thermocouples are premium-grade Chromel-Alumel except for the Platinel thermocouples that are supplied with the capacitive strain gages. The accuracy is ±7°C (±13°F).

†For each capacitive strain gage, one thermocouple is mounted on the specimen and one additional thermocouple is mounted on the gage rod.

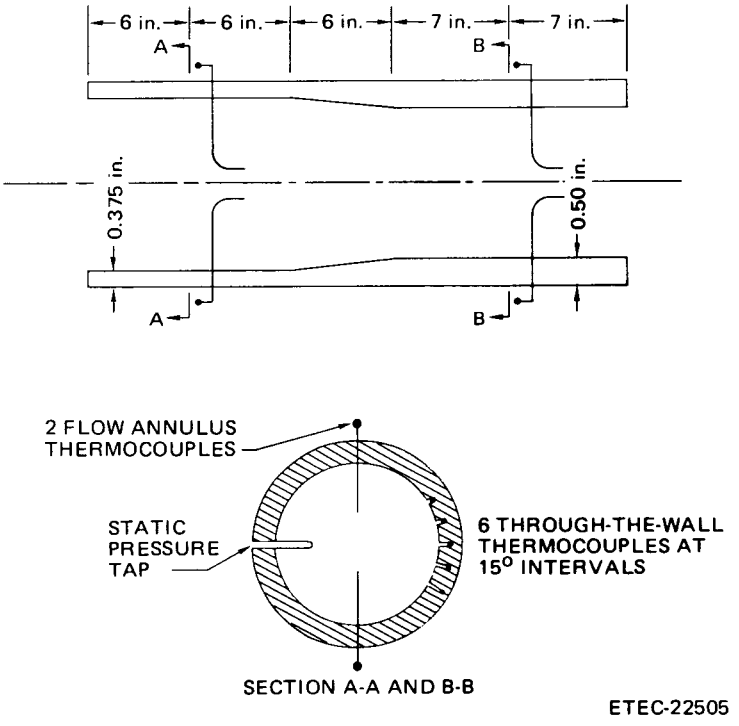

Figure XV-3. Central Section of Type 304 Stainless Steel Centerbody

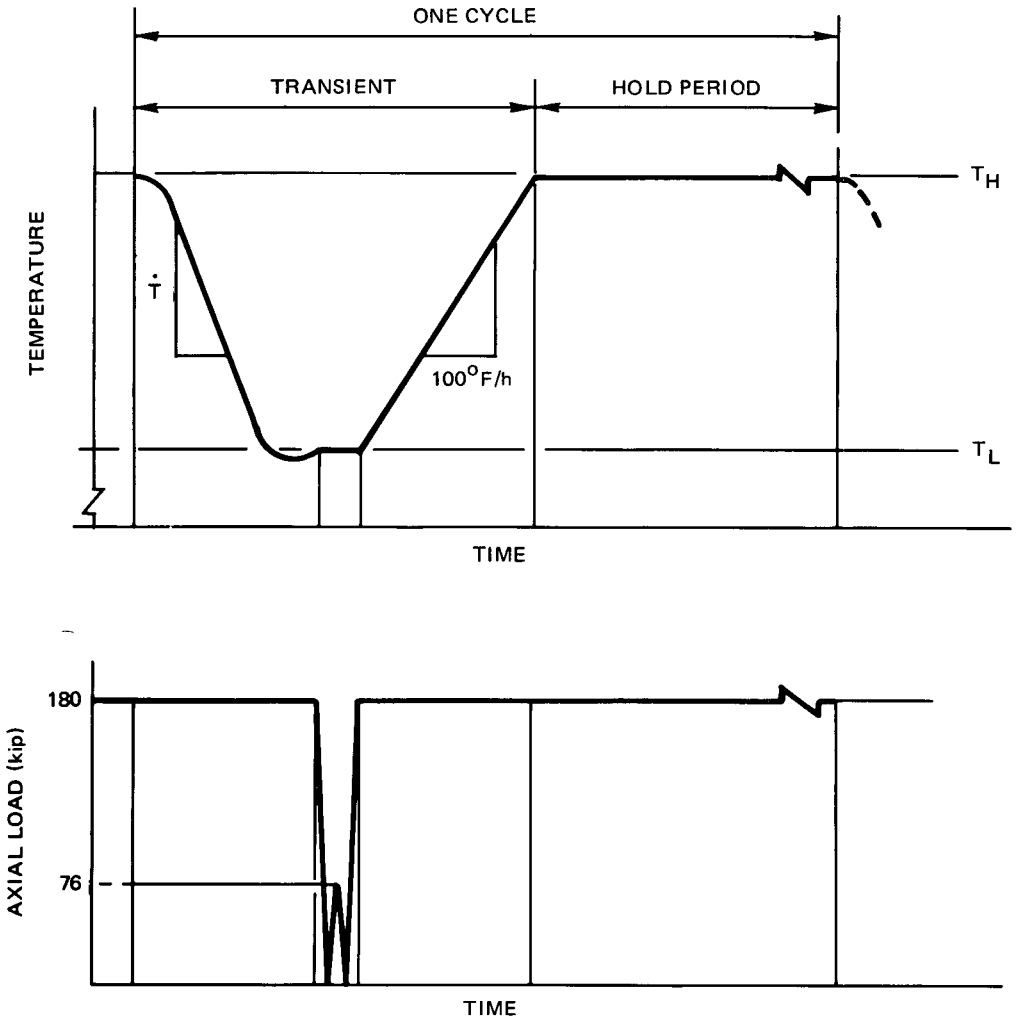

1. DOWNTRANSIENT RATE $\dot{T}$	60°F/s
2. HOLD TEMPERATURE T_H	1100°F
3. LOW-CYCLE TEMPERATURE T_L	500°F
4. HOLD PERIOD	16 h
5. CYCLE DURATION	24 h
6. REMOVAL AND REAPPLICATION OF LOAD EVERY THIRD CYCLE	

Figure XV-4. Test Cycle Histogram

C. TEST RESULTS

Installation of the test article was started on December 4, 1980. Low-temperature strain gages and HITEC capacitive gages were installed adjacent to each other to enable calibration of the capacitive gages. Loads were applied at ambient temperature, 250°F (121°C), and 400°F (204°C), and comparative data obtained for calibration of the capacitive gages yielded good results. The temperature was then increased to 1000°F (538°C) and the capacitive gages were conditioned throughout the load and temperature spectra. By heating the test article to various temperatures and performing load cycles at these temperatures, the stresses locked up in the gage assemblies during installation are removed. Table XV-2 indicates the manner in which nine HITEC Model HTC-DC-025-09 1/4-in. capacitive gages were installed. For some of these gages, the measurement range was doubled by spacing the attachment welds 1/8-in. apart. Some gages were offset to either the positive or negative end of travel before welding to the test article to extend the range.

The test sequence performed to achieve stabilization was:

1) Five load cycles at 275°F (135°C) with a maximum load of 180,000 lb (0.8 MN)
2) Five load cycles at 400°F (204°C) with a maximum load of 180,000 lb (0.8 MN)
3) Five load cycles at 1100°F (593°C) with a maximum load of 180,000 lb (0.8 MN)
4) Cooldown to 275°F (135°C)
5) Five temperature cycles consisting of heatup to 1100°F (593°C) followed by cooldown to 450°F (232°C)
6) Five load cycles at 500°F (260°C) with a maximum load of 180,000 lb (0.8 MN)
7) Five load cycles at 1100°F (593°C) with a maximum load of 180,000 lb (0.8 MN).

TABLE XV-2

GAGE INSTALLATION

GAGE DESCRIPTION	CONFIGURATION	GAGE LENGTH	BIAS	GAGE RANGE
Cap Strain Gage WE-2440, Sect. B, 0 DEG	Axial	1/4-Inch	Unbiased	± 8%
Cap Strain Gage WE-2441, Sect. B, 90 DEG	Axial	1/8-Inch	Negative	0-32%
Cap Strain Gage WE-2442, Sect. B, 180 DEG	Axial	1/4-Inch	Unbiased	± 8%
Cap Strain Gage WE-2443, Sect. B, 270 DEG	Axial	1/8-Inch	Negative	0-32%
Cap Strain Gage WE-2444, Sect. B, 135 DEG	Circumferential	1/4-Inch	Unbiased	± 8%
Cap Strain Gage WE-2445, Sect. B, 315 DEG	Circumferential	1/4-Inch	Positive	- 16-0%
Cap Strain Gage WE-2446, Sect. C, 0 DEG	Axial	1/4-Inch	Unbiased	± 8%
Cap Strain Gage WE-2447, Sect. C, 180 DEG	Axial	1/8-Inch	Negative	0-32%
Cap Strain Gage WE-2448, Sect. C, 135 DEG	Circumferential	1/4-Inch	Positive	- 16-0%

Typical examples of the strain gage data obtained are shown in Figures XV-5 and -6.

On January 23, the test article was heated to 1000°F (538°C) and a load of 180,000 lb (0.80 MN) was applied to verify the settings of the load maintainer and actuators and to assure that any induced bending moment was within the allowable tolerance. Analysis of the data indicated that the test section appeared to have yielded as shown in Figure XV-7. These data were discussed with ORNL, who had expressed a preference for limiting the load to 100,000 lb (0.44 MN) during strain gage conditioning since they anticipated some yield at 1000°F (538°C). However, ORNL agreed that, given the complete load-temperature history, they could account for this event in their analysis. ORNL agreed to proceed with testing. After five cycles at 1100°F (593°C), the load was removed and the test article was allowed to cool to 275°F (135°C). Temperature cycling was then achieved by heating the test article to 1100°F (293°C), then cooling to 400°F (204°C) for a total of five cycles. Figure XV-8 is a typical plot of the temperature obtained.

The apparent strain correction factor was determined by performing a least-squares curve fit of Cycle 5 strain gage data vs temperature data. It can be seen from Figure XV-9 that the temperature difference between the test article and the HITEC gage rod was within ±5°F. The effect on the apparent strain correction at this level is negligible. Figure XV-10 is a plot of apparent strain data from the five temperature cycles during cooldown with no load applied. This plot demonstrates the repeatability obtained and is typical of the data obtained during cooldown from 1100°F (593°C). The final steps in the stabilization process were load cycles performed at both 500°F (260°C) and 1100°F (593°C). Figures XV-11 and XV-12 are typical plots of data obtained during these tests.

Table XV-3 lists the anomalies observed during the gage conditioning procedure and illustrates that Gages WE-2442 and WE-2443 consistently had problems. The problems were found to be originating in the power supplies and signal conditioner mode cards. New cards were installed, and a second series of cycling tests was performed to verify the performance of these gages.

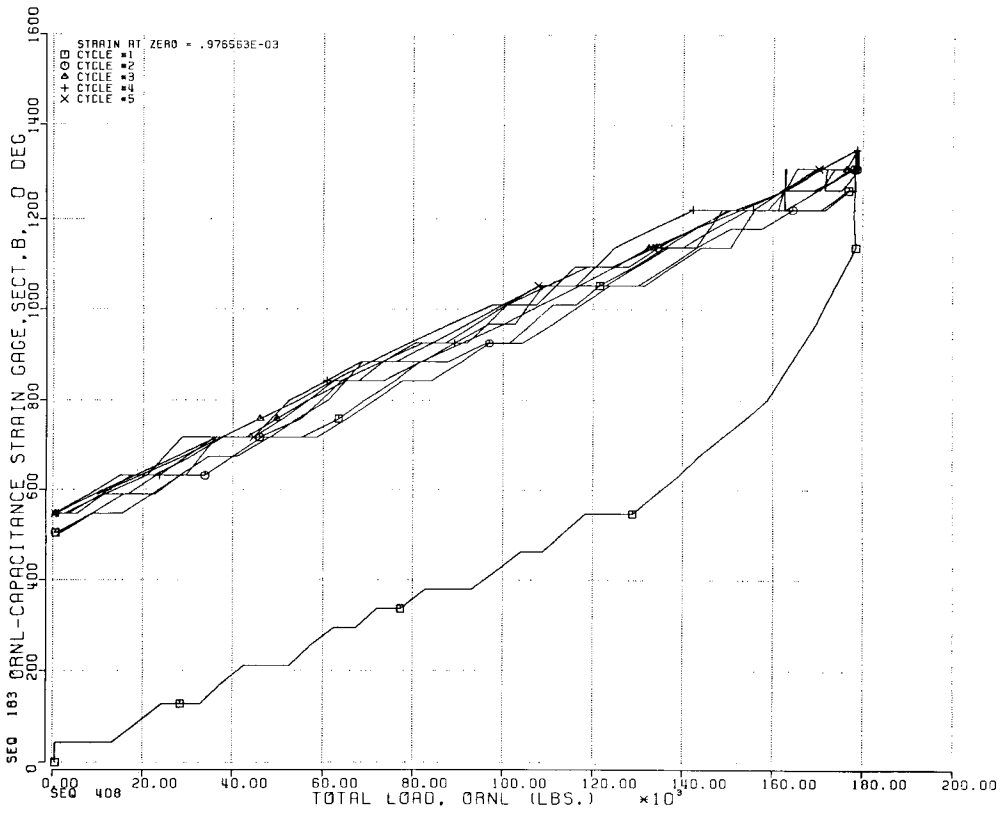

Figure XV-5. ORNL Load Cycles at 275°F

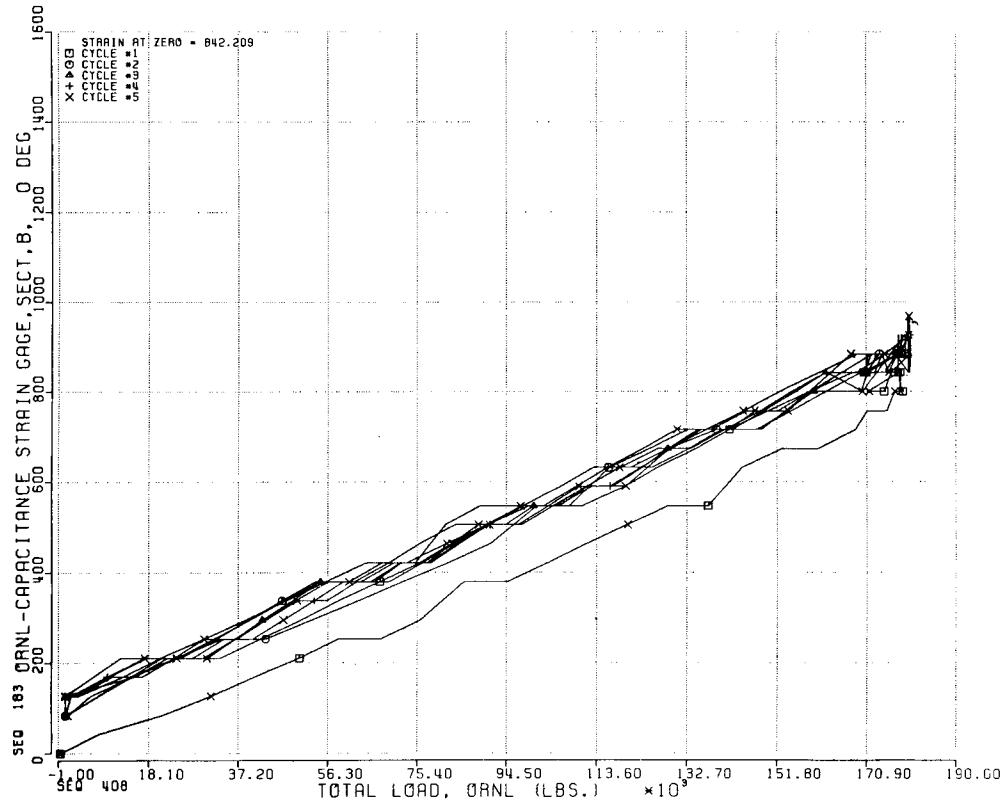

Figure XV-6. ORNL Load Cycles at 400°F

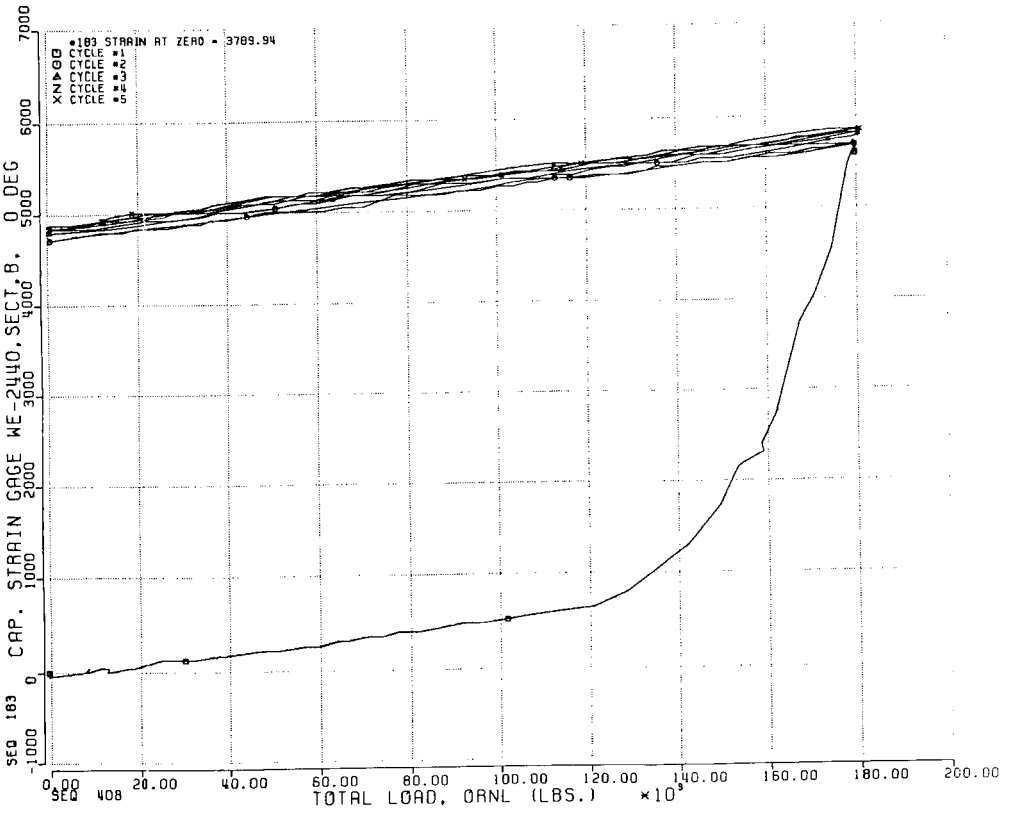

Figure XV-7. ORNL Load Cycles at 1100°F (January 13, 1981, 1:26-2:10 p.m.)

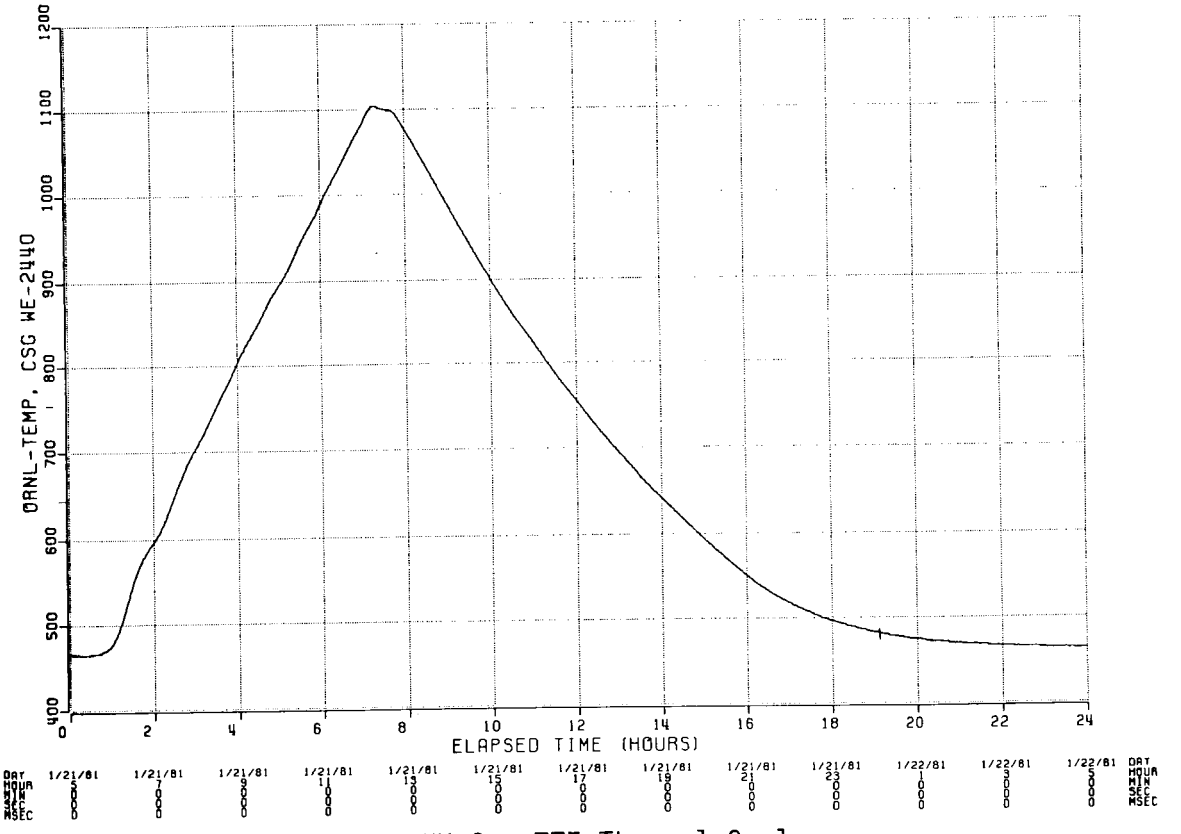

Figure XV-8. TTF Thermal Cycles

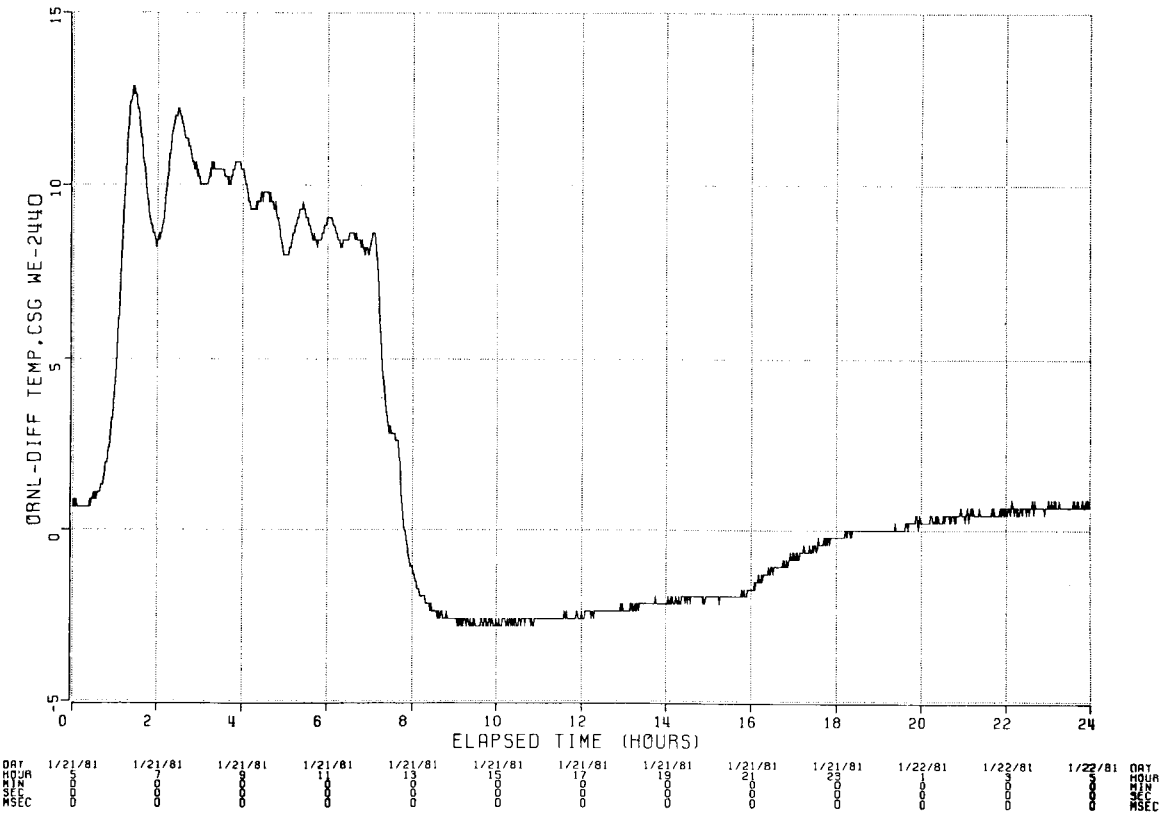

Figure XV-9. TTF Thermal Cycles

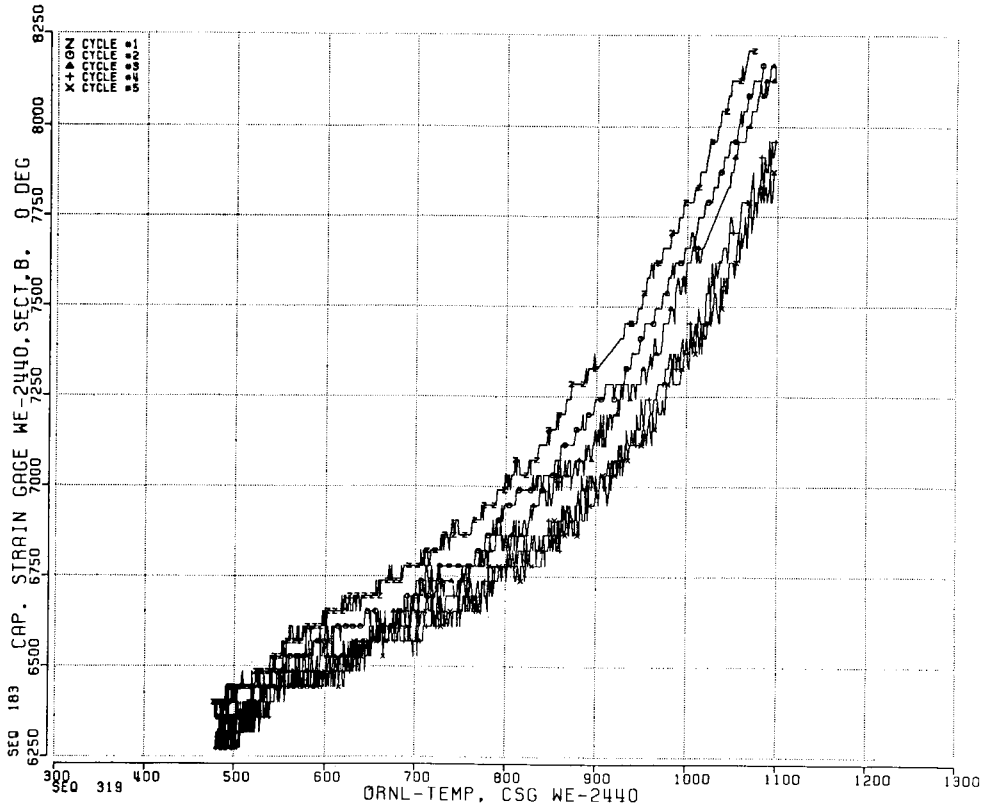

Figure XV-10. ORNL Thermal Cycles

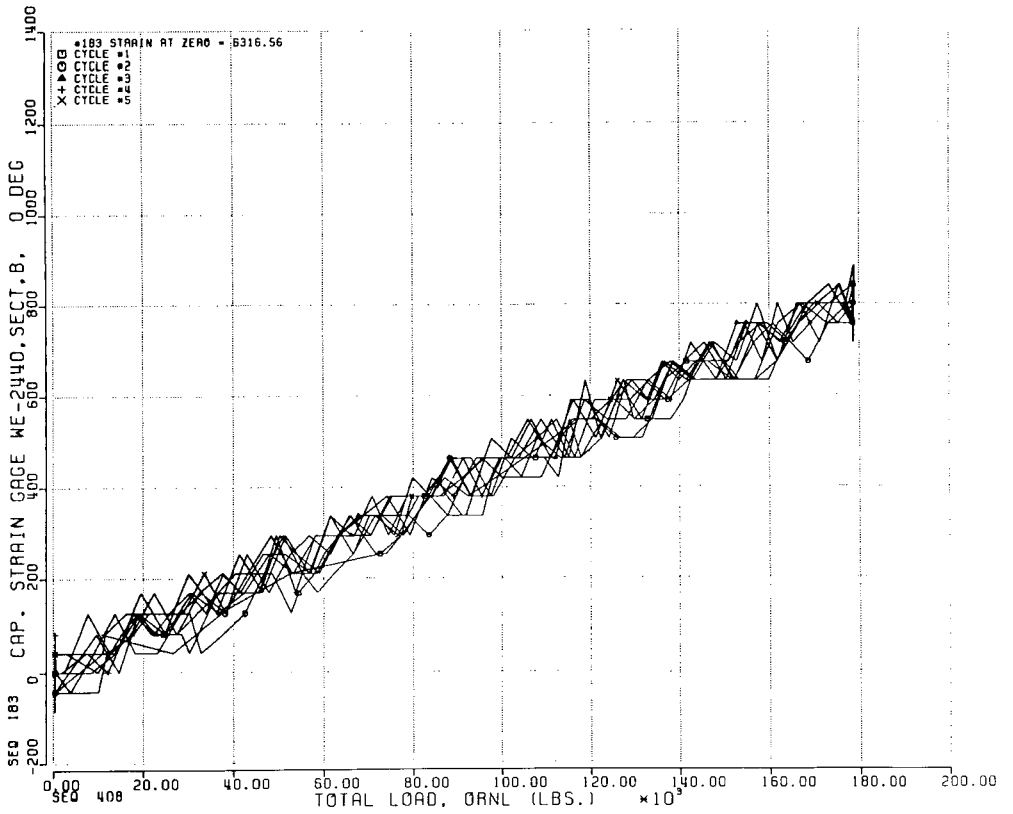

Figure XV-11. ORNL Load Cycles at 500°F

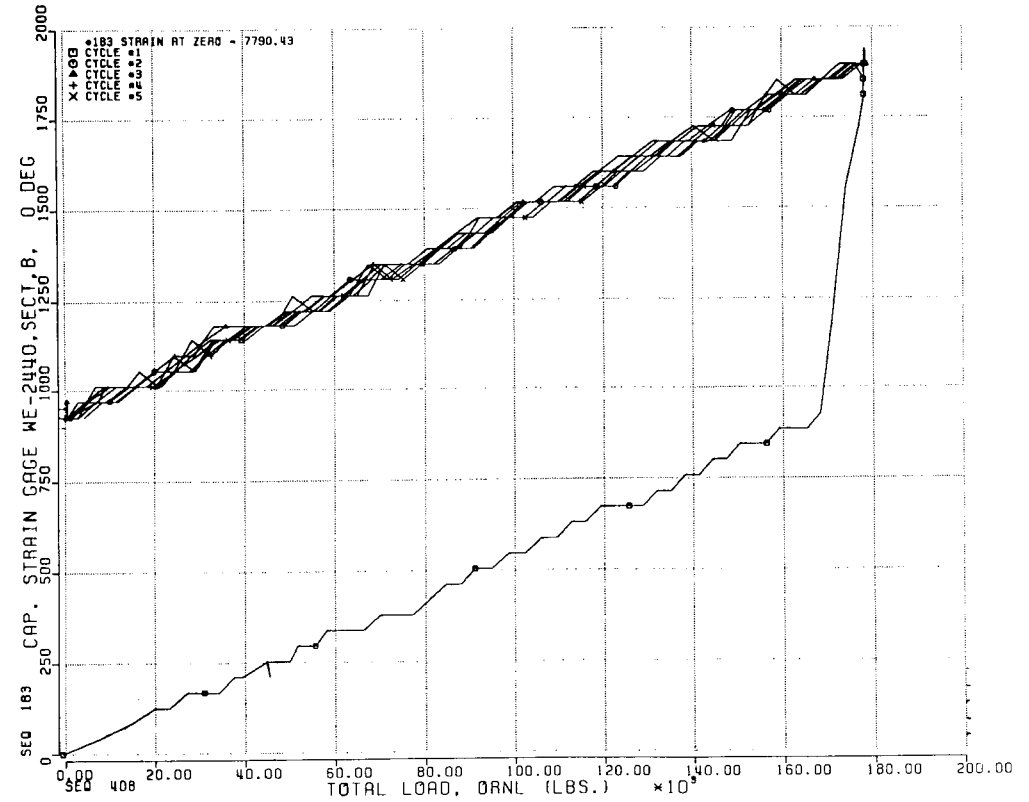

Figure XV-12. ORNL Load Cycles at 1100°F

TABLE XV-3

ANOMALOUS DATA

Test	Gage	Comment
275°F Load Cycles	WE-2445	Positive response to load, while corresponding resist. gage responds negatively. Magnitude OK.
	WE-2447	No response to load.
400°F Load Cycles	No Problems	
1100°F Load Cycles	WE-2443	Gage drifted positively by 120,000 microstrain during five cycles.
	WE-2446	Large shifts in output (~600 ME) between Cycles 3 and 4.
Temperature Cycles	WE-2442	Large change in shape of curve between Cycles 2 and 3.
	WE-2443	Shape of curve shifting throughout all five cycles.
500°F Load Cycles	WE-2442	No response to load
1100°F Load Cycles	WE-2442	Responded to load, but large drift throughout test.

1) Two temperature cycles — Heatup to 1100°F (593°C) followed by cooldown to 450°F (232°C)
2) Two load cycles at 1100°F (593°C) with a maximum load of 100,000 lb (0.44 MN).

The results were still unsatisfactory, and further changes were made in the signal conditioning equipment. Two more load cycles at 1100°F (593°C) up to a maximum of 100,000 lb (0.44 MN) were followed by cooldown to 400°F (204°C). All gages performed satisfactorily, and the apparent strain and temperature corrections

were determined. These values were used in the following data reduction equation for HITEC gages:

$$S = B*C + A - F(T) - (\alpha * \Delta T)$$

where

S = strain gage output corrected for apparent strain and differential temperature effects

B = slope coefficients to convert counts to uncorrected gage output in microstrain

C = strain gage counts as stored on data tape

A = intercept coefficient in microstrain

F(T) = apparent strain correction in microstrain, up to sixth-order function of temperature (F)

α = mean coefficient of thermal expansion for stainless steel = 9.7 microstrain/^{o}F

ΔT = differential temperature between pipe surface and HITEC compensating rod (^{o}F).

First- through sixth-order least-squares curve fits were made for each capacitive strain gage; from the curve that best fit the data over the required temperature range 500^{o}F (260^{o}C) to 1100^{o}F (593^{o}C), the apparent strain corrections were obtained as shown in Table XV-4.

Figure XV-13 is a typical plot of data and best-fit line using data from the Cycle 5 cooldown. This cycle was used for all gages except WE-2442 and WE-2443. Data for these gages were taken during the final cooldown on February 12, 1981.

As a final check that the apparent strain correction was valid, data from the five temperature cycles were processed using the equation shown above. Figure XV-14 is a typical plot of the results obtained during both increasing and decreasing temperature phases.

TABLE XV-4

ORNL THERMAL RATCHETTING TEST
APPARENT STRAIN EQUATION COEFFICIENTS

$$(F(T) = A_0 + A_1 * T + A_2 * T^2 + A_3 * T^3 + A_4 * T^4 + A_5 * T^5)$$

Gage Identification	A_0	A_1	A_2	A_3	A_4	A_5
WE-2440	2778.875	14.83378	- .2060015 E-1	.1033400 E-4		
WE-2441	-75147.30	570.0233	- .1565884	.2093907 E-2	- .1363777 E-5	.3452633 E-9
WE-2442	-1139.879	8.242205	- .1491375 E-1	.6970417 E-5		
WE-2443	4085.054	6.208152	- .1686036 E-1	.7511185 E-5		
WE-2444	-7683.208	29.66277	- .5834512 E-1	.5046738 E-4	- .1631277 E-7	
WE-2445	-10726.05	52.06448	- .1089189	.1008528 E-3	- .3439070 E-7	
WE-2446	2046.797	2.891313	.1335055 E-2			
WE-2447	79595.05	- 606.6965	1.820509	-.2700351 E-2	.1967924 E-5	- .5645431 E-9
WE-2448	-14151.71	113.3261	- .3562362	.5370617 E-3	- .3873296 E-6	.1078559 E-9

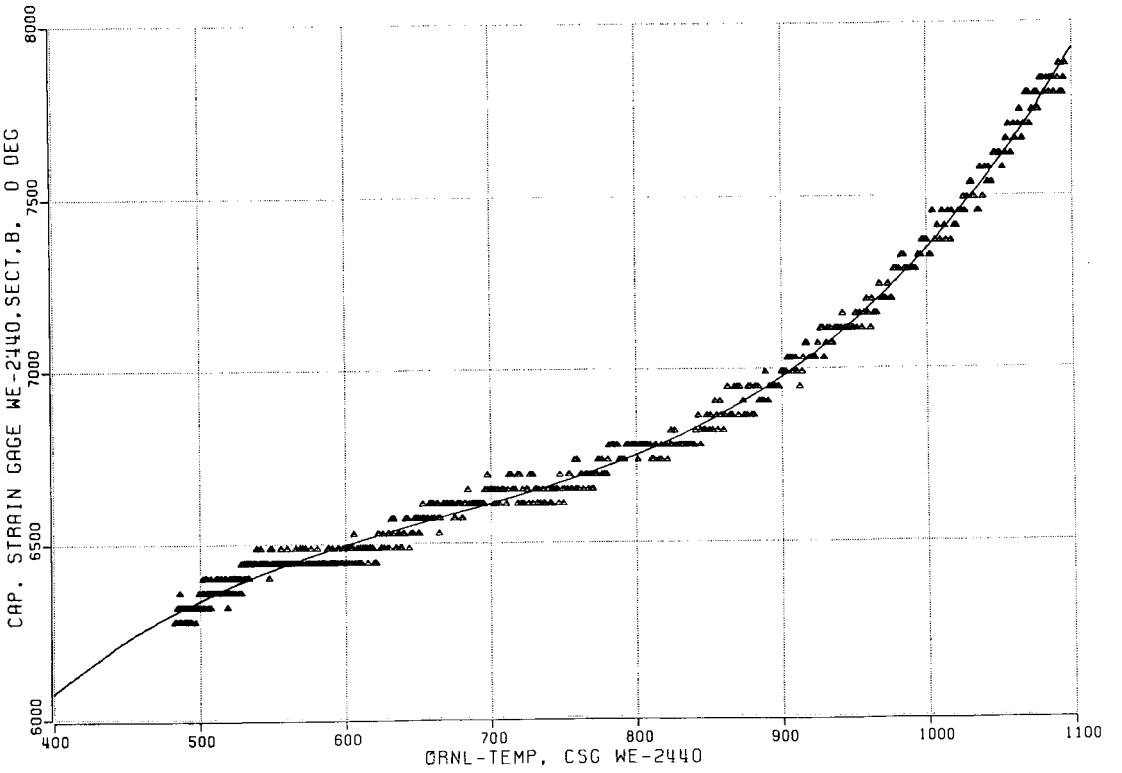

Figure XV-13. TTF ORNL Thermal Cycle 5
(January 21, 1981, 12:45-12 p.m.)

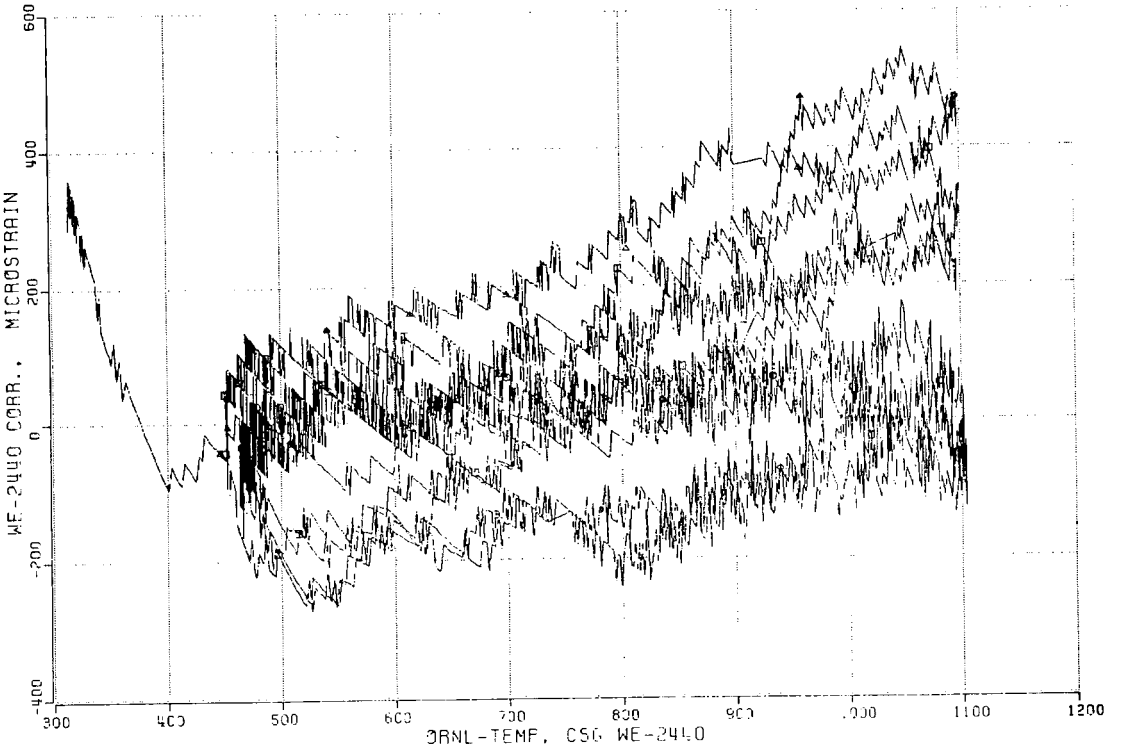

Figure XV-14. ORNL Temperature Cycles with Corrections

On February 17, 1981, testing was started with a downtransient in accordance with Test Procedure TP-42-PA-012. Heatup was initiated so that the transient could be performed at 8 a.m., thus allowing for one-shift operation on a 24-h cycle. The first downtransient was completed on February 18 and a second transient was performed on February 19. Three transients were completed, followed by a load cycle in accordance with the histogram. The data were reviewed and, since it looked good, a second series of three cycles was performed, followed by a load cycle and cooldown to ambient temperature in accordance with the histogram. During the sixth cycle high-temperature hold period, there was a facility power dip that resulted in a load decay from 180,000 to 163,000 lb (0.80 to 0.72 MN) over a period of 3 h. This event was reported to ORNL, and they agreed to completion of the sixth cycle as scheduled. Examination of the data at this time showed a maximum accumulated total strain of about 2%, as shown in Figure XV-15.

After cooldown, the test-section diameter was measured at several locations; the results are shown in Table XV-5. A dye-penetrant examination of the outside surface showed no evidence of cracking. Soil tab data were taken using an instrument supplied by ORNL. Comparison of this data with the strain gage data showed very good agreement. Based on the results of this examination, which were transmitted to ORNL, authorization was obtained to proceed with a second series of six cycles. ORNL also agreed that if using their instrument with the soil tabs in a circumferential direction might break off the tabs, we could limit the measurements to the axial direction.

Heatup for Cycle 7 was started on March 4, but because of another facility power dip, the heaup was restarted on March 5 in order to maintain the 24-h cycle schedule. The downtransient was performed on March 6; then the test was put on hold with the test article at 500^{o}F (260^{o}C) while new transducers were installed for the flow measurements. Cycle 9 was completed on March 11, at which time the data indicated a maximum accumulated strain of $\sim$3%. The program was again put on hold while a noise problem on the new transducers was resolved. This was accomplished by March 13, and heatup for Cycle 10 was initiated on March 16. Cycle 12 was completed by March 19, and cooldown was started for mechanical inspection in accordance with the histogram. Analysis of the data

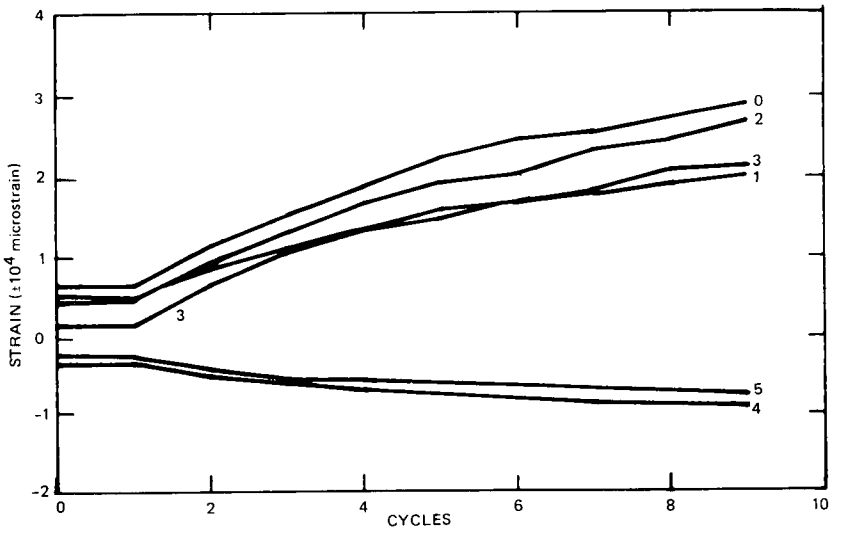

Figure XV-15. ORNL Thermal Ratchetting Test — Section B Strain Gages

TABLE XV-5

OUTSIDE DIAMETER MEASUREMENTS

CYCLE NO. / DATE	DIAMETER	SECTION a	b	c	d	e	f
6 / 3-2-81	HORIZ	8.175	8.176	8.171	8.178	8.182	8.205
	VERT	8.172	8.175	–	8.187	8.187	8.196
12 / 3-23-81	HORIZ	8.167	8.156	8.155	8.164	8.170	8.180
	VERT	8.175	8.175	–	8.172	8.169	8.175
15 / 4-7-81	HORIZ	8.169	8.153	8.154	8.163	8.169	8.200
	VERT	8.188	8.177	–	8.175	8.172	8.186
18 / 4-21-81	HORIZ	8.163	8.149	8.153	8.161	8.164	8.173
	VERT	8.182	8.175	–	8.167	8.167	8.177
	HORIZ						
	VERT						

NOTE: SECTION C VERTICAL MEASUREMENT AND CENTER-SECTION MEASUREMENTS RESTRICTED BY TEST INSTRUMENTATION

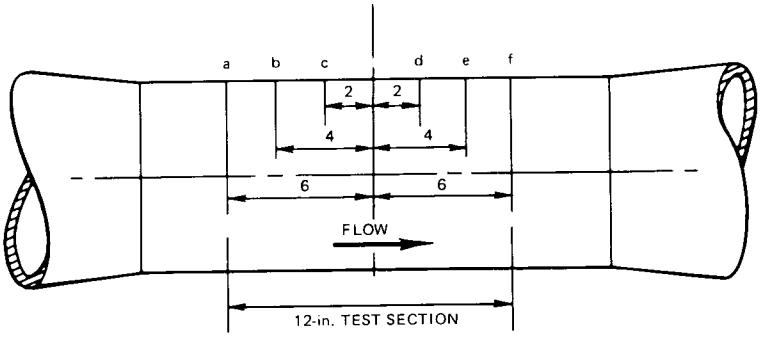

revealed a temperature variation along the test article from 1100°F (593°C) to 850°F (454°C), which was found to be the result of loss of one heating element. This element was replaced. On March 23, the outside diameter of the test article was measured and dye penetrant was applied. Circumferential cracks were observed in the last 2 in. (5.08 cm) of the downstream end on the right side looking from the inlet and near the center of the test section on the opposite side. The cracks are shown in Figures XV-16 and XV-17. Helium leak testing produced no evidence of through-cracks.

On March 27, the test article was heated to 500°F (260°C), with no load applied, to permit checkout of the oven and temperature alarm system. On March 31, heatup for Cycle 13 was started, and three cycles were completed by April 3. Cooldown for mechanical inspection was initiated immediately after the load test and measurements were taken, and dye-penetrant inspection was completed by April 8. The results indicated a deepening of the cracks, and an area of $\sim$1 in.^{2} was ground down a few thousandths of an inch and polished. A repeat of the dye-penetrant test indicated the cracks were quite deep, but a helium leak test still showed no evidence of through-cracking. The data showed that the maximum cumulative strain was still below 4%. ORNL authorized another series of three cycles using the same load. This series was completed by April 17, and cooldown was started for inspection. Indications were that the cracks had continued to grow but still showed no evidence of through-cracking. At least one strain gage had reached 5% accumulated strain. A decision was made to perform six cycles before the next examination. Heatup for Cycle 19 was started on April 27. Failure occurred, as shown in Figure XV-18, after 1 h in the high-temperature creep hold period. The fracture appeared to be typical of a high-temperature low-cycle fatigue break. The test article was removed and the test section was sent to ORNL for analysis.

On June 1, 1981, a new specimen consisting of a 30-in. (0.76 m) section of 0.375-in. (0.95-cm) wall Type 304 stainless steel pipe was received from ORNL. The original extension spools were cleaned up and weld-prepped to accommodate this 30-in. (0.76-m) section and maintain the original overall length. Sleeves were fabricated and installed to protect the new welds from direct effects of the

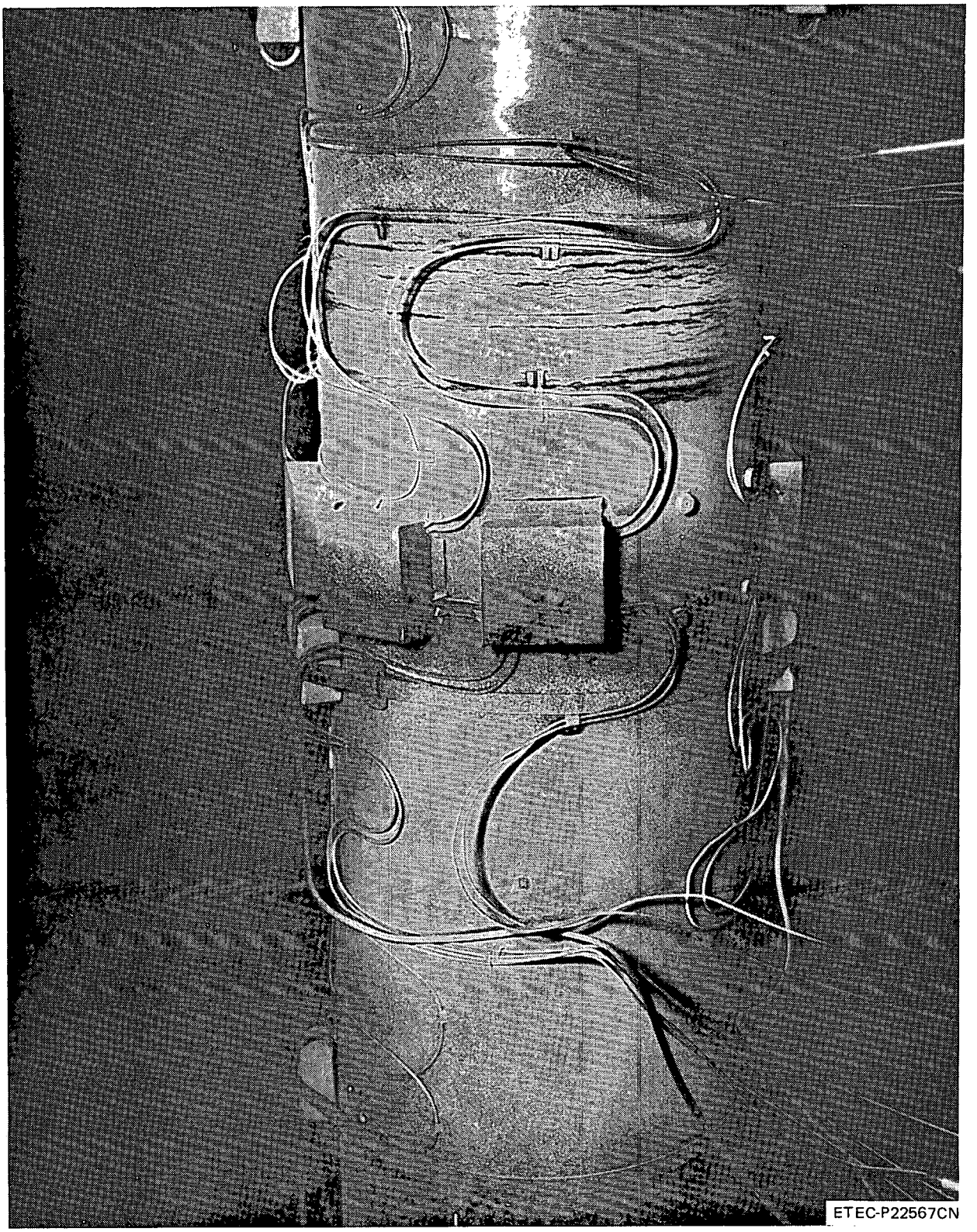

Figure XV-16. Onset of Surface Cracking, Right Side, Viewed from Inlet

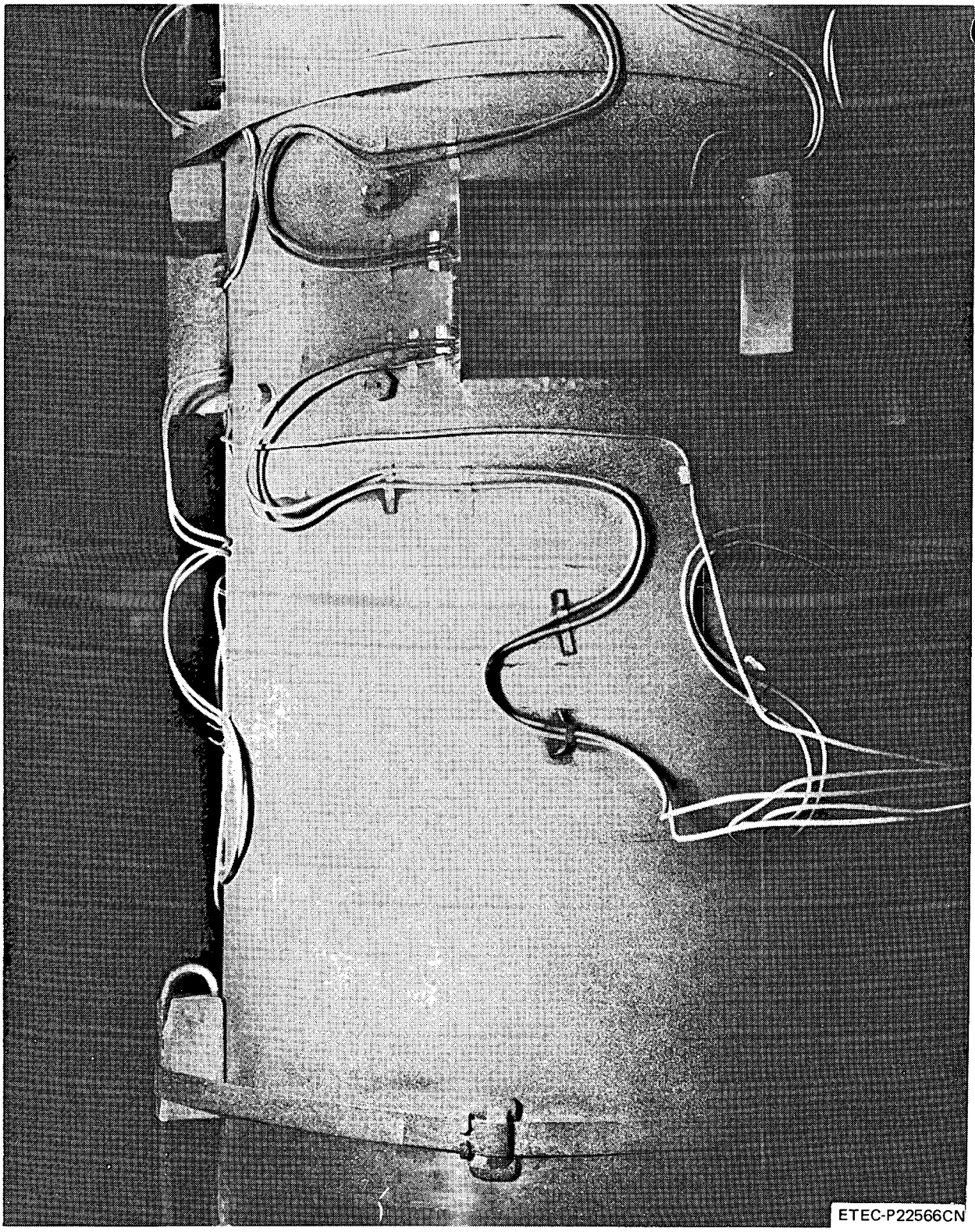

Figure XV-17. Onset of Surface Cracking, Left Side, Viewed from Inlet

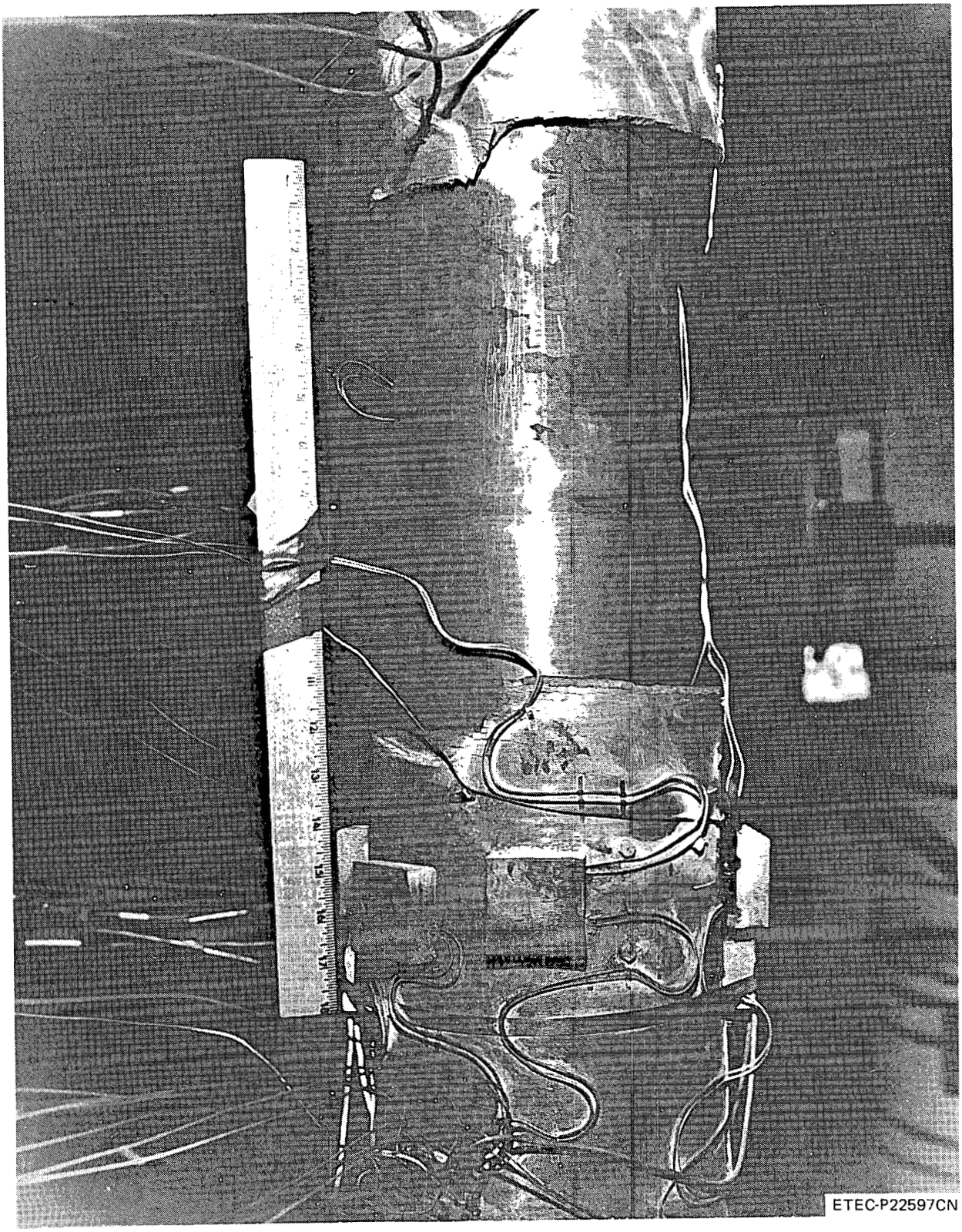

Figure XV-18. Failed Test Article

transient. Figure XV-19 illustrates the composition of Test Article 2. Installation of this assembly was initiated on July 14, 1981, and by August 14, installation and checkout of the instrumentation was completed. Figure XV-20 shows the arrangement of the available capacitive strain gages that had been agreed to by ORNL. They further requested that a modified procedure be used to condition these gages.

The modified procedure consisted of the following steps:

1) Bake out at 275°F (135°C) for 24 h.
2) Perform five load cycles at 275°F (135°C).
3) Perform five load cycles at 1100°F (593°C).

The load limitation requested for stabilization load cycles was 75,000 lb (0.33 MN) total load. During the initial load cycles at 275°F (135°C), the load was allowed to go to the full test load of 180,000 lb (0.80 MN). There was evidence that the specimen yielded, and ORNL was advised. Data will be made available for factoring into the analysis. Strain gage conditioning was completed by September 12, when heatup to 1100°F (593°C) was started, and as soon as the temperature had stabilized at 1100°F (593°C), the first downtransient was performed. Testing then continued in accordance with the histogram shown in Figure XV-4. After the third cycle, the load was cycled as a check on the calibration of the capacitive strain gages. The gages seemed to be functioning as expected and cycling was resumed. The fifth cycle was completed on September 18, and the test article was maintained at 500°F (260°C) until September 20, when heatup was initiated for the sixth cycle.

After completing the sixth cycle, the load was again cycled in accordance with the test histogram. Three more cycles were performed, followed by another load cycle; then the test article was held at 500°F (260°C) from September 25 to September 28. Starting on September 28, Cycles 10, 11, and 12 were completed and a load cycle was performed; then Cycle 13 was completed. The test article was held at 500°F (260°C) at the end of Cycle 13 until October 4 at 10:03 a.m., when heatup was started for Cycle 14. At 1:56 a.m. on October 5, the load cylinders

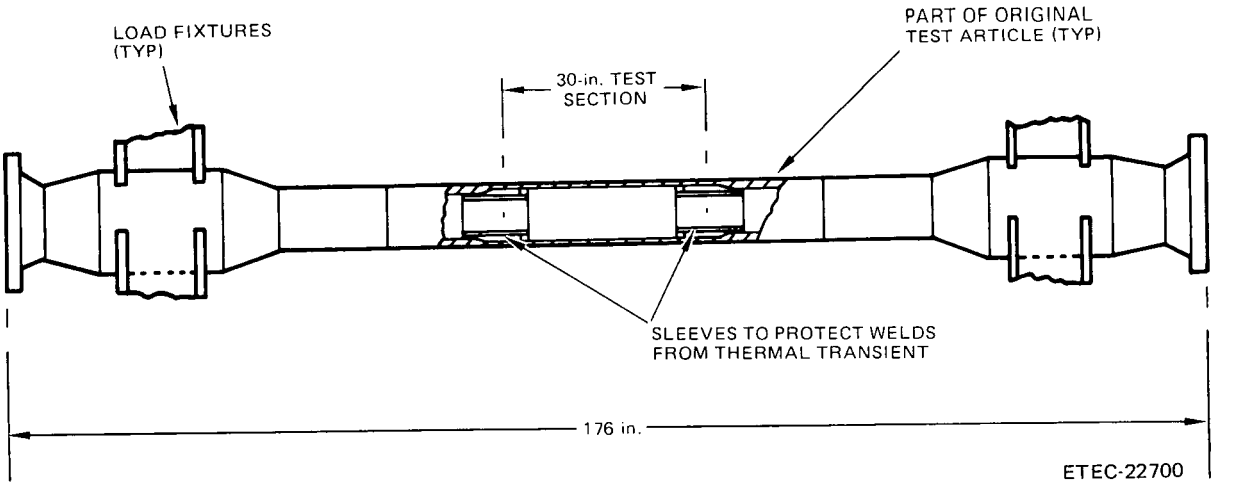

Figure XV-19. Test Article 2

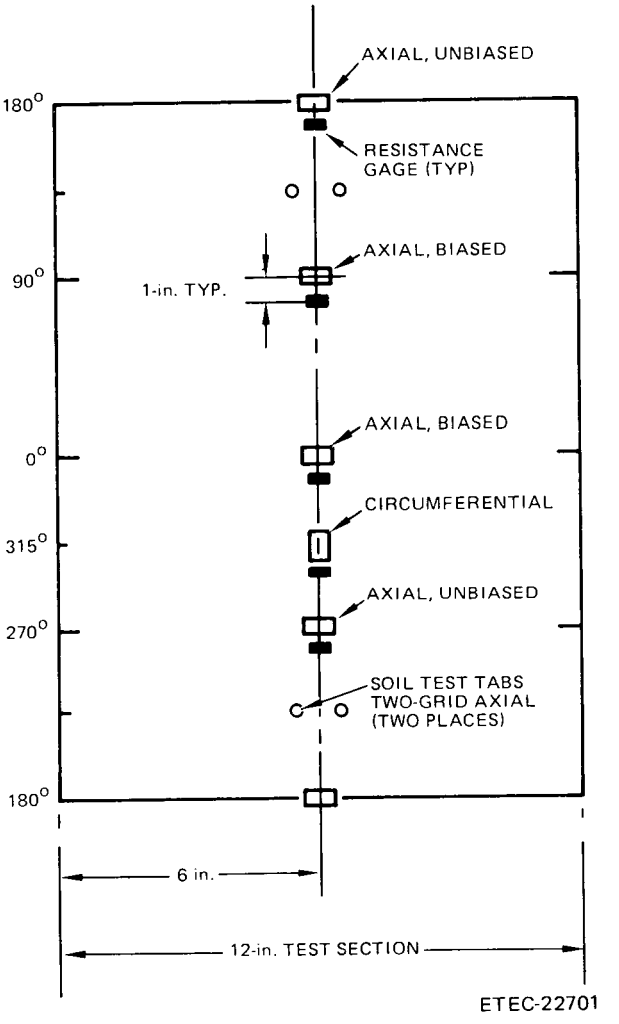

Figure XV-20. Strain-Measuring Instrumentation

extended fully, indicating a failure. Cooldown was started immediately and by October 6, the oven had been removed. The failure was found to be in the extension spool on the upstream end of the test section. This spool was part of the original test article supplied by ORNL and had been exposed to a total of 32 transient cycles. The fracture looked similar to the fracture in the original test section. Dye penetrant was applied to both upstream and downstream spools and the center test section. There was no evidence of cracking in the test section, but both spools had well-defined cracks similar to those experience in the original test article before failure. The test article was removed from the facility piping, and replacement spools have been fabricated and will be welded to the test section to allow testing to continue to failure.

Plots for the completed cycles have been transmitted to ORNL, along with a duplicate tape of the test data, to enable an analysis of the spool failure. Data from thermocouples mounted in the vicinity of the break are recorded on the tape and should provide information on what level of transient was experienced at the location of the break.

XVI. SODIUM-TO-GAS LEAK DETECTION

K. A. DAVIS

A. INTRODUCTION

During recent years, a number of test programs have been performed at ETEC to enable the selection of candidate leak detectors for LMFBR applications. The tests were designed to evaluate the basic functional capabilities of these detectors. In 1977, two aerosol-type detectors, which appeared qualified, were placed in a long-term test in a practical operating plant environment to provide performance data under these conditions. These data were needed to enable the design of sodium leak detection systems, writing procurement specifications, and writing operating guidelines.

The present test articles are sodium ionization-type aerosol detectors, one from each of two manufacturers, and plugging filter-type aerosol detectors, two from one manufacturer.

B. TEST DESCRIPTION

1. Facility

Since the EBR-II is an operating LMFBR plant and could provide the desired test conditions, it was selected as the site for the tests. The detectors monitor the gas in the upper plenum region of two sodium-heated steam generators. A diagram of the gas flow circuit through the detectors is presented in Figure XVI-1. Each of the "1/4-in." stainless steel gas lines from the steam generators to the detectors is 46 m (150 ft) long. Signals from the four detectors are recorded continuously by a multipoint strip-chart recorder. The filter analyzers are used to determine the aerosol concentration and chemical composition of a sample of the gas that passes through the detectors (test articles). These filters have the same characteristics as those used in the plugging filter aerosol detectors.

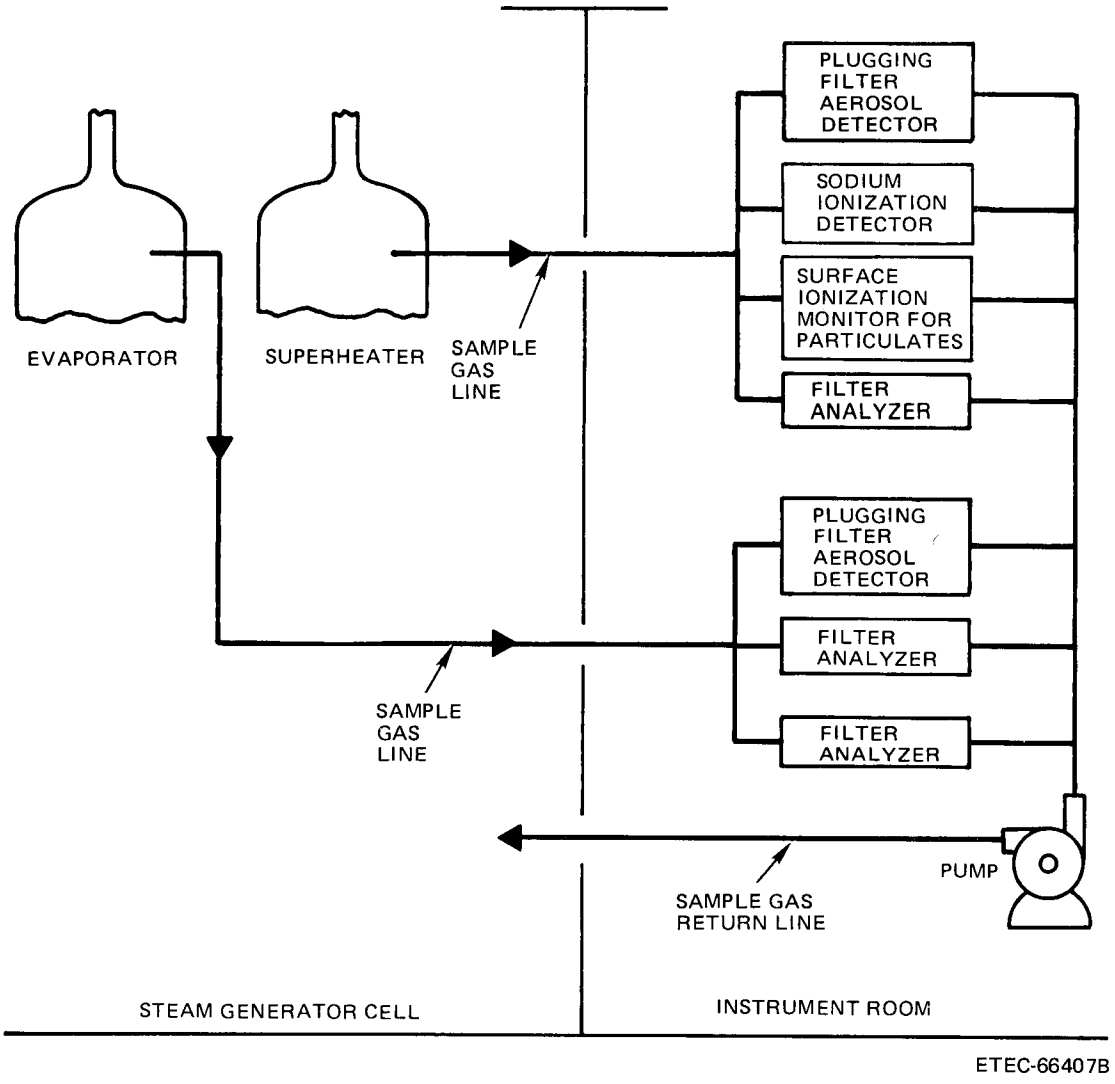

Figure XVI-1. Diagram of Gas Flow

2. Test Articles

The plugging filter aerosol detectors (PFAD) were designed by the Atomics International Division of the Energy Systems Group of Rockwell International and were manufactured by Controls for Industry. The detector consists of a gas flow system in which sample gas flows through a filter disc, across which is a differential pressure transducer. It then flows on through a valve and flowmeter. The filter is a 47-mm (1.85-in.), 0.8-μm pore size disc. Until March 1980, these discs were composed of a copolymer of acrylonitrile and polyvinyl chloride. Since then, filters composed of mixed esters of cellulose have been used because these provide lower "blank" values of sodium. In operation, a constant gas flow of 83×10^{-6} m^3/s (305 $in.^3/min$) is established, and in the absence of any particulates becoming entrained on the filter, the pressure across the filter remains constant. Any particulates in the gas stream cause plugging of the filter, and this is indicated by a differential pressure rise. An output signal for recording is provided. The filter disc is easily removable for analysis to identify the deposited material.

The sodium ionization detector (SID) was developed and manufactured by the Nuclear Instrumentation and Control Department of Westinghouse Electric Corporation for use as a sodium leak detector. The detector consists of a sensor and an "electronics module" that provides sensor power and the current measuring instrumentation. The sensor consists of a hot filament and a plate enclosed in a housing through which sample gas is passed. The plate is electrically charged negative relative to the filament so that in the absence of sodium (or any other easily ionizable material) arriving at the filament, the current is negligible. Upon contacting the filament, however, sodium is ionized and the sodium ions flowing to the plate result in a small but easily detectable current. The sensitivity of the detector is quoted by the manufacturer as approximately "3 nanoamperes per nanogram of sodium per cm^3 of gas." The detector provides a recorder signal output and high and low alarms.

The surface ionization monitor for particulates (SIMP) is an instrument developed and manufactured by Extranuclear Laboratories Inc. for air pollution monitoring. This instrument is similar in operating principle to the sodium ionization detector described above. This similarity led to adding this detector to the various sodium leak detector testing programs.

3. Test Method

Sample gas at a rate of 15 l/min is drawn continuously through each of the two lines from the steam generators and is distributed to each of the instruments according to the individual instrument requirements. Each instrument is monitored and adjusted as needed according to a fixed schedule to ensure proper operation.

The SID requires occasional filament current adjustments as the filament resistance increases with age. The only other operational activities are verification that the sample gas is flowing through the sensor and an operational verification at 5-month intervals by injecting a small quantity of smoke into the gas sample stream. The SIMP does not require any filament adjustment. Otherwise, the operational attention needed is the same as that for the SID. The PFADs require periodic filter replacement. At the beginning of this test program, the filters were exposed to the sample gas for periods of 1 week. Each exposed filter was sent to ETEC for examination consisting of visual inspection, weight gain, and analysis for sodium (and other materials when the need was evident). Later, the filter exposure time was increased to 2 weeks, and then in April 1979, the time was increased to 4 weeks. Strip-chart recordings of the SID and SIMP ion currents and the two PFADs' differential pressure as a function of time are transmitted to ETEC weekly.

In addition to the filters in the PFADs, three additional filters connected as shown in Figure XVI-1 are used to provide additional information on aerosols in the sample gas and on the use of filters for analysis.

All of the data obtained are reported monthly.

4. Test Results

This test continues to provide a considerable amount of useful data on the practical aspects of operating sodium aerosol-type leak detectors in a typical sodium heat transfer system. The test of the SID and SIMP has shown the nature of their respective background signals to be expected during periods of normal system operation and during periods of various levels of operating disturbances and plant maintenance activities. Such information is of value in setting alarm limits. The tests have also provided data on the effect of filament aging, the need for filament current adjustment and the consequent signal disturbance, and the filament life expectancy. The performances of the SID and SIMP are similar. The significance is in the filament life expectancy. The last three SID filaments operated 7926, 6648, and 5448 h, respectively. In this test of the SIMP, the original filament is still operating. It has operated 15,744 h at EBR-II in addition to several hundred hours at ETEC prior to its transfer to EBR-II. The experiment on the different types of filter material shows that the millipore filters made of mixed esters of cellulose are satisfactory and enable a better analytical resolution (lower blank value) than the Gelman filters, which are composed of a copolymer of acrylonitrile and polyvinyl chloride. An experiment on the effect of pore size on the differential pressure showed that the differential pressure for pores of 0.45 μm was 2.35 times that of pores of 0.80-μm size. When the SID filament failed at about mid-year, the failure was preceded by erratic operation for several days. This characteristic had been observed previously. A test was performed to determine the effect of power failure on the SID. The results showed that the ion current overshoot was no more than 38% upon restoration of power and that recovery occurs within 15 min or less. This was of concern since there have been instances in which disturbances have caused very long (many hours') recovery time.

This effort is being continued to provide a longer evaluation interval and to provide more data to improve the statistical aspects of the data.

XVII. INTERMEDIATE-SIZE INDUCER PUMP-II

W. H. MUNYON

A. INTRODUCTION

The Intermediate-Size Sodium Pump-II was tested at the Energy Technology Engineering Center (ETEC). Installation of the pump into the pump tank began February 19, 1981. Sodium testing was completed and sodium drained from the system on August 30, 1981.

The purpose of this test program was to demonstrate the applicability of the pump inducer concept to large, high-temperature sodium pumps.

The test program included steady-state performance tests over wide ranges of speed, flow, and sodium temperature. Also included was a cavitation test to establish the critical net positive suction head (NPSH). Endurance tests at 155% of the critical NPSH at 950^{o}F and at an NPSH of 60 ft at 1050^{o}F were also performed.

The test article was a modified Fast Flux Test Facility (FFTF) primary pump. The modification consisted of replacing the standard impeller with an integral inducer-impeller combination. Other components to adapt the new impeller assembly to the existing FFTF pump were included.

The ISIP-II pump was tested at the Sodium Pump Test Facility (SPTF) during FY 1981. An unmodified FFTF pump was tested during 1977 at the same ETEC facility.

B. TEST DESCRIPTION

1. Facility

The primary function of the SPTF is to test liquid sodium pumps. The test pump is installed in a pump tank that is part of a piping loop housed within a

test building. The pump is controlled remotely from a control building. The flowing sodium loop is serviced by another loop used to control the sodium temperature. SPTF is also provided with tanks and piping for adding and removing sodium. Various other systems support the operation of the sodium loop by providing purification and sampling capability, cover gas control, and temperature control. Assembly, disassembly, and cleaning of the test pump are done in the Component Handling and Cleaning Facility (CHCF) located west of the SPTF. The stiffleg derrick at the CHCF is used for handling the test pump and other components. Figure XVII-1 shows the CHCF and stiffleg derrick in relation to the SPTF.

Descriptions of the major components and systems at the SPTF are presented in the following paragraphs.

a. Main Flow Loop System

The main flow loop (MFL) system includes the main flow loop, the test pump, the feed line and tank, the drain line and tank, the sodium cooler, and piping. The main flow loop consists of 16-, 18-, and 28-in. (40.6-, 45.7-, and 71.1-cm) piping with five butterfly-type control valves, a mixing tee, a drain tee, a cooler tee, a venturi flowmeter, and a pressure reducing device. The permanent portion of the loop is 18-in.-diameter (45.7-cm) Type 304-H stainless steel pipe, arranged in a U-shape. The suction piping and discharge piping for the pump have a configuration designed to hydraulically simulate the FFTF piping.

The pump tank serves as the anchor point for the main flow loop. Feed and drain tanks are connected to the MFL by 12-in. (30.5-cm) piping.

Excess heat generated in the main flow loop sodium by the test pump is rejected to the atmosphere by the sodium cooler.

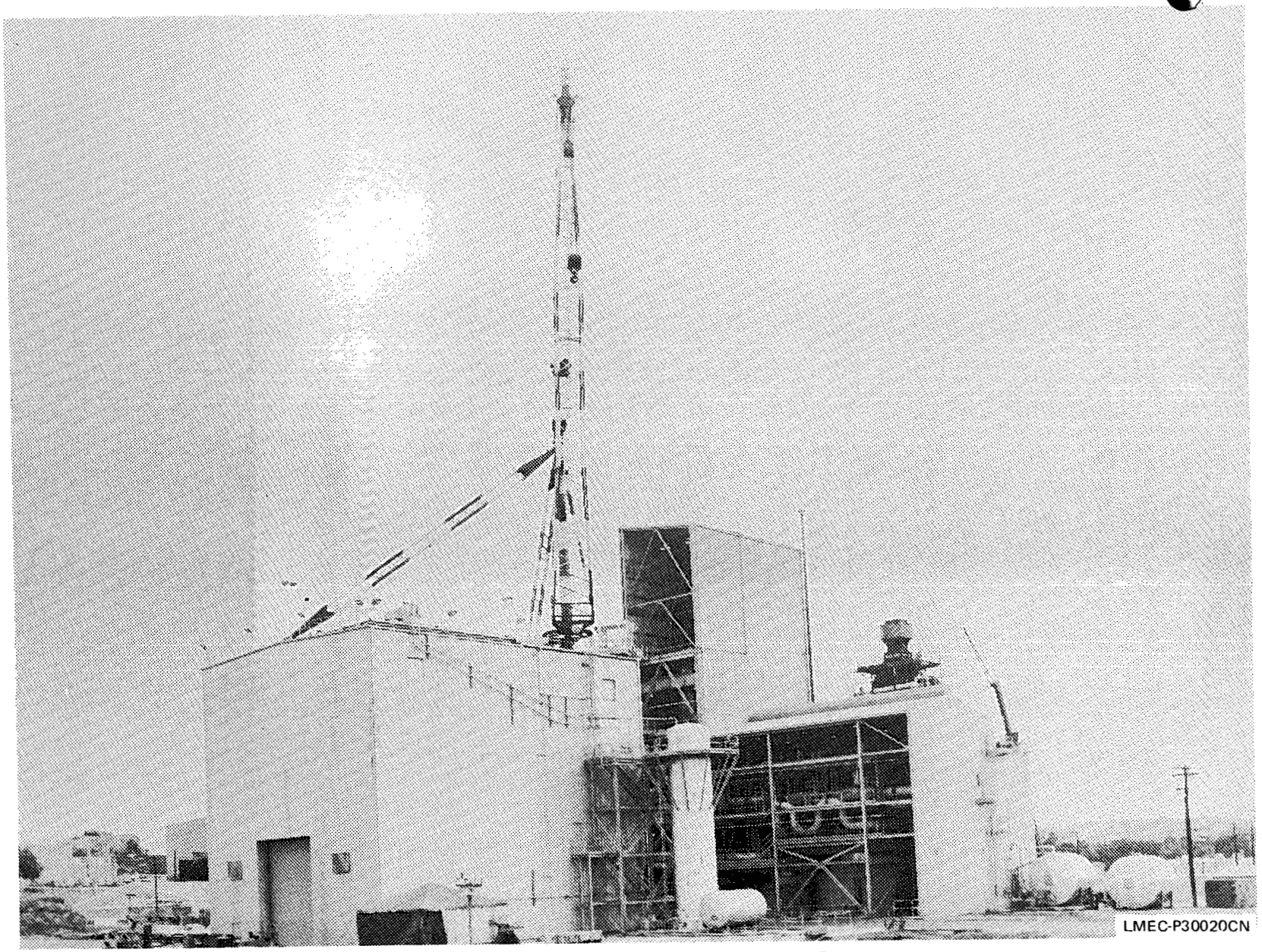

Figure XVII-1. SPTF and CHCF Complex

The piping is supported by spring hangers and tied to the building structure by vibration snubbers so that the combination of hangers and snubbers allows controlled movement during thermal expansion and contraction, as well as seismic activity.

b. Component Cleaning and Handling Facility

The CHCF provides the capabilities for assembling, disassembling, cleaning, and handling the pump internals. The facility consists of a building in which the pump can be assembled and disassembled while protected from the elements. Included is an outdoor cleaning tank in which the pump internals assembly can be immersed in an alcohol cleaning solution. Mounted on top of the building is a 70-ton (63.5- Mg) derrick capable of lifting the pump internals assembly (∿66 tons, or ∿60 Mg) out of the pump tank in SPTF and transporting that assembly to the cleaning tank and into the building through one of the roof hatches. The building has three 18-ft^2 (5.49-m^2) roof hatches. Inside the building, under one of the hatches, is a 40-ft-high (12.2-m) assembly/disassembly (A/D) station designed to hold components of the pump internals and provide personnel access during assembly and disassembly operations.

The building also has a bridge crane inside with 60- and 15-ton (54.4- and 13.6-Mg) hooks to permit handling of component parts without opening the roof hatch to the derrick.

2. Description of Test Article

The intermediate-size inducer pump is an FFTF primary pump modified by replacing the original impeller with an inducer, a new impeller, and other components needed to adapt the existing pump for use with the new pump rotating elements.

Outwardly, the intermediate-size inducer pump is identical to the FFTF prototype pump previously tested at ETEC. Physical interfaces are identical, and functional interfaces remain basically unchanged from the original FFTF configuration.

The test article is a vertical, free-surface, centrifugal pump designed to deliver 14,500 gal/min (0.9148 m^3/s) of 1050°F (565.6°C) sodium at a differential head of 500 ft (152.3 m). The actual head produced by the pump was 550 ft (167.6 m) because the impeller had not been trimmed to achieve the design head.

Included with the pump are: (1) a vertical wound-rotor drive motor, (2) a liquid rheostat to control motor speed, (3) an oil lubrication system, (4) two control cabinets, and (5) various pump-mounted instruments.

The hydraulic end of the pump (impeller, inducer, diffuser, sodium bearing, thermal shield, and radiation shield) is enclosed in a Type 304 stainless steel tank ∿35 ft (10.7 m) long and 7 ft (2.1 m) in diameter. The internal parts are also stainless steel. The upper bearings and shaft seal are oil lubricated; the lower bearing is a sodium-lubricated hydrostatic bearing.

Figure XVII-2 is a simplified illustration of the general arrangement of major components in the pump. Inlet suction flow enters the pump hydraulic assembly via the internal suction elbow (located in direct line with the suction nozzle), passes through the elbow length, enters the inducer, and is directed to the impeller eye traveling in an upward direction. The impeller increases the flow velocity. This flow is discharged radially from the impeller and enters the diffuser and then the turning vane that converts velocity head to pressure head and redirects the flow from a radial direction to a downward direction. The high-pressure fluid then moves downward along the hydraulic discharge passage and exits from the pump through the discharge nozzle.

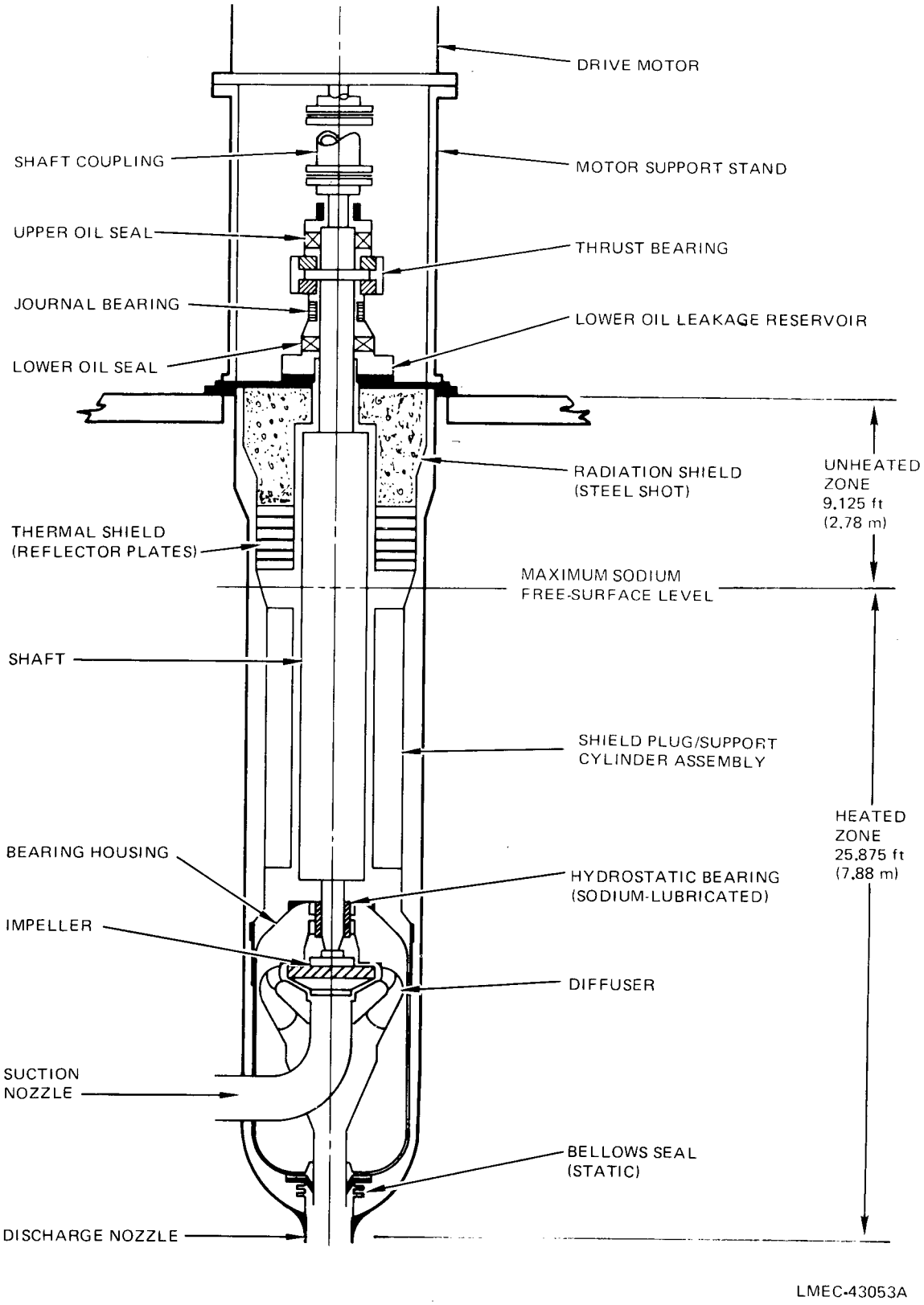

Figure XVII-2. ISIP-II Sodium Pump — Simplified Illustration

Within the hydraulic assembly, a secondary flow pattern exists in conjunction with the main flow described above. At the extreme bottom end of the diffuser/turning vane assembly, ~0.3% of the main flow is directed into the cavity formed by the pressure casing. This fluid is thoroughly mixed before flowing upward between the casing and the diffuser/turning vane assembly walls into the bearing supply reservoir portion of the bearing support housing. From this reservoir, flow is injected through control orifices into the inner pressure pockets of the sodium-lubricated hydrostatic bearing. It is by means of this secondary high-pressure flow that the load-carrying capabilities of the bearing are developed and lateral support to the pump rotor is provided.

3. Test Methods

Performance tests of the ISIP-II pump were conducted in a manner similar to those previously run on the FFTF prototype pump. However, thermal transient tests were not performed with the ISIP-II pump.

a. Sodium Melt and Heatup

Melting of sodium in the drain and feed tanks and dry preheat of the main flow loop (MFL) and pump tank were accomplished by means of electrical trace heaters on the tanks and piping. Heatup to 700°F (371.1°C) and wetting were accomplished by pump rotation at ~600 rpm. Melting of sodium in the drain and feed tanks was begun on March 13, 1981.

The main flow loop, purification system, vent lines, and other sodium system lines were also dry preheated to 400°F (204.4°C) by means of electrical heaters.

Dry preheat of the pump tank was initiated on April 14, 1981 — a day ahead of schedule. It required 180 h to bring the pump bearing temperature to 400°F. Figure XVII-3 shows typical pump tank and bearing temperatures during the preheat period. The rate of heatup was controlled so it would not exceed 10°F (5.6°C)

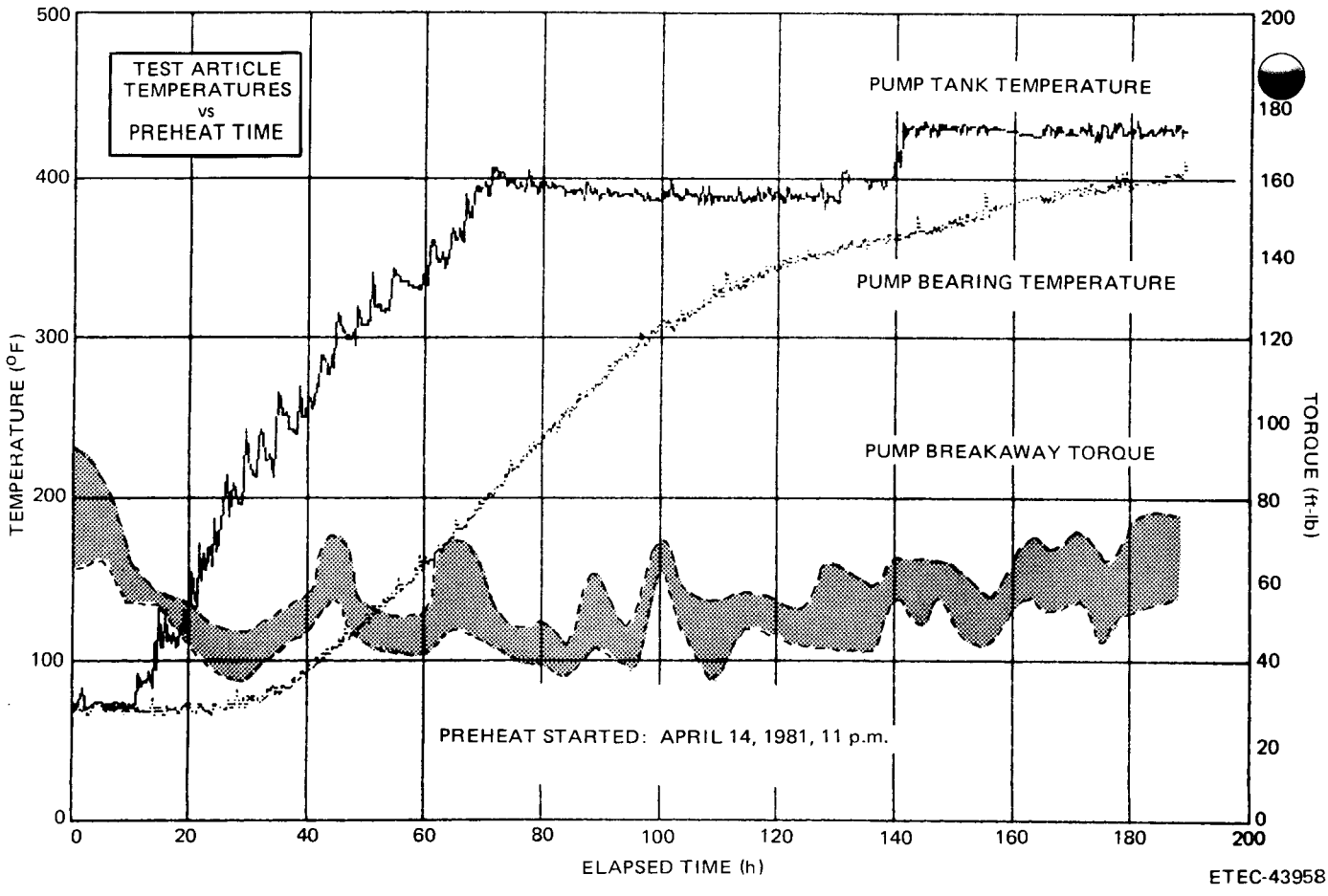

Figure XVII-3. Test Article Preheat History

per hour. Pump breakaway torque was measured at 1-h intervals during the preheat period. Pump shaft breakaway torque values were compared to ambient temperature breakaway torques. The purpose of frequently checking shaft breakaway torque was to ensure that pump shaft binding could be detected and corrected early. Neither shaft binding nor unusually high shaft breakaway torque was encountered at any time during the test program.

b. Testing Approach

Testing proceeded from less severe to increasingly severe conditions. Speed scans and flow scans were performed at discrete temperature levels from 700°F

(371.1°C) to 1050°F (565.6°C). A cavitation "head drop limit" test was performed 950°F (510°C). Endurance runs at 1050°F (565.6°C) at NPSH of 60 ft (18.29 m) and 950°F (510°C) at NPSH of 29 ft (8.84 m) were also performed.

Increase of sodium temperature in the flow loop was accomplished by heat input due to pump work. The sodium temperature was reduced by slowing the pump speed and by utilizing the facility sodium cooler.

Pump head, flow, electrical power consumption, and efficiency were measured for all test conditions. Several of the critical pump and facility operating parameters were displayed on a TV screen and continuously updated for the convenience of the operators.

Speed scans were run at two system resistance values, R4 and R5. System resistance is defined as a function of the flow divided by the pump speed (Q/N) as follows:

Resistance	Flow/Speed (Q/N)
R4	$\frac{14500 \text{ gpm}}{1110 \text{ rpm}} = 13.063 \text{ gal/rev} \left(\frac{0.9148 \text{ m}^3/\text{s}}{1110 \text{ rpm}} = 8.24 \times 10^{-4} \text{ m}^3/\text{rev}\right)$
R5	$\frac{18000 \text{ gpm}}{1110 \text{ rpm}} = 16.216 \text{ gal/rev} \left(\frac{1.1356 \text{ m}^3/\text{s}}{1110 \text{ rpm}} = 1.023 \times 10^{-3} \text{ m}^3/\text{rev}\right)$

Changes in system resistance were accomplished by adjusting five butterfly valves in the main flow loop. The location of the MFL butterfly valves is shown schematically in Figure XVII-4.

Flow scans (seven points) were run at sodium temperatures of 700°F (371.1°C) and 950°F (510°C). The flow rate was varied in discrete steps from ∿13800 gal/min (0.8706 m^3/s) to 18000 gal/min (1.1356 m^3/s) by use of the facility butterfly valves while maintaining pump speed constant at 1110 rpm.

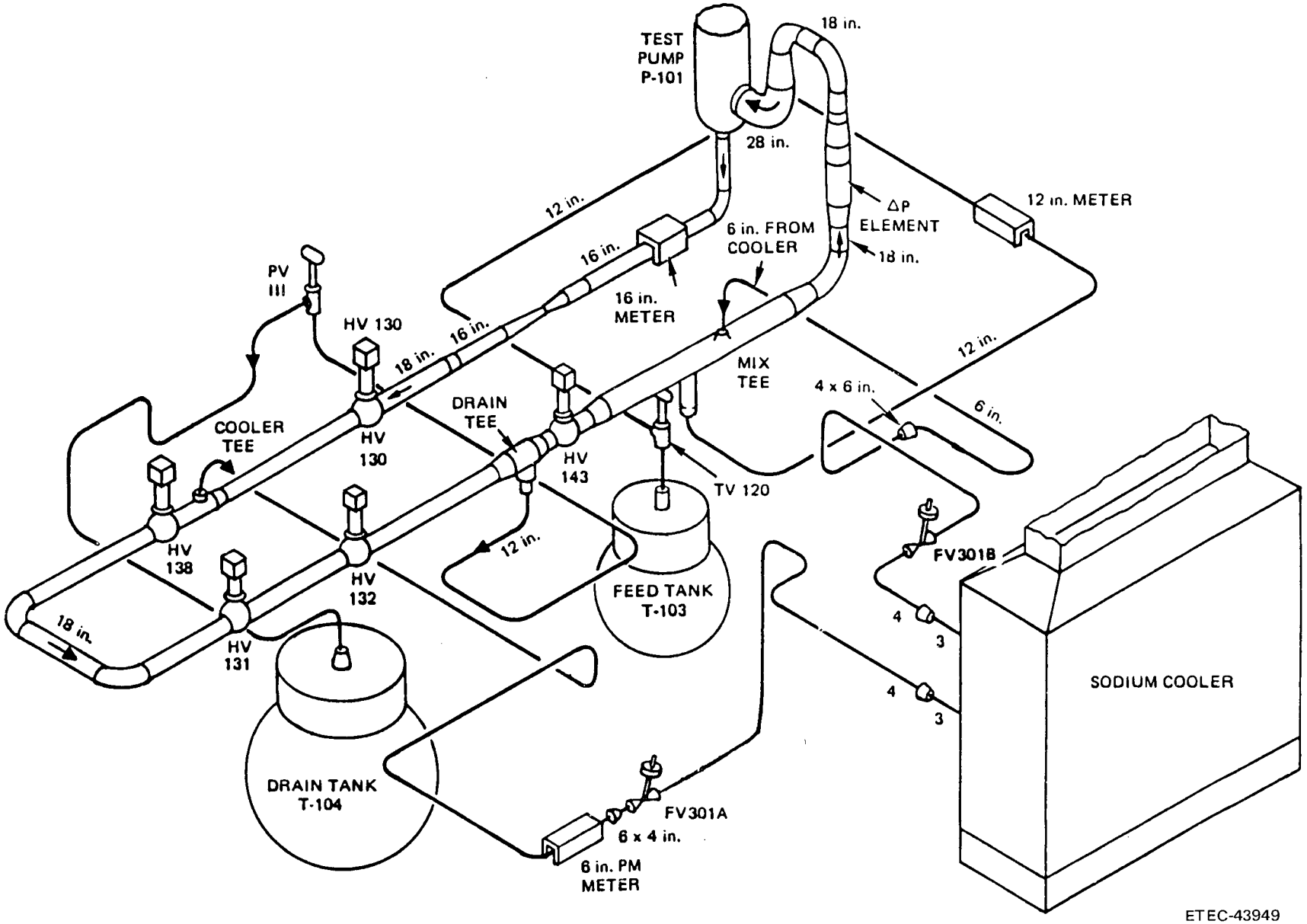

Figure XVII-4. SPTF Pump Flow Loop — Isometric Sketch

A four-point flow scan at 950°F (510°C) was also performed to calibrate the system resistance characteristics prior to performing the cavitation test. These data were used to predict the cavitation test initial flow rate.

The general technique of performing a flow scan was to set the flow-divided-by-speed variable (Q/N) to the desired set point at a speed of 750 rpm. The speed was then increased to 1110 rpm to take data. The speed was then reduced to 750 rpm to set the new value of Q/N and the procedure repeated for all values of Q/N. This technique was employed to avoid operating the facility butterfly valves at high flow conditions.

c. Adjustments to Data

Actual pump operating conditions rarely exactly match the targeted operating points. Therefore, test data were adjusted to the targeted test conditions in order to present all test data on the same basis.

Speed scan data points were adjusted to the specified targeted operating speeds of 600, 700, 800, 900, 950, 1000, 1025, 1050, 1075, and 1110 rpm. However, every specified operating speed was not achieved for every test.

Flow scan data and adjusted cavitation test data were adjusted to 1110 rpm. Data points outside of a band width of ±7 rpm of the specified operating speed were not shown on the data plots unless it is specifically noted that all points are plotted.

The following notations are used in the expressions for adjusted parameters:

Notation

N = pump speed (rpm)
Q = flow rate [gal/min (m^3/s)]
Head = total head, [ft of sodium (m)]
PWR = total input power to main motor (kW)

Greek Letters

η = efficiency (%)
ρ = density [lb/ft^3 (kg/m^3)]

Subscripts

p = projected value
m = measured value

Flow Adjustments — Flow was adjusted to the specified operating speed as follows:

$$Q_p = Q_m \left(\frac{N_p}{N_m}\right) \tag{1}$$

Head Adjustments — The adjusted total head shown plotted in the data curves was adjusted to the specified speed as follows:

$$\text{Head}_p = \text{Head}_m \left(\frac{N_p}{N_m}\right)^2 \tag{2}$$

Power Adjustments — The measured power to drive the pump is the total main motor input power, which includes liquid rheostat losses. The measured input power, therefore, cannot be projected from the (speed ratio)^3 relationship as is common practice for centrifugal pumps.

An empirical relationship established for FFTF prototype pump testing was used to project measured pump power to the specified speed and temperature as follows:

$$PWR_p = PWR_m \left(\frac{N_p}{N_m}\right)^{1.895} \left(\frac{\rho_p}{\rho_m}\right) \frac{[1 + 9.8(10^{-6})(T_p - 70)]}{[1 + 9.8(10^{-6})(T_m - 70)]} \tag{3}$$

Equation 3 was shortened for the ISIP-II program as follows:

$$PWR_p = PWR_m \left(\frac{N_p}{N_m}\right)^{1.895} \left(\frac{\rho_p}{\rho_m}\right) \qquad (4)$$

Temperature adjustments were less than $10^{o}F$ ($5.6^{o}C$) for all data; therefore, the temperature adjustment factor of Equation 3 became very small. The density ratio factor was left in Expression 4 as a temperature correction.

Curve Fits and Plots – The performance curves were curve fit with a best-fit computer-generated equation. The curve-fit equation generally was in the form of a second-order polynomial, even though the pump affinity laws might indicate that another form was more appropriate. Therefore, caution should be exercised in using the curve-fit equations to extrapolate the data beyond the test values.

The data presented in the speed scan and flow scan plots are steady-state data. Speed scan data were selected for points within ±7 rpm of the specified operating speed. Flow-divided-by-speed (Q/N) points within ∿0.75% of the specified Q/N target value were selected. Transient data are thus eliminated.

C. TEST RESULTS

1. Chronology of Events

An overview of the chronology of test activity is presented in Table XVII-1 and Figure XVII-5. Four basic types of tests (speed, scans, flow scans, cavitation tests, and endurance runs) at six discrete sodium temperature levels were performed. The test matrix is shown in Table XVII-2.

TABLE XVII-1

ISIP-II PUMP TEST CHRONOLOGY OF EVENTS
(Sheet 1 of 2)

Day	Event
02/19/81	Pump internals installed into pump tank
02/22-23	Seventeen drums of shot loaded into pump tank shot cavity
04/14	Initiated pump tank preheat
03/05	Installed drive motor onto pump
05/19	Initial sodium load (400°F) to MFL. Leak at flow venturi discovered. Emptied MFL and repaired leak.
05/26	Started initial MFL sodium flush
06/05	Initiated pony motor rotation of pump
	Initiated main motor rotation of pump
06/13	Completed wetting of pump and facility system at 700°F sodium temperature
06/16-21	Performed 700°F R4 Speed Scan 1
06/19-20	Performed 700°F R5 speed scan
06/20	Performed 700°F flow scan
06/21	Performed 750°F R4 speed scan
06/23-24	Performed 850°F R4 speed scan
06/28	Performed 950°F R4 Speed Scan 1
06/28-29	Performed 950°F R5 speed scan
06/29	Performed 950°F R4 Speed Scan 2
06/30	Performed 950°F flow scan
07/02	Performed 950°F cavitation calibration flow scan
07/02-03	Performed cavitation test
07/03-05	Initiated endurance run at NPSH = 29 ft, speed - 1110 rpm, flow = 14,500 gal/min
07/08	Performed 1000°F R4 speed scan
07/09-10	Performed 1050°F R4 speed scan
07/10-12	Performed 48-h duration run at 1050°F
07/12	Returned to endurance run conditions at NPSH = 29 ft
07/15	Performed 950°F R4 Speed Scan 3
07/16	Returned to endurance run conditions at NPSH = 29 ft
07/21	Replaced a section of pump tank line. Reduced shaft seal purge. Restarted endurance run at NPSH = 29 ft.

TABLE XVII-1

ISIP-II PUMP TEST CHRONOLOGY OF EVENTS
(Sheet 2 of 2)

Day	Event
07/25	Sodium leak discovered in purification system. Reduced speed to pony motor speed and repaired leak.
07/27-28	Performed 700°F R4 Speed Scan 2
07/28	Returned to endurance conditions at NPSH = 29 ft
08/07	Utilized Hewlett-Packard time interval counter to measure shaft speed. Still on endurance run at NPSH = 29 ft.
08/11	Increased NPSH to 86 ft (N = 1110 rpm) for UKAEA cavitation listening test. Returned to endurance run at NPSH = 29 ft.
08/12	Performed UKAEA cavitation listening test at 690 rpm, NPSH excursion. Returned to endurance run at NPSH = 29 ft.
08/13	Completed UKAEA cavitation listening test at minimum main motor speed. Returned to endurance run at NPSH = 29 ft.
08/25	Removed Hewlett-Packard counter used for speed measurement. Partially completed HEDL coastdown tests. Returned to endurance run conditions at NPSH = 29 ft.
08/26	Partially completed HEDL coastdown tests. Returned to endurance run conditions at NPSH = 29 ft.
08/27	Completed HEDL coastdown tests and returned to endurance run conditions. Terminated endurance run at midnight. Accumulated 942.3-h endurance run duration.
08/28	Begin sodium system cooldown
08/29	Perform ANL flowmeter tests at 400°F. Perform HEDL coupled main motor noise test.
08/30	Perform ANL flowmeter tests at 600°F. Drain sodium system.
08/31	Perform HEDL uncoupled main motor noise test.

Total Operating Time	
Pony motor only operation	109.4 h
Main motor operation	1759.8 h
Including:	
950°F endurance run (NPSH = 29 ft)	941.0 h
Cavitation (NPSH <29 ft)	1.3 h
Total	942.3 h
1050°F endurance run (NPSH = 60 ft)	48.1 h

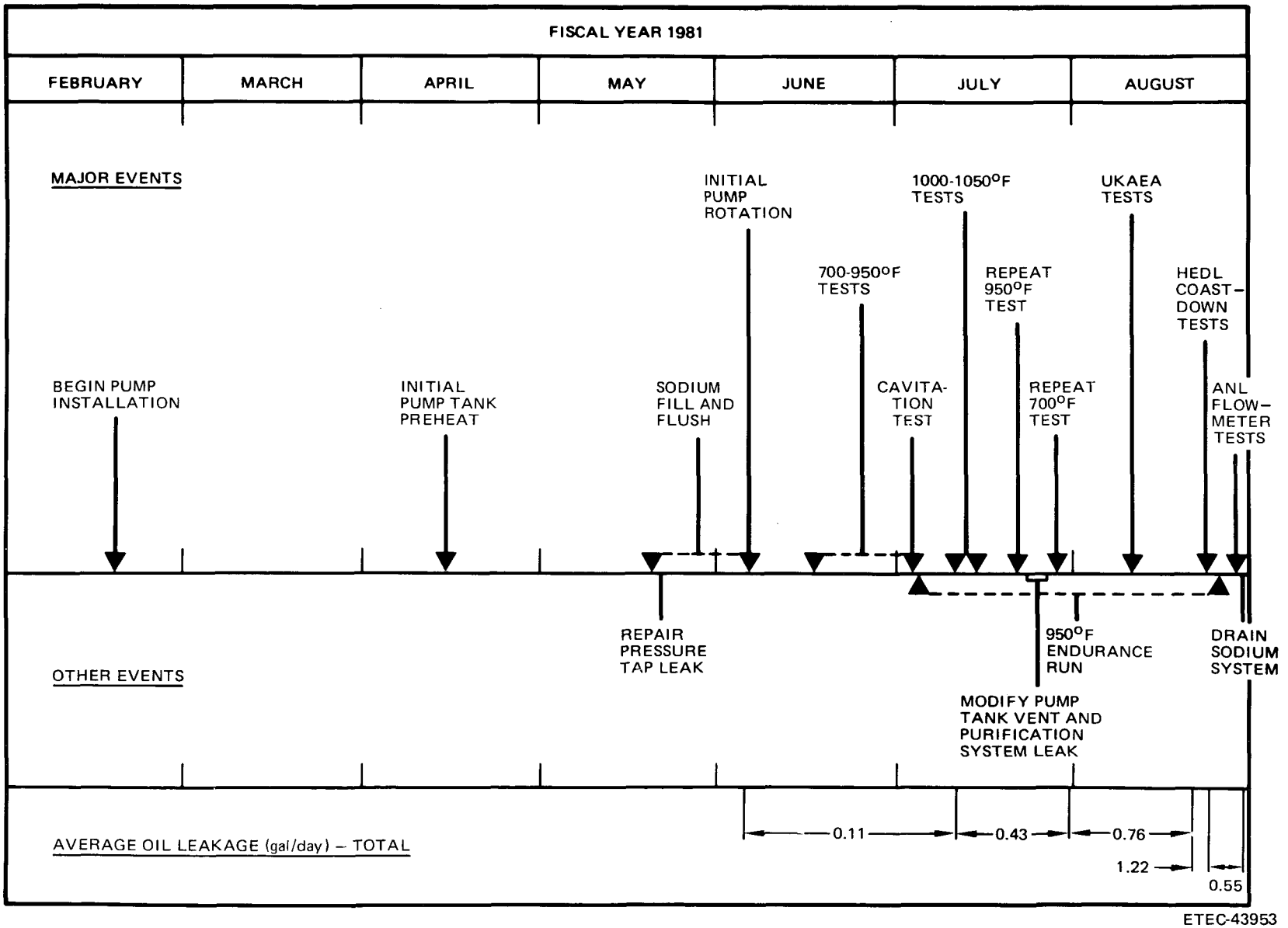

Figure XVII-5. ISIP-II Test Program Chronology

TABLE XVII-2

ISIP-II TEST MATRIX

SODIUM TEMPERATURE	R4 SPEED SCAN	R5 SPEED SCAN	FLOW SCAN	CAVITATION TEST	ENDURANCE RUN (h)
700°F (371.1°C)	X(2)	X	X		
750°F (398.9°C)	X				
850°F (454.4°C)	X				
950°F (510°C)	X(3)	X	X	X	942.3
1000°F (537.8°C)	X				
1050°F (565.6°C)	X				48.1

2. Operating Condition History

A summary of the pump operating history from the time of initial powered pump rotation until the final motor shutdown is presented in Table XVII-3.

TABLE XVII-3

ISIP-II OPERATING CONDITION HISTORY

Speed (SE-47) (rpm)	Temperature (°F)				Total Hours
	Less Than 575	575 to 775	775 to 975	Over 975	
Less than 400	140.4	89.7	57.4	7.7	295.2
400 to 800	39.0	193.0	364.2	35.4	631.6
800 to 1000	0.6	7.9	20.3	3.2	32.0
Over 1000	0.4	15.0	1011.0	52.1	1078.5
Total					2037.3

Interval from 6/5/81 at 15:42 to 8/29/81 at 13:58

Time exposure (hours):

Pony motor only	109.4
Main motor	1759.8
Motor stopped during this period	68.1
950°F endurance run (NPSH = 29 ft)	941.0
Cavitation test (NPSH < 29 ft)	1.3
1050°F endurance run	48.1

The pump was operated under power for 1869.2 h, of which 1759.8 h were at main motor speed. A total of 1011 h of pump operation was accumulated at a pump speed above 1000 rpm with the sodium temperature ranging from 775°F (412.8°C) to 975°F (523.9°C). A total of 941 h at the 950°F (510°C) reduced-NPSH endurance run condition was accumulated. This was the longest run duration practical because another pump test program was scheduled to be run in SPTF.

3. Performance Summary

All objectives of demonstrating pump performance as outlined in the Request for Test were met within schedule. The following objectives were successfully accomplished:

1) To characterize pump head, flow, power, and speed relationships in the operating region between design and two-loop flow impedance over a range of sodium temperatures
2) To determine the pump's critical NPSH
3) To demonstrate pump operation at 1050°F (566°C)
4) To demonstrate pump operation at a reduced NPSH.

The test program was extended 2 weeks beyond the originally scheduled shutdown date to permit additional run duration at reduced NPSH for the endurance run.

Performance tests, which consisted of speed scans at two flow resistances and two flow scans, were performed over a range of sodium temperatures from 700°F (371°C) to 1050°F (566°C). The developed head was determined to be significantly higher than that achieved during the FFTF test program. The developed head at a 1110-rpm pump speed and a flow of 14,500 gal/min (0.9148 m^3/s) was 562 ft (171.3 m). This is slightly higher than the Rocketdyne prediction of 546 ft (166.4 m) for these operating conditions. It should be noted that the impeller was not trimmed to achieve the design head.

The critical NPSH was established during a cavitation test. The NPSH was reduced to 11.3 ft (3.44 m) to achieve a head reduction of 2.2%. The cavitation test was terminated before the targeted 3.0% head drop was reached because of what was perceived to be excessive cavitation in the facility pressure reduction device.

A 48-h endurance run was successfully performed at 1050°F (566°C) to verify that pump shaft rework performed prior to test was satisfactory.

An endurance run of 941-h duration was performed at an NPSH of 29 ft (8.84 m). This NPSH was 155% of the established critical NPSH. The desired run duration of 2000 h was not achieved because of schedule interference with the next pump test program for SPTF. There were no technical reasons for limiting the endurance test program.

The pump performance tests for flow, head, power consumption, and computed efficiency (adjusted to 1110 rpm) are presented in Tables XVII-4A and -4B. Table XVII-4A also contains the test description, the date and time of the test, and the flow/speed (Q/N) range plotted. Note that the pump data presented in Table XVII-4A are in British units, whereas the same data presented in Table XVII-4B are in SI units.

a. Performance Parameters

Total Head – The head or total head, as used herein, is defined as the total dynamic head, expressed as the height of a column of sodium corresponding to the pressure increase produced by the pump. Included in the value for the head is the difference in velocity heads at points in the inlet and discharge line where the pressure is measured.

The discharge pressure is measured at a point downstream of the pump in the discharge ducting. The velocity head is calculated for the piping cross-sectional

TABLE XVII-4A

ISIP-II ADJUSTED TEST DATA SUMMARY (BRITISH UNITS)

Date of Test	Type of Test[b]	Time of Test	Q/N Range Plotted	Measured Data Adjusted to 1110 rpm				Data Adjusted to Target Flow[a]		@ 1110 rpm Operating Specific Speed	@ 14,500 gpm Operating Specific Speed
				Flow (gpm)	Head (ft)	Power (kW)	Efficiency (%)	Head (ft)	Power (kW)		
July 27-28, 1981	700°F R4 SS	2300 start 0150 end	12.96-13.16	14,485	564.1	1,920	69.1	565.3	1,924	1,154.2	1,152.9
June 21, 1981	750°F R4 SS	1920-2320	12.7-13.0	14,100	553.5	1,850	68.0	---[c]	---[c]	---[c]	---[c]
June 24, 1981	850°F R4 SS	0000-0400	12.96-13.16	14,365	556.2	1,883	67.3	566.7	1,917	1,161.6	1,150.8
July 15-16, 1981	950°F R4 SS	2025 start 0040 end	12.96-13.16	14,500	562.9	1,838	69.4	562.9	1,838	1,156.6	1,156.6
July 8, 1981	1000°F R4 SS	0200-0635	12.96-13.16	14,475	568.8	1,845	68.8	570.8	1,851	1,146.6	1,144.6
July 9-10, 1981	1050°F R4 SS	2150 start 0215 end	12.96-13.16	14,495	565.1	1,828	68.9	565.5	1,829	1,153.0	1,152.6
June 19-20, 1981	700°F R5 SS	0110-0320, 0655-1120	15.70-16.37	17,475	509.1	2,107	68.5	540.1	2,229	1,369.1	1,329.2
June 29, 1981	950°F R5 SS	0230-0745	15.9-16.16	17,745	512.3	2,070	68.6	527.1	2,127	1,373.1	1,353.8
June 20, 1981	700°F 7-PT FS	1830-2240	12.96-13.16	14,500[c]	558.0	1,904	68.8	558.0	1,904	1,164.2	1,164.2
June 30, 1981	950°F 7-PT FS	0140-0620	12.96-13.16	14,500[c]	561.1	1,849	68.7	561.1	1,849	1,159.4	1,159.4
July 2, 1981	950°F 4-PT FS	0320-0535	13.08-13.28	14,500[c]	561.6	1,850	68.8	561.6	1,850	1,158.6	1,158.6
								ON_S R4 = 1,156.8 $_{Avg}$ @ 1,110 rpm		ON_S R5 = 1,7.11 $_{Avg}$ @ 1,110 rpm	
								ON_S R4 = 1,155.0 $_{Avg}$ @ 14,500 gpm		ON_S R5 = 1,341.5 $_{Avg}$ @ 14,500 gpm	

[a] Data adjusted to targeted flows:
R4 = 14,500 gal/min at 1,110 rpm
R5 = 18,000 gal/min at 1,110 rpm

[b] SS = speed scan, FS = flow scan

[c] Data out of Q/N range; not extrapolated

TABLE XVII-4B

ISIP-II ADJUSTED TEST DATA SUMMARY (SI UNITS)

Test Date	Type of Test[b]	Measured Data Adjusted to 1110 rpm			Data Adjusted to Target Flow[a]	
		Flow (m^3/s)	Head (m)	Power (kW)	Head (m)	Power (kW)
July 27-28, 1981	371.1°C R4 SS	0.9139	171.9	1920	172.3	1924
June 21, 1981	398.9°C R4 SS	0.8896	168.7	1850	---[c]	---[c]
June 24, 1981	454.4°C R4 SS	0.9063	169.5	1883	172.7	1917
July 15-16, 1981	510°C R4 SS	0.9148	171.6	1838	171.6	1838
July 8, 1981	537.8°C R4 SS	0.9132	173.4	1845	174.0	1851
July 9-10, 1981	565.6°C R4 SS	0.9145	172.2	1828	172.4	1829
June 19-20, 1981	371.1°C R5 SS	1.1025	155.2	2107	164.6	2229
June 29, 1981	510°C R5 SS	1.1195	156.1	2070	160.7	2127
June 20, 1981	371.1°C 7-PT FS	0.9148	170.0	1909	170.1	1909
June 30, 1981	510°C 7-PT FS	0.9148	171.0	1849	171.0	1849
July 2, 1981	510°C 4-PT FS	0.9148	171.2	1850	171.2	1850

[a]Data adjusted to targeted flows:
R4 = 0.91481 m^3/s
R5 = 1.13672 m^3/s

[b]SS = speed scan, FS = flow scan

[c]Data out of Q/N range, not extrapolated

area at that point. The fluid friction loss from the pump discharge to the point where the discharge pressure is measured is calculated and added to the calculated discharge head.

The head at the inlet is determined from the height of the column of sodium above the reference point (inducer inlet) plus the cover gas pressure equivalent head in the pump tank. The inlet velocity head is computed at the inducer inlet cross-sectional area and added to the inlet head computed above.

This method of computing the inlet head was used during the latter part of the FFTF pump test program. It is believed to be a more accurate and stable technique of determining the inlet head than computing the inlet head from the pressure reading in the inlet ducting.

The pump demonstrated good head-vs-flow mapping repeatability at all temperatures. Mapping at R4 and R5 speed scans and flow scans was performed at sodium temperatures of 700°F (371.1°C) and 950°F (510°C). The head-flow and power-flow maps for 700°F (371.1°C) are presented in Figures XVII-6a and -6b, respectively. The head- and power-vs-flow maps at 950°F (510°C) are presented in Figures XVII-7a and -7b, respectively.

The head- and power-vs-flow characteristics at the extremes of operating temperatures, 700°F (371.1°C) and 1050°F (565.6°C) for the R4 system resistance condition is shown in Figures XVII-8a and -8b. It can be seen from Figure XVII-7a that the head-vs-flow characteristics are essentially the same. Minor deviation is due to normal random data scatter and to the diurnal effect on the speed indicator tachometer generator.

Total head data for each test series were extracted from Tables XVII-4A and -4B and are presented in Table XVII-5 for clarity. The data presented in Table XVII-5 are adjusted to 1110 rpm.

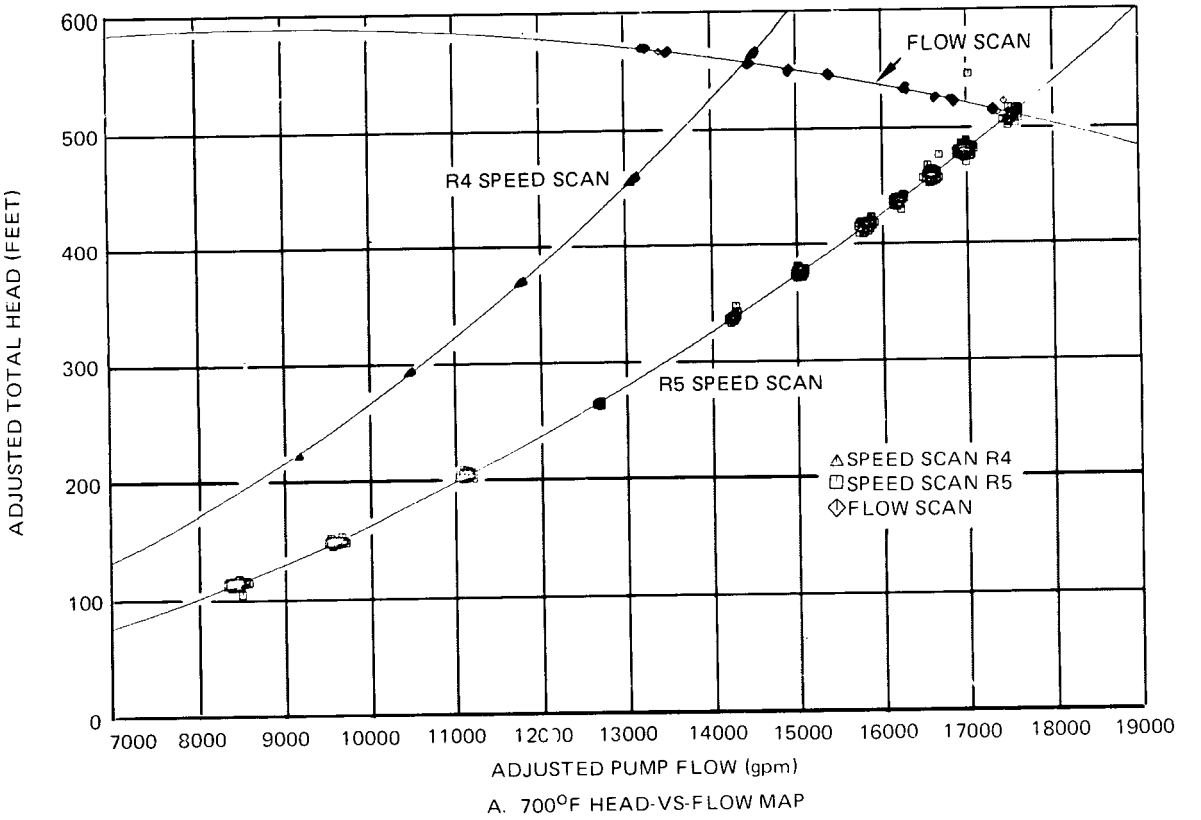

A. 700°F HEAD-VS-FLOW MAP

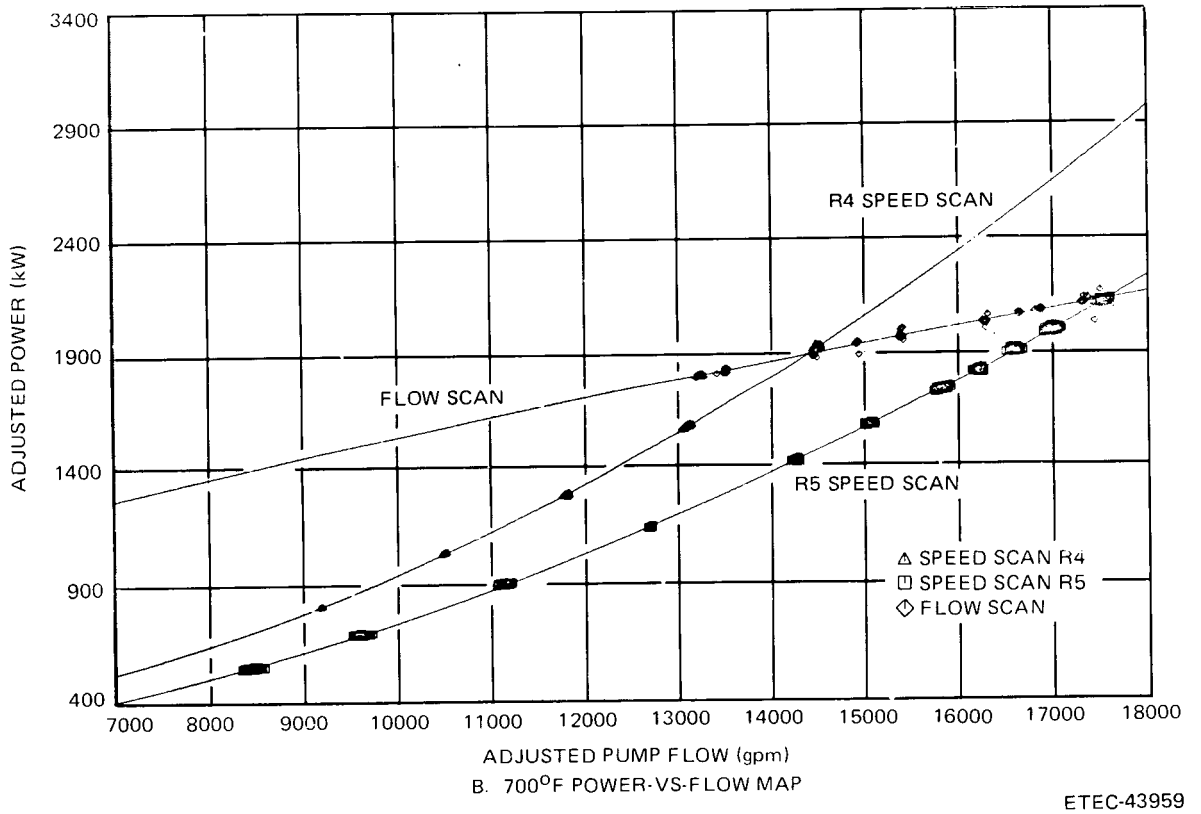

B. 700°F POWER-VS-FLOW MAP

ETEC-43959

Figure XVII-6. 700°F Performance Map

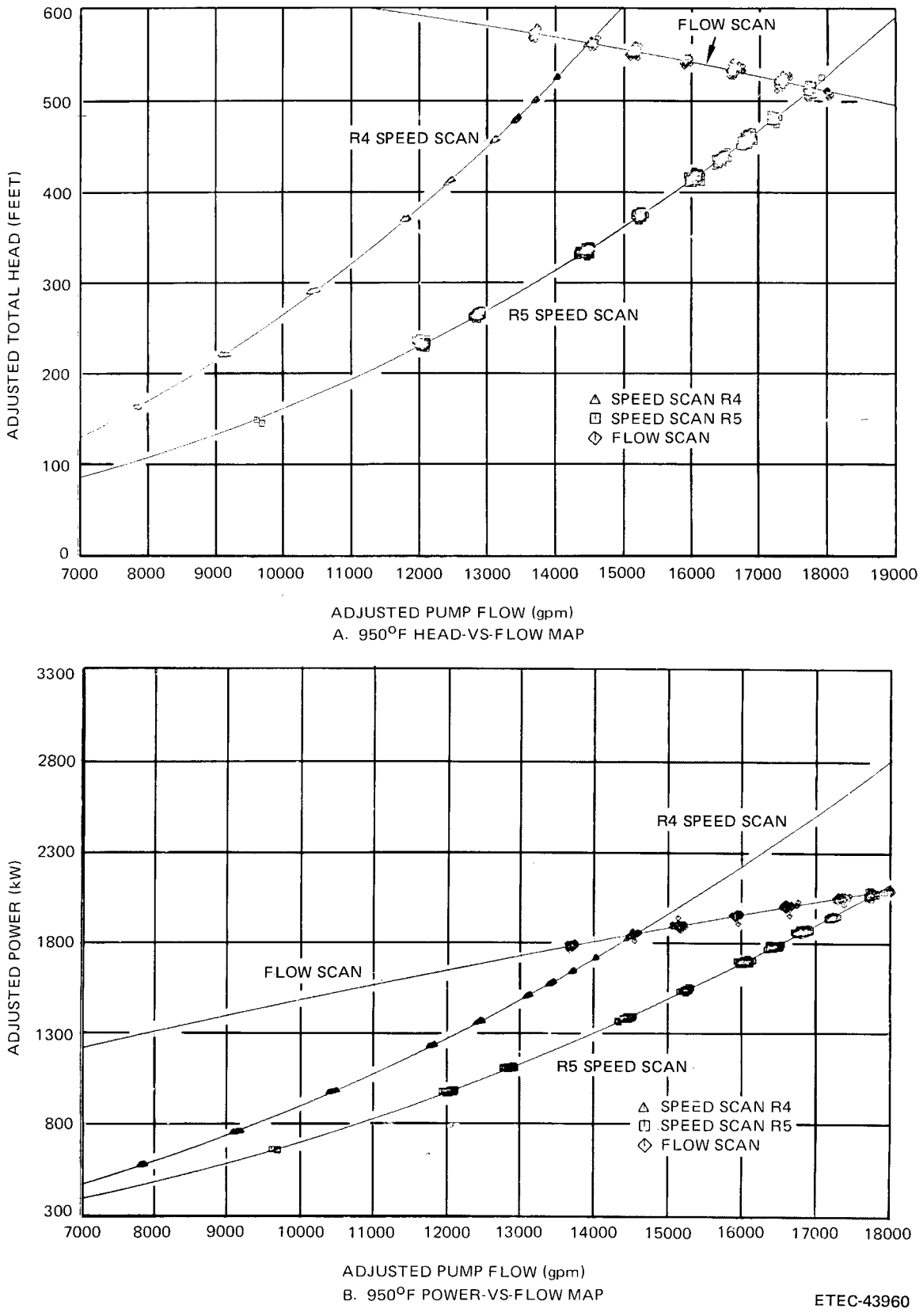

Figure XVII-7. 950°F Performance Map

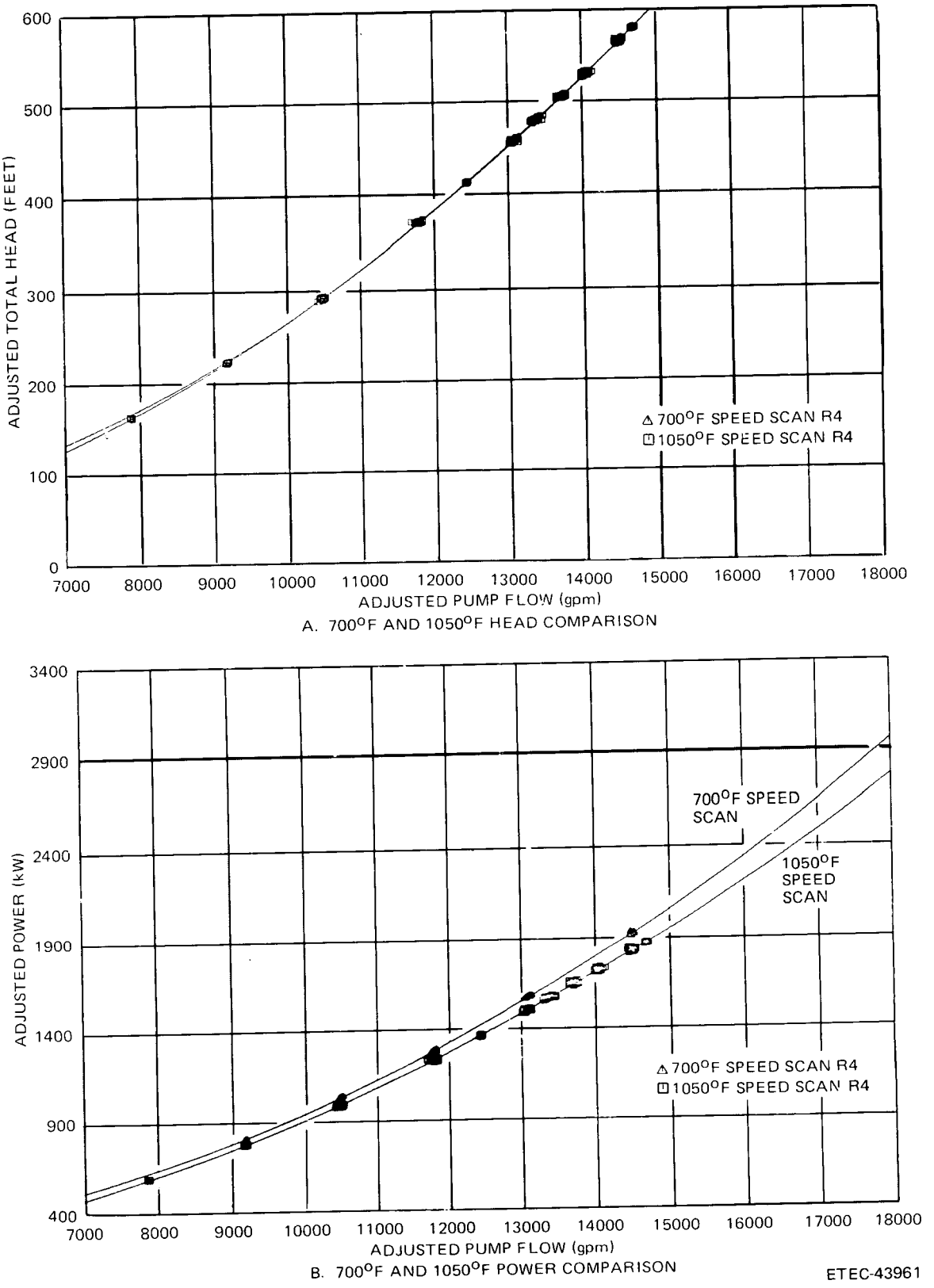

Figure XVII-8. 700°F and 1050°F Performance Comparison Plots

TABLE XVII-5

ISIP-II TOTAL HEAD AT 1110 rpm

Test Date	Type Test, R4[a]	Head[b]	
		ft	m
July 27-28, 1981	700°F (371.1°C) SS	564.1	171.9
June 24, 1981	850°F (454.4°C) SS	556.2	169.5
July 15-16, 1981	950°F (510°C) SS	562.9	171.6
July 8, 1981	1000°F (537.8°C) SS	568.8	173.4 (maximum)
July 9-10, 1981	1050°F (565.6°C) SS	565.1	172.2
June 20, 1981	700°F (371.1°C) 7-PT FS	558.0	170.1 (minimum)
June 30, 1981	950°F (510°C) 7-PT FS	561.1	171.0
July 2, 1981	950°F (510°C) 4-PT FS	561.6	171.2
		562.2	171.4 average
		+1.2, -0.7 maximum deviation (%)	
		3.99 ft (1.22 m) standard deviation	

Test Date	Type Test, R5[a]	Head	
		ft	m
June 19-20, 1981	700°F (371.1°C) SS	509.1	155.2
June 29, 1981	950°F (510°C) SS	512.3	156.1
		510.7	155.7 average

[a]SS = speed scan, FS = flow scan
[b]NPSH = 60 ft (18.3 m)

The average head at R4 resistance is 562 ft (171.3 m). The maximum deviation is +1.0%, -0.8%. Data for the 750°F (398.9°C) R4 speed scan are not included because they are outside the range of all other data presented.

The average head at R5 resistance is 510 ft (155.4 m). It should be noted that there are only two data points for the R5 resistance at 1110 rpm.

Power — The measured power as used herein refers to the total input power to the main motor, including losses due to the liquid rheostat. There was no provision to isolate the main motor power consumption from the rheostat losses. The similarity relations regarding power, therefore, do not strictly apply. A special correlation factor was used to extrapolate power data for different speed conditions.

The power-flow maps for the 700°F (371.1°C) and 950°F (510°C) temperature runs were shown in Figures XVII-6b and -7b, respectively. R4 and R5 speed scans and a flow scan (at constant speed of 1110 rpm) comprise each of the maps.

A comparison of the power-flow characteristics for the test program extremes of 700°F (371.1°C) and 1050°F (565.6°C) temperature conditions at R4 system resistance was shown in Figure XVII-8b. The higher power requirements at the 700°F (371.1°C) temperature is to be expected because of the higher density sodium being pumped at the lower temperature.

The measured power requirement was 1925.2 kW at a sodium temperature of 700°F (371.1°C) adjusted to 1110 rpm. The projected power at 1050°F (565.6°C) at 1110 rpm using Equation 4 is 1827.5 kW. This falls within 0.1% of the actual measured power of 1829.8 kW at 1050°F (565.6°C) adjusted to 1110 rpm for the R4 system resistance.

The power-vs-flow curve at R4 resistance for 950°F is shown in Figure XVII-7b. The projected power requirement at 950°F and 1110 rpm using Equation 4 is 1855.5 kW. The projected value is within 1.2% of the actual measured power of 1833.4 kW. This discrepancy is considered to be due to the diurnal effect on the speed indicator tachometer generator.

The power-vs-flow curves for the 700°F (371.1°C) and the 950°F (510°C) R5 resistance tests are shown in Figures XVII-6b and -7b, respectively. The power required at 1110 rpm for the 700°F (371.1°C) R5 test was 2120 kW. The required power at 950°C (510°C), 1110 rpm, projected from Equation 4 is 2043.4 kW. The projected value at 950°F (510°C) was within 1.4% of the actual measured power of 2071.6 kW.

Pump Efficiency — Pump efficiency was calculated from the expression:

$$\eta = (0.01883)\ \frac{(\text{Head})(Q)(\text{Sp g})}{(\text{PWR})} \qquad (5)$$

The average efficiency for the R4 resistance data (adjusted to 1110 rpm) is 68.6%, with the maximum deviation ∿1.0%.

The efficiency quoted is meaningful only for the ISIP-II pump-motor combination (including the liquid rheostat).

Cavitation Performance — The purpose of the cavitation test was to determine the critical NPSH required to cause a 3% head loss. The pump was to be operating at the design speed (1110 rpm) and design flow rate of 14,500 gal/min (0.9148 m^3/s). NPSH was referenced to the inducer blade tip elevation.

The targeted 3% head drop was not achieved. The cavitation test data in Figure XVII-9 show that ∿2.1% head drop was realized. There were sufficient data acquired to confidently predict that the critical NPSH would be 11.3 ft (3.44 m) at the extrapolated 3% head drop.

The initial flow rate for the cavitation test was determined from a four-point flow scan performed just prior to the cavitation test. The flow scan was performed to calibrate the pump and facility at the same conditions as those at which the cavitation test was to be run.

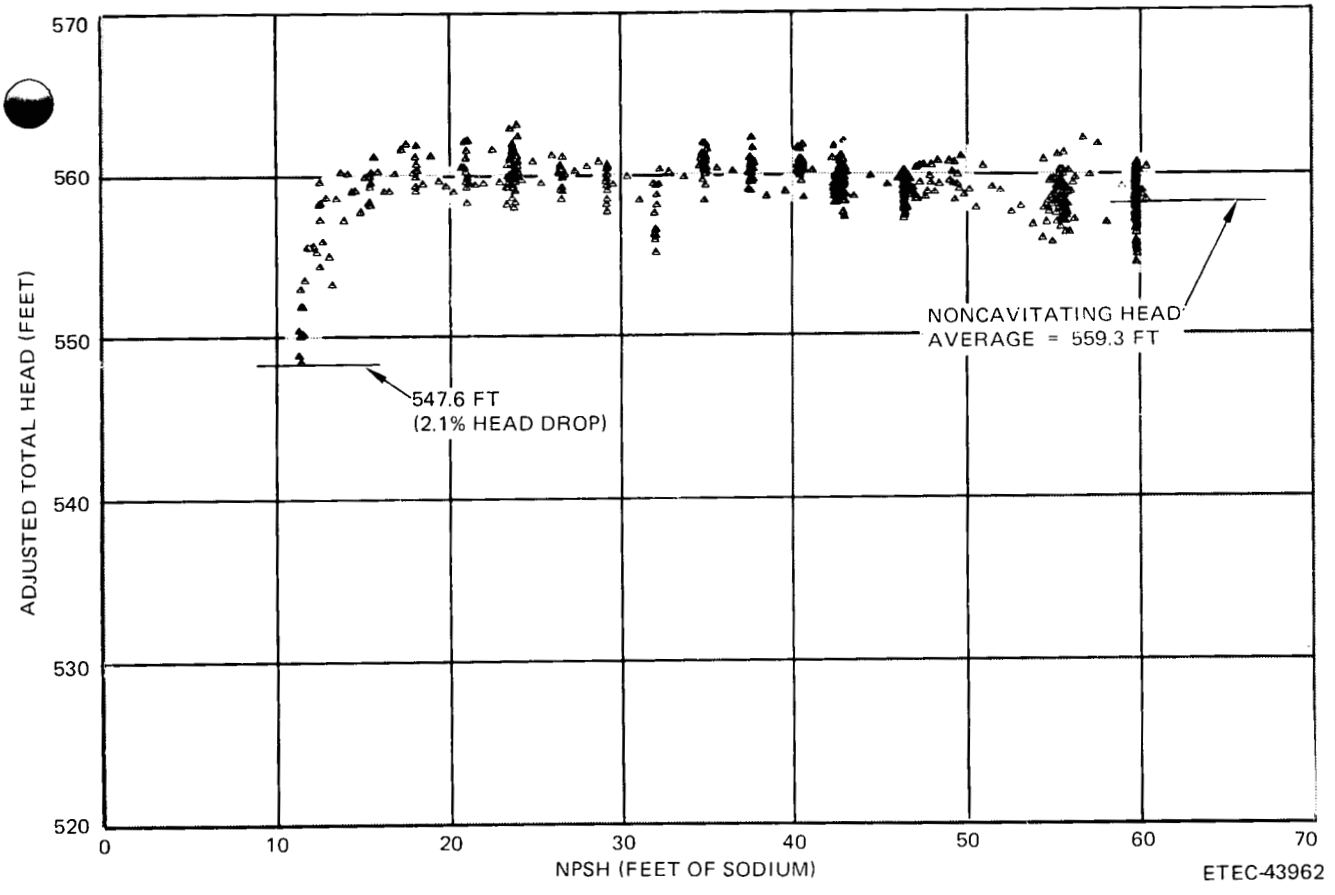

Figure XVII-9. 950°F Cavitation Test Data Plot

The head-vs-flow data for the four-point calibration flow scan were used to establish the initial operating point such that the flow rate would be 14,500 gal/min (0.9148 m^3/s) at the 3% head drop limit. The required initial cavitation test flow rate was determined to be 14,690 gal/min (0.9268 m^3/s).

The noncavitating baseline head was established by operating for 1 h at the following conditions:

NPSH	60 ft (18.29 m)
Speed	1110 rpm
Flow rate	14,690 gal/min (0.9268 m^3/s)
Temperature	950°F (510°C)
Sodium level	125 in. (3.175 m) above impeller
Total head	559.3 ft (170.5 m)

The baseline head for noncavitation was verified by operating at NPSH of 80 ft (26.21 m) for 1 h at the same speed, flow rate, temperature, and sodium level. The developed total head for NPSH of 86 ft (26.21 m) was 562 ft (171.3 m).

Reduction of NPSH was accomplished by two methods: The first was to lower the sodium level in the pump tank from 125 in. (3.175 m) (normal operating level) to 48 in. (1.219 m) above the impeller centerline. The second method was to reduce the pump tank cover gas pressure below atmospheric pressure by means of a vacuum pump.

The cover gas pressure was reduced in small increments, ~1-2 psi (6.89-13.79 kPa), until cavitation was achieved. The cover gas pressure had to be reduced to 1.6 psia (6.89 kPa) to achieve 2.1% head drop.

XVIII. 1/5-SCALE PUMP

J. J. CORUGEDO

A. INTRODUCTION

The 1/5-scale model pump built by Atomics International and Rocketdyne Divisions of Rockwell International is being tested at the Hydraulic Test Facility (HTF) at ETEC.

The item under test is a 1/5-scale hydrodynamic model of a large-scale breeder reactor (LSBR) primary sodium pump, including components such as an inducer, an impeller, a diffuser, a collector bowl, inlet ducting, and inlet and discharge nozzles. Geometric and operational similarities between the model and the full-size prototype have been maintained.

Accessory equipment needed to support operation of the test article includes a drive assembly, a circulating oil lubrication system, instrumentation and controls, and the water loop.

The water testing of this test article emphasizes the quantification of operating net positive suction head (NPSH) margin, characterization of head-flow and efficiency relationships, and determination of protection against cavitation damage to the inducer, impeller, and diffuser.

B. TEST DESCRIPTION

1. Facility

The Hydraulic Test Facility performs hydraulic tests, utilizing water as the test fluid, on components to be used in the Fast Breeder Reactor Program. Three special test sections (one 10-in., one 8-in., and one 6-in.-diameter pipe) hold the components to be tested. The test sections are incorporated in the hydraulic loop that circulates water through the test articles.

Water circulation is provided by three centrifugal pumps arranged in a parallel configuration. One pump (P-3) is rated at 3000 gal/min (0.189 m^3/s) at 300 ft of head (0.89 kPa); two pumps (P-2 and P-1) are each rated at 750 gal/min (0.045 m^3/s) and 900-ft head (2.67 kPa). These pumps may be run one at a time or together. The pumps' energy input heats the water above ambient temperature if required.

In the 10-in. (0.254-m) loop, water flows from the pumps through a 10-in. line, through the test article section, through a deaeration tank, and back to the facility pump suction manifold. A water-cooled heat exchanger provides for temperature control. This is the loop currently being used for the 1/5-scale model pump.

In the 8-in. (0.203-m) loop, water flows from the pump discharge through an 8-in. line, through a manifolded pipe array test section, and then back to the pump suction manifold. The manifold pipe array consists of a 2-in. (0.05-m), a 4-in. (0.1-m), and a 6-in. (0.15-m) pipe run in parallel, with each pipe run containing a flowmeter and shutoff valve. Large test articles may also be installed in the 8-in. piping downstream of the manifold. An airblast heat exchanger provides temperature control.

The 6-in. (0.152-m) test loop is installed in parallel with the 10-in. test loop. This configuration permits installation of a test article in either section while testing continues in the other.

A 700-hp variable-speed (0 to 3460 rpm) dc motor, currently being utilized to drive the 1/5-scale model pump, will be available for future tests.

A lube-oil system capable of providing and controlling oil is being used to supply the bearings on the 1/5-scale model pump.

The 7600-gal (29.6-m^3) deaeration tank's primary function is to remove entrained gases from circulating water. An internal anti-vortex baffle has been installed in the deaeration tank over the outlet nozzle to prevent reentrainment of gas by vortex action. A vacuum system is provided for reducing the pressure of the gas above the water surface; a nitrogen system is provided for pressurization.

A digital data acquisition system (DDAS) is provided that records data on disc for on-line processing and on tape for a more permanent record and off-line processing of data.

An X-Y plotter-printer is provided for either on-line or off-line plotting of test data.

The computer is currently programmed with a complete set of equations for on-line reduction of data on pump performance. Several special programs are also included, providing real-time display of data on two cathode ray tubes (CRTs) in the form of plots, with the advantage of on-line comparison with predicted data.

An isometric of the Hydraulic Test Facility (HTF) is shown in Figure XVIII-1.

2. Test Article

The item under test, shown in Figure XVIII-2, is a 1/5-scale hydrodynamic model of the hot (930°F) dimensions of the pumping elements of an LSBR primary sodium pump, including components such as inducer blades and hub, impeller blades and shrouds, diffuser vanes, collector bowl configuration, inlet duct, and discharge nozzle. The same scaling will be used for the subscale rotor substitution (SRS) pump sodium test assembly, such that identical pumping element components will be fabricated. The rear impeller labyrinth leakage and hydrostatic bearing flow rates are simulated by use of overflow lines with valves to set the scaled flow rates. Specific pressure measurements will be included in the inlet and discharge ducting and the test rig to obtain inlet velocity profile, labyrinth

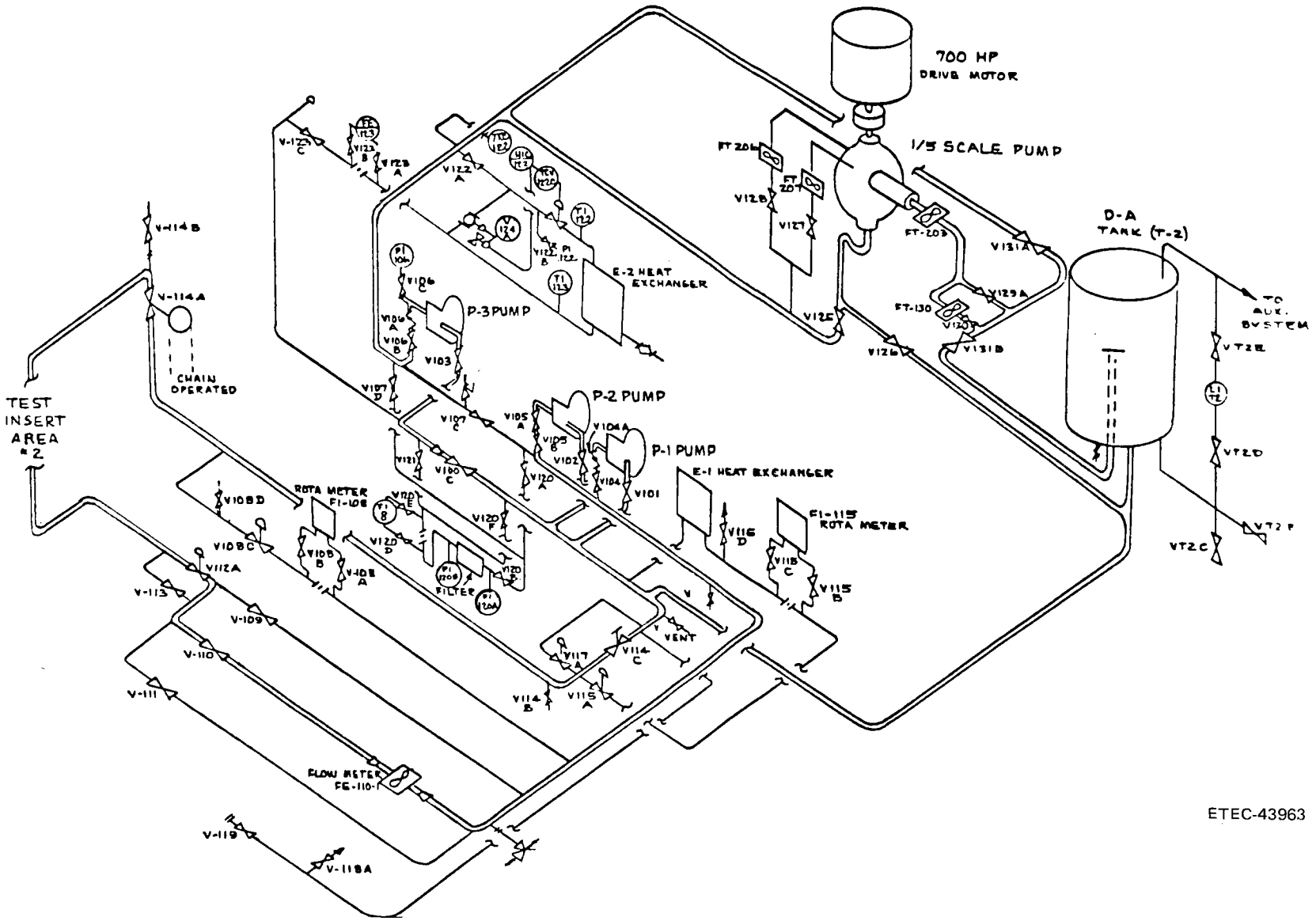

Figure XVIII-1. Hydraulic Test Facility P&I Diagram

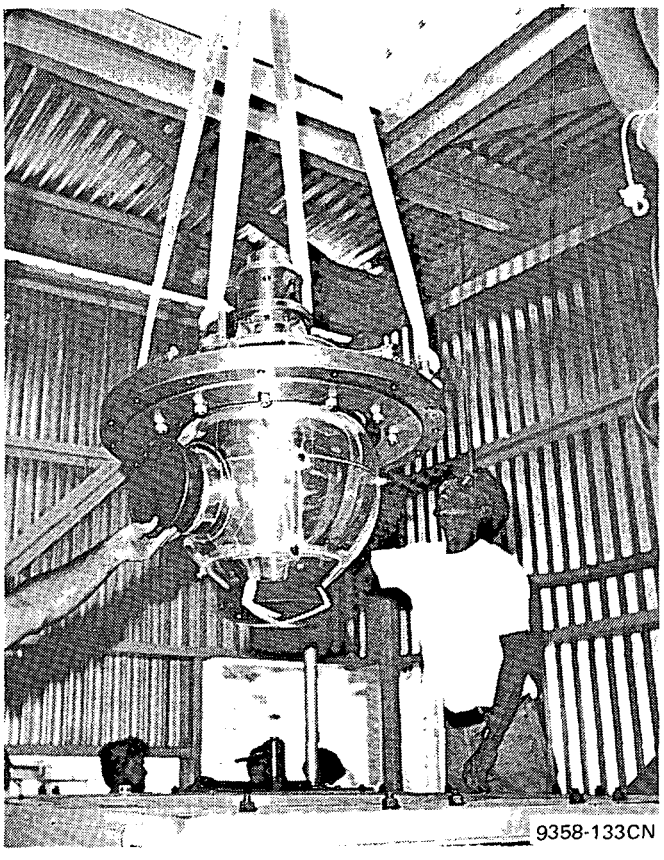

Figure XVIII-2. 1/5-Scale Model Pump
Being Lowered Onto the Test Stand

seal pressure drops, inducer/impeller pressures, and pump performance. A special shaft support system will use rolling element bearings with instrumented supports. This will allow measurement of dynamic radial and axial loads of the inducer and impeller rotating assembly.

The pump is driven by a 700-hp variable-speed (0-3460 rpm) dc motor through a flexible coupling assembly fitted with a Himmelstein MCRT-8-02TA (15-3) torque transmitter.

Figure XVIII-3 shows the pump installed with all the instrumentation and nozzles connected to it, while Figure XVIII-4 shows the variable-speed drive motor.

Table XVIII-1 lists the parameters recorded for this test program, while Figure XVIII-5 shows the location of the test article instrumentation.

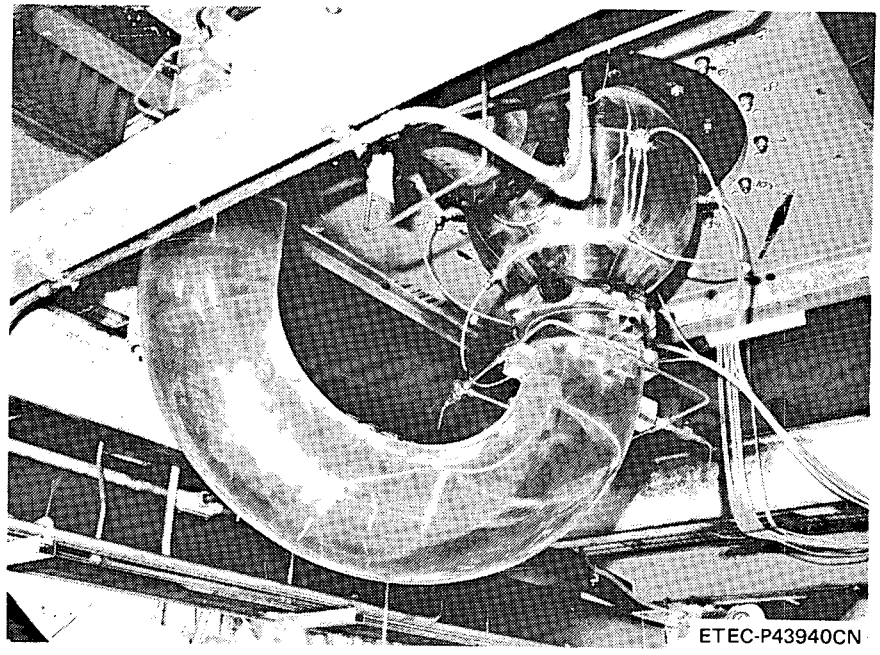

Figure XVIII-3. Test Article Installed in Place With Prototypical Inlet Configuration and Ready for Test

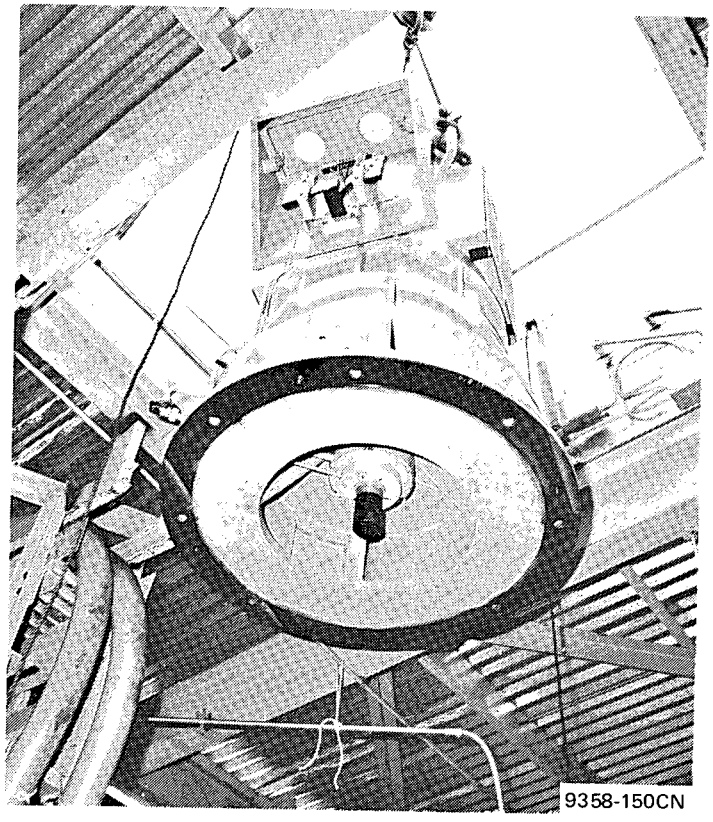

Figure XVIII-4. 700-hp dc-Drive Motor Being Installed

TABLE XVIII-1

INSTRUMENTATION
(Sheet 1 of 3)

Pump Instrumentation	
PT-1111	Pump bowl pressure port 18 psig
PT-1112	Pump bowl pressure port 22 psig
PT-1113	Pump bowl pressure port 19 psig
PT-1114	Pump bowl pressure port 16 psig
PT-1115	Pump bowl pressure port 21 psig
PT-1116	Pump bowl pressure port 17 psig
PT-1117	Pump bowl pressure port 20 psig
PT-1118	Pump bowl pressure port 15 psig
PT-1121	Impeller discharge port 30 psig
PT-1122	Impeller discharge port 25 psig
PT-1123	Impeller discharge port 26 psig
PT-1124	Impeller discharge port 27 psig
PT-1125	Impeller discharge port 28 psig
PT-1126	Impeller discharge port 29 psig
PT-1140	Shaft lab. downstream psig
PT-1141	Shaft lab. upstream psig
PT-1142	Front impeller lab. downstream psig
PT-1143	Front impeller lab. upstream psig
PT-1144	Rear impeller lab. downstream psig
PT-1145	Rear impeller lab. upstream psig
YT-1132	Pump vibration – lower NE (g)
YT-1133	Pump vibration – lower NW (g)
YT-1134	Pump vibration – upper NE (g)
YT-1135	Pump vibration – upper NW (g)
ZT-1127A	Pump shaft position – lower SE (mils)
ZT-1127B	Pump shaft position – lower SW (mils)
ZT-1127C	Pump shaft position – upper SE (mils)
ZT-1127D	Pump shaft position – upper SW (mils)

TABLE XVIII-1

INSTRUMENTATION
(Sheet 2 of 3)

GT-1150 through -1164	Bearing support strain gages (in.)
GT-1180 through -1185	Bearing support strain gages (in.)
Facility Instrumentation	
ST-1110	Pump speed (rpm)
ST-1106	Motor speed (rpm)
FIT-203	Discharge flow – high (gpm)
FIT-130	Discharge flow – low (gpm)
FIT-207	Hydrostatic bearing overflow (gpm)
FIT-206	Shaft labyrinth overflow (gpm)
PT-202A	Inlet pressure Sta. 1A (psia)
PT-202B	Inlet pressure Sta. 1B (psia)
PDT-203	Delta-P Sta. 2 - 1A (psid)
PT-203	Outlet pressure (psig)
TT-202	Water-in temperature (^{O}F)
TT-203	Water-out temperature (^{O}F)
TT-302	Oil-in temperature (^{O}F)
TT-301	Oil-out temperature (^{O}F)
FT-302	Lower bearing oil flow (gpm)
FT-303	Upper bearing oil flow (gpm)
PT-302	Oil inlet pressure (psig)
XT-1110-1	Pump torque (in.-lb)
JT-1109	Motor power (hp)
YT-1130	Drive motor vibration – lower (g)
YT-1131	Drive motor vibration – upper (g)
PT-203A	Pump dynamic discharge pressure (psi)
ZT-V129	Valve Position Ind. V129A (% open)
ZT-V131	Valve Position Ind. V131B (% open)

TABLE XVIII-1

INSTRUMENTATION
(Sheet 3 of 3)

Calculated Parameters	
Q1 (or Q6)	Inlet flow (gpm)
Q1N1	Q/N FIT-203 based (gal/rev)
Q2N2	Q/N FIT-130 based (gal/rev)
H1	Head Sta. 2 and 1A (ft)
H2	Head Sta. 2 and 1B (ft)
H3	Head Delta-P (ft)
NPSH1	NPSH – Sta. 1A based (ft)
NPSH2	NPSH – Sta. 1B based (ft)
NPSH3	NPSH – Sta. 1A – 180^{o} inlet only (ft)
BHP	Brake horsepower (hp)
FHP1	Fluid HP-H1 based (hp)
FHP2	Fluid HP-H2 based (hp)
FHP3	Fluid HP-H3 based (hp)
EFF1	Efficiency-H1 based (%)
EFF2	Efficiency-H2 based (%)
EFF3	Efficiency-H3 based (%)
Q2C1	Dis. flow corr. (3295 rpm) (gpm)
H2C1	Head corr. to (3295 rpm) (ft)
H3C1	Overall head corr. to (3295 rpm) (ft)
Q2C2	Dis. flow corr. (2657 rpm) (gpm)
H2C2	Head corr. to (2657 rpm) (ft)
H3C2	Overall head corr. to (2657 rpm) (ft)

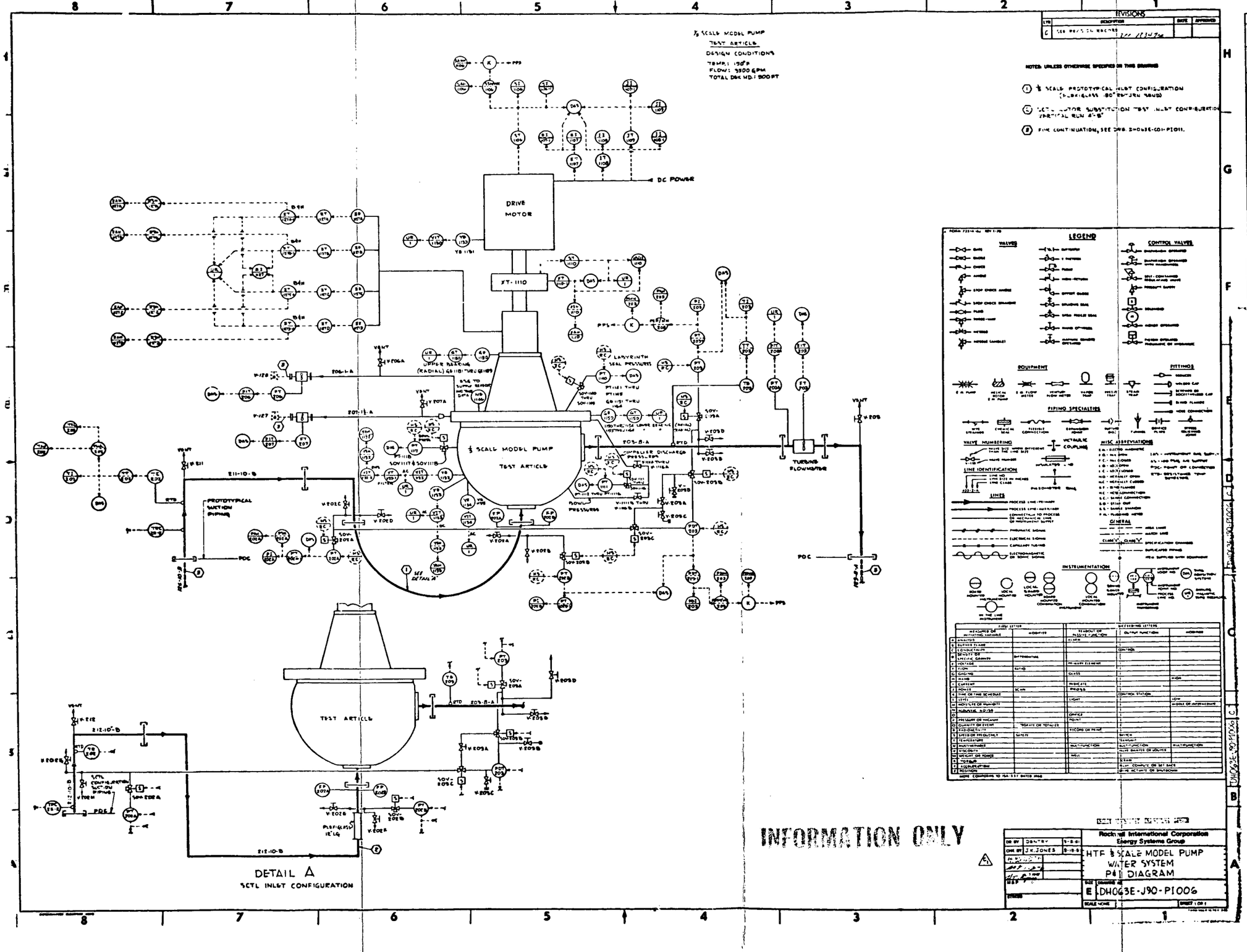

REVISIONS

LTR	DESCRIPTION	DATE	APPROVED
C	SEE REVISION RECORD	3/4/83	

NOTES: UNLESS OTHERWISE SPECIFIED ON THIS DRAWING

1. ⅛ SCALE PROTOTYPICAL INLET CONFIGURATION (5 ELBOWS CLASS -80° ELBOW RADIUS)
2. SCTL INLET SUBSTITUTION TEST INLET CONFIGUERTION (VERTICAL RUN 4'-8")
3. PIPE CONTINUATION, SEE DWG. SHOWSE-COMPIOII.

REVISION RECORD

LTR	DESCRIPTION	DATE	APPROVED
A2	1		

Rocketdyne International Corporation Energy Systems Group — RR-DH063E-J90-P1006 — C

LEGEND

VALVES | CONTROL VALVES | EQUIPMENT | PIPING SPECIALTIES | FITTINGS | VALVE NUMBERING | VICTAULIC COUPLING | MISC ABBREVIATIONS | LINE IDENTIFICATION | LINES | GENERAL | INSTRUMENTATION

FIRST LETTER		SUCCEEDING LETTERS		
MEASURED OR INITIATING VARIABLE	MODIFIER	READOUT OR PASSIVE FUNCTION	OUTPUT FUNCTION	MODIFIER
A ANALYSIS		ALARM		
B BURNER FLAME				
C CONDUCTIVITY			CONTROL	
D DENSITY OR SPECIFIC GRAVITY	DIFFERENTIAL			
E VOLTAGE		PRIMARY ELEMENT		
F FLOW	RATIO			
G GAGING		GLASS		
H HAND				HIGH
I CURRENT		INDICATE		
J POWER	SCAN	PROBE		
K TIME OR TIME SCHEDULE			CONTROL STATION	
L LEVEL		LIGHT		LOW
M MOISTURE OR HUMIDITY				MIDDLE OR INTERMEDIATE
N NUMBER OR TOTAL				
O PRESSURE OR VACUUM		ORIFICE POINT		
P QUANTITY OR EVENT	INTEGRATE OR TOTALIZE			
Q RADIOACTIVITY		RECORD OR PRINT		
R SPEED OR FREQUENCY	SAFETY		SWITCH	
S TEMPERATURE			TRANSMIT	
T MULTIVARIABLE		MULTIFUNCTION	MULTIFUNCTION	MULTIFUNCTION
U VISCOSITY			VALVE DAMPER OR LOUVER	
V VIBRATION				
W WEIGHT OR FORCE		WELL		
X UNCLASSIFIED			STEAM	
Y EVALUATION			ALARM, CONVERTER OR SET POINT	
Z POSITION			DRIVE ACTUATE OR SHUTDOWN	

MORE COMPARING TO ISA-S37 DATED 1968

DR BY	DBUTTRY	9-8-83	Rocketdyne International Corporation Energy Systems Group
CHK BY	J.V. JONES	9-18-83	HTF ⅛ SCALE MODEL PUMP WATER SYSTEM P&I DIAGRAM
SIZE	DRAWING NO.		
E	DH063E-J90-P1006		
SCALE NONE		SHEET 1 OF 1	

Figure XVIII-5. Test Article Instrumentation

3. Test Method

The purpose of this test program is to demonstrate and verify pump hydrodynamic operational characteristics of the LSBR primary pump by testing a 1/5-scale pump in water. Results will substantiate the inducer, impeller, and diffuser designs for large primary system sodium prototype pumps. The overall test program includes installation, testing, removal, and inspection of the test pump. Testing includes head-flow characterization, suction performance, and bearing load determination. Dye tests will be conducted to verify cavitation damage avoidance at the steady-state operating conditions. Design and off-design steady-state tests will be conducted to demonstrate operational stability and cavitation damage protection by this inducer pump design. Cavitation tests will give the critical NPSH and suction performance capability. A special shaft support system will use rolling element bearings with instrumented supports. This will allow measurement of dynamic radial and axial loads of the inducer and impeller rotating assembly for analysis and verification of the hydrostatic bearing design of the LSBR primary pump.

Special tests include locked rotor forward and reverse flow impedance, inlet probe survey, bearing load tests, second quadrant operation, and negative head rise. Pump disassembly at HTF during the dye tests, dye application, and reassembly of the pump will be performed by ETEC to approved procedures. ESG QA will witness these operations. Photographic recording of test article parts will show the cavitation damage protection margin offered by this inducer and impeller design. A duplicate small-component test loop (SCTL) inlet duct will be used to determine if any difference in pump performance occurs when compared to the prototype inlet duct test results.

The method of testing the 1/5-scale model pump consists of manually controlling the following pump parameters:

1) Pump Speed – Shown on the Himmelstein digital display and on the cathode ray tube (CRT), and recorded on the DAS.

2) Pump Head and Flow — Displayable on the CRT and recorded on the DAS. Testing at the various system resistances is accomplished throttling Valves V-131B and V-129A at the pump discharge from the control room. Thus, adjustments to pump speed and the position of the valves allow pump testing at specified speeds and Q/N values.

3) NPSH — Pump suction pressure is controlled by varying the cover gas pressure on the DA tank (T-2). Generally, the tank is either pressurized with nitrogen or under a vacuum condition.

The DAS is used to monitor test conditions and to provide facility and test article performance parameters during each test.

Oil flows to the bearings are manually set, while oil temperature is controlled by the lube oil system. Both oil pressures and temperature are recorded on the DAS.

Acoustic measurements were made by AI personnel during cavitation tests and are in their possession.

Table XVIII-2 describes the major events in chronological order.

C. TEST RESULTS

1. Pony Motor Testing

Tests were conducted to obtain the operating characteristics of the test article at pony motor speeds. Data were obtained for a range of flows at pump speeds equal to 2.5, 4, and 7% of design speed. Special testing included negative head rise and second quadrant test at speeds of 4 and 7% of design speed. A composite plot of all these data is shown in Figure XVIII-6. The pump impedance for positive and negative flow (locked rotor forward and reverse flow) is shown in Figure XVIII-7.

TABLE XVIII-2

CHRONOLOGY OF MAJOR EVENTS
(Sheet 1 of 2)

Completion Date	Event	Test
June 18, 1981	Pump delivered to ETEC	
August 14, 1981	Readiness review	
September 1, 1981	Pony motor dry spin test	1A
September 29, 1981	Pony motor speed checkout	1B
October 2, 1981	Pony motor head-flow (2.5% speed)	2
October 5, 1981	Pony motor head-flow (4% speed)	3
October 6, 1981	Pony motor head-flow (7% speed)	4
October 8, 1981	Windmilling	5
October 9, 1981	Negative head rise (4% speed)	6
October 9, 1981	Negative head rise (7% speed)	7
Deleted	Locked rotor – low forward flow	8
October 9, 1981	Locked rotor – reverse flow	9
October 13, 1981	Second quadrant, reverse flow (4% speed)	10
October 13, 1981	Second quadrant, reverse flow (7% speed)	11
October 22, 1981	Main motor dry spin test	12A
November 2, 1981	Main motor checkout test	12B
November 13, 1981	Head flow – 1320 rpm	13A
November 13, 1981	Head flow – 2020 rpm	13B
November 16, 1981	Head flow – 2657 rpm	14
November 16, 1981	Head flow – 3295 rpm	15
November 16, 1981	Head flow – 3460 rpm	16
November 19, 1981	Cavitation – 3295 rpm, Q/N = 1.03	17
November 23, 1981	Cavitation – 3295 rpm, Q/N = 1.13	18
November 23, 1981	Cavitation – 3295 rpm, Q/N = 1.24	19
November 24, 1981	Cavitation – 3295 rpm, Q/N = 1.34	20
November 24, 1981	Cavitation – 3295 rpm, Q/N = 1.44	21
November 24, 1981	Cavitation – 3295 rpm, Q/N = 0.93	22
November 30, 1981	Cavitation – 3295 rpm, Q/N = 0.83	23

TABLE XVIII-2

CHRONOLOGY OF MAJOR EVENTS
(Continued)

Completion Date	Event	Test
December 1, 1981	Cavitation – 3295 rpm, Q/N = 0.72	24
December 1, 1981	Cavitation – 2657 rpm, Q/N = 1.23	27
December 1, 1981	Cavitation – 2657 rpm, Q/N = 1.33	28
December 1, 1981	Cavitation – 2657 rpm, Q/N = 1.44	29
December 2, 1981	Cavitation – 3295 rpm, Q/N = 0.69	25
December 2, 1981	Cavitation – 3295 rpm, Q/N = 1.03 – Repeat	17
December 2, 1981	Cavitation – 2657 rpm, Q/N = 1.55	26

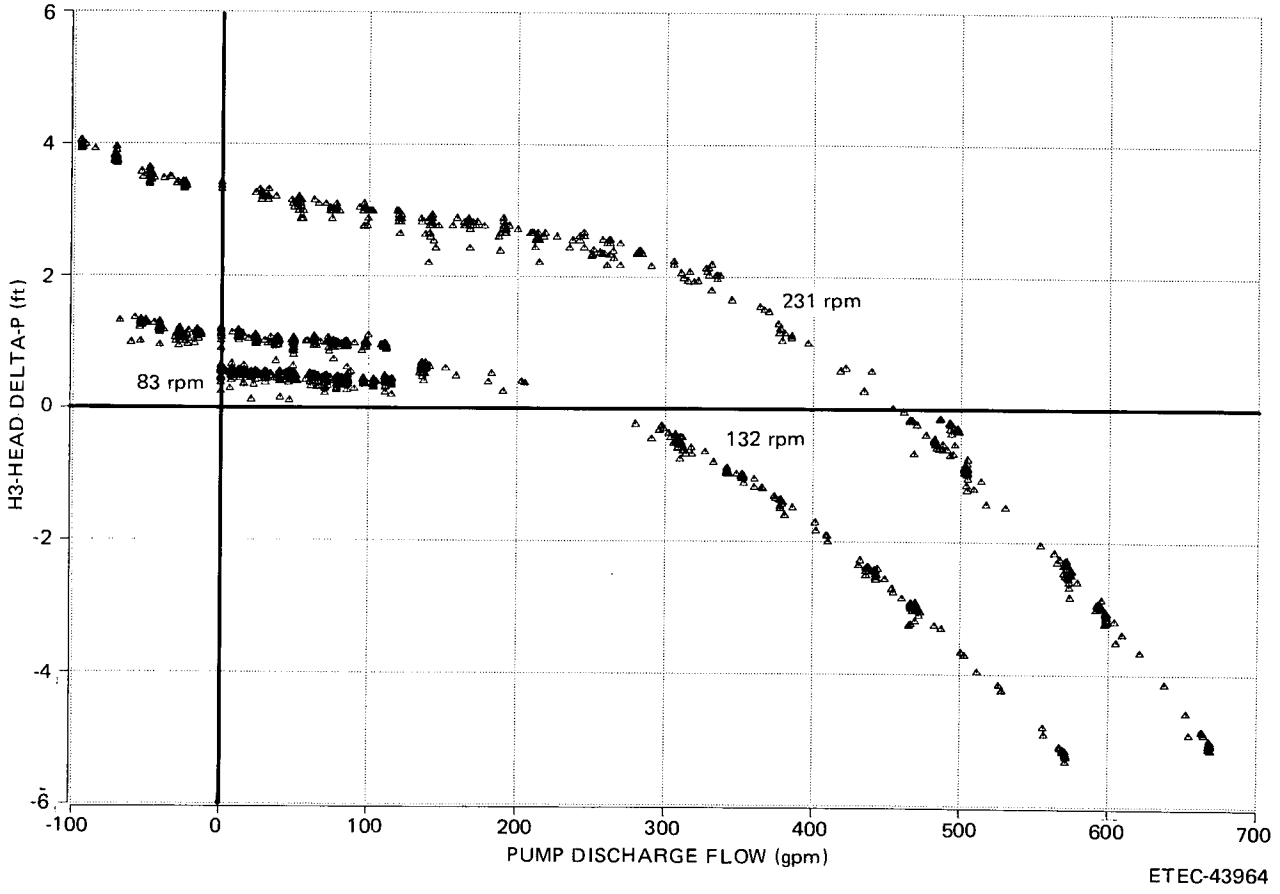

Figure XVIII-6. 1/5-Scale Model Pump Head-Flow Mapping at Pony Motor Speeds

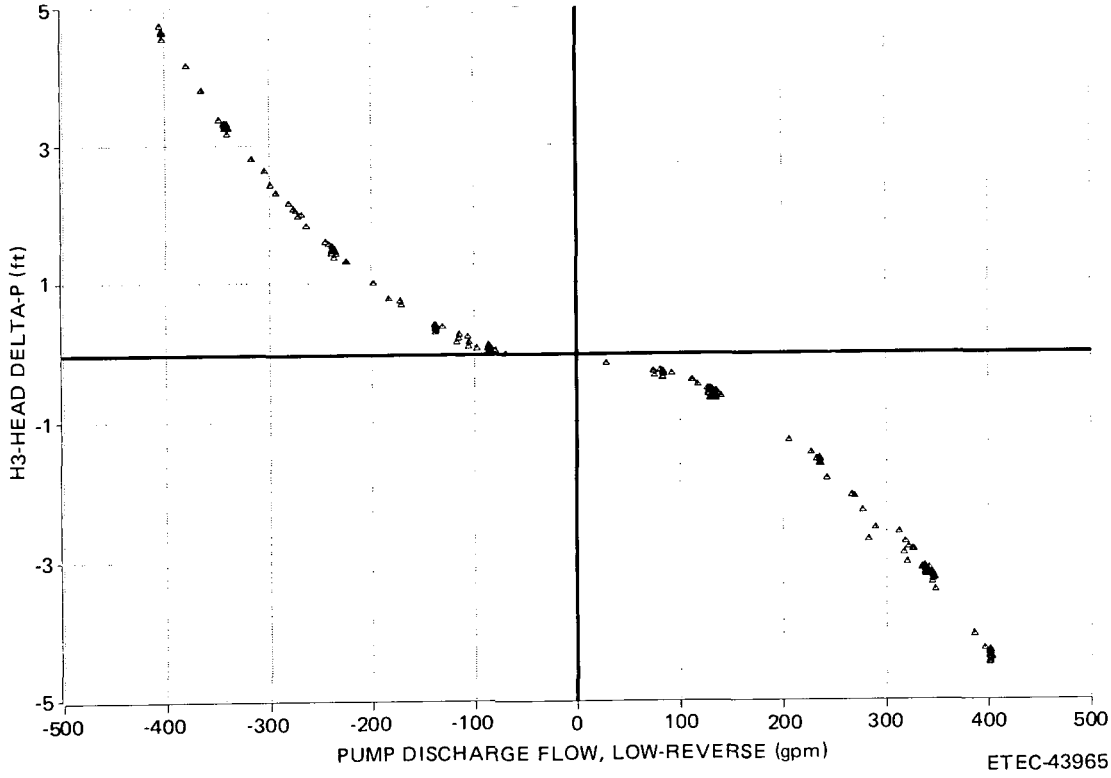

Figure XVIII-7. 1/5-Scale Model Pump Impedance Mapping for Locked Rotor Forward and Reverse Flow (Pony Motor Ranges)

2. Main Motor Testing

Head Flow (H-Q) Tests — These tests defined the characteristic developed head of this pump as a function of flow rate at five test speeds (40, 61.3, 80.65, 100, and 105% of design). Figure XVIII-8 demonstrates the results from these tests compared to the respective predicted curves.

NPSH Tests — Initial suction performance tests were unsuccessful because of air in solution in the water. The water in the loop was deaerated using the facility pumps, circulating through Test Insert Area 3 and while pulling a vacuum on the DA tank (T-2). Deaerating for ∿20 min before testing provided the necessary protection against air in solution.

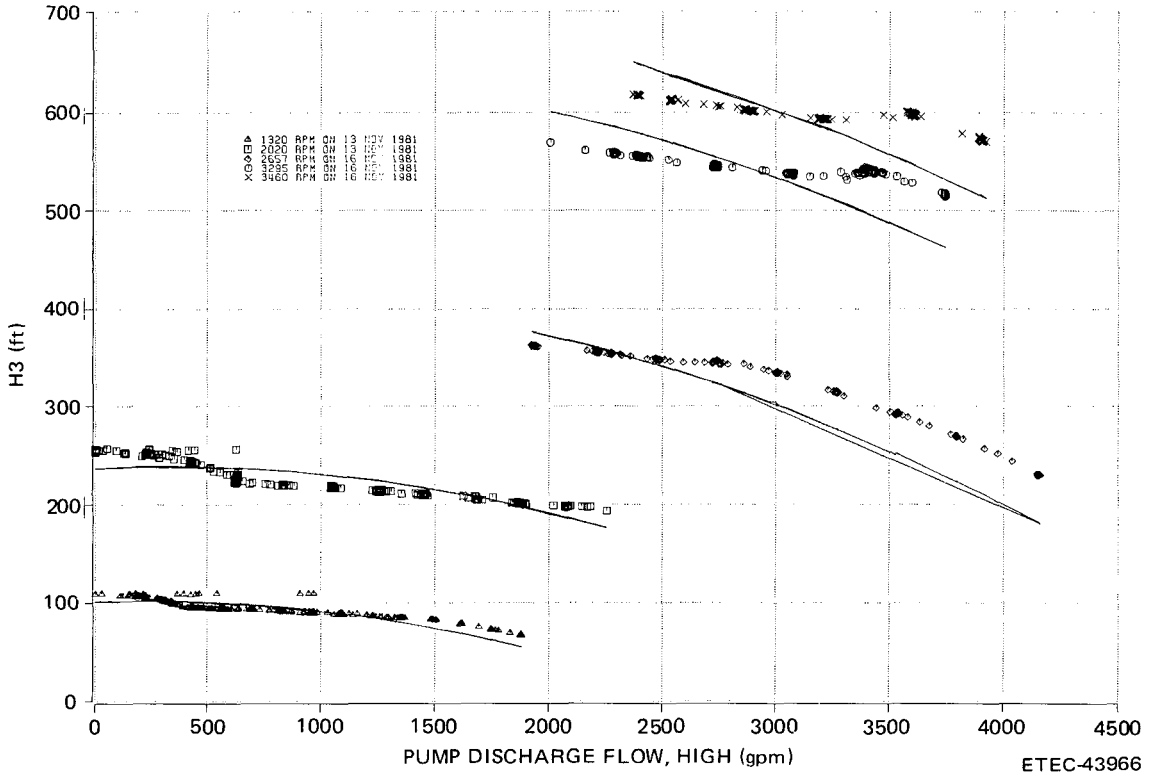

Figure XVIII-8. 1/5-Scale Model Pump Head-Flow Mapping at Main Motor Speeds, Showing Both Predicted and Actual Data

Figure XVIII-9 shows a H-Q map of cavitation data for design speed and design flow, with lines showing 100, 97, and 95% of the noncavitating head for this test point. Figure XVIII-10 shows a head-vs-NPSH plot for the same test. Data still have to be corrected for speed and flow.

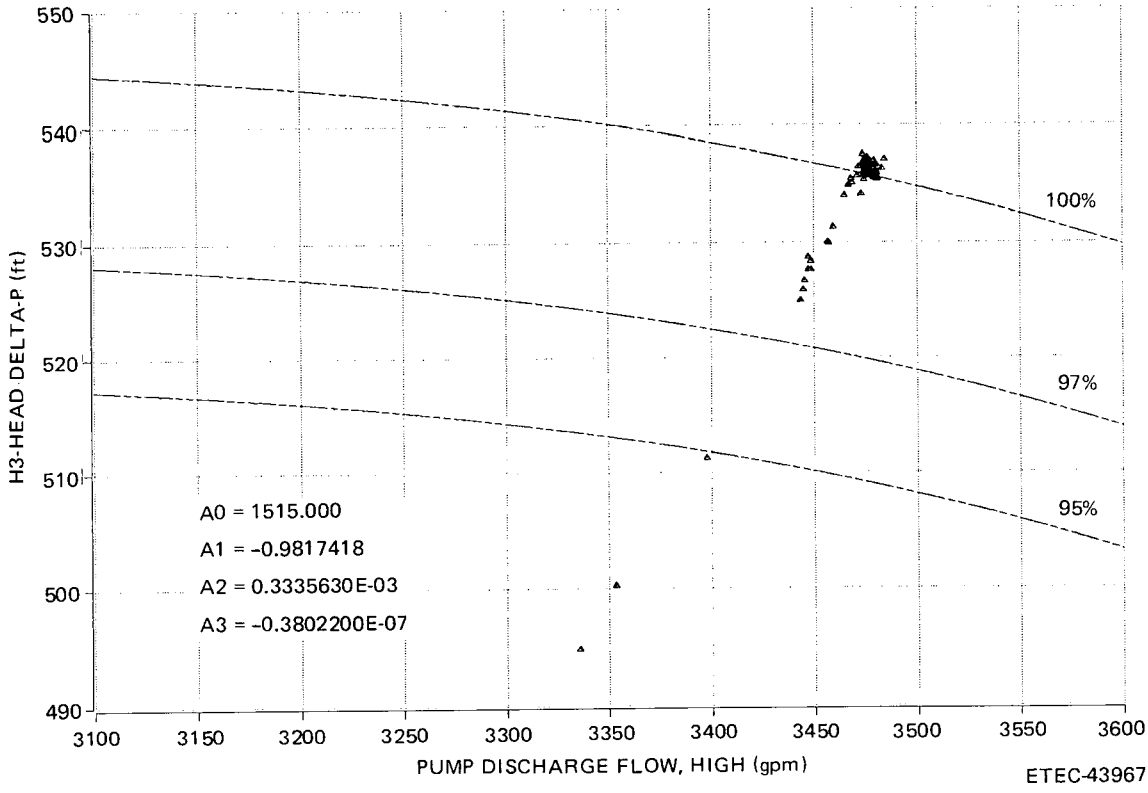

Figure XVIII-9. 1/5-Scale Model Pump Point 1 Suction Performance Test — Developed Head (Data Not Corrected)

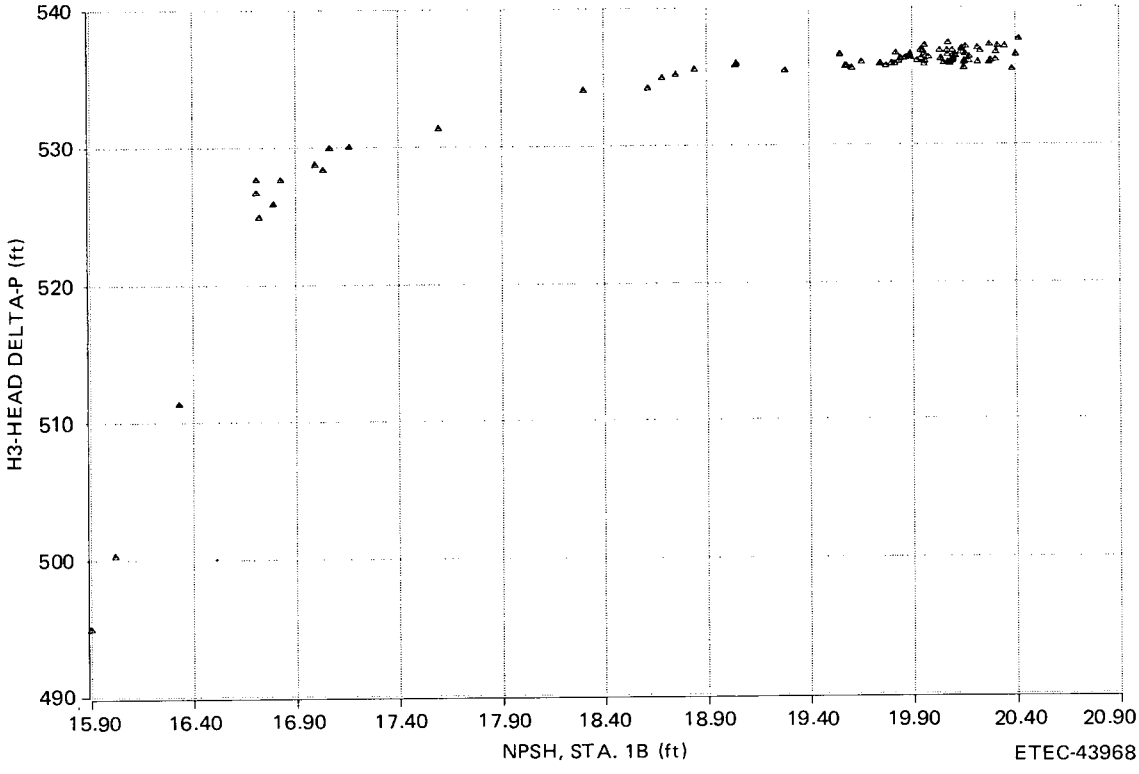

Figure XVIII-10. 1/5-Scale Model Pump Point 1 Suction Performance Test — Available NPSH (Data Not Corrected)

XIX. ENERGY CONSERVATION

H. R. ZWEIG

A. ORGANIZATION

The position of Manager, Energy Conservation, was established in FY 1980 to implement plans and programs for reducing energy consumption and cost in ETEC operations. To focus on the importance of these goals, the position initially reported to the Vice-President, ETEC, in a staff capacity; however, now that the activity is well established, the position has been merged into the Test Systems Unit in the Test Engineering Department. This change is very appropriate, since most of the energy consumption at ETEC is related to the testing activity and test facility operation.

B. ACCOMPLISHMENTS AND ACTIVITIES

To achieve measurable conservation of energy, it is necessary to forecast energy needs for future test programs and to identify cost-effective methods and investment opportunities. Forecasts of energy consumption for the decade of the 1980s were made during FY 1980. While these will change as test schedules change, they remain, in FY 1981, fairly accurate yardsticks of future demand and the potential effectiveness of conservation measures.

Conservation activities fall into several categories:

1) Test program optimization
2) Capital investments in conservation retrofits
3) Studies and surveys to identify conservation opportunities
4) Administrative actions to guide personnel in energy savings
5) Promotion of energy savings through ridesharing to aid rational objectives of fuel conservation
6) Metering of processes and appropriate recordkeeping.

1. Test Program Optimization

The ISIP-II test program in the Sodium Pump Test Facility (SPTF) was conducted with a goal of reducing both the consumption and the cost of energy, compared to the manner in which the Fast Flux Test Facility (FFTF) pump had been tested previously. Powered testing was performed during off-peak hours relative to electrical demand charges. Also, in the period between test points, the pump was run at the lowest speed (550 to 700 rpm) consistent with sustaining isothermal conditions in the loop. This contrasts to the FFTF pump test program, in which most of the testing was done on the first shift, during peak demand hours, and the pump was run at 750 rpm or higher between tests in order to accumulate running time.

During FY 1980, selected ETEC procedures were revised to incorporate energy conservation directives. The method of conducting the ISIP-II program to meet energy conservation goals was consistent with those changes in ETEC procedures.

2. Capital Investments

The DOE Division of In-House Energy Management provides funding for capital projects that result in a reduction of energy costs to the extent that payback is achieved in less than 10 years and where the lifetime discounted savings exceed the investment by a good margin. ETEC has proposed projects that satisfy these criteria, a listing of which is found in Table XIX-1.

3. Survey and Studies

During FY 1981, a new building and facility survey was contracted for completion in FY 1982. This survey should reveal new energy conservation opportunities.

TABLE XIX-1

ENERGY CONSERVATION PROJECTS

Project Description	TEC ($000)	SPB	SIR	Annual Energy Savings (10^9 Btu)	Annual Energy Savings (Btu/$PVI)
Projects With TEC Less Than $1 Million					
SCTI Preheater: Add a heat exchanger to the flue of H-1 to utilize combustion gases to preheat sodium	264	1.7	9.6	23.4	123,200
Outdoor floodlight and building exterior lighting modifications	63	3.12	3.30	2.3	47,600
Replace existing high-bay lighting with high-pressure sodium luminaries	67	3.80	2.7	2.1	39,700
Automated energy management system	490	4.35	2.5	15.7	41,100
Economizer cycles on existing HVAC units	76	5.3	1.9	1.8	30,000
Retrofit exterior lights at SCTI	21	5.4	1.9	0.4	22,300
SCTI H-1 and H-2 combustion efficiency improvement	95	1.63	3.68	7.3	76,400
Projects With TEC Greater Than $1 Million					
SCTI Economizer: Utilite the CRBR prototype steam generator as an economizer to reheat sodium by partial condensation of steam. This project is in Title I design.	10,500	3.08	4.50	428	54,700
SCTI Cogeneration: Add an organic Rankine cycle to SCTI to convert waste heat to electrical capacity.	1,280	2.23	3.40	61	71,400
SPTF Cogeneration: Add a helical rotor pump/turbine to convert fluid power to electrical capacity.	6,447	5.12	1.73	121	29,800
SCTI Combustion Air Preheaters: Add heat exchanger to utilize high-temperature exhaust gas to preheat incoming combustion air.	2,998	6.7	1.88	46.7	24,122

Key: TEC = total estimated cost
SPB = simple payback
SIR = savings-to-investment ratio
PVI = present value of investment

4. Administrative Actions

A campaign to turn off lights in individual offices when unoccupied has led to a heightened awareness on the part of personnel of the need to conserve, as well as to some real reductions in electrical energy use in the office trailers.

5. Ridesharing

ETEC employees participate in ridesharing at a 50% level. Since this level holds fairly constant, overt promotion is not necessary. Help to new employees seeking carpools is provided by local management and senior personnel.

6. Metering and Recordkeeping

ETEC processes are fully metered; however, an additional project ($79,000) has been proposed to improve the quality of fuel flow measurement and recording in the SCTI heaters.

C. ENERGY CONSUMPTION

ETEC's energy consumption is illustrated by the following:

1) Figure XIX-1 shows FY 1981 energy consumption by fuel use category.
2) Figure XIX-2 shows energy consumption by fuel type.
3) Figure XIX-3, showing electrical energy use in the Component Handling and Cleaning Facility (CHCF), illustrates the effect of changing from mercury-vapor to high-pressure sodium luminaries.
4) Figure XIX-4, which shows the electrical consumption in the office trailers, illustrates the effect of turning off office lights. Excessively hot weather during this past summer produced higher than normal air conditioning loads, so the small year-to-year increase in consumption was due mainly to those who regularly turned off their office lights.

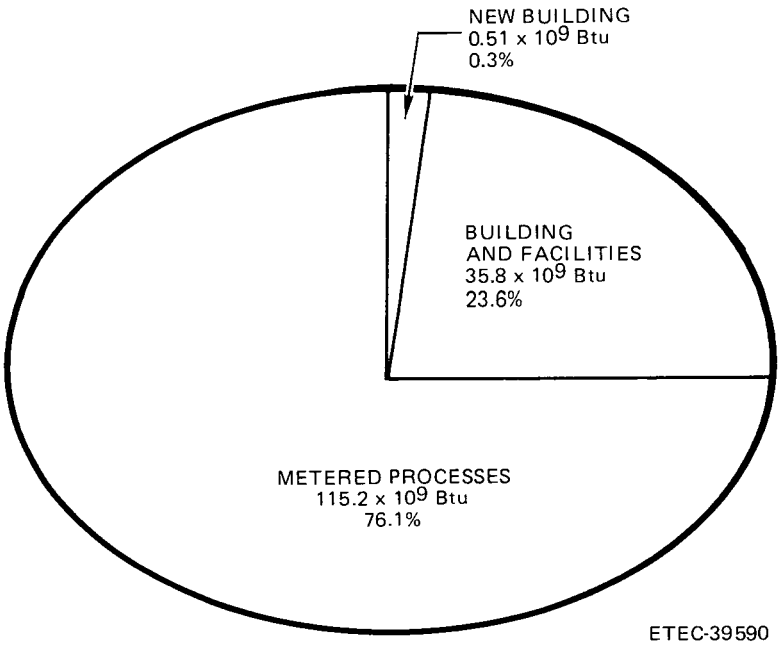

Figure XIX-1. FY 1981 Energy Consumption by Fuel Use Category

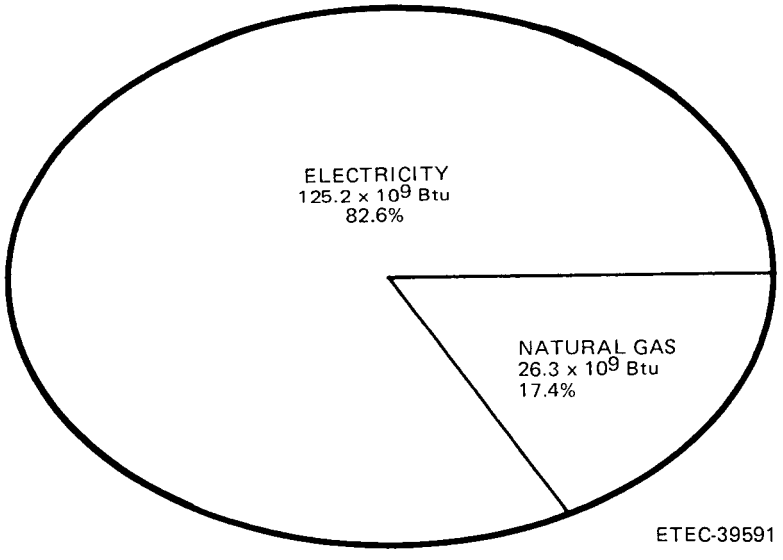

Figure XIX-2. Energy Consumption by Fuel Type

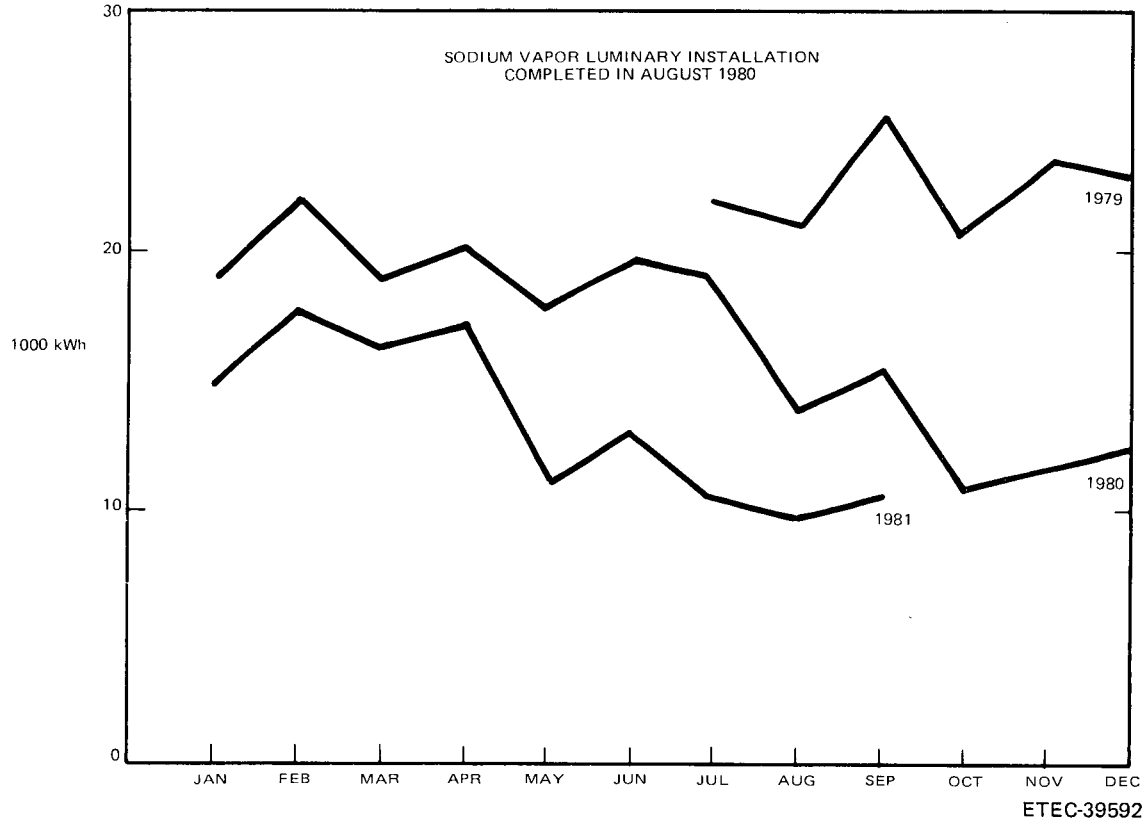

Figure XIX-3. Electrical Energy Use in CHCF

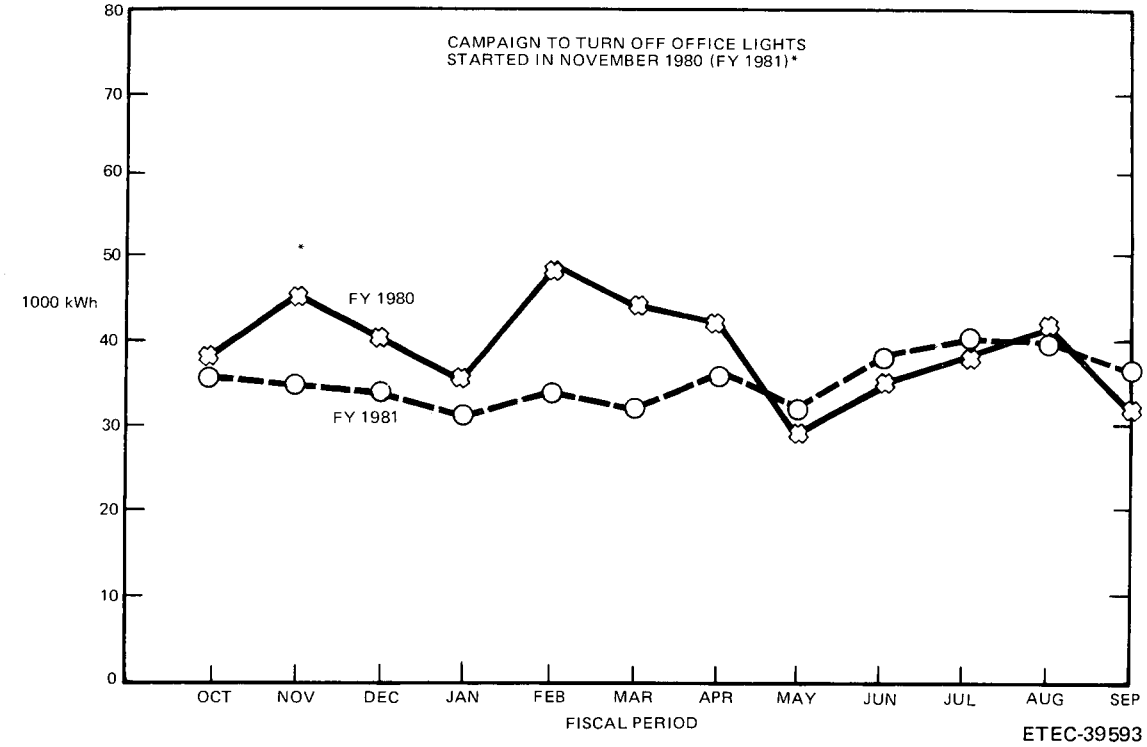

Figure XIX-4. Electrical Consumption in the Office Trailers

XX. ABSORBER BALL MATERIALS TESTS

R. L. EICHELBERGER

A. INTRODUCTION

Atomics International (AI) is developing a self-actuated shutdown system for sodium-cooled reactors. One concept for such a system requires small spheres of a neutron-absorbing material to be in contact with flowing sodium at the maximum sodium temperature in the reactor. Tantalum and its alloys are candidates for this service. Therefore, screening tests in hot sodium were needed before further development of the concept could proceed.

B. TEST DESCRIPTION

1. Facility

The prospective absorber ball materials were exposed to sodium in a tank maintained at the desired test temperature. The sodium was continuously purified by passing through a cold trap that was held at a temperature at which the solubility of oxygen in sodium is <2 ppm. The volume of sodium in the system was about 55 gal (0.21 m^3), and cold trap flow was about 1 gal/min (6.3×10^{-5} m^3/s).

2. Test Specimens

Six tantalum-based materials were exposed to sodium: unalloyed tantalum, T-111 alloy, Ta-10W, Ta with a carburized surface, Ta coated with tantalum carbide (not formed in situ), and Ta coated with Al ("aluminized"). Two kinds of specimens of each material were tested, flat corrosion specimens 0.5 in. (1.3 cm) in diameter and 0.04 in. (0.1 cm) thick and cylindrical specimens 0.5 in. (1.3 cm) in diameter and 0.5 in. (1.3 cm) long. The cylindrical specimens were placed in contact with other cylinders at right angles in 12 combinations, each of the six

materials vs itself and each of the six materials vs Type 304 stainless steel. Each pair of cylinders was loaded with 6.4 lb (2.9 kg) dead weight to produce a stress at the point of contact of 30×10^3 to 100×10^3 lb/in.^{2} (2.1×10^7 to 7×10^7 kg/m^2).

In addition, two iron-silicon materials were exposed to sodium in the longest test (1500 h at 1020°F (820 K)). Specimens were 0.5 in. (1.3 cm) square by 0.04 in. (0.1 cm) thick with the nominal compositions of Fe - 3% Si and Fe - 3% Si - 0.5% Al.

3. Test Method

The tantalum-based test specimens as described above were immersed in liquid sodium in the test facility in three identical groups. The groups were exposed to sodium for 500 h at 700°F, 900°F, and 1200°F (644 K, 755 K, and 921 K), respectively. A fourth group of specimens including the two iron-silicon compositions was exposed to sodium for 1500 h at 1020°F (820 K).

After being removed from the sodium, the specimens were cleaned of sodium by immersion in Dowanol-PM (propylene glycol methyl ether) and then rinsed in deionized water. Photomacrographs and scanning electron micrographs of each specimen were prepared.

C. TEST RESULTS

The test specimens and before-and-after photographs and electron micrographs taken for the sodium exposure tests were delivered to the Test Requester. The Test Requester will make the complete evaluation of the results and issue necessary reports. However, the following observations were made at ETEC in the course of the test.

Exposure to sodium at 700°F (644 K) for 500 h caused no appreciable change weight or appearance in any of the specimens. The point of contact between cylinders exposed under stress was slightly flattened for the uncoated Ta, both when in contact with itself and when in contact with stainless steel. The tantalum carbide coating appeared to be significantly damaged at the point of contact. None of the coatings was uniformly smooth as received, and small changes in appearance were difficult to detect.

After exposure to sodium at 900°F (755 K), the corrosion specimens showed slight discoloration, but no generalizations were made on the relative discoloration of the various materials. Weight changes of these discs were small, probably within weighing reproducibility, except for the tantalum coated with tantalum carbide, for which the two discs gained 1.9 mg and 0.9 mg. Weight changes for the tantalum coated with tantalum carbide stress specimens were in the opposite direction, the three cylinders losing 45.4, 15.6, and 17.0 mg. No other material showed consistent weight changes.

The observations that can be reported on the stress specimens are similar to those reported for the 700°F exposure. All the materials show some apparent deformation at the point of contact, with uncoated tantalum perhaps the most deformed. The tantalum carbide coating on tantalum had flaked away over a small area on one specimen. No firm evidence of diffusion bonding was seen, although several scanning electron microscope (SEM) photomicrographs might be interpreted to show that some tearing of metal occurred when two specimens were separated.

Specimens exposed to sodium at 1200°F (921 K) for 500 h all showed significant weight losses and deformation at the points of contact between stressed specimens. The surfaces of the aluminized tantalum and the tantalum carbide-coated specimens were disrupted at the points of contact. The carburized tantalum, however, seemed to have suffered no surface damage. The greatest attack, accompanied by apparent self-welding, occurred with the unalloyed tantalum.

After exposure to sodium at 1020°F (820 K) for 1500 h, all tantalum-based materials showed slight discoloration. No inferences were made on the relative discoloration of the various tantalum alloys. No significant dimensional changes were measured.

Weight changes for all the materials showed a loss of material an order of magnitude less than that observed in the 500-h tests at 1200°F and about an order of magnitude greater than the 500-h tests at 900°F. The latter, however, were only a few tenths of a milligram, and perhaps within the reproducibility of weighing.

Both of the magnetic materials (Fe - 3% Si and Fe - 3% Si - 0.5% Al) were lighter in color after the sodium exposure. Both alloys lost weight, although three of the four specimens of Fe - 3% Si changed only 0.1 mg. The fourth Fe - 3% Si specimen lost 0.6 mg. The weight loss of three of the four Fe - 3% Si - 0.5% Al specimens was 0.6 mg, and the fourth lost 0.10 mg.

Magnetic alloys containing substantially more Si and/or Al are of interest for safe-shutdown hardware. Without testing them, no generalizations may be made about how they would fare in sodium. The present tests suggest that the presence of 0.5% Al in the Fe - 3% Si material causes it to be more strongly attacked by 1020°F sodium than the alloy without Al is.

Qualitative evaluation of the results discussed above suggests that pure Ta, Ta coated with tantalum carbide, and aluminized Ta are not satisfactory for the intended service. The two tantalum alloys and the carburized tantalum appear sufficiently promising to warrant further testing if work continues on the absorber-ball concept for a self-actuated shutdown system.

XXI. FLAT, LINEAR INDUCTION PUMP TESTING

R. A. GRANGER

A. INTRODUCTION

Sodium tests have been completed on a full-scale 400-gal/min (0.025-m^3/s) flat, linear induction electromagnetic (EM) pump. The pump was designed as a prototypical model containing all of the pumping elements found in the CRBR electromagnetic pump.

During testing, the pump met or exceeded all requirements of performance, both normal and emergency, as required by the test requester. In addition, the pump exhibited stability under all operating modes, whether obtained by voltage control or by changing the loop resistance. The pump also exhibited considerable excess capacity and low coil temperatures. This was a result of designing for minimum coil temperatures to obtain the required 30-yr life for the pump.

B. TEST DESCRIPTION

1. Facility

The tests were performed with the EM pump installed in a sodium loop in the Sodium Component Test Installation (SCTI) at the Energy Technology Engineering Center (ETEC). The sodium loop is shown in Figure XXI-1.

The T6 sodium tank served as a cooler and expansion tank during the testing by accommodating changes in the sodium volume and provided an elevated free surface between the sodium and the cover gas. The tank, 5.5 ft (1.67 m) high, consisted of 24-in. (61-cm) Schedule 20 pipe with two hemispherical caps, each having a 24-in. (61-cm) curvature radius. Inside the tank was a manual level dipstick and a 12-in. (30.5-cm) Schedule 40 standpipe, connected to a 4-in. (10-cm) inlet with 4-in. x 8-in. (10-cm x 20-cm) and 8-in. x 12-in. (20-cm x 30.5-cm) reducers. Inside the tank, the sodium flows radially out of the top of the standpipe through 50 1-in.-diameter (2.54-cm) holes arranged in two rows of 25.

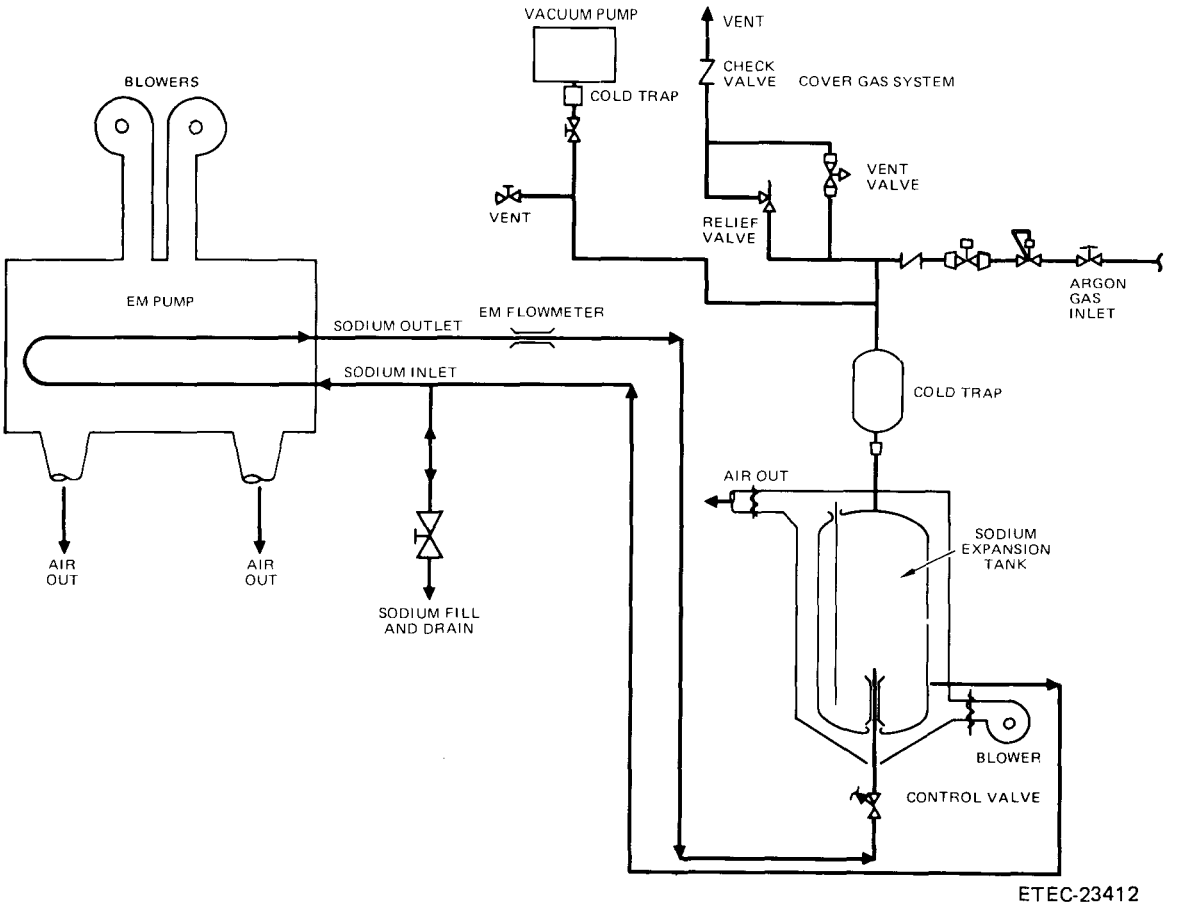

Figure XXI-1. EM Pump Cooling and Cover Gas

To remove heat from the sodium, air was blown through a 1-in. (2.54-cm) annular region between the tank and the blower ducting. The cooling capacity of the expansion tank was designed to function as a counterflow heat exchanger. Air was blown upward through the annular space, and sodium flowed downward through another annulus, inside the tank, formed by the standpipe and the inside wall of the tank. The blower was sized to lower the sodium heatup at the test point having the greatest cooling requirement, which is at the conditions of lowest sodium temperature and flow with maximum applied voltage.

The sodium loop consisted of 4-in. (10-cm) pipe and included a flowmeter and 4-in. (10-cm) Sargent Y-angle globe valve with a full-open C_V of 324. The valve was equipped with a position indicator and a local readout indicator.

The argon cover gas system consisted of the required regulators, controllers, and vent valves to provide a positive regulated pressure on the sodium and also included a vacuum pump to lower the sodium pressure during the head-flow cavitation tests.

Forced cooling of the EM pump coils was provided by two blowers and air ductwork. The blowers were rated at 1500 scfm each. Experience gained during testing indicated that the blowers could be throttled to 2100 scfm (total). This provided a more stable thermal condition in the pump coils and did not require turning the blowers on and off. The cooling air pressure drop across the pump at 2100 scfm was found to be 1.75 in. (4.4 cm) H_2O.

During the testing, the following instrumentation was recorded:

Sequence Number	Description	Tag Name
446	Sodium flow rate	FE-670
	Pressure rise	*
	Pressure rise (corrected)	*
	Efficiency	*
	NPSH	*
445	Sodium outlet temperature	TE-6700
479	Pump throat inlet pressure	PT-671
478	Pump throat outlet pressure	PT-670
488	Input current Phase A	IT-TA-AI
489	Input current Phase B	IT-TA-BI
490	Input current Phase C	IT-TA-CI
491	Output current Phase A	IT-TA-AO
492	Output current Phase B	IT-TA-BO
493	Output current Phase C	IT-TA-CO
485	Excitation voltage (A-B)	ETTA A-B
486	Excitation voltage (B-C)	ETTA B-C
487	Excitation voltage (C-A)	ETTA C-N
494	Output power	J1-1A

Sequence Number	Description	Tag Name
477	Pump throat vibration	YE-TA
433	Upper throat aft left (SP)	TE-4B
435	Upper throat fwd left (SP)	TE-6B
436	Lower throat aft right (SP)	TE-7B
438	Lower throat fwd left (SP)	TE-9B
465	Upper throat aft left	TE-4A
466	Upper throat C.L. center	TE-5A
467	Upper throat fwd right	TE-6A
468	Lower throat aft right	TE-7A
469	Lower throat C.L. center	TE-8A
470	Lower throat fwd left	TE-9A
449	Air inlet temperature (B1)	TE-B1
450	Air inlet temperature (B2)	TE-B2
451	Air outlet temperature #1	TEB1/B21
452	Air outlet temperature #2	TEB1/B22
483	Cooling air flow (B1)	PDT-B1
484	Cooling air flow (A2)	PDT-B2
407	Cooling air flow rate	*
401	Pump frame temperature #1	TE-F1
402	Pump frame temperature #2	TE-F2
353	Up. pipe cone to elbow fwd	TE-2A-1
354	Up. pipe cone to elbow aft	TE-2C-1
355	Up. elbow – aft throat-P	TE-3A-1
356	Up. elbow – aft throat-C.L.	TE-3B-1
357	Up. elbow – aft throat	TE-3C-1
358	Up. elbow – aft throat-bot.	TE-3D-1
359	Forward header	TE-10A-1
360	Forward header	TE-10B-1
439	Lower stator Phase B (SP)	TE-16B
440	Lower stator Phase A (SP)	TE-17B
441	Lower stator Phase C (SP)	TE-18B
442	Upper stator Phase B (SP)	TE-19B
443	Upper stator Phase A (SP)	TE-20B
444	Upper stator Phase C (SP)	TE-21B
471	Lower stator Phase B	TE-16A
472	Lower stator Phase A	TE-17A
473	Lower stator Phase C	TE-18A
474	Upper stator Phase B	TE-19A
475	Upper stator Phase A	TE-20A
476	Upper stator Phase C	TE-21A
480	T6 cover gas pressure	PT-T6

*Calculated parameters

2. Test Article

The test article consisted of the functional model electromagnetic pump containing all of the pumping elements to be found in the CRBRP electromagnetic pump, Type I. All of the component parts were installed in a frame assembly for a completed pump assembly as shown in Figures XXI-2 and -3. This assembly includes the flow pipe, thermal insulation, heaters, thermocouples, stators, snubbers, and various miscellaneous parts. This final assembly results in a boxlike structure capable of resisting pipe stresses and suitable for mounting on a relatively flat surface.

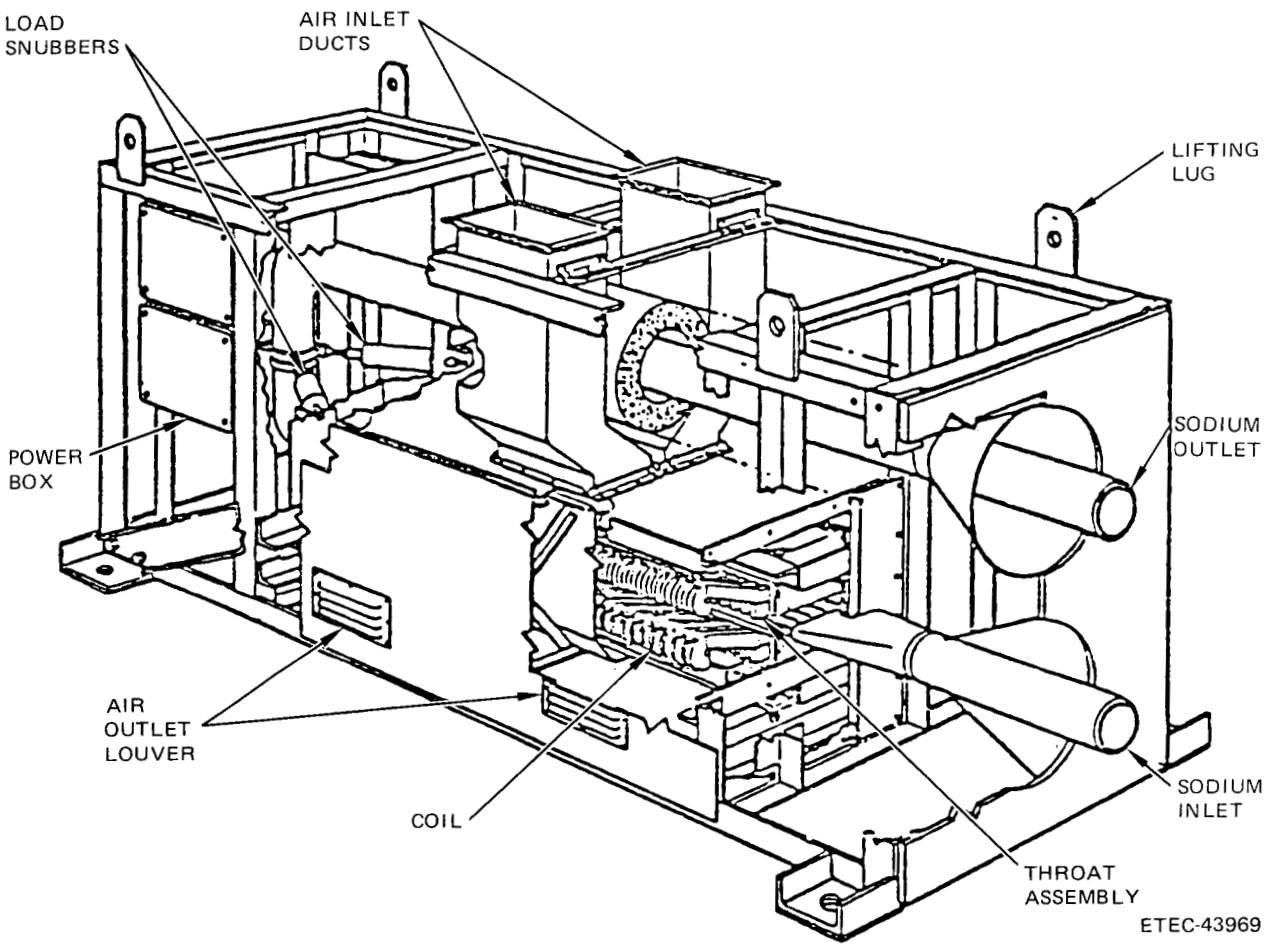

Figure XXI-2. 400-gal/min (0.025 m^3/s) Flat, Linear Induction Pump

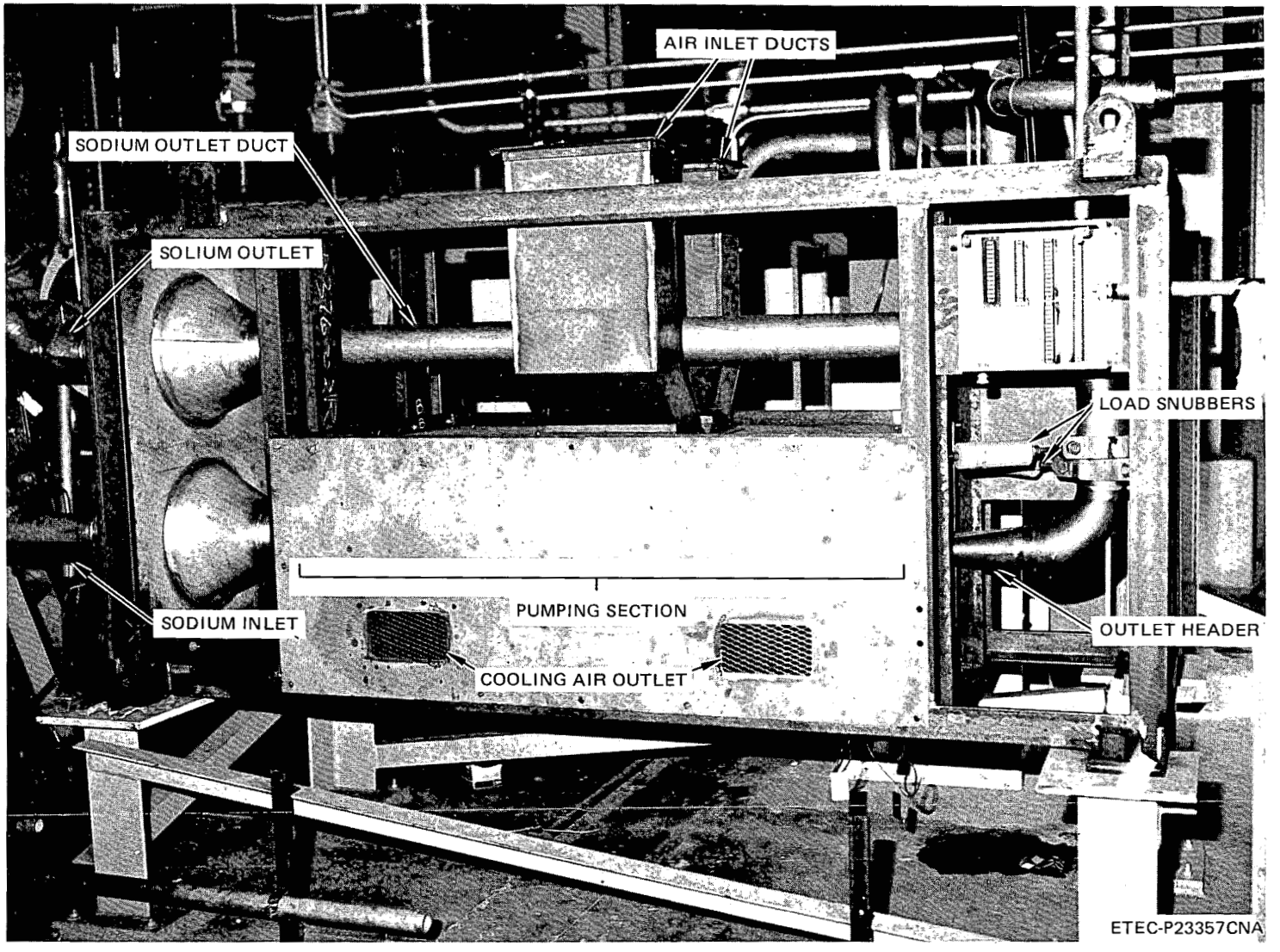

Figure XXI-3. Linear Induction Pump

The stators and hydraulic assembly were constructed identically to and of the materials proposed for the CRBR EM pump, Type I. The two stators, between which passes a flat assembly of multiple ducts for passing liquid metal, comprise the electromagnetic portion of the pump. Each stator contained 48 coils connected to produce a traveling magnetic field, which passes through the multiple ducts containing liquid metal. Currents are induced in the liquid metal, dragging the liquid metal with the moving field.

The voltage was set by a device commercially known as an "inductrol." The "inductrol" voltage regulator is a variable-ratio autotransformer consisting of a laminated steel stator, on which is wound the regulating or series winding, and a laminated steel rotor, on which is wound the exciting or shunt winding. The basic construction is similar to that of an electric motor, except that the rotor rotates only 180 mechanical and electrical degrees.

3. Test Method

The functional test program is described below.

a. Dry Preheat Test

The EM pump, facility piping, and components were heated at a controlled rate of $50^{o}F/h$ ($0.17^{o}C/s$) up to $400^{o}F$ ($204^{o}C$). During the heatup, a vacuum was applied to the system and then dry argon gas was introduced into the system through Vapor Trap VT-6. This process was repeated several times during the preheat until the dew point of the removed gas was below $-40^{o}F$ ($-40^{o}C$).

b. Sodium Fill

After the preheat temperature of $400^{o}F$ ($204^{o}C$) had stabilized, the EM pump and test system was filled with sodium. The basic method for filling was to apply a vacuum on the system, pressurize the facility sodium supply tank, and throttle the sodium into the system by opening Supply Valve V626.

c. Wetting

With the sodium flow from the EM pump set at 100 gal/min, and a pressure rise across the pump of 10 psi (69 kPa), the sodium temperature was increased to 750°F (399°C) at a controlled rate of 50°F/h (0.17°C/s). This condition was held for 48 h to "wet" the pump. The sodium was then drained back to the facility storage tanks and the EM pump cooled down to 400°F (204°C). The EM pump was then refilled with 350°F (177°C) sodium. The sodium temperature was then increased to 1130°F (610°C) at a controlled rate of 50°F/h (0.17°C/s).

d. Head-Flow Test

(1) 1130°F (610°C) Tests

Cavitation Test – With the EM pump operating at 300 gal/min (0.019 m^3/s) and 60 psi (414 kPa), the 1130°F (610°C) cavitation test was performed by slowly reducing the cover gas pressure until there was a 3% loss in the pressure rise across the pump or the pump nozzle accelerometer triggered an alarm.

Variable-Voltage Test at Reference System Resistance – The 1130°F (610°C) variable-voltage test was performed at 300 gal/min (0.019 m^3/s) and a 60-psi (414-kPa) pressure rise across the pump. During the test, the pump voltage was varied by 105, 85, 75, 50, and 25% of the value at the reference system resistance.

Variable-Voltage Test at 133% of Reference System Resistance – This test was performed with the sodium system set at the reference resistance of 300 gal/min (0.019 m^3/s) and a pressure rise across the pump of 60 psi (414 kPa). The sodium system valve position was then changed to obtain the required flow rate. The pump voltage was then varied by 105, 85, 75, 50, and 25%. The same variable-voltage tests were repeated for 200 and 400% of the reference system resistance.

Head-Flow Mapping – The test was initiated at the reference system resistance of 300 gal/min (0.019 m^3/s) and a pressure rise of 60 psi (414 kPa) across the pump. The sodium valve was positioned to obtain a sodium flow of 400, 500,

and 600 gal/min (0.025, 0.032, and 0.037 m^3/s). The EM pump voltage was then adjusted to 184 V and the sodium valve was positioned to obtain sodium flows of 100, 200, 300, 400, and 500 gal/min (0.0063, 0.013, 0.019, 0.025, and 0.032 m^3/s). This was repeated at pump voltages of 92, 368, and 450 V.

(2) 800^oF (427^oC) Test

The sodium system was cooled to 800^oF (427^oC) at a controlled rate of $50^oF/h$ ($0.17^oC/s$). The cavitation test, variable-voltage test at reference system resistance, variable-voltage test at 133% of reference system resistance, and head-flow mapping test were all performed in the same sequence as in the 1130^oF (610^oC) test.

(3) 600^oF (316^oC) Test

The sodium system was cooled to 600^oF (316^oC) at a controlled rate of $50^oF/h$ ($0.17^oC/s$). The cavitation test, variable-voltage test at reference system resistance, variable-voltage test at 133% of reference system resistance, and head-flow mapping test were all performed in the same sequence as in the 1130^oF (610^oC) test.

(4) 450^oF (232^oC) Test

The sodium system was cooled to 450^oF (232^oC) at a controlled rate of $50^oF/h$ ($0.17^oC/s$). The cavitation test, variable-voltage test at reference system resistance, variable-voltage test at 133% of reference system resistance, and head-flow mapping test were all performed in the same sequence as in the 1130^oF (610^oC) test.

e. Extended Operations Test

The EM pump was operated at a steady-state condition of 900^oF (482^oC), 300 gal/min (0.019 m^3/s), against a head rise of 60 psi (414 kPa) for 200 h.

f. Design Limit Test

(1) 450°F (232°C) Test

The test was initiated with the sodium temperature at 450°F (232°C) and the EM pump flow at 800 gal/min (0.050 m^3/s). The developed pressure of the pump was then increased by 40 psi (286 kPa) by adjusting the sodium system valve. The EM pump flow rate was then increased to 800 gal/min (0.050 m^3/s). The developed pressure of the pump was again increased by 40 psi (276 kPa). This operation was continued until a maximum pump discharge pressure of 200 psia (1380 kPa) was reached.

(2) 600°F (316°C) Test

This test was performed in the same sequence as in the 450°F (232°C) design limit test.

g. Blocked-Flow Test

(1) 600°F (316°C) Test

With the pump operating at 25% voltage and 100 gal/min (0.0063 m^3/s), the sodium flow was rapidly shut off.

(2) 450°F (232°C) Test

This test was performed in the same sequence as in the 600°F (316°C) test.

h. Heat Soak Test

The sodium temperature was lowered to 400°F (204°C), at which time the EM pump and air blowers were turned off. Pump temperatures were recorded every 5 min until they stabilized.

i. Preheat Test (With Sodium in the Lines)

The EM pump was allowed to cool to ambient temperature. The pump was then preheated to 830°F.

j. Emergency Conditions Test

The EM pump and facility piping was drained of sodium and cooled to ambient temperature. With the interlocks disabled, 230 V ac was applied to the pump for 20 s with the pump temperatures being recorded until they stabilized.

C. TEST RESULTS

1. Dry Preheat

Power was applied to the pump, pump heaters, and loop heaters to increase the temperature at the rate of 50°F/h (0.17°C/s) from the initial pump ambient temperature. Preheat temperature of 400°F (204°C) was reached with 100 V applied to the pump. The pump was then cooled to ambient conditions at 50°F/h (0.17°C/s). When the pump preheat was terminated, the pump current was 60 A and the maximum coil temperature was 127°F (53°C) with a 71°F (22°C) ambient temperature without forced air cooling.

2. Sodium Fill

EM pump testing was resumed with a repeat of preheating to 400°F (204°C), followed by filling the pump and loop with 350°F (177°C) sodium. After filling, the pump was operated at 100 gal/min (0.0063 m^3/s) at a 10-psi (69-kPa) developed head and the sodium temperature was increased to 750°F (399°C). This operation continued until the pump and loop were drained at 750°F (399°C). After the pump and loop temperatures were reduced to 400°F (204°C), the pump and loop were refilled with 350°F (177°C) sodium. Operation at 100 gal/min (0.0063 m^3/s) developing 10-psi (69-kPa) head required a pump voltage of 128 V line-to-line with a pump current of 118 A, and the maximum measured coil temperature was 124°F (51°C) with a 62.5°F (17°C) ambient temperature.

3. Wetting

After refilling the pump and loop with 350°F (177°C) sodium, the wetting procedure was started by setting a flow and head of 100 gal/min (0.0063 m^3/s) and 10-psi (69-kPa) developed head. This required 107 V, line-to-line, applied to the pump. The sodium temperature was increased to 750°F (399°C) at a maximum heatup rate of 50°F/h (0.17°C/s). The sodium wetting of the system had occurred when the flow and head stabilized.

4. Head-Flow Test

After the wetting tests, the flow was increased to 300 gal/min (0.019 m^3/s) with 60-psi (141-kPa) developed head. This required 255 V line-to-line. As the temperature of the sodium increased to 1130°F (610°C), the valve position and pump supply voltage were changed to maintain the flow and head. The final voltage was 271 V line-to-line.

a. Testing at 1130°F

Cavitation — Cavitation testing was performed at a flow of 300 gal/min (0.019 m^3/s). The 3% loss in pressure rise was visually monitored on a programmed DAS graphical TV display.

Variable-Voltage Tests — This test was performed using four different loop resistances obtained by changing the valve position to obtain loop resistance of 100, 133, 200, and 400% of base loop resistances. Base loop resistance was established as providing for a 60-psi (414-kPa) head drop for 300-gal/min (0.019-m^3/s) flow. The line voltage for this operating point is called 100% line voltage for this test. For each resistance curve, data were acquired at 100, 105, 85, 75, 50, and 25% of the line voltage as established above.

Flow-Mapping — This test was performed by changing valve position while constant voltage was applied to the pump. The voltages selected for this testing were: 460, 368, 276, 184, and 92 V line-to-line as applied to the pump. Flow-mapping testing at 460 V could not be performed at less than 200 gal/min due to excessive discharge pressure. A limit of 200-psi gauge pressure was established as the testing limit for the pump.

b. Testing at 800°F (427°C)

Cavitation — The 3% loss in pressure rise was visually monitored on the programmed DAS graphical TV display.

Variable-Voltage Test — Test results were consistent with the 1130°F (610°C) test.

Flow-Mapping — Flow-mapping testing at 460 V could not be performed at less than 500 gal/min due to excessive discharge pressure. A limit of 200-psi gauge pressure was established as the testing limit for the pump.

c. Testing at 600°F (316°C)

Cavitation — The 3% loss in pressure rise was visually monitored on the programmed DAS graphical TV display.

Variable-Voltage Test — These test results showed excellent stability. The application near this temperature is for the EVST sodium pump's emergency condition.

Flow-Mapping — Flow-mapping testing at 460 V could not be performed at less than 500 gal/min (0.032 m^3/s) due to excessive discharge pressure. A limit of 200-psi (1380-kPa) gauge pressure was established as the testing limit for the pump.

d. Testing at 450°F (232°C)

Cavitation – The 3% loss in pressure rise was visually monitored on the programmed DAS graphical TV display.

It is concluded the pump will operate without cavitation at all specified conditions of flow and head with 0-psi (14.7-psia) input pressure. Test data indicate an inlet pressure of 7.5 psia is adequate to prevent cavitation at flows of 300 gal/min or less, but for flows of 300 to 500 gal/min, the inlet pressure should be 12 psia minimum.

Variable-Voltage Test – The test data indicated excellent stability. There are two applications near this tested condition: (1) the primary sodium makeup pump and (2) the EVST sodium pump condition, Condition 1 at a higher system resistance and Condition 2 at a system flow resistance somewhat lower. The flow requirement of Condition 2 can be obtained at a voltage of less than 276 V line-to-line.

Flow-Mapping – Flow-mapping testing at 460 V could not be performed at less than 500 gal/min (0.032 m^3/s) due to excessive dischrage pressure. A limit of 200-psi (1380-kPa) gauge pressure was established as the testing limit for the pump. Test data indicated a head abnormality at 200 gal/min (0.013 m^3/s). This is the flow at which there was excessive valve vibration at higher line voltages. This vibration was responsive to cover gas pressure and is believed to be caused by valve cavitation.

e. Extended Performance

Pump performance was constant during the test period without any change in performance. Electrical conditions were as follows: 264 V line-to-line, 244 A at 35% power factor, requiring 39.3 kW of power for a 20% pumping efficiency. The coil temperature rise was 143°F (62°C) over the ambient temperature.

f. Design Limits

During the test, the maximum measured coil temperature rise was 160°F (71°C) over a 66°F (19°C) ambient temperature, and as such, coil temperature limit was not a problem. The maximum efficiency was attained at maximum flow and head to produce the maximum output. The maximum efficiency was slightly over 40% at the transition between maximum flow limit and 460-V line-to-line limit.

g. Heat Soak Test

The thermocouples attached to the pump duct showed an immediate drop in temperature. The period of the oscillation was about 15 min. The coil temperature thermocouples indicated a temperature drop in the first 10 to 15 min and a steady decrease from there on. There was no evidence of a temperature overshoot, as convectional cooling is adequate to cool the pumps upon loss of power to the pump and blower at 400°F (204°C).

h. Preheat Test With Sodium in the Pump

This test verifies that the pump can be thawed after freezing without incurring damage. The last section of sodium to melt was the aft part of the pumping section between the stator and transition heater locations.

As heat was added to a given part of the pump, the temperature would rise until the sodium started to melt; then the temperature would remain constant as the sodium melted, and after the sodium was melted, the temperature would resume its rise. When the last of the sodium was melted, pump flow was quickly established.

i. Emergency Conditions Test

This test was run for 2 min at power of 28 kW at 224 V and 35 kW at 235 V with a maximum temperature rise of 241°F (116°C).

Subsequent inspection, including disassembly and visual inspection of the lower surface of the pumping duct, determined there was no distortion, warpage, defect, or any anomaly of the ducts or of its attachments during testing.